In Vitro and *In Vivo* Feasibility Study of Ultrasound for Monitoring Tooth Surface Loss

Khalid Hussain F Sindi

Submitted in accordance with the requirements for the degree of
Doctor of Philosophy

As part of the requirements for the Integrated degree of Doctor of Philosophy and
Master of Science (Restorative Dentistry)

The University of Leeds

School of Dentistry

December 2013

The candidate confirms that the work submitted is his own and that appropriate credit has been given where reference has been made to the work of others.

Acknowledgments

I am deeply grateful to my supervisors: Dr. Nigel Bubb, Dr. Tony Evans and Miss Lynn Gutteridge for their guidance, help, encouragement and support, which they have extended to me, without their advice and feedback, this thesis would have not been completed. I would like to express thanks to the Saudi Ministry of Health for their sponsorship and for giving me the opportunity to join the University of Leeds as an Integrated PhD and MSc student, and gain unmatched educational experience in the fields of dental research and clinical dentistry.

My gratitude extends to my father, Prof. Hussain Sindi, who has always been there for me, and has always supported me in the shadow and in the light. I love you and will always be grateful to you dad. My warmest appreciation extends to my wife and soul mate, Mrs Noha Affan, for her unconditional love, kindness, and support that she has shown throughout my studies. I want to tell her she is the best thing that happened in my life and that I love her endlessly and unconditionally. A lot of family time had to be sacrificed and she was very understanding. Special thanks to my lovely sister Mrs Suzan Sindi, the heart of our family whom is a true blessing from God. She is not only my sister, but a friend and a mother. Thanks are due to my fantastic sister Miss Razan Sindi, my brothers Mr. Fouad Sindi, Mr. Abdulrahman Sindi, Mr Mohammed Sindi, Mr Faisal Sindi and Mr Osama Sindi; I would like to tell them that I love them very much and I will always be there for them. Last but not least, I would like to tell my daughter, Miss Tuleen Sindi, how much I love her and that I will always be there for her, to protect her, to cherish her and make sure she is always happy and loved.

I would also like to take this opportunity to thank Mr David Foakes and Mr Mick Devlin for their help with the purpose-built and ultrasound apparatuses (Chapters 2 and 3, respectively); Mr Mike Pullan for his help with the design and construction of the purpose-built apparatus in Chapter 2 and Dr. Daniel Skrzypiec for help with the μ-CT images in Chapter 4. I would like to thank some of my fellow colleagues: Dr. Sevan Harput for his help with setting up the apparatus, Mr John Blockley for his help with the preliminary results in Chapter 2, Dr. Mostafa Abdelrahman for his help with some of the imaging work using the commercial ultrasound scanner in Chapter 4. Thanks are extended to Mr Mohammed Khan for the programme codes used in Chapter 3 for automating signal capture, in Chapter 4 for automating image formation, Chapter 5 and 6 for automating signal capture.

Thanks to Dr. Jing Kang and Mrs Theresa Munoumbwe for their statistical support, Dr. Catherine Fernandez, Mrs Gillian Ducanovic, Miss Ashna Chavda for their help with the setting up and management of the clinical trial through DentCTRU (Chapter 6). Thanks are also extended to Mrs Jackie Hudson and Mrs Claire Godfrey for their assistance at various stages in my studies. I would also like to thank Mrs Julie McDermott for her help in coordinating my ethical approval application and Mr Adam Steel for his help throughout my time in the Oral Biology Department, University of Leeds.

Abstract

This work attempted to appraise the usefulness of ultrasound as a diagnostic tool for use in dentistry. A number of possibilities were modelled and the most promising, at this time, was monitoring tooth surface loss (TSL). TSL is a serious dental condition affecting patients worldwide. Current methods used to monitor TSL in the dental surgery are subjective and unreliable. Laboratory-based monitoring methods are time consuming and costly. Ultrasound is a non-invasive, non-destructive method that is mainly used in the medical field. Its use in dentistry started in the 1950s but is still limited to therapeutics (e.g. periodontics and endodontics) and head and neck imaging. There are several modes of ultrasound imaging. Of particular note are amplitude mode (A-mode) and brightness mode (B-mode) ultrasound. In A-mode, a single beam is sent to an object, and its reflected echo is captured. This mode does not produce an image but is rather displayed as a waveform in time and amplitude domains. B-mode ultrasound has two spatial axes and therefore is used as a cross-sectional imaging tool.

To date, there are no *in vivo* studies investigating the use of ultrasound to directly monitor TSL in the dental surgery. The aim of this thesis was to assess the feasibility and optimisation of ultrasound as a potential clinical dental tool in monitoring erosive TSL *in vivo*. This thesis investigated the coupling efficiency of various dental and other materials and their suitability as couplants. The results showed that Perspex was a suitable ultrasonic couplant for the purpose of enamel thickness measurements and the tightness of the coupling at an interface was of importance for efficient transmission of ultrasound energy into an object. However, a purpose-built apparatus was required for this as the ultrasound echoes were angle dependent. It further investigates the angle dependency of echoes arising from premolars compared to synthetic maxillary central incisors, as natural incisors were not available. The results demonstrated that the more planar incisors reflected ultrasound more readily and were less angle dependent than premolars (p-value < 0.001).

B-mode ultrasound imaging was then investigated to measure intact enamel in human teeth and validated with μ-computed tomography (μ-CT). Two systems were evaluated for this purpose; the first was an in-house ultrasound apparatus and the second was a commercial ultrasound scanner, with the data obtained validated with μ-CT. The results showed that the commercial ultrasound scanner was more accurate than the in-house scanner with Bland-Altman 95% limits of agreement of -0.48 to 0.47 mm and -1.21 to 0.87 mm respectively. However, the B-mode images produced were not of sufficient clarity and consequently the accuracy of the enamel thickness measurements was not suitable for monitoring progressive enamel loss. Therefore, the simpler A-mode ultrasound approach was investigated for enamel thickness measurements and validated with histological sections of the same teeth. A study of speed of sound (SOS) variations in enamel was also performed. It was found that A-mode ultrasound was able to measure enamel thickness *in vitro* with an accuracy of 10% compared to histology and the mean SOS in enamel was 6191 ±199 ms^{-1}.

Finally, A-mode ultrasound was assessed *in vivo* (n = 30) to determine if it could monitor enamel thickness reliably and reproducibly on the labial surface of maxillary central incisors. The results showed that ultrasound was a highly reproducible and reliable technique for monitoring enamel thickness with 95% limits of agreement of -0.04 to 0.05 mm. The results demonstrated for the first time *in vivo* that A-mode ultrasound had sufficient precision (0.05 mm) to allow it to be used as a direct method for serial assessment of erosive TSL. The preferable site for making ultrasonic measurements was the cervical site (site 1) followed by the mid-buccal site (site 2). Therefore ultrasound is a promising and simple method to monitor early erosive changes in thickness of the enamel layer, especially in vulnerable patients with frequent acidic intake or in patients with gastro-oesophageal reflux disease (GORD).

Table of Contents

List of Tables

List of Figures

List of Abbreviations

%	Percentage
<	Less Than
>	More Than
μ-CT	Micro computed tomography
μm	Micrometre
μs	Microsecond
2D	Two dimensional
3D	Three dimensional
ADA	American Dental Association
ADHS	Adult dental health survey
ADJ	Amelo-dentinal junction
AFM	Atomic force microscopy
A-mode	Amplitude mode
ANSI	American National Standard Institute
ASCII	American Standard Code for Information Interchange
BEWE	Basic erosive wear examination
B-mode	Brightness mode
BMUS	British Medical Ultrasound Society
BSODR	British Society for Oral and Dental Research
CA	California
CAD	Computer aided design
CAM	Computer aided manufacturing
CEJ	Cemento-enamel junction
CI	Confidence interval
CLSM	Confocal laser scanning microscopy
CT	Computed tomography
d	Distance
DenTCRU	Dental Translational and Clinical Research Unit
Df	Degrees of freedom
DICOM	Digital imaging and communications in medicine
DREC	Dental Research Ethics Committee
e.g.	For example
FOTI	Fibre optic trans-illumination
FrFT	Fractional Fourier transform
FWHM	Full width at half maximum
g	Gram(s)

GCP	Good clinical practice
GDP	General dental practitioner
GORD	Gastro-oesophageal reflux disease
HBSS	Hanks balanced saline solution
i.e.	That is
ICC	Intra-class correlation
Inc.	Incorporated
IPEM	Institute of Physics and Engineering in Medicine
ISO	International Standards Organisation
kHz	Kilohertz
LFM	Linear frequency modulated
LIGHT	Leeds Institute of Genetics Health and Therapeutics
Ltd.	Limited company
LTHT	Leeds Teaching Hospital Trust
MA	Massachusetts
MHz	Megahertz
mm	Millimetre
MO	Missouri
MRayls	MegaRayls
MS/s	Megasample per second
mV	Millivolt(s)
mW	Milliwatt(s)
N	Newton(s)
n	Sample size
NJ	New Jersey
No.	Number
NY	New York
º	Degrees of arc
ºC	Degrees Celsius
OCT	Optical coherence tomography
PC	Personal computer
pH	Acidity
PTFE	Polytetrafluorethylene
PZT	Lead zirconite titanate
QLF	Quantitative light-induced fluorescence
R	Intensity reflection coefficient
r	Amplitude reflection coefficient
r'	Reflector

R & D	Research and Development
RCM	Reflectance confocal microscopy
S	Second(s)
SD	Standard deviation
SE	Standard error
SEM	Scanning electron microscopy
S_F	Normalised focal length
Sig	Significance value
SMADDA	Surface Matching and Difference Detection Algorithm
SOS	Speed of Sound
t	Time
T	t-value
TIFF	Tagged image file format
TOF	Time of Flight
TSL	Tooth surface loss
UK	United Kingdom
USA	United States of America
USB	Universal serial bus
v	Speed
V	Volt(s)
V_L	Longitudinal speed of sound
WHO	World Health Organisation
WI	Wisconsin
Z	Acoustic impedance
ρ	Density of material

1 Introduction

Ultrasound has been used in the medical field since the 1940s to image human organs, such as the liver, heart, muscles, tendons, spleen and kidneys. The preferred diagnostic range is 3–15 MHz. However, the use of ultrasound as a diagnostic tool in the dental arena is still limited to research studies. This Chapter explores ultrasound use in dentistry, basic principles of ultrasound, the areas in which ultrasound has been used therapeutically and diagnostically thus far and areas in which it can potentially be used as a diagnostic device.

1.1 Ultrasound in Dentistry

Ultrasound has been used in dentistry as a therapeutic method since the 1950s. It was first used as a cutting tool to prepare cavities in teeth using a powder slurry (Catuna, 1953; Postle, 1958) and was later used to remove plaque and calculus from teeth (Zinner, 1955; Johnson and Wilson, 1957). This type of ultrasound—therapeutic ultrasound—is used at relatively high intensity and low frequency in the 25–42 kHz range (Lea and Walmsley, 2009). Ultrasound has since gained more popularity in dentistry, and its use as a therapeutic modality encompasses periodontics, endodontics, operative dentistry, the cleaning of dental instruments, dental tissue repair (Walmsley, 1988; Scheven *et al.*, 2009) and toothbrush technology (Zimmer *et al.*, 2002; Costa *et al.*, 2007).

Diagnostic ultrasound has followed a similar path, and its non-ionising nature is a key advantage supporting its multifaceted use. Diagnostic applications include the assessment of the temporomandibular joint (Stefanoff *et al.*, 1992; Gateno *et al.*, 1993; Assaf *et al.*, 2013), pulpal blood flow measurements (Yoon *et al.*, 2010; Yoon

et al., 2012), detection of periapical radiolucencies (Cotti *et al.*, 2002; Gundappa *et al.*, 2006; Raghav *et al.*, 2010), periodontal diagnosis (Spranger, 1971; Fukukita *et al.*, 1985; Tsiolis *et al.*, 2003; Chifor *et al.*, 2010; Mahmoud *et al.*, 2010) caries detection (Peck and Briggs, 1987; Ng *et al.*, 1988; Bab *et al.*, 1997; Yanikoğlu *et al.*, 2000; Zheng *et al.*, 2002; Pretty, 2006; Harput *et al.*, 2011), crack detection (Culjat *et al.*, 2005a; Singh *et al.*, 2007), cement bond failure (Wichard *et al.*, 1996; Denisova *et al.*, 2009) and enamel thickness (Lees *et al.*, 1970; Louwerse *et al.*, 2004; Bozkurt *et al.*, 2005; Hua *et al.*, 2009; Hughes *et al.*, 2009; Lewis *et al.*, 2010; Slak *et al.*, 2011).

Numerous studies have been conducted on diagnostic ultrasound and have demonstrated its potential to detect dental pathology and structural defects in teeth (Baum *et al.*, 1963; Kossoff and Sharpe, 1966; Lees, 1968; Barber *et al.*, 1969; Lees *et al.*, 1970; Lees, 1971; Lees and Barber, 1971; Lees and Rollins Jr, 1972; Lees *et al.*, 1973). Nevertheless, ultrasound is still not used as a routine diagnostic modality in dental surgeries. It is therefore reasonable to examine why this is the case and to identify areas where some progress might be made. To do this, it is useful to consider the principles of ultrasound in detail.

1.2 Ultrasound Principles

Sound waves are longitudinal pressure waves that travel in solids, gases and liquids (Hall and Girkin, 2004). Sound is generated when a vibrating object, such as a string, forces air molecules to vibrate. Ultrasound is a sound pressure wave at frequencies above the level of human acoustic hearing (> 20 kHz) (Zagzebski, 1996).

The simplest technique in ultrasound testing is the pulse-echo technique, whereby an ultrasonic pulse is generated in a particular direction, and if there is an object in the path of this pulse, part or all of the pulse will be reflected as an echo that is captured by a transducer. When the energy is reflected from a surface in the pulse-echo technique, the same transducer converts the mechanical energy back to electrical energy, which is then displayed on an oscilloscope screen. A transducer can act as both a transmitter of signals and a receiver of echoes (see Figure 1.1 below).

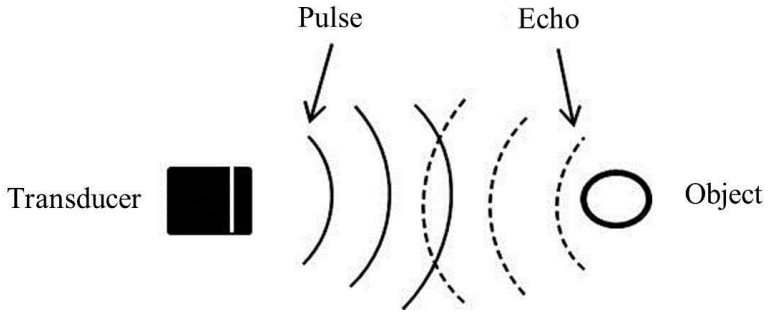

Figure 1.1. Pulse-echo technique with one object and its echo.

By measuring the time of flight (TOF) between the transmitted pulse and the received echo, it is possible to know the thickness (*d*) of the object, such that

$$d = \frac{vt}{2}$$

Equation 1.1

where

d = distance (thickness),

v = speed of sound (SOS) in medium and

t = time.

Reflections at a boundary between two materials are governed by the acoustic impedance, *Z*, of the materials. For any material, its *Z* value can be expressed as

$$Z = \rho v$$

Equation 1.2

where

ρ = density of material and

v = SOS in material.

The fraction of the energy reflected at a boundary is determined by the difference in acoustic impedance across the boundary. We can define an intensity reflection coefficient, *R*, between two materials with *Z* values, Z_1 and Z_2, using the following equation:

$$R = \left(\frac{Z_2 - Z_1}{Z_2 + Z_1}\right)^2$$

Equation 1.3

It is also possible to describe the relationship between the amplitude of the incident wave and that of the reflected wave using an amplitude reflection coefficient, *r*. In this case, we have,

$$r = \left(\frac{Z_1 - Z_2}{Z_1 + Z_2}\right)$$

Equation 1.4

This is because of the square relationship between amplitude and intensity.

It should be noted that this expression applies to theoretical interfaces which are flat and smooth on the scale of the wavelength, and the wave is normally incident. Real interfaces will deviate from this.

It follows that the delivery of ultrasonic waves from a source to another medium will be inefficient if the difference in Z value between the two is large. This is a significant problem in medicine and dentistry because the sources normally used (piezoelectric transducers) have a high Z value. To minimise energy loss, couplants that have acoustic impedance values intermediate between the source and target material are used.

A couplant is simply a medium through which ultrasound waves pass as they penetrate the target under investigation. It can be shown that the maximum energy transfer between two media with acoustic impedances Z_1 and Z_2 is achieved using a coupling material with acoustic impedance Z_3, such that:

$$Z_3 = \sqrt{Z_1 Z_2}$$

Equation 1.5

where

Z_1 = impedance of the transducer assembly,
Z_2 = impedance of the target material and
Z_3 = impedance of the couplant.

Ultrasound is generated by a transducer, which is a device that converts one form of energy (electrical) into another (mechanical) and *vice versa*. The most common type is the piezoelectric transducer, which has a layer of piezoelectric lead zirconate

titanate (PZT) crystals that vibrates when excited by an electrical pulse (Lempriere, 2002).

Transducers come in a variety of shapes, sizes and frequencies, and should be selected based on their suitability for a particular task. The thickness of the test target is also important and this will normally dictate which type of transducer to use. In general, higher frequencies lead to higher signal loss (attenuation) in the material, although the actual depth penetrated at any frequency depends strongly on the nature of the material.

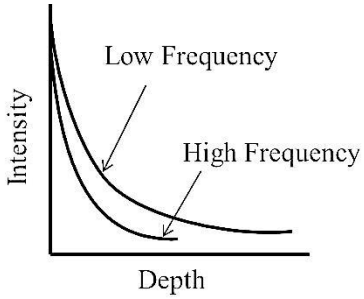

Figure 1.2. Penetration depth is inversely proportional to frequency

As the frequency increases, the absorption rate increases, which limits penetration depth (Figure 1.2 above). If two strongly reflecting interfaces are positioned close to each other and are parallel, then multiple reflections will occur. This is known as reverberation, which gives rise to a series of reflections equidistant from each other with decaying amplitude. When an ultrasound wave is transmitted through an object, it loses some of its energy as it passes through. This loss is mainly due to absorption, scatter and refraction. Absorption occurs when the ultrasound waves are dissipated in the target as heat and do not return to their source (i.e. the transducer). Absorption leads to an exponential decrease in intensity and amplitude as a function of distance. The term “attenuation” is used to express the sum of all the energy loss mechanisms.

Thus attenuation = absorption + reflection + scatter + refraction (the latter two are discussed below).

Equation 1.3 describes reflection under the ideal circumstance of the beam striking a large flat boundary at a right angle (normal incidence). If the beam strikes the boundary at an angle differing from 90°, then the reflected wave will not follow the path of the incident one (Figure 1.3 below). The situation is the same as when light strikes a mirror where the reflected angle will be equal to the incident angle. If the same transducer is used for both the creation of the beam and its detection, then non-normal incidence will result in the echo not being detected. Consequently, ultrasound imaging has a strong angle dependency. This becomes more evident if the surface is rounded rather than planar.

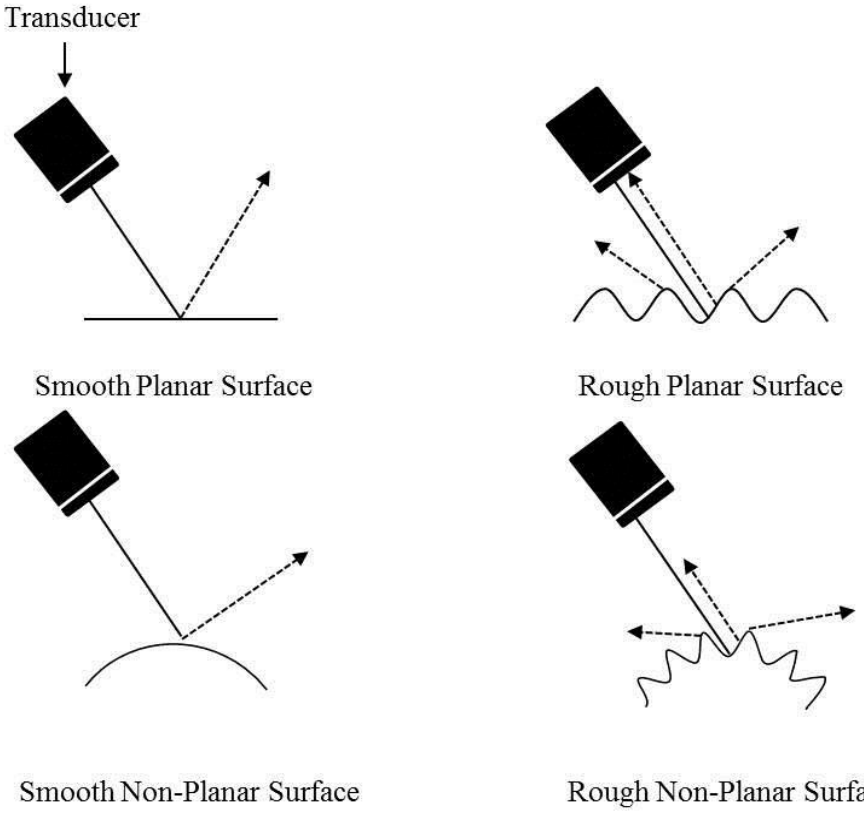

Figure 1.3. Schematic depicting the effects of topography on ultrasound echo reflection angle.

On the other hand, if the boundary is not smooth, then scattering will occur. This leads to redirection of the echo signal over a wide range of angles. Therefore, if the ultrasound wave meets a rough surface at a right angle, then a lower signal will return to the transducer and some of the energy will be scattered and lost. This is sometimes advantageous as a signal arising from a rough surface becomes less angle-dependent. Figure 1.3 shows that when an ultrasound beam does not hit a smooth planar surface at a right angle, no echo is received compared to the planar rough surface. This is because there are greater chances of a beam hitting the rough planar surface at a right angle compared to the smooth surface. In the same figure, the second set of schematics depicts ultrasound reflections and their angles when they meet a non-planar smooth surface and a planar rough surface. It can be seen that the non-planar roughened surface still produces an echo that is stronger than its non-planar smooth counterpart.

The fraction of the beam energy which is not reflected or scattered is transmitted into the material beyond the boundary. If the SOS in this material differs from that in the original material, then refraction (beam bending) will occur. This is described by Snell's Law,

$$\frac{Sin\theta_1}{V_{L1}} = \frac{Sin\theta_2}{V_{L2}}$$

Equation 1.6

where

$Sin\ \theta_1$ = incident angle,

$Sin\ \theta_2$ = refraction angle,

V_{L1} = longitudinal SOS in the first material and

V_{L2} = longitudinal SOS in the second material.

We will see later that in hard dental tissues, refraction can have a significant effect because SOS in enamel, dentine and pulp exhibit wide differences.

There are several types of ultrasound imaging mode. Of particular note are amplitude mode (A-mode) and brightness mode (B-mode) ultrasound. In A-mode, a single beam is sent to an object, and its reflected echo is captured. This mode does not produce an image but is rather displayed as a waveform in time and amplitude domains (Figure 1.4 below). On the other hand, B-mode ultrasound has two spatial axes and therefore is a cross-sectional imaging tool. The amplitude information is displayed in the grey level of the echoes on the oscilloscope screen. Each pixel corresponds to the intensity of ultrasound signals received from that location (Figure 1.5).

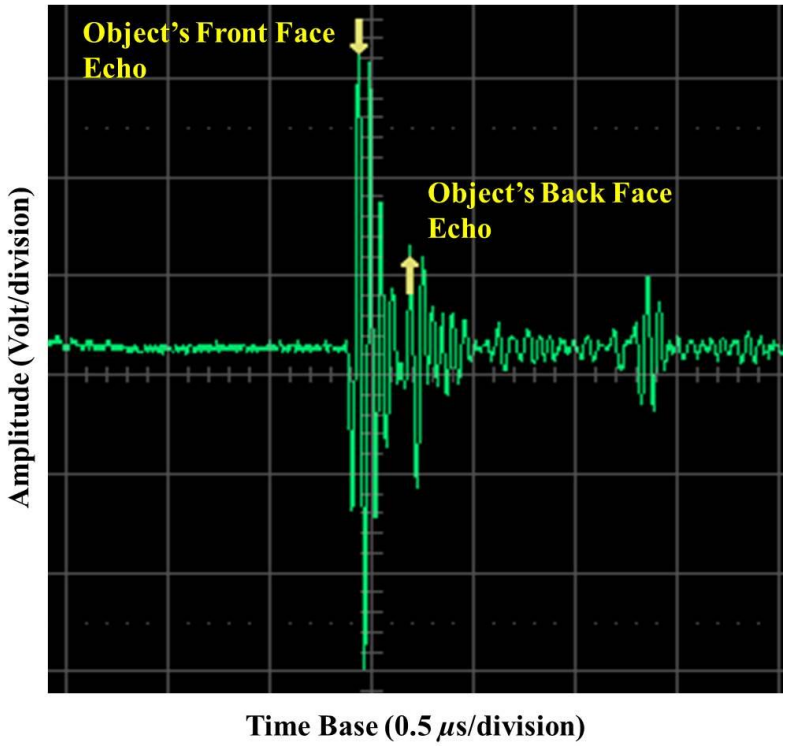

Figure 1.4. A-mode ultrasound waveform and echoes reflected from an object, as seen on a digital oscilloscope display. The TOF is calculated by measuring the time between the yellow arrows on the waveform and is used to derive the object's thickness.

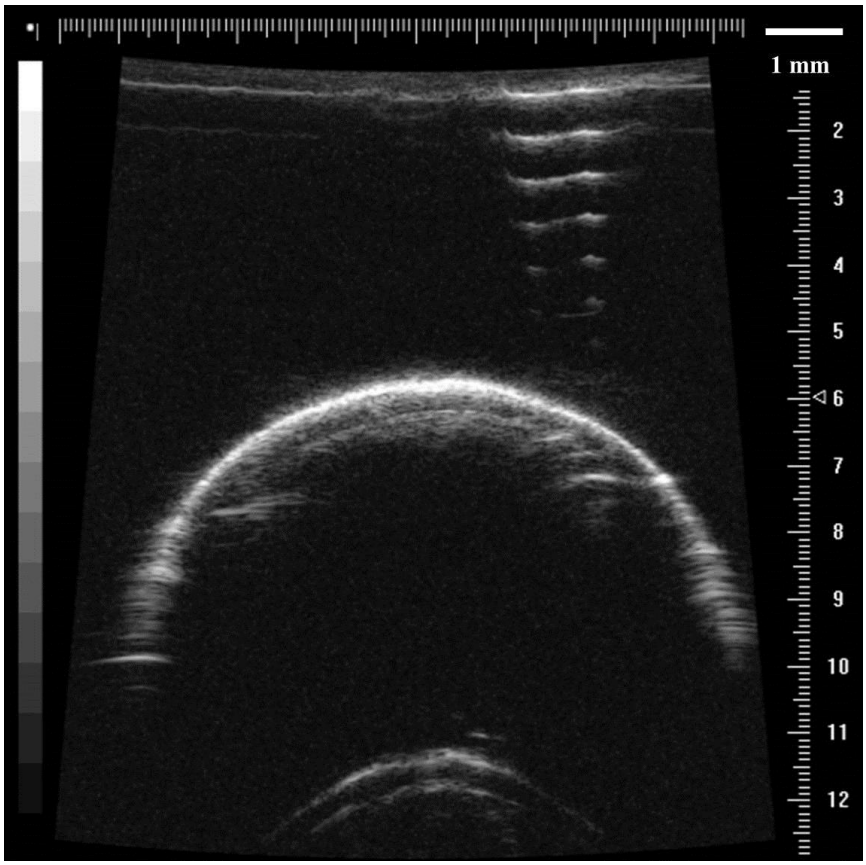

Figure 1.5. B-mode ultrasound image of the enamel layer in a human premolar tooth.

The ultrasound beam in Figure 1.5 was perpendicular to the crown of the tooth on the distal surface generating a ‘slice’ in the coronal direction. To reduce noise in an ultrasound waveform, time averaging is sometimes applied. This technique sends multiple waves into the target and takes an ‘average’ of all waves received by assuming that the noise differs from waveform to waveform, while the signal from the transducer does not (Lempriere, 2002).

One of the key parameters of an ultrasound imaging system is resolution, which is how clearly an ultrasound beam can distinguish two adjacent points separated by a specified distance. If the points are resolved with ease, then this is a high-resolution ultrasound system, and if the points are superimposed, then this is a low-resolution ultrasound system. The term axial resolution is used when two targets lie along the

axis of a single beam (Figure 1.6 below). Axial resolution is related to pulse length with shorter pulses associated with better axial resolution.

Lateral resolution refers to how good an ultrasonic system is in differentiating between two points lying at the same distance from the transducer but along the axis of different beams (Figure 1.6). For lateral resolution, we need more than one beam; the narrower the beam, the better the resolution. However, beam width is not constant with depth and hence, lateral resolution will vary with depth. Lateral resolution can be improved by the use of lenses that will reduce the beam width at one depth, albeit at the expense of degrading it at another.

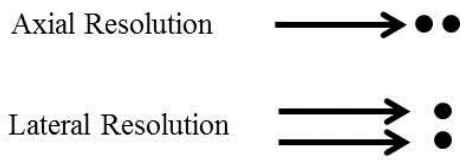

Figure 1.6. Ultrasound beam (arrow) encountering two points. The first depicts axial resolution and the second depicts lateral resolution.

An unfocussed transducer will generate a relatively wide ultrasound beam, which may be suitable for many non-destructive testing purposes. On the other hand, a focussed transducer produces a beam that narrows down to a small spot that effectively increases the sensitivity of the beam to any structural defects at the depth of the focus.

For axial resolution, the pulse length is typically 2–3 cycles (i.e. 2–3 wavelengths). It follows that this will improve with increasing frequency. The beam width for both focussed and unfocussed beams is also dependent on the wavelength, and hence, it too improves with increasing frequency. Hence, higher frequencies give better resolution but more absorption and therefore more noise.

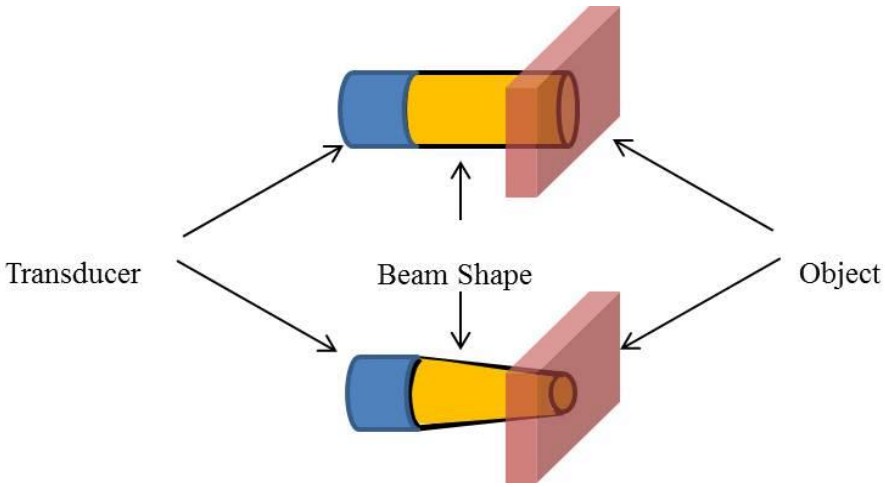

Figure 1.7. Schematic depicting two beam shapes.

The circular beam shape in Figure 1.7 belongs to an unfocussed transducer, and the cone beam shape belongs to a focussed transducer. The relative spot size can be seen on the object where the unfocussed transducer generates a larger spot size compared to the focussed one.

1.3 Diagnostic Applications of Ultrasound in Dentistry

Although there is an extensive literature on the diagnostic applications of ultrasound in dentistry, it can be usefully discussed under two broad headings; applications in which boundaries and/or layers are characterised and applications which are primarily aimed at measuring dimensions. They are therefore reviewed below under these headings.

1.3.1 Detection of Layers and Boundaries with Ultrasound

The first reported use of diagnostic ultrasound in dentistry was by Baum *et al.* (1963), who imaged human teeth with an ultrasonic probe originally manufactured for use in ophthalmology. Although the B-mode images obtained with the ultrasonic device were not very clear, a cross-sectional image of the maxillary anterior teeth

was generated. In the image, there appears to be a bridge cantilevered from the upper left canine, as shown in Figure 1.8 below.

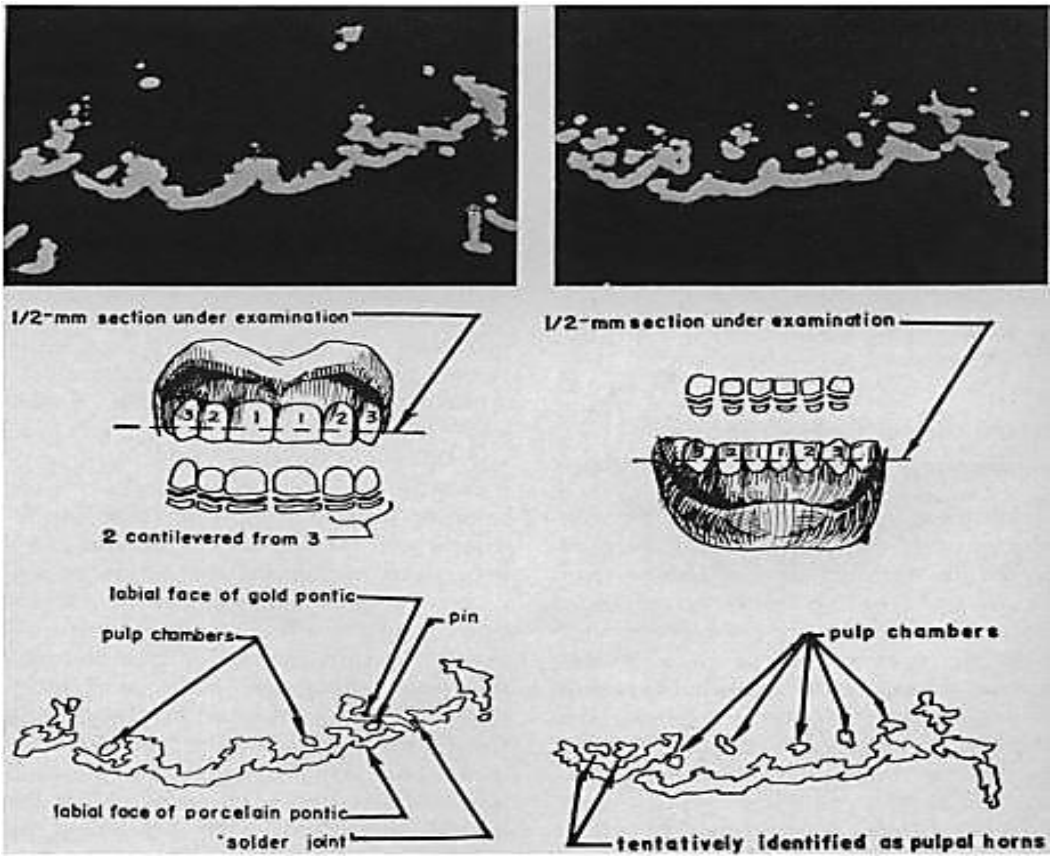

Figure 1.8. A B-mode image (top) portraying a cross section of teeth from the maxillary right canine to the maxillary left canine (Baum *et al.*, 1963, p.495). The bottom illustrations depict the location of the structures in the images. [Reproduced with permission from *Science*].

The images in the work of Baum *et al.* were obtained with a 15 MHz ultrasound probe traditionally used in ophthalmology, which may be why the B-mode images were distorted.

X-rays are the gold standard in dental imaging, but they possess inherent limitations, such as the production of a film emulsion that is a 2D image of 3D anatomical structures. In addition, X-rays are a source of ionising radiation and must be used with care. The radiographic signs of a tooth with degenerating pulp include widening

of periodontal ligament space, thickened lamina dura, root resorption and/or periapical radiolucency. However, pulp tissue is invisible on X-rays, and so the state of the pulp—whether it is undergoing reversible pulpitis, irreversible pulpitis or if it is necrotic—cannot be ascertained. The following section discusses the use of ultrasound as an adjunct to X-rays in pulpal disease characterisation.

1.3.1.1 Ultrasound and Pulp Degeneration

Kossoff and Sharpe (1966) suggested the use of ultrasound to diagnose pulpal disease *in vitro*. This study relied on the principle of acoustic impedance mismatch (see section 1.2), where it proved beneficial in differentiating between vital and necrotic pulp. As mentioned in section 1.2, the intensity of the reflected ultrasound signal is dependent on the *Z* values of the materials at either side of the interface.

In the case of vital pulp, the ultrasound waves will pass through dentine that has an acoustic impedance value of ~8 MRayls and then through vital pulp that has an acoustic impedance similar to that of water, ~1.5 MRayls. The acoustic impedance mismatch between dentine and water resulted in an echo that was detected by Kossoff and Sharpe's ultrasound system. In the case of necrotic pulp, ultrasound will penetrate through dentine and then air that is present in the pulpal cavity. The acoustic impedance mismatch here will be higher, as air has significantly lower acoustic impedance than water; therefore, a higher ultrasonic reflection will occur at this interface. Following these observations, the focus then shifted to caries detection with ultrasound, which is discussed in the next section.

1.3.1.2 Ultrasound and Caries Detection

Dental caries is defined as the loss of tooth minerals due to a shift from the process of remineralisation to demineralisation. Caries is detected by visual examination,

fibre-optic trans-illumination (FOTI), dyes, laser fluorescence, quantitative light-induced fluorescence (QLF), optical coherence tomography (OCT) and also can be done using an electrical caries monitor (Pretty, 2006). However, early caries is often difficult to diagnose, which delays preventative measures that aid in halting the progression of caries from enamel into dentine.

Lees and Barber (1968) started examining teeth and their internal layers using ultrasound and successfully detected demineralisation *in vitro*. These studies resulted in several papers highlighting the role that ultrasound could play in the diagnostic dental arena (Lees *et al.*, 1970; Lees, 1971; Lees *et al.*, 1973). They suggested that if ultrasound was very sensitive to *Z* value changes across interfaces and boundaries, it might be useful in detecting demineralisation in teeth. Because a demineralised layer in a tooth will have lower density and consequently a different *Z* value from the original layer, it will result in a stronger ultrasound reflection from the demineralised outer layer.

Utilising the same principle of acoustic impedance mismatch, other researchers looked at the possible use of ultrasound in crack detection and periodontal tissue assessment (Culjat *et al.*, 2005a), which is discussed in the following section.

1.3.1.3 Ultrasound and Crack Detection

Cracks in teeth are often invisible on X-rays unless the beam meets the crack at 90°. The traditional way of diagnosing cracks in teeth is by dental history, unaided visual examination, FOTI, tooth sleuth and dyes, all of which can only be used in certain cases. For this reason, Culjat *et al.* (2005a) used ultrasound to detect a 25 μm thick crack in the crown of a tooth phantom. They were able to receive a reflection from that crack, indicating that ultrasound can be useful in such conditions. However,

further research is required on natural teeth to see if the same results are achievable *in vivo*.

1.3.1.4 Ultrasound and Periodontal Probing

One of the signs of a healthy periodontium is the absence of periodontal pockets, which are assessed by periodontal probing (Chapple, 1997). Periodontal probing is performed using a Williams probe or a World Health Organisation (WHO) 621 probe, which are inserted inside the pocket to measure the pocket depth. Clinical attachment levels can also be measured using the Williams probe. However, these probes sometimes cause pain and resolution is limited to ±1 mm.

A study by Freed *et al.* (1983) showed that the mean probing force across dental professionals was 0.44 N (equivalent to a weight of 44 g), which is higher than the norm of 0.25–0.30 N (25–30 g). This led Lynch and Hinders (2002) to develop and test an ultrasound system for the purpose of measuring pocket depth. They utilised a 10 MHz ultrasound transducer with a specially designed 0.5 mm tip that slips in the gingival margin, thereby sending and receiving ultrasound signals from anatomic features in that area. However, they had to perform signal analysis (a lengthy process) on the received signal before deducing information from it, which resulted in more accurate pocket depth measurements.

1.3.1.5 Ultrasound and Alveolar Bone Assessment

The assessment of alveolar bone levels is crucial in patients suffering periodontal disease. This is normally assessed using X-rays that have the limitation of not being able to detect alveolar bone loss until 30–50% of the bone minerals are lost. In the 1980s, Fukukita *et al.* (1985) used a 20 MHz ultrasound scanner to image the periodontium of the maxillary anterior teeth with the hope of detecting alveolar bone

loss. They measured the alveolar bone levels with ultrasound first and then compared that with the true value by raising a flap surgically and obtaining measurements. There was good agreement between both techniques.

1.3.1.6 Ultrasound and Bond Failure

Other researchers investigated the use of ultrasound to detect cement failure and the de-bonding of restorations. Wichard *et al.* (1996) investigated the cement bond between crowns and the tooth structure with a 30 MHz ultrasound transducer using a pulse-echo technique in a water tank. The crowns with failing cement were more 'echogenic' than the adequately cemented crowns. When a cement fails, microleakage and caries of the underlying tooth structure may follow (Wichard *et al.*, 1996), which in turn affects crown retention and functionality. Although the results were from prepared specimens, these findings demonstrated that ultrasound was able to detect interface changes (cement failure and secondary caries) that were otherwise invisible on X-rays. These findings were supported by Ghorayeb and Valle (2002), who established that ultrasound can be useful in detecting de-bonding between a restoration and a tooth.

The clinical significance of these findings is intriguing. The success and longevity of simple dental restorations primarily depends on the bond strength between the restoration and the tooth surface, which is mainly dentine (Zheng *et al.*, 2002); therefore, keeping this interface intact is of paramount importance. However, X-rays cannot determine the quality of this interface; they can only detect the consequences of the failing interface in the form of a radiolucent area at the interface (i.e. secondary caries). Ultrasound, on the other hand, differentiates between good (adequate bond) or bad (weak bond) restoration-tooth interfaces (Ghorayeb and

Valle, 2002; Singh *et al.*, 2007). Ultrasound is highly sensitive to interface changes (see Figure 1.9 below). When an ultrasound pulse is directed at an 'imperfectly bonded' interface it results in a higher echo arising from the de-bonded interface (Denisova *et al.*, 2009). If the interface is 'air tight' and adequately bonded there would be minimal (nearly indistinguishable) echoes arising from the interface because the interface becomes acoustically 'invisible'.

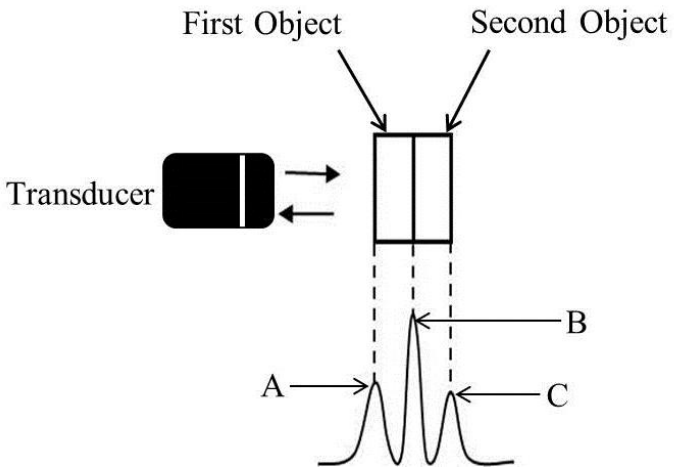

Figure 1.9. A schematic of a transducer aimed at two objects placed adjacent to each other. The dashed lines point toward the echoes generated at the first interface, A, followed by the second interface echo, B, and finally the last interface echo, C. It can be seen that echo B is higher than the other echoes because the interface between the two objects is not adequately bonded, therefore, the air trapped at this interface will generate a higher echo due to the high impedance mismatch between the objects and air.

1.3.2 Characterisation of Dimensions, Thicknesses and Sizes with Ultrasound

As described in section 1.2 (page 2), ultrasound can be used to measure the thickness of a material, and this has been exploited in dentistry specifically to measure the thickness of enamel and dentine. Tooth surface loss (TSL) is an area where much of the ultrasound work has been directed. TSL is a significant dental problem that is becoming increasingly evident in patients' dentition (White *et al.*, 2011). The fact that patients are retaining more teeth, along with increased consumption of acidic food and fizzy drinks, underscores the importance of using a method that can be used

to monitor the disease. Unfortunately, to date, there is no way of *directly* monitoring TSL accurately and reproducibly *in vivo*.

1.3.2.1 Ultrasound and Enamel Thickness

The role of ultrasound in studying enamel thickness and surface topography has yet to be fully developed, and the topic is still limited to small research studies. Possible reasons for this include the large signal losses that arise because of impedance mismatches (enamel, dentine and pulp) and the angle dependency caused by the curvaceous nature of teeth (Walmsley, 1988).

Several laboratory-based studies reported relatively good results, but the need for improvement in technique and clinical applicability remains (Barber *et al.*, 1969; Huysmans and Thijssen, 2000; Culjat *et al.*, 2003; Louwerse *et al.*, 2004; Toda *et al.*, 2005; Ghorayeb *et al.*, 2008; Harput *et al.*, 2009; Lewis *et al.*, 2010; Harput *et al.*, 2011; Slak *et al.*, 2011). However, much of the work involving diagnostic ultrasound has been performed *in vitro* and there are no studies that investigated ultrasound *in vivo* to measure and monitor erosive TSL. It is important to mention that what is being measured with ultrasound *in vivo* is the relative loss in enamel thickness and not the early demineralised layer.

To assess whether ultrasound can measure enamel thickness (d in Equation 1.1), the SOS in enamel (v) must first be determined. A summary of reported values reported in the literature is shown in Table 1.1.

Table 1.1. Speed of sound (SOS) in enamel as reported in several published studies (ms^{-1}).

Study	SOS (±SD)	Teeth
Blodgett (2002)	6250	Human incisors
Lees and Barber (1971)	6000 ±190	Human molars
Huysmans and Thijssen (2000)	6500	Human incisors
Barber (1969)	6250 ±410	Human incisors
Kossof and Sharpe (1966)	4500 ±410	Human incisors and molars
Hedrick *et al.* (1995)	5800	Incisors and molars
Bozkurt *et al.* (2005)	6132	Human premolars
Ng *et al.* (1989)	6450 ±210	Human incisors and molars
Ghorayeb and Valle (2002)	6200	Human molars
Maev *et al.* (2002)	5900	Human molars
Reich *et al.* (1967)	5700	-
Slak *et al.* (2011)	6100	Human incisors
Hamano *et al.* (2003)	6244	Human molars

It is evident from the table above that there is quite a large range in the reported SOS in enamel (4500-6500 ms^{-1}). These variations might have arisen for several reasons. For example, teeth that are extracted from the mouth and left to dry will exhibit a significant change in SOS. It has been shown that the type of storage media will affect the acoustic properties of hard tissues and that Hank's balanced saline solution (HBSS) is the best medium to preserve their elastic properties (Raum *et al.*, 2007).

Another possible source of the reported variation in SOS is the anisotropic nature of enamel (Lees and Rollins Jr, 1972; Habelitz *et al.*, 2001; Lussi *et al.*, 2004) and thus the SOS varies depending on the orientation of the ultrasound wave, where it might be 'faster' in one plane and 'slower' in another. Also, true variations in enamel structure that might be related to age, gender and ethnicity may well play a role in this variation. The type of tooth, its curvature and 'hidden' demineralisation also contribute to this variation (Peck and Briggs, 1987). Also, technical variations and

the use of different ultrasonic equipment and techniques might have contributed to the varied SOS values reported in the literature (Hamano *et al.*, 2003).

1.4 Tooth Surface Loss

Before defining TSL (or tooth wear), it seems logical to step back and define the meaning of the term 'wear'. According to the International Standards Organisation (ISO), wear is defined as *"the loss of material from a surface, caused by mechanical contact, movement of a solid or liquid body, chemical action or both chemical and mechanical action simultaneously"* (ISO No. 14569-2, 1999). There are two nomenclatures used to describe the loss of tooth structure due to non-bacterial sources; the first is non-carious TSL and the second is tooth wear. Both terms are often quoted in the literature and are used interchangeably to mean the same thing. Throughout this thesis, the term TSL will be adopted.

It is established that TSL is a condition affecting dentate people of all ages and is a gradual process that involves one or more mechanisms—erosion, attrition, abrasion and abfraction—or a combination of these (Pindborg, 1970). These mechanisms rarely operate singly, and the overlap of two or more of them aggravates TSL and increases the complexity of the problem (Carlsson *et al.*, 1985). According to the 2009 United Kingdom (UK) Adult Dental Health Survey (ADHS), more than two-thirds (77%) of the British population had some wear on their anterior teeth (White *et al.*, 2011) compared to 66% in the 1998 survey (Nuttall *et al.*, 2001). What is more concerning is the small but increasing percentage of adults with moderate wear of 11% in 1998 compared with 15% in 2009 (Hill, 2012). This trend is likely to continue as more teeth are retained by the aging population, which was demonstrated by the recent ADHS.

It is important to differentiate between physiological TSL that results from natural wear of tooth substance due to tooth-to-tooth contact estimated by Lambrechts *et al.* (1989) to be 32 μm/year for premolars, 51 μm/year for molars and pathological TSL with a range of 17.6 - 108.2 μm/6 months (Bartlett *et al.*, 1997), where higher rates of tooth tissue loss occurs (Schlueter *et al.*, 2005). Pathological TSL can be a result of parafunctional habits, such as bruxism (attritive TSL) or overzealous tooth brushing (abrasive TSL). Attrition is defined as the loss of tooth tissue due to tooth-to-tooth contact (e.g. bruxism), while abrasion is the loss of tooth tissue due to mechanical factors (e.g. pipe smoking, fingernail biting and overzealous tooth brushing). Abfraction refers to the development of a non-carious cervical V-shaped lesion resulting from tensile stresses generated by occlusal loading, leading to the micro-fracture of cervical enamel rods (Assaf *et al.*, 2013).

Another form of pathological TSL is erosion, defined as the loss of tooth tissue due to non-bacterial acidic sources. This is the most common cause of TSL and has been implicated in 89% of all cases (Smith and Knight, 1984a). Another term for erosion is tribo-chemical wear or corrosive wear (d'Incau *et al.*, 2012). These terms are used by tribologists to describe TSL caused by chemical or electrochemical action. Mair (1992) raised an important point about the terms erosion, attrition and abrasion. Mair explains that these terms are used in dentistry to describe a clinical manifestation that has been observed and not to describe the underlying process for wear; there is a difference in understanding across disciplines. It is not within the remit of this thesis to favour one term over another but just to mention the existing nomenclatures and how they are viewed in different disciplines.

Erosion occurs when there are excessive amounts and frequencies of acids, which could be extrinsic, intrinsic or a combination of both (Pindborg, 1970). Extrinsic acidic (erosive TSL) sources include beverages (Lussi *et al.*, 1991; Milosevic, 1997; Moazzez *et al.*, 2000; Johansson *et al.*, 2002; Lussi *et al.*, 2004), citrus fruits (Jarvinen *et al.*, 1991; Toumba *et al.*, 2003), medications including tranquilisers, antihistamines, and antiemetics (Hellwig and Lussi, 2006), as well as dietary supplements such as vitamin C and iron (Giunta, 1983). Furthermore, frequent swimming in chlorinated water has also been reported as an extrinsic causative factor of erosive TSL (Centerwall *et al.*, 1986). Intrinsic acidic sources of erosion are gastric acids, which gain access to the oral cavity in gastro-oesophageal reflux disease (GORD)**,** vomiting (bulimia nervosa and anorexia nervosa) and rumination.

The prevalence of erosive TSL is evidently on the rise (Lussi and Jaeggi, 2008), with an alarming increase in children and young adults over the past 30 years (Mehta *et al.*, 2012). A recent prevalence study of 3187 patients aged 18-35 years from seven European countries reported that 27% of the patients had signs of TSL (Bartlett *et al.*, 2013). A systematic review reported that TSL is a common disease with a positive relationship between the severity of TSL and age (Van't Spijker *et al.*, 2009), with prevalence figures increasing in adults from 3% at the age of 20 years to 17% at the age of 70 years. A retrospective study comparing 68 study models of TSL patients over a median time of 26 months, found that the progression of TSL is inevitable (Bartlett, 2003). In a cross-sectional study of 1007 patients, Smith and Robb (1996) found that 22% (224) of those patients had unacceptable levels of TSL on more than 10% of their tooth surface, while the remaining 78% had less than 10% of unacceptable TSL levels.

Children and adolescents are also displaying signs of TSL and its association with age is evident. A systematic review of the prevalence of TSL in children reported a range of 0-82% up to the age of 7 years (Kreulen *et al.*, 2010). Therefore, monitoring this common disease is very important. In the UK, Dugmore and Rock (2004) conducted an erosion prevalence study of a random sample of 1753 children and found that 59.7% of the children had erosion of their teeth. Other studies in children and young adults reported a similar increase in this condition (Millward *et al.*, 1994; Milosevic *et al.*, 1994; Hinds and Gregory, 1995; Jones and Nunn, 1995; Bartlett *et al.*, 1998; Williams *et al.*, 1999; Walker *et al.*, 2000; Al-Dlaigan *et al.*, 2001; Bardsley *et al.*, 2004; Chadwick and Pendry, 2004).

A study of a random sample of 12-year-old children (n = 1686) has shown that general dental practitioners (GDP) have low awareness of erosive wear, and more importantly, 67.5% of dentists (n = 227) only rarely or occasionally advised their patients about erosion (Dugmore and Rock, 2003).

It appears that the prevalence figures reported across various TSL studies are not consistent because data are obtained using different scoring criteria, study designs and examiner calibration. Some studies examined more than one tooth surface, while other studies examined only one surface and this renders comparison between studies difficult. However, the evidence suggests that erosive TSL in adults, adolescents and children is on the rise.

Prevention of erosive TSL is the first weapon in a dentist's arsenal, and utmost thoroughness must be exercised during diet analysis, which may help uncover excessive dietary acidic intake. Importantly, early detection of erosion is crucial to prevent its progression and avoid complications, such as hypersensitivity.

Erosive TSL can also lead to functional and aesthetic problems, which are often detrimental to the patient's overall oral health and wellbeing. Therefore, erosion risk factors, described by Lussi (2006) as behavioural, chemical and biological, should be identified.

Behavioural factors are those related to eating and drinking habits, tooth brushing, medications and occupation. Chemical factors refer to the types of acid consumed, the buffering capacity of saliva, pH and levels of calcium, phosphorous and fluoride ions. Finally, biological factors should be accounted for including tooth structure, salivary flow and buffering capacity, pellicle formation and soft tissue movement (see Figure 1.10 below).

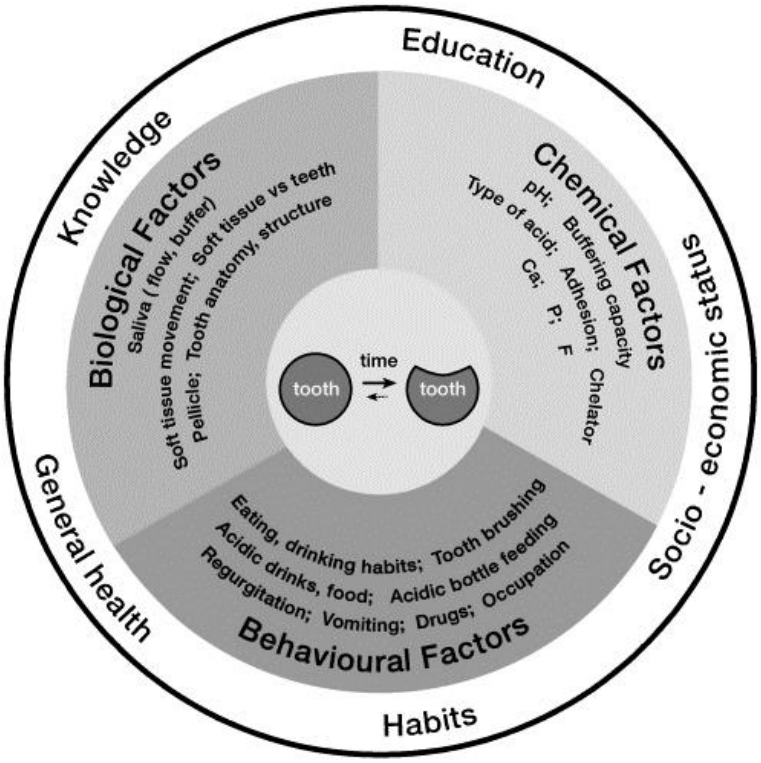

Figure 1.10. Multifactorial origins of erosive TSL (Lussi, 2006, p.6). [Reproduced with permission from *Karger*].

1.4.1 Diagnosis and Monitoring of Erosive TSL

Laboratory studies demonstrated that when acids of non-bacterial origin (0.3% citric acid buffered to pH 3.2) are in contact with enamel, they demineralise ~2-12 μm of the outer enamel layer (Eisenburger *et al.,* 2000; Eisenburger *et al.,* 2004). This softer layer is often abraded away and a new, fresh layer is created which will encounter another acid attack. When this happens multiple times an erosive crater develops (Elton *et al.*, 2009). This crater is impossible to measure clinically but can be measured in the laboratory using profilometry, as described in the study by West and co-workers (1998), or using transverse microradiography (Elton *et al.*, 2009). Therefore, the ability to quantify erosive TSL directly in a clinical setting (without laboratory work) is of importance.

1.4.2 *In Vivo* Methods for Monitoring Erosive TSL

Several erosion indices have been developed based on the Eccles (1979) erosion index and Smith and Knight's (1984b) tooth wear index. These include the Linkosalo and Markannen (1985) index, Lussi *et. al*'s (1991) index, O'Brien's (1994) index, O'Sullivan's (2000) index and Larsen *et. al*'s (2000) index. These indices aim to monitor erosion by ascribing a numerical score to affected teeth surfaces, corresponding to the severity of erosive TSL. The indices can also be used *in vitro* on study models as well as *in vivo*.

Interestingly, Wetselaar *et al.* (2009) assessed the reliability of a newly developed TSL scoring index to detect TSL both *in vivo* and on study models *in vitro*. They found that using this scoring system *in vivo* resulted in more reliable TSL scores, especially for buccal and palatal surfaces, compared to the *in vitro* study model counterpart. On the other hand, they reported occlusal and incisal TSL assessment of

study models had a reliability of ‘fair to good’ and ‘excellent’. The authors of this study mentioned the advantages of this scoring index over traditional indices in that it measures TSL in easy-to-use small steps and allows for measuring more extensive TSL levels.

Because there is *“no agreed consensus on a universally accepted tooth wear index”* (Bartlett and Dugmore, 2008), an attempt was made to use a standardised and reproducible index that is easily used by GDPs (Young *et al.*, 2008). Thus, the basic erosive wear examination (BEWE) index was proposed (Bartlett *et al.*, 2008). However, as with other indices, it is not able to detect small changes of 17.6 - 108.2 μm/6 months caused by the erosion (Bartlett *et al.*, 1997). These conventional indices are only beneficial for epidemiological studies because they measure erosion in a crude way that is rarely reproducible or reliable, rendering them subjective, inaccurate and variable across dentists (Hall *et al.*, 1997; Azzopardi *et al.*, 2000). Therefore, dentists monitoring erosive TSL using such indices should bear in mind the problem of intra-examiner reproducibility and remember the precise diagnostic criteria for the index used (O'Sullivan and Milosevic, 2008).

There are currently six non-destructive methods in research and development for use *in vivo* to ***directly*** monitor erosive TSL. These methods are QLF (Pretty *et al.*, 2004), OCT (Wilder-Smith *et al.*, 2009), spectroradiometry (Krikken *et al.*, 2008) (measuring light reflectance from enamel), reflectance confocal microscopy (RCM) (Contaldo *et al.*, 2013), computer automated design-computer automated machinery (CAD-CAM) and ultrasound (Fukukita *et al.*, 1985; Huysmans and Thijssen, 2000; Louwerse *et al.*, 2004; Bozkurt *et al.*, 2005; Tagtekin *et al.*, 2005; Toda *et al.*, 2005;

Harput *et al.*, 2009; Hua *et al.*, 2009; Hughes *et al.*, 2009; Dwyer-Joyce *et al.*, 2010; Harput *et al.*, 2011)

Some of these methods were able to detect the demineralised superficial enamel layer, such as QLF (Field *et al.*, 2010), while other methods were able to measure the crater depth (e.g. ultrasound) relative to a stable reference *in vitro*. These non-destructive methods may offer a solution for measuring and monitoring the enamel layer chair-side.

Quantitative light-induced fluorescence is an optical method to detect early caries that measures the difference in fluorescence between sound and unsound teeth via a hand-held probe (de Josselin de Jong *et al.*, 1995). Quantitative light-induced fluorescence has been investigated *in vitro* to detect and quantify artificially-induced erosive lesions with good results (Pretty *et al.*, 2004). A drawback with this method is that it requires an intact reference area to compare it to the relative loss in fluorescence from the eroded surface (Huysmans *et al.*, 2011), which rarely occurs in erosive TSL. In addition, it shows a 'trend' of fluorescence from teeth and does not yield an enamel layer thickness (Field *et al.*, 2010). Thus, further research is required to assess its feasibility in a clinical environment and to validate its use *in vivo* to know if it is able to quantify and monitor erosive TSL reliably.

Another interesting *in vivo* study on GORD patients was completed by Wilder-Smith and co-workers (2009) in which they were able to measure a decrease in enamel thickness of 15 ±0.17 μm using an OCT scanner. The OCT device was able to detect enamel erosion in GORD patients taking omeprazole or a placebo (Wilder-Smith *et al.*, 2009), but the device required a positioning stent made from a silicone

impression material that had 3 mm holes drilled into it (where the OCT probe was placed) for optimal positioning.

Before the enamel thickness scans were performed on each patient, the stent was placed inside the patient's mouth to accurately position the OCT probe on the scan site. Again, this is time consuming and will need to be remade if a patient receives a new restoration (cast or direct), as this alters the seating of the stent. On the other hand, spectroradiometry measures the relative 'yellowish' colour of enamel that emanates from underlying dentine (Krikken *et al.*, 2008). This requires the superficial enamel layer to wear away to some extent until a 'difference' in colour reflectance can be detected. In addition, the spectroradiometer was bulky and cumbersome to manoeuvre around teeth.

Contaldo and co-workers (2013) investigated a hand-held RCM device, originally used in dermatology, to image the surface and subsurface topography of enamel *in vivo*. However, the device could not image more than 300 μm into enamel and was bulky, which did not allow for imaging teeth other than central incisors. Further research and development is required to render RCM a clinically viable approach to monitor erosive TSL.

The CAD-CAM approach has developed at a fast pace bringing with it refinements in technology where *in vivo* 3D images of teeth are now replacing conventional study models. In fact, DeLong (2006) argues that the best method for accurately measuring wear of any material *in vitro* and *in vivo* is sequential 3D imaging. The 3D images (e.g. the baseline image and the image after 6 months) are then superimposed on each other and the 'difference' is calculated by a process known as image registration (DeLong, 2006). Al-Omiri *et al.* (2010) compared the accuracy of a new CAD-CAM

laser scanning machine against a toolmaker's microscope and Smith and Knight's index in detecting TSL over a six-month period. They found that Smith and Knight's index was the least sensitive in quantifying TSL and was not able to monitor progression in most cases. However, CAD-CAM scanners are too cumbersome for routine use in a dental setting and are costly (Al-Omiri *et al.*, 2010). These scanners also require further development to render them fully capable of monitoring erosive TSL (Huysmans *et al.*, 2011).

1.4.3 *In Vitro* Methods for Monitoring Erosive TSL

Current methods for monitoring erosive TSL include silicone putty indices (Shaw *et al.*, 1999) and taking clinical photographs of the teeth. However, when clinical photographs are used, care must be exercised before drawing conclusions as these have a level of unreliability in assessing and monitoring erosion (Grenby, 1996). Sequential study models are also used in monitoring erosive TSL (Wickens, 1999). Chadwick (1998) performed a survey on consultants in restorative dentistry in the UK and found that one-third of the consultants believed that the use of sequential study models is a crude method of measuring TSL. Sequential study models were only able to detect gross changes in surface topography and by inference were not sensitive enough to detect finer changes. Overall, 94% of the consultants thought that a sensitive and quantitative technique that is able to determine small changes in TSL would be of great help in the assessment of this condition. Therefore, it might be suggested that GDPs, having less clinical expertise in diagnosing TSL, would have more difficulties assessing and monitoring it with sequential study models, compared to consultants in restorative dentistry. These *in vitro* methods are in fairly common use.

In an attempt to address the shortcomings of conventional erosion detection and monitoring methods, Mitchell *et al.* (2003) assessed an electromechanical device (surface profilometer) in the UK that scans study model replicas of the upper arch for a cohort of 10–11-year-old children (n = 100). The technique involves taking study models at baseline, 9 and 18 months (including eroded palatal areas of maxillary central incisors) for each arch and replicating them. The replica is then sprayed with an electro-conductive paint, which renders the topographical terrain of the replica recognisable by the electromechanical device whilst scanning. Each individual replica is scanned and the topographical map of the eroded surfaces is generated and saved.

However, because there are no fixed intra-oral reference points (consequently, there are no fixed points on the study models and replicas either) from which to take measurements, the device assumes reference points through mathematical surface matching and a difference detection algorithm (SMADDA). This algorithm has dual functions: first, it allows the device to estimate the best fit of surfaces of the replicas; second, it estimates the change that occurs between each replica. The authors reported initial results at 9 months for 53 children (106 electroconductive replicas) and the machine was able to measure erosion levels of 50 ±15 μm in one-quarter of the teeth over the 9 month period. However, only one assessor analysed the erosion measurements. Full automation of the system was not possible due to some abnormalities which occurred (air bubbles in impressions and replicas). Therefore, human examination of graphs from the surface matching programme was unavoidable.

The surface profilometer approach, though successful, has several drawbacks. First, it is only able to measure erosion on replicas of study models; this necessitates taking impressions in the clinic and sending them to the dental lab for casting, which is time consuming. Second, it uses a mathematical algorithm that 'estimates' the location of the baseline erosion levels, which introduces uncertainties to the measurements. Third, it is performed *in vitro* and so it does not yield real-time measurement of erosion levels and therefore does not overcome the shortcomings of conventional methods. Fourth, cast replicas can have dimensional changes which occur during and after setting or when in storage (McCabe and Walls, 2009), in addition to shrinkage or expansion of impression materials, which introduces errors in the measurements. Nevertheless, a miniaturised chair-side electromechanical device that can scan teeth *in vivo* would be beneficial, but this is something that may take industry some time to develop.

In vitro methods used for quantifying erosive TSL include the following: 3D scanners, such as micro/cone-CT and laser (DeLong, 2006); stereo microscopes, image analysis, scanning-electron microscopy (Azzopardi *et al.*, 2000); confocal laser scanning microscopy (CLSM), iodide permeability testing, surface hardness, microradiography, nanoindentation, atomic force microscopy (AFM), chemical analysis of dissolved minerals and element analysis of solid samples (Attin, 2006). These methods require substantial amounts of time, are technique sensitive and cannot be used at the clinical level in their current state of development, which is a major drawback.

GDPs are the backbone of the general dental care service and their ability to diagnose and monitor erosive TSL at its earliest stage is very important. Therefore, a

quick, accurate and reliable method is needed to diagnose and monitor TSL (Bartlett *et al.*, 1997; Azzopardi *et al.*, 2000). This method preferentially would be in the form of an adjunctive chair-side dental tool able to accurately and reproducibly monitor progressive TSL (Johansson *et al.*, 1993).

1.5 Erosive TSL Measurement with Ultrasound

Angle dependency is one of the most often cited, yet less explored limitations of ultrasound in the measurement of TSL. If the standard pulse-echo technique is used, then an echo will only be detected from a surface or boundary when its path is similar to that of the original beam. In other words, a significant deviation from 90º incidence will lead to the echo being re-directed and not detected. Precisely how rapidly the echo strength decays as the angle changes depends on the topography and roughness of the surface and hence the relative amount of scattering involved (Wichard *et al.*, 1996). The non-planar nature of human teeth limits the manoeuvrability of the ultrasound beam and consequently, measuring the thickness of enamel becomes more difficult. This has been mentioned in several research papers (see section 1.3) and is often described as an inherent limitation dictated by the shape of human teeth.

Incisors are obviously more planar than the remainder of the teeth in the arch and therefore might be considered as attractive targets for ultrasound investigation. They are prone to acid attack, from acidic fizzy drinks for example (unless a straw was used, passing the anterior teeth) and therefore can act as a reference for monitoring the acidic intake for patients. Furthermore, incisors are most vulnerable in bulimics and GORD patients, especially on the palatal surface, but access *in vivo* might be problematic. It might be predicted that other teeth (premolars and molars) may have

a different angle dependency to incisors, however this does not seem to have been the focus of much research.

It is not clear whether a reliable measurement of enamel thickness requires the acquisition of an image. Some studies have used B-mode imaging (Culjat *et al.*, 2003; Harput *et al.*, 2011) to measure enamel thickness, but this seems to have been limited to *in vitro* work. One of the earliest efforts to produce a B-mode image of a tooth (to measure bone levels around the tooth) was performed by Fukukita *et al.* (1985). The B-mode images, however, revealed the crown, gingiva and alveolar bone but not enamel thickness. This work was replicated by Berson *et al.* (1999), where they imaged a tooth and its periodontium, highlighting the potential of ultrasound in diagnosing periodontal disease by measuring alveolar bone height.

In an attempt to develop an ultrasound image of a tooth to quantify enamel layer thickness, Hua *et al.* (2009) used an ultrasound (13 MHz) medical scanner to image a molar tooth. The raw B-mode image required image processing to enhance it. Both images in Figure 1.11 below are not of adequate resolution to obtain enamel thickness measurements.

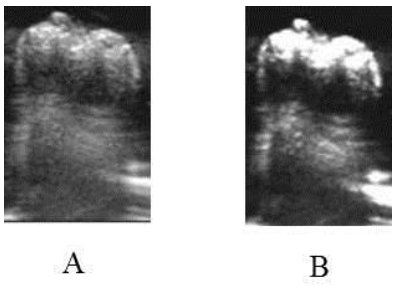

Figure 1.11. B-mode image of a molar before image processing, ‘A’ and after image processing, ‘B’ (Hua *et al.*, 2009, p.441).

Another study examined the ultrasound (35 MHz) resonance method to obtain a 3D image of the enamel layer (Hughes *et al.*, 2009). The study reported good results

with a 3D image of a tooth, however the study used a sectioned tooth specimen that was conditioned by polishing. This method is relatively ‘destructive’ and cannot be translated to the clinical level.

Whether or not a B-mode image is beneficial when making an ultrasonic scan of enamel thickness is an intriguing question. B-mode images can be saved on a computer and compared with future B-mode images to assess the level of erosive TSL that occurred. However, as enamel has a high SOS (see section 1.2, page 3), several echoes are generated within the tooth that obscure ‘real’ enamel layer echoes, which renders B-mode imaging more challenging. Nevertheless, using high frequency ultrasound improves axial resolution and therefore enhances B-mode images (discussed in Chapter 4).

Quantifying the thickness of the enamel layer would certainly help in monitoring erosive TSL. Enamel thickness measurements have been made by several researchers with A-mode ultrasound (see section 1.3.2). The reproducibility and accuracy of the measurements were often the two main outcomes reported. However, most of the reported results were from *in vitro* studies, mainly on extracted human teeth.

An *in vitro* A-mode study carried out in the Netherlands and Sweden (Louwerse *et al.,* 2004) tested the reproducibility of a 15 MHz ultrasonic device in measuring enamel thickness on 12 anterior teeth across four observers. They concluded that there was high inter-observer variability in measurements (between baseline and repeat measurements) and that a thickness of less than 0.33 mm could not be reliably detected. The authors attributed this to poor reproducibility and probe positioning. However, they did not attribute the variation to the two inexperienced observers who only had two-hours of training in ultrasound measurements and waveform

recognition beforehand. In the same study, a reproducibility test was undertaken for the placement of the delay line type ultrasonic transducer. This was achieved by taking digital photographs of an ink-marked area (one-third of the tooth length from the gingival margin and one-half of the tooth width) of the tip of the ultrasound probe. This experiment was repeated after one week to test probe positioning reproducibility between two observers, and how that might impact enamel thickness measurements, but the variation in probe positioning between the two observers was negligible.

A similar *in vitro* study (Huysmans and Thijssen, 2000) to measure enamel thickness on extracted human incisors was successful but with limitations. Of note was the difficulty in obtaining a recognisable ultrasonic waveform from cervical areas on both buccal and palatal surfaces due to the very thin enamel layer (< 0.5 mm) and the non-planar surface at these sites (Huysmans and Thijssen, 2000). The problems caused by the curvature of the teeth in these areas were compounded by holding the tooth in one hand and the ultrasonic probe in the other. The authors pointed out that if these measurements were to be made *in vivo*, probe alignment and measurements would be easier. Nevertheless, the reproducibility (intra- and inter-examiner agreement) was good with intra-examiner limits of agreement for the first examiner (n = 20) at -0.064 to 0.061 mm and -0.084 to 0.061 mm for the second examiner. The inter-examiner limits of agreement (n = 42) were -0.09 and 0.09 mm. The majority of the studies investigating enamel thickness assumed a constant SOS in enamel (see section 1.3.2). This assumption produces uncertainties of the enamel thickness results obtained using a constant SOS, because SOS varies within the same tooth and across teeth (Slak *et al.*, 2011). To assess the accuracy of the ultrasonic system, the SOS for

each tooth and each section of the tooth must be obtained first, and then the thickness of each section is derived and compared with histology (discussed in Chapter 5).

Bozkurt *et al.* (2005) investigated the accuracy of an ultrasonic system in detecting progressive occlusal wear on 20 human premolars *in vitro*. Thickness measurements were obtained using an ultrasonic system with a frequency of 11 MHz. The authors selected occlusal areas with some wear to guarantee a planar surface, which was scanned with a delay-line ultrasonic probe, with a tip diameter of 1.5 mm. The study reported a good agreement between ultrasound thickness measurements and histological sections of the teeth examined under a stereo microscope, as well as good inter-examiner reproducibility.

Because TSL is a progressive phenomenon (Lee *et al.*, 2012), locating planar areas on occlusal surfaces to measure enamel thickness *in vivo* might be challenging, as fixed reference points are lost in erosive TSL (Mitchell *et al.*, 2003). Also, the same planar reference that served as a baseline would not be present in successive scans. The value of an *in vivo* investigation of A-mode ultrasound reproducibility on teeth with naturally planar surfaces becomes very important, as these surfaces can serve as baselines for monitoring the condition. This would help determine how beneficial ultrasound can be in monitoring erosive TSL.

One of the main problems of applying diagnostic ultrasound in dentistry is coupling, which is required to transfer the ultrasound energy into the tooth and back to the transducer (see section 1.2). The outer surface of a tooth (enamel) is full of porosities (Crabb, 1976) which contain air. Air is acoustically ‘unfriendly’ and does not transmit ultrasound waves; ultrasound does not pass through air because of the impedance mismatch between the highly dense enamel and the less dense air (Harput

et al., 2011). On the microscopic scale, these porosities decrease the amount of contact (surface area) between the transducer and the enamel surface (Lempriere, 2002). Therefore, a couplant such as water could be used to inhibit this effect.

Several research groups investigated the use of couplants, such as glycerine, castor oil, aluminium and mercury (mercury would not be used in an *in vivo* situation because of its toxicity). The aim of these investigations was to find the best coupling agent that would transmit most of the ultrasound wave with minimal loss of signal. This is done by selecting a coupling material with an impedance value that lies between the impedance values of the ultrasound wave source (transducer) and the tooth (enamel). Ideally it should be a solid, but that is clinically impractical.

Aluminium has an impedance value that is similar to enamel (Lees and Barber, 1968) and the piezoelectric transducer; theoretically, it is an ideal couplant. However, the use of aluminium is not practical in a clinical environment because it requires a perfectly planar surface to achieve good contact and thus coupling with enamel. Therefore, it is useful to know what materials are suitable for coupling transducers to teeth. This will be investigated in more detail in Chapter 2.

It would be sensible, therefore, to establish clinical reproducibility in an *in vivo* situation, which would pinpoint any limitations that might arise in a clinical situation and inform future research in this field (discussed in Chapter 6). Initial work to look at the possibility of identifying interfaces would also be valuable as enamel thickness is of central importance in the monitoring of TSL.

The aim of this thesis is to assess the feasibility and optimisation of ultrasound as a potential clinical dental tool aiding in quantifying the enamel layer to assess the possibility of using this tool in monitoring erosive TSL *in vitro* and *in vivo*.

1.6 Objectives

To achieve the aim stated above, the following were established.

1. To investigate the suitability of certain dental materials as couplants, as well as other potential couplants.

2. To determine the angle dependency of echoes arising from premolars and compare it to maxillary central incisors. Synthetic incisors would be used here because of the lack of available natural teeth.

3. To explore the feasibility of using B-mode ultrasound in imaging intact enamel in human teeth. Two systems are evaluated for this purpose. The first uses an in-house ultrasound scanner and the second is a commercial ultrasound machine. The data obtained are validated with μ-CT.

4. To determine the feasibility of using A-mode imaging for enamel thickness measurements, including a study of SOS variations. Such measurements are validated with histological sections of the same teeth.

5. To determine whether A-mode ultrasound is able to monitor human enamel thickness reliably and reproducibly *in vivo*.

The work to achieve each of these objectives is described in the following Chapters.

2 Coupling, Boundaries and Interfaces

2.1 Introduction

The problem of coupling ultrasound energy between the transducer and the target material is significant in dentistry because of the high *Z* values in enamel and the transducer as compared with low *Z* values in saliva and water. This creates a large mismatch and hence a significant loss of signal both on transmission and on reflection. In the ultrasound field, this problem has been traditionally addressed by the use of coupling materials with intermediate impedance values. However, in dentistry there are extra constraints on the choice of coupling materials since it is critical that they are safe for oral use. An additional problem is the need for delay lines, since the materials used for delay lines have to satisfy the same demands.

Delay lines are important because of the need to delineate the first enamel border clearly. In the absence of a delay line, the echo from the proximal enamel surface would arrive during the excitation period of the transducer and therefore be lost. Delay lines create a time gap between the transducer excitation and the arrival of the first echo. The material from which the delay line and coupling is constructed therefore requires investigation and the suitability of various dental materials for this purpose is the subject of this Chapter.

2.2 Materials and Methods

To investigate coupling efficiency two different experimental designs were used: a water tank apparatus and a purpose-built apparatus.

2.2.1 Water Tank Apparatus

In this experiment, several relevant and commercially available dental materials were investigated as couplants—namely: alginate, silicone, tooth carding wax, orthodontic

wax, plaster, stone and cobalt-chromium (Co-Cr). Aluminium and Polymethylmethacrylate (Perspex) were also investigated. These were tested in a water-filled tank which was made of Perspex and filled with fresh tap water until the transducer and specimen were completely immersed.

2.2.1.1 Preparation of Coupling Materials

Mixing of the addition silicone, alginate, plaster and stone was carried out according to the manufacturer's instructions. Before they were completely set, silicone and alginate were placed into a custom-made polytetrafluoroethylene (PTFE) mould (Ø = 10 mm and depth of 5.5 mm) and a glass slide was placed on top of the mould to ensure a planar surface was present. Aluminium and Perspex were supplied by their manufacturer as rods, which were machined by a lathe to the required length. Co-Cr was used in its original cylindrical form (ingot). Tooth carding wax and orthodontic wax were moulded by hand and pressed between two glass slides until and an even surface was created. These materials and their thicknesses are shown in Table 2.1.

Table 2.1. Materials used as coupling agents for ultrasound investigations

Material	Thickness (mm)	Brand	Part Number and Manufacturer
Addition silicone	5.60	Aquasil™ (soft putty)	60578320, DENTSPLY, PA, USA
Alginate	5.48	Cavex ColourChange	AA323, Cavex Holland BV, The Netherlands
Polymethyl-methacrylate	4.92	Perspex*	ME303055, Goodfellow, UK
Aluminium	9.96	-	AL007912, Goodfellow, UK
Tooth carding wax	5.25	-	DWS304, Kemdent®, UK
Orthodontic wax	4.41	-	860111B, Ortho-care, Ltd, UK
Plaster	5.87	éclair	ECL20, Lafarge Prestia, France
Stone	5.36	Crystacal 'D'	CD045, John Winter and Co., Ltd, UK
Co-Cr	15.00	Sheralit-Cylindra	401043, John Winter and Co., Ltd, UK

*The term Perspex will be used throughout this thesis instead of polymethylmethacrylate (for simplicity).

Each material was attached to a glass slide (an interface that has a similar SOS to enamel) inside the water-filled tank to see which of these coupling materials transfers most of the ultrasound signal into the glass slide and back to the transducer (Culjat *et al.*, 2005b). Ten specimens of each material were used.

2.2.1.2 Ultrasonic Setup for Water-filled Tank Studies

The transducer was secured in a clamp and suspended vertically in the water tank. The glass slide was placed in the bottom of the water tank, and the coupling material was placed on top of the glass slide, such that a straight line ran across the centre of the transducer, the coupling material and the glass slide. This ensures that the ultrasound beam meets the material surface at normal incidence (Figure 2.1 below). The transducers used had a frequency of 10 and 20 MHz and had a detachable Perspex delay line which was removed prior commencing the experiment because a time offset was not required (V203-RM and V208-RM, Olympus® Inc., MA, USA). The transducers were excited by a pulser/receiver (PR-5742, Olympus® Inc., MA, USA) and the ultrasonic echoes were displayed on a digital oscilloscope (LT-3542, Teledyne LeCroy®, NY, USA). The waveform files were subsequently saved in an American Standard Code for Information Interchange (ASCII) format on the lab PC (connected to the oscilloscope with an RS-232 cable) for further analysis.

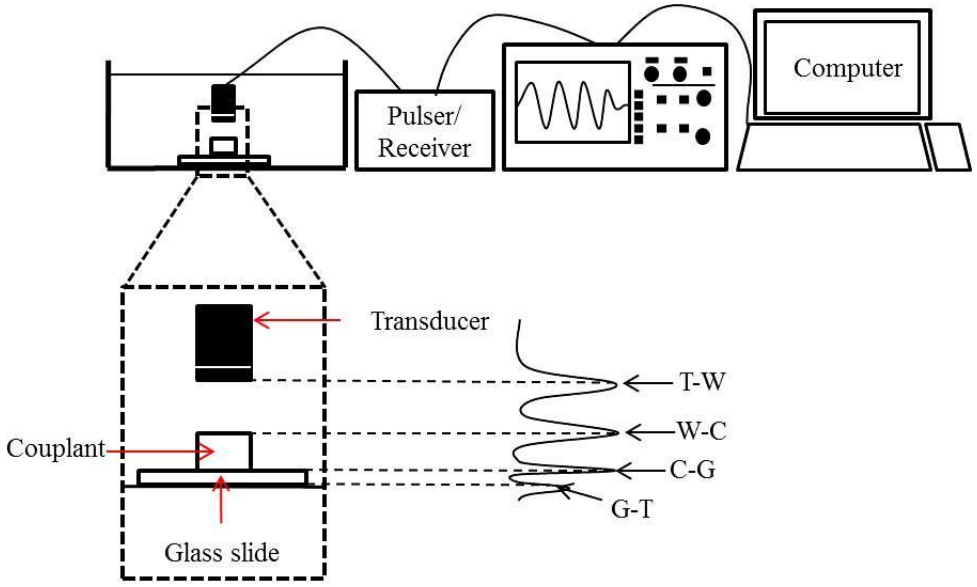

Figure 2.1. Water-filled tank depicting couplant and the interfaces echoes 'T-W' denotes the echo arising from the transducer-water interface; 'W-C' refers to the water-couplant echo; 'C-G' refers to the couplant-glass slide echo and 'G-T' refers to the glass-tank base echo.

2.2.1.3 Statistical Methods for Water-filled Tank Studies

Two-way analysis of variance (ANOVA) was performed (coupling material and frequency as the two factors) to determine if there were statistically significant differences in reflection across the coupling materials. The significance level was set at $\alpha = 0.05$. All statistical analyses were done using IBM® SPSS® version 20 (IBM SPSS®, IBM® Corp., NY, USA)

2.2.2 Purpose-built Apparatus

This apparatus had a railway-like design, with the specimen held in a cone-shaped PTFE holder that translates on two steel rods. A manual knob controlled the translation movement of the holder (and specimen), which was attached to a vernier scale (±0.1 mm) for consistent movement. The rational for choosing a cone-shaped holder was to scatter the ultrasound echoes arising from the holder. This guaranteed that any visible echoes were those of the specimen (Figure 2.2 below).

2.2.2.1 Preparation of Composite and Perspex Discs

Micro-hybrid dental composite of shade A3 (Herculite® XRV, Kerr, Germany) was packed into a custom-made PTFE mould and light cured for 30 s (according to manufacturer's instructions) with a light curing unit (DENTSPLY, PA, USA) with an intensity of 500 mW/cm^2. Ten composite disc-shaped specimens were produced with a diameter and thickness of 4 mm and 10 Perspex discs were machined to yield disc-shaped specimens with the same dimensions.

2.2.2.2 Ultrasonic Setup for Purpose-built Apparatus Studies

Three transducers with frequencies of 2.25 MHz, 3.5 MHz and 5 MHz (V304, V380 and V307, Olympus® Inc., MA, USA) were chosen. The transducer was mounted in the purpose-built apparatus (with a linear translation and a vernier scale) that secured it parallel to and in contact with the Perspex-composite interface (Figure 2.2). A thin layer of coupling gel (Aquasonic® 100, Parker Laboratories Inc., NJ, USA) was placed at the transducer-Perspex and Perspex-composite interfaces.

The remainder of the ultrasonic setup is similar to the one in section 2.2.1.2.

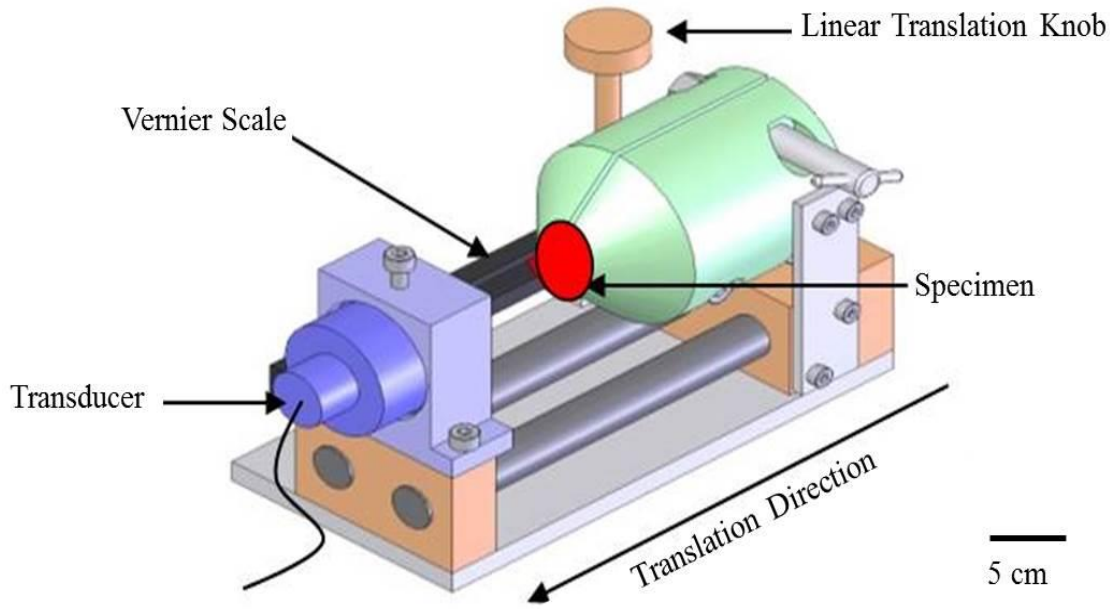

Figure 2.2. Purpose-built apparatus with transducer and specimen in place.

To couple the transducer to the composite disc, the Perspex was placed in front of and in contact with the composite disc facing the ultrasound transducer (red specimen in Figure 2.2). To achieve optimum contact between the transducer and specimen, the linear translation knob was rotated to translate the specimen holder (green) and specimen until it was in contact with the transducer (Figure 2.3 below).

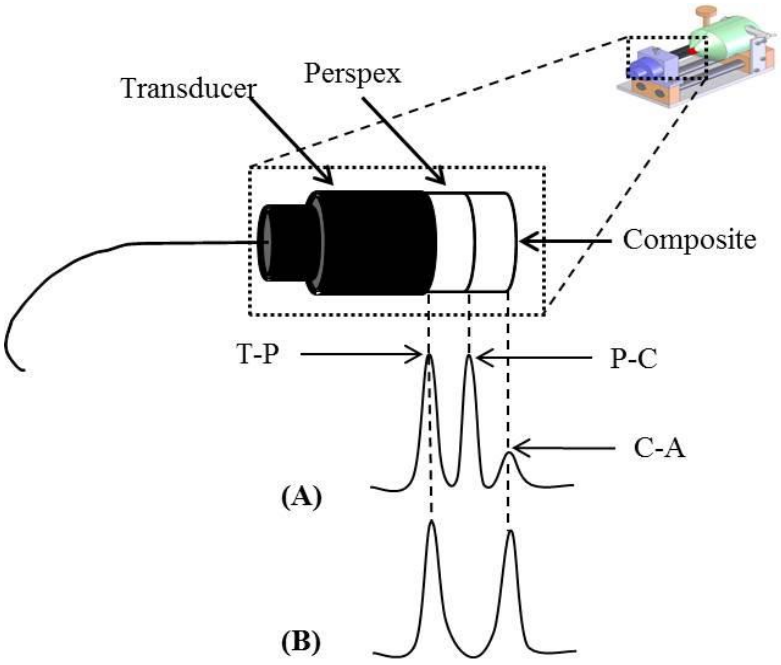

Figure 2.3. Transducer and Perspex-composite setup. Depicts the ultrasonic reflections from the Transducer-Perspex 'T-P', Perspex-Composite 'P-C', and Composite-Air 'C-A' interfaces when Perspex is used as a couplant.

The first (front face) echo, 'T-P', arising from the transducer-Perspex interface was captured along with its amplitude. The second (interface) echo, 'P-C', arising from the Perspex-composite interface was also captured and its amplitude recorded. The same was applied to the third (back face) waveform, 'C-A', arising from the composite-air interface and the waveform and amplitude recorded. The same experiment was repeated using a cyanoacrylate adhesive (853188, Loctite® Super Glue, Henkel, CT, USA) to improve coupling at the 'P-C' interface and the echoes were recorded ('B' in Figure 2.3). The strength of the reflection at the

Perspex-composite interface should be dependent on the quality of the bond between the two materials. A larger amplitude 'P-C' suggests a stronger reflection and hence a poorer bond.

The amplitude reflection coefficient (*r*) was also calculated, using Equation 1.4 (see section 1.2). Knowing the impedance values of both Perspex (P) and composite (C), the amplitude reflection coefficient (*r*) can be derived. Perspex has an impedance value of 3.6 MRayls and composite has a value of 6.9 MRayls (Singh *et al.*, 2008).

2.2.2.3 Statistical Methods for Purpose-built Apparatus Studies

An independent *t*-test was used to assess if there is a statistically significant difference between the two groups (with and without adhesive at 'P-C') in section 2.2.2. The significance level was set $\alpha = 0.05$. All statistical analyses were done using IBM® SPSS® version 20 (IBM SPSS®, IBM® Corp., NY, USA).

2.3 Results

2.3.1 Water Tank Apparatus

The amplitude of the reflected ultrasonic echoes was used as an indication of which coupling materials are most efficient in transferring ultrasonic energy out of and back to the transducer (Table 2.1 below). Some useful data was obtained from this apparatus. However, problems were encountered with alignment and orientation and a different, more precise device was constructed to investigate the Perspex-composite interface (as described in section 2.2.2).

Table 2.2. Interface echo amplitudes (Volts) between several materials and a glass slide

Frequency (MHz)	Material	Thickness (±0.01 mm)	W-C Front face echo (SD ±0.01)	C-G Interface echo (SD ±0.01)	G-T Glass back face echo (SD ±0.01)
10	Addition silicone	5.60	3.03	0.29	3.23
20		5.60	2.86	0.00	3.26
10	Alginate	5.48	2.46	0.00	2.78
20		5.48	3.07	0.00	3.26
10	Perspex	4.92	2.14	3.14	3.69
20		4.92	2.78	1.18	3.10
10	Aluminium	9.96	3.69	3.67	0.60
20		9.96	3.21	3.21	3.00
10	Tooth carding wax	5.25	2.53	0.00	3.52
20		5.25	3.02	0.91	3.02
10	Orthodontic wax	4.41	1.87	0.16	3.53
20		4.41	2.64	0.00	3.35
10	Plaster	5.87	3.17	0.00	3.51
20		5.87	2.73	0.00	3.19
10	Stone	5.36	3.00	0.35	3.52
20		5.36	2.12	0.23	3.30
10	Co-Cr	15.00	3.50	2.30	3.04
20		15.00	3.20	2.89	3.04

Table 2.3. Key for Table 2.3

W-C	Water-couplant interface
C-G	Couplant-glass slide interface
G-T	Glass-tank base interface

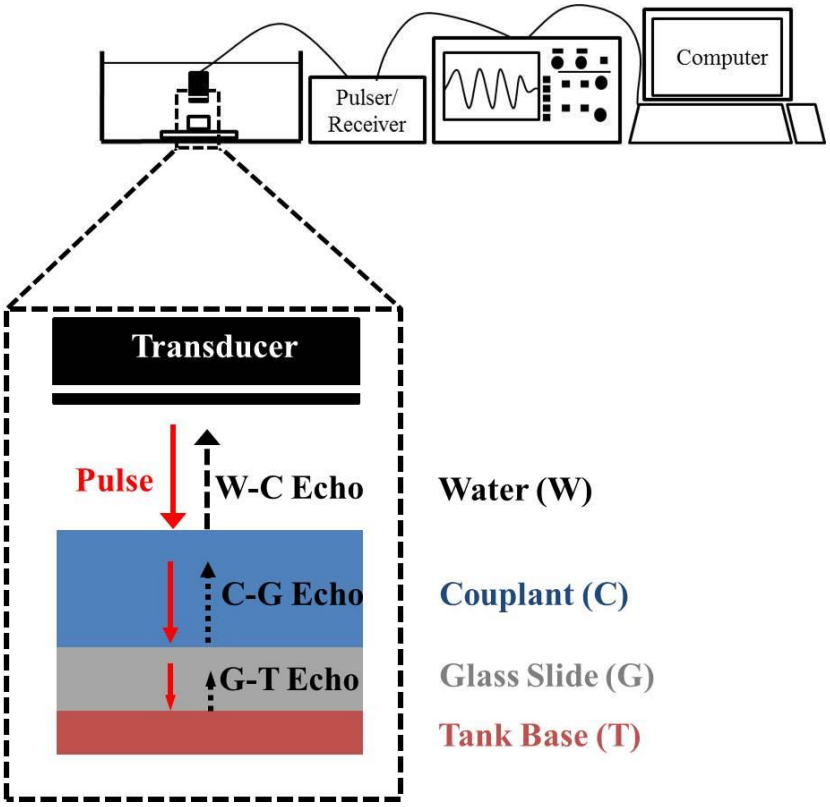

Figure 2.4. Schematic depicting the origin of echoes in Table 2.2. The fired pulse encounters the water-couplant interface (W-C) and an echo registers (W-C Echo). Part of the pulse continues its path through the couplant and encounters the couplant-glass slide interface (C-G), and a second echo registers (C-G Echo). When the pulse meets the glass slide-tank base interface, a final echo develops (G-T Echo).

It was found that the high frequency (10 and 20 MHz) transducers led to a poor signal-to-noise ratio, which was why lower frequencies were used for the Purpose-built apparatus.

Table 2.4. Two-way ANOVA results for the coupling materials' reflection at the 'G-T' interface.

Coupling Material	G-T (V) Mean (±SD)
Alginate	3.02 (0.34)
Aluminium	1.80 (1.70)
Tooth carding wax	3.27 (0.35)
Co-Cr	3.04 (0.00)
Orthodontic wax	3.44 (0.13)
Perspex	3.40 (0.42)
Plaster	3.35 (0.23)
Addition Silicone	3.25 (0.02)
Stone	3.41 (0.16)
P-value	0.37

The water tank apparatus was suitable for measurements of coupling between bulk materials without firm adhesion between them. The purpose-built apparatus was designed for use on small discs of materials which could be firmly pressed together.

2.3.2 Purpose-built Apparatus

2.3.2.1 Reflection Calculation (No Adhesive Applied)

The first set of echoes in Figure 2.3, 'A', were from the transducer-Perspex-composite interface. It can be seen from this illustration that the Perspex transmits the ultrasonic signal to the back face of the composite, but it is not of high amplitude ('C-A').

Table 2.5. Echo amplitudes at transducer-Perspex (T-P), Perspex-composite (P-C) and composite-air (C-A) interfaces with no adhesive at (P-C)

Frequency (MHz)	Mean T-P Front face echo (mV)	±SD	Mean **P-C** Interface echo (mV)	±SD	Mean C-A Back face echo (mV)	±SD
5	480	13	**285**	**21**	51	8
3.5	549	15	**301**	**10**	64	11
2.25	109	8	**77**	**4**	35	4

2.3.2.2 Reflection Calculation (Adhesive Applied)

It can be seen in Figure 2.3, 'B', that the 'P-C' echo amplitude has diminished in favour of the 'C-A' echo amplitude. This means that the thin layer of adhesive, which in effect was as an additional couplant, has improved the ultrasonic transmission by improving the coupling and minimising the reflection at the 'P-C' interface.

Table 2.6. Echo amplitudes at transducer-Perspex (T-P), Perspex-composite (P-C) and composite-air (C-A) interfaces with adhesive at (P-C).

Frequency (MHz)	Mean T-P Front face echo (mV)	±SD	Mean **P-C** Interface echo (mV)	±SD	Mean C-A Back face echo (mV)	±SD
5	480	30	**184**	**24**	43	4
3.5	552	17	**219**	**10**	77	10
2.25	99	8	**67**	**22**	32	-

Table 2.7. Statistical analysis of amplitudes between two groups: with and without adhesive at the 'P-C' interface.

Frequency (MHz)	*p*-value
5	0.01
3.5	0.00
2.25	0.56

Table 2.8. Amplitude reflection coefficient calculation.

Interface	**Amplitude Reflection Coefficient (*r*)**
Perspex-composite	-0.314 (-31.4%)

2.4 Discussion

2.4.1 Water Tank Apparatus

The use of couplants for ultrasonic use in dentistry was investigated as early as the 1960s, when Lees and Barber (1968) examined aluminium as a couplant for enamel because of its similar *Z* value. They found that it was difficult to adapt the aluminium rod to the enamel surface because of the lack of a planar surface in the teeth they used. However, they reported good results and concluded that aluminium was a suitable couplant.

In the present study, all the materials had good coupling abilities, as seen from the 'G-T' interface echo amplitudes, where most of the signal has reached this interface. The results showed no significant difference between the different coupling materials for the 'G-T' interfaces (p-value > 0.05). Aluminium displayed good ultrasound coupling when the 20 MHz transducer was used, but not with the 10 MHz transducer, where only a small fraction of the ultrasound signal reached the 'G-T' interface (the echo amplitude was 0.6 V in Table 2.2). This may be due to insufficient pressure applied on the aluminium and the glass slide, which may have caused ultrasound signal loss. A small ultrasound signal renders it difficult to detect on the oscilloscope and consequently, no data can be obtained. This highlights the importance of having good contact between the couplant and the object. In addition, aluminium generated reverberations that obscured the echo in question (G-T echo in Figure 2.1, p.44).

Alginate was not a good couplant because it was not durable and can be easily torn. Wax was also an unreliable couplant due to its ability to change shape. Stone, plaster and Co-Cr are unsuitable due to the time required to adapt to a transducer. In addition, stone and plaster have a rough texture and are not suitable for *in vivo* use.

Silicone requires mixing a base and a catalyst and consistency in mixing may not be achievable and in addition, it is costly. Therefore, silicone was regarded as an unsuitable couplant.

It seems reasonable to assume that the ultrasonic energy reaching the glass slide would have been higher if water was not present between the main couplant and the transducer (i.e. the transducer is in direct contact with the main couplant). The use of water was inevitable because even contact between the transducer and some materials was not possible in contact mode.

When Perspex was used, the 'G-T' interface had a visible echo (echo amplitude was 3.69 V at 10 MHz and 3.10 V at 20 MHz), which indicates its relatively good coupling ability. However, because the transducer that will be used in later Chapters was manufactured with a Perspex tip, Perspex was used in section 2.2.2.

2.4.2 Purpose-built Apparatus

For this phase of the work, it was decided to use a Perspex-composite interface as an experimental model. The rationale for this was that Perspex is the default material for use in delay lines and that dental composite was readily available in addition to being a dentally relevant material. After deciding that Perspex was the best coupling material, an experiment was run to examine bonding at the Perspex-composite interface. The first experiment used gel between the Perspex and composite and the data from this experiment demonstrated that the majority of the ultrasonic signal had been reflected at the second interface, 'P-C', where the bond (or coupling) between the Perspex and composite was suboptimal (echo amplitude at this interface was 285 mV; see Table 2.5). This premature signal loss affected the echo amplitude at the composite-air interface, 'C-A'. However, when the adhesive was used at the 'P-C'

interface, the echo amplitude decreased to 184 mV (Table 2.6), and more ultrasonic signal reached the ‘C-A’ interface. It was thought that the pressure applied on the specimens affected the coupling at the ‘P-C’ interface and the amplitude of the reflected echoes.

Another factor that affected the coupling at the ‘P-C’ interface was that the coupling gel at the ‘P-C’ interface had a larger impedance difference compared to the adhesive. The findings demonstrate that ultrasound is sensitive to interface changes, such that when a gel was used much ultrasound energy was reflected at the ‘P-C’ interface. These changes in echo amplitudes, although slight, showed that the adhesive was more efficient than gel in transferring ultrasound to and from the composite (p-value < 0.05 for 5 and 3.5 MHz in Table 2.7). These findings are in agreement with Denisova *et al.* (2009), who performed similar studies on a cement-dentine interface.

This experiment was performed on planar Perspex and composite discs that were machined to have parallel surfaces. It is expected that parallel surfaces will result in larger echo amplitudes than in a real tooth where the interface between the Perspex and enamel would rarely be planar. Therefore, the echo amplitude is expected to be smaller in the clinical situation. For improved coupling, Culjat *et al.* (2005b) investigated the use of a mouldable alloy couplant that can conform to the shape of the target surface. This is unlike Lees and Barber’s (1968) approach, where they ground the surface of the tooth to become planar to adapt the aluminium rod to it. In the approach described in this Chapter, the conformity problem was eliminated by machining both Perspex and composite to planar surfaces. Although not ideal, this sufficed as a simple approach to test echo amplitudes. One of the main reasons for

choosing this approach was to eliminate other variables that could decrease (or increase) echo amplitudes.

Bringing the findings of this Chapter to a scenario with a restoration–tooth interface, the consequences of ultrasonic echo reflections can be anticipated. When a restoration fails, it is expected that the tight seal begins to disintegrate, forming a micro-gap into which bacteria from oral fluid seep (microleakage). The hypothesis is that ultrasound would recognise this change in restoration-tooth interface as an increase in echo amplitude (if the interface failed) or a decrease in echo amplitude (if the interface is intact). This could then inform the dentist whether the restoration merits replacement or not. Denisova *et al.* (2009), Ghorayeb and Valle (2002) and others have previously investigated this situation. When an ultrasound wave propagates in a material and meets an interface, an echo will return from this interface. The amplitude of this echo (large or small) will depend on the qualities of this interface. If the interface is acoustically invisible (i.e. having a similar impedance value to the materials on either side), then the ultrasound echo would be very minimal, if not absent. However, when the interface has a very different impedance value relative to the materials on either side of it, a large ultrasound echo will develop.

2.5 Conclusions

The results demonstrate that ultrasound can detect interface changes in the form of echo amplitudes (A-mode). Some general useful conclusions can be drawn:

- Intimate contact is important when coupling a material to a specimen for ultrasound scanning.
- The use of Perspex as a coupling material (while not ideal) should be adequate for further studies.

3 Angle Dependency Assessment

3.1 Introduction

A potential drawback associated with the use of ultrasound is angle-dependency which can lead to loss of ultrasound signal (Dwyer-Joyce *et al.*, 2010). As discussed in section 1.5 there are two aspects to the problem. First, since the surface of the tooth is curved, the amplitude of the echo from the enamel surface will vary considerably in terms of angle and is likely to disappear completely if the angle deviates significantly from 90°. In addition, the echo amplitude will also vary with surface roughness. Second, if the intention is to measure enamel thickness, then the echo from the amelo-dentinal junction (ADJ) is also needed. It too is curved, but it is not necessarily parallel to the enamel surface. In other words, the angle which will maximise the echo from the enamel surface generally will not be the same as that for maximising the ADJ echo.

It therefore seems logical that the extent of the angle-dependency problem will depend on the curvature of the tooth. This would imply that premolars will exhibit more extreme angle dependency than incisors since they are normally more curved. That said, an echo received from the outer enamel surface is dependent on two angles; the first along the horizontal plane and the second across the vertical plane (Figure 3.1 below).

Dwyer-Joyce *et al.* (2010) explored this issue in molar teeth, using three different beam angles relative to the tooth. They measured the effect of angle change on the TOF and enamel thickness measurements. The technique they used to measure this change was not described in detail, but unsurprisingly, they reported that the best TOF measurements were achieved when the transducer was at a right angle to the

tooth's surface. Furthermore, the ADJ echo was not apparent when the ultrasound beam was tilted more than 10° from the optimal position, which means that at this point, the angle of reflection was so great that no echo returned to the transducer (see section 1.2, Equation 1.6).

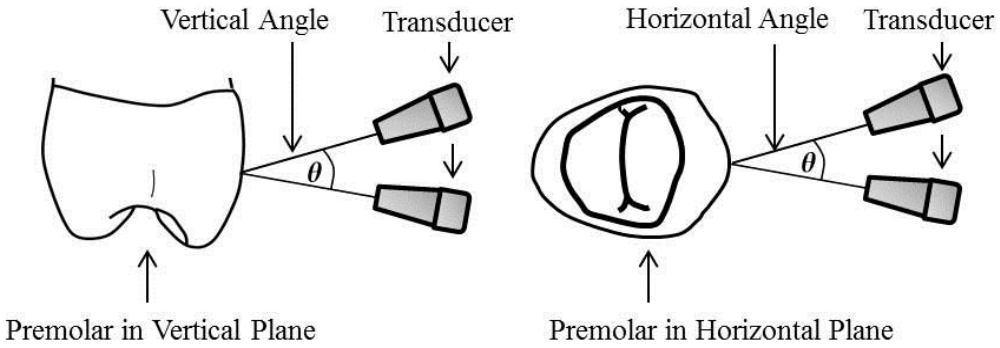

Figure 3.1. Schematic depicting vertical and horizontal ultrasonic signal angles

This Chapter deals with horizontal angle change and its effects on the ultrasound signal received from the outer enamel surface. The curvature and surface roughness of the teeth will add to the problem, but they are not discussed here.

The difference between the work described in this Chapter and that of Dwyer-Joyce *et al.* (2010) is in the comparison of incisors with premolars to see if they have different tolerance to angle change. Another difference is that the echo under investigation here arises from the enamel's front surface (water–enamel interface) rather than the ADJ interface as in the work of Dwyer-Joyce *et al.* (2010). The aim of the work described in this Chapter is twofold: First, to determine how much deviation is possible from this ideal angle while still producing an interpretable echo from the surface of a relatively curved tooth (premolar) and a relatively planar one (incisor); second, to test the hypothesis that there is considerable variation in reflectivity between teeth of different types.

3.2 Materials and Methods

Human premolars and synthetic central incisors were used to investigate how the incident ultrasound beam angle affects the received ultrasound echo amplitude. The angle comparison was between the buccal (more curved) premolar surface and the labial central incisor surface (planar).

3.2.1 Tooth Selection and Storage

Twenty-seven human premolar teeth extracted for orthodontic purposes were obtained from the University of Leeds Skeletal Tissue Bank (130109/DS/19). The teeth roots were cleaned to remove soft tissue remnants with a spoon excavator and a toothbrush with pumice powder and stone. Teeth were then placed in distilled water and 0.1% thymol (Sigma Aldrich, MO, USA) and stored in the refrigerator at 5 ºC.

In addition to premolars, two synthetic maxillary central incisors (AG-3, Frasaco GmbH, Tettnang, Germany) were included for testing. Because natural maxillary central incisors were not available from the tissue bank at the time of the experiment, synthetic maxillary incisors were the best available option. Nevertheless, crowns of synthetic teeth have approximate labial topographical resemblance to natural maxillary central incisors, which is sufficient for the purpose of this experiment.

3.2.2 Ultrasound Apparatus

Based on previous preliminary experiments, a proper holding mechanism had to be designed to address the angle dependency question. The design was simple yet provided the required conditions for conducting the experiment. The holding mechanism was assembled in the School of Dentistry's workshop, after obtaining the necessary components. An acrylic tank, filled with tap water, was used to investigate the angle dependency issue.

To control the angle movement, a stepper motor with a step angle of 1.8° ±0.09º (RS-191-8299, RS Components, Oxford, UK) was used to mount the tooth, via a steel axle connected to the motor. The stepper motor rotated the tooth with a predetermined angle. The angle was controlled by a stepper drive (ST5-Si-NN, Applied Motion Products, Inc., CA, USA), which controlled the stepper motor. The stepper drive was connected to a PC running proprietary software (Si Programmer™, V2.7.22, Applied Motion Products Inc., CA, USA) in which the desired angle was programmed.

After assembling the components of the system, it was possible to suspend a 15 MHz focussed transducer with a Perspex delay line (VR-260, Olympus® Inc., MA, USA) from an *x-y* translation stage with a resolution of 10 μm (XYR1, Thorlabs, NJ, USA) mounted on the acrylic tank (Figure 3.2 below). Although, for this purpose, the transducer was not being used in contact mode, a transducer with a delay line was selected. This was done in order to allow use of the same transducer in contact mode at a later stage. The *x-y* translation stage provided a platform for reproducible transducer movement in the x and y planes. It was important to align the centre of both the stepper motor and *x-y* translation stage, so that the ultrasound measurements were always at the centre of the tooth. The tooth was then rotated in increments of 5º ±0.25° via the PC-controlled stepper motor and the averaged ultrasound echo (echo ‘B’ in Figure 3.3) was saved for each increment.

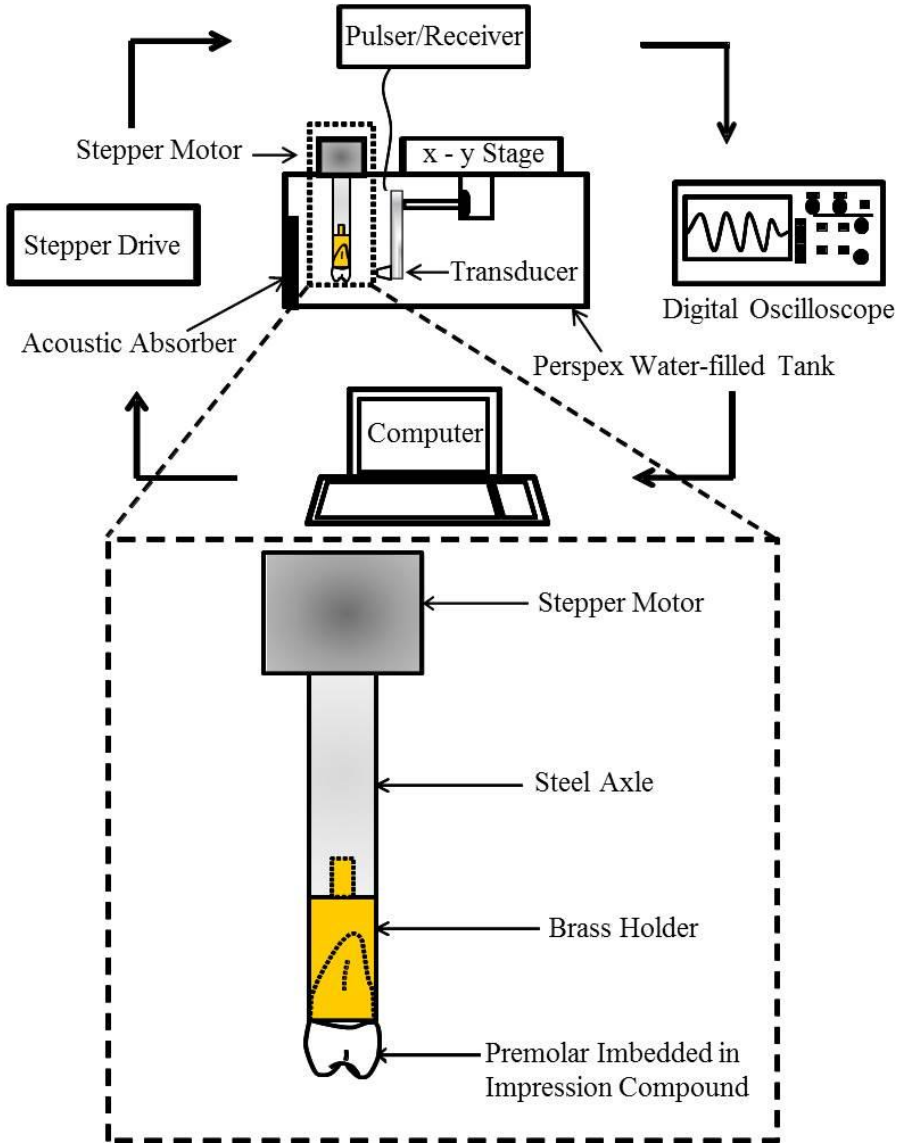

Figure 3.2. Ultrasound apparatus depicting the tooth *in-situ*.

In Figure 3.2, the tooth to be scanned was embedded in the brass holder and secured with impression compound (Kemco, Kemdent®, UK) until the material was set. It was important that the long axis of the tooth was in line with the centre of the steel axle and brass holder, so that accurate angle measurements were taken. The steel axle with a brass holder at one end was attached to the stepper motor which enabled the tooth to rotate in the centre of rotation of the stepper motor.

The transducer was excited by a pulser/receiver (PR-5742, Olympus® Inc., MA, USA), and the ultrasound waveform was captured on a digital oscilloscope

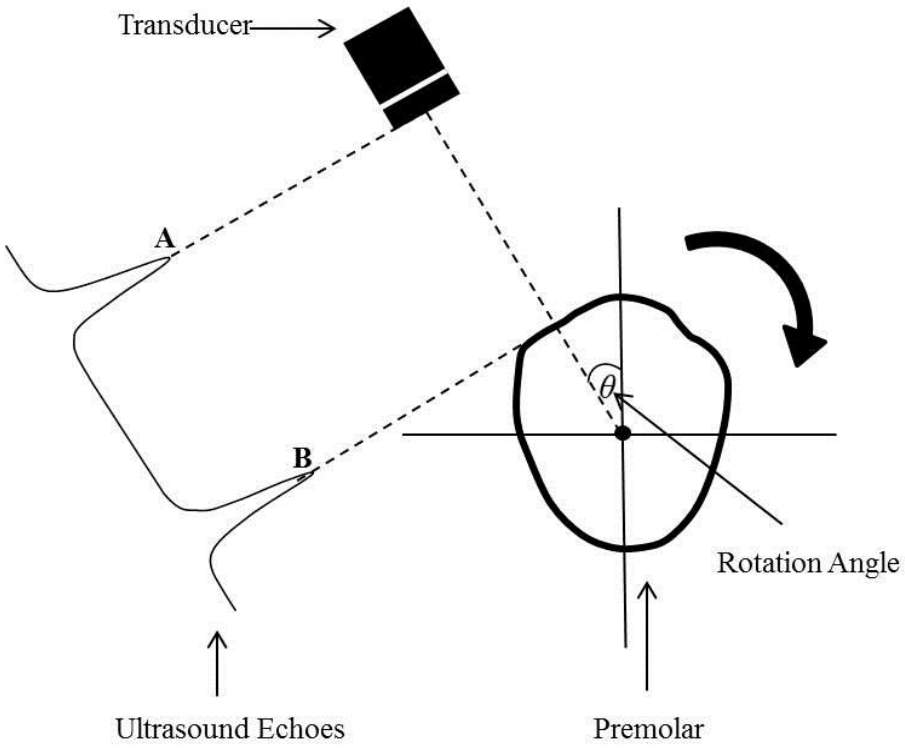

Figure 3.3. Schematic of the rotation angle and the ultrasonic echoes generated at the interfaces of interest in the premolar.

(LT-3542, Teledyne LeCroy®, NY, USA) and digitised to 2500 data points. To improve the signal-to-noise ratio, 1000 such pulses were averaged by the oscilloscope to create an ASCII data file for export to a PC via an RS-232 cable. To automate the waveform capturing and saving process, a macro programme, written by Mr Mohammed Khan, University of Leeds, was used. In Figure 3.3 echo 'A' denotes the transducer–water interface, while echo 'B' denotes the water–enamel interface. The echo of interest here is 'B', which is affected by the angle change, 'θ'. When the tooth rotates, the ultrasonic echo hits the tooth surface at another angle (horizontal angle in Figure 3.3 above) because of the curvature of the tooth's surface (Figure 3.4 below).

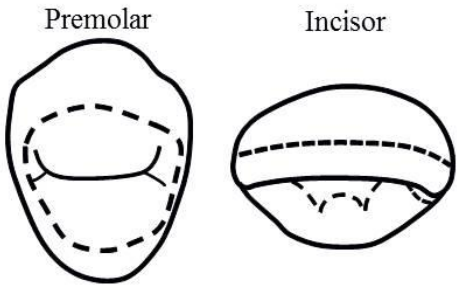

Figure 3.4. Curvature of premolars versus incisors.

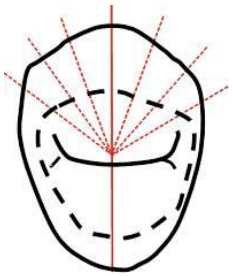

Figure 3.5. Premolar tooth relative to rotation angle (θ = 5º ±0.25°).

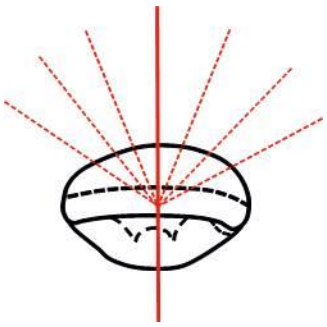

Figure 3.6. Synthetic maxillary central incisor tooth relative to rotation angle (θ = 5º ±0.25°).

3.2.3 Ultrasound Scans

A trial scan was performed to make sure that the tooth rotated freely and was in line with the delay line of the transducer, and also that the ultrasound scans could be successfully stored. The trial scan was done by selecting a 5º ±0.25° increment from the stepper drive's software, capturing the ultrasound waveform and automatically saving each file via the macro programme.

The macro programme had control over the rotation of the tooth, taking an ultrasound scan and saving the averaged waveform in the ASCII format for analysis. At the start of the scan, the delay line was 1 mm away from and perpendicular to the buccal surface of the premolar. The baseline waveform was captured and saved. Clockwise rotations in steps of 5º ±0.25° were performed until no echo was received from the tooth and the waveforms were saved for analysis. At each angle, the measurement was repeated twice and the mean amplitude taken.

After completing the scans for a tooth, the axle and the tooth attached to it were removed from the stepper motor and placed in a bowl of warm water so that the tooth could be removed from the brass holder. The next tooth to be scanned was placed in the holder while the impression compound was still mouldable. Caution was exercised while the material was cooling down, to make sure that when the material set, the tooth was still in the centre of the brass holder and in line with the stepper motor's centre of rotation.

3.2.4 Data Analysis

A total of 766 ASCII data files were analysed using OriginPro® version 8.6 (OriginLabs®, MA, USA). Each file was plotted (each plot was a mean of two repeat measurements) against the angle of rotation (θ = 5º ±0.25°) and a waveform was produced to demonstrate the angle dependency of the signal. A 'find peak' function was used to locate the peak and record its amplitude. The first peak corresponded to the transducer-water interface, while the second peak corresponded to the water-enamel interface (see Figure 3.3). When the second echo, 'B', in Figure 3.3 had multiple peaks, the highest peak was used to record the amplitude (the second peak was a reverberation). When a waveform was uninterpretable, its measurement was omitted.

3.2.5 Statistical Methods

The statistical test used to analyse the data from the premolars and synthetic incisors was multilevel (mixed) regression. This analysis allows for comparing premolars and incisors in terms of repeat amplitude measurement (the outcome variable) over different angles. For each angle, the amplitude of the signal was measured twice and the mean was taken. Prior to performing the analysis, a Shapiro-Wilk normality test was done to see if the data followed a normal distribution. The significance level for this test was set at $\alpha = 0.05$. If the test yields a *p*-value that was < 0.05 then the data did not follow a normal distribution. On the other hand, if the test yields a *p*-value > 0.05 then the data followed a normal distribution.

If the data did not follow a normal distribution, a log transformation was made for the amplitude data before the statistical test was performed. All statistical analyses were done using IBM® SPSS® version 20 (IBM SPSS®, IBM® Corp., NY, USA)

3.3 Results

Data was collected from 27 premolar teeth and 2 synthetic incisors using the ultrasound apparatus described in materials and methods. The data were successfully analysed and the echo amplitudes from both groups were saved for each angle.

3.3.1 Normality Test

The Shapiro-Wilk test result was > 0.05 (*p*-value = 0.000), therefore the data were not normally distributed.

3.3.2 Premolars

Overall, the signal angle dependency for premolars displayed a wide range of angles, 0–120° (Appendix 1). As expected, there were large differences in both amplitude and angle range between premolars, as each premolar had its own unique amplitude values and angle range. In Figure 3.7 below, 50% of the signal amplitude was between 15° and 85° (when the ultrasound beam met a planar surface), and the signal diminished significantly beyond this range. The full width at half maximum (FWHM) is the standard way to describe the width of plotted curves.

It is important to note that not all premolars reflected ultrasound at the start position and that some premolar had to rotate 50° ±2.50° before the echo with the highest amplitude was reached.

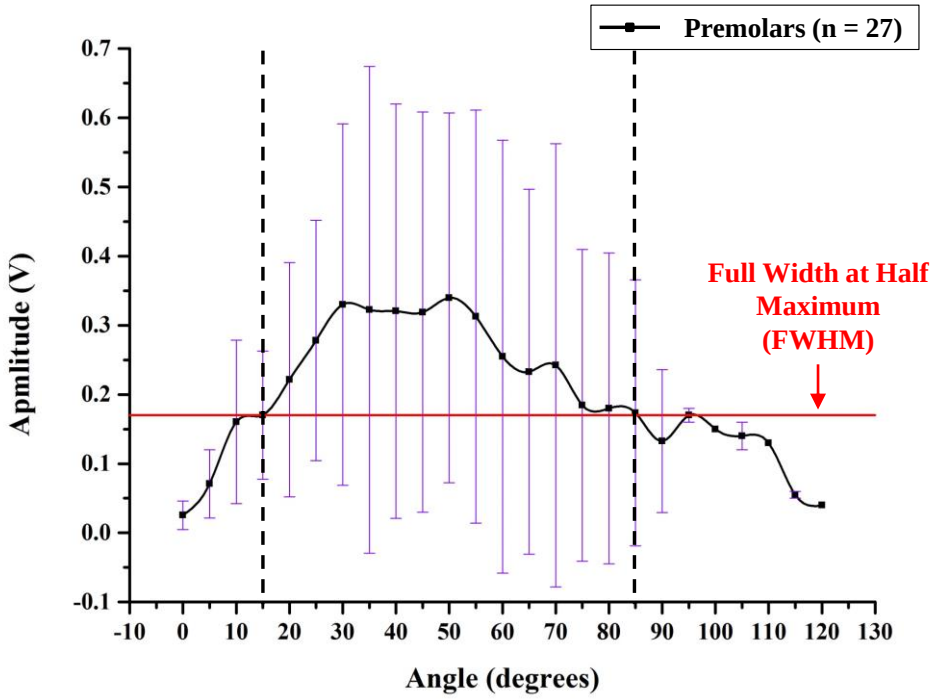

Figure 3.7. Mean of ultrasonic signal-angle dependency from 27 premolars. The line connecting the data points in Figure 3.7 was made to help the reader; it was not a waveform, *per se*.

3.3.3 Synthetic Maxillary Central Incisors

The synthetic maxillary central incisors displayed a narrower angle range than the premolars (Appendix 1). However, the incisors reflected an ultrasonic echo with the highest amplitude at 10° ±0.50° from the 'start' position, and by the second rotation, the highest amplitude appeared (Figure 3.8 below). Fifty per cent of the signal amplitude in Figure 3.8 was between 5° and 31° (when the ultrasound beam met a planar surface) and the signal diminished significantly beyond this range.

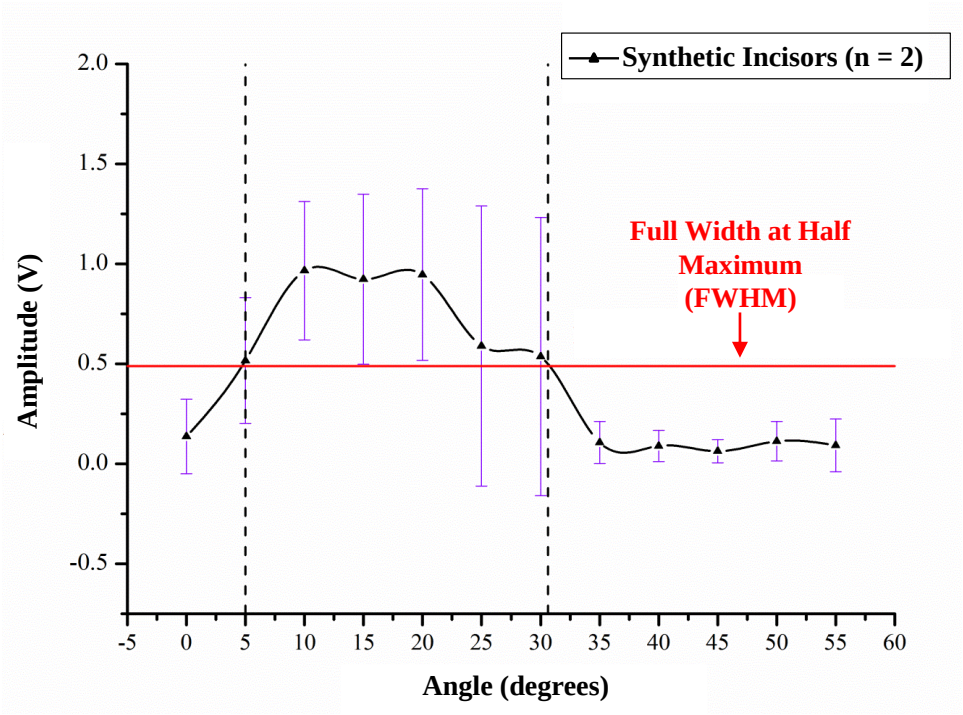

Figure 3.8. Mean ultrasonic angle dependency from two synthetic maxillary central incisors.

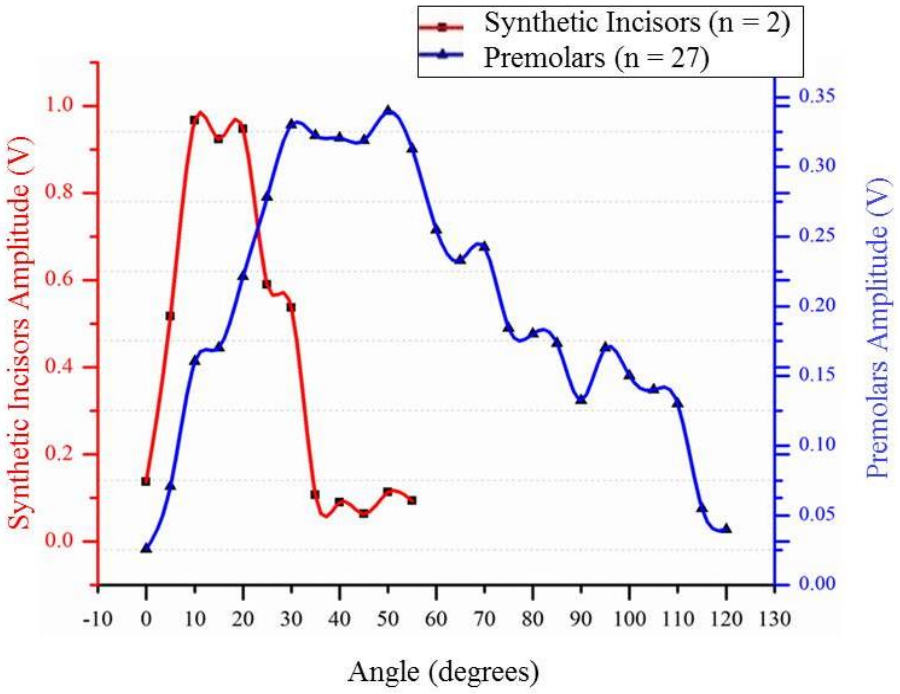

Figure 3.9. Signal-angle dependency of all premolars in blue and synthetic maxillary central incisors in red (observed values).

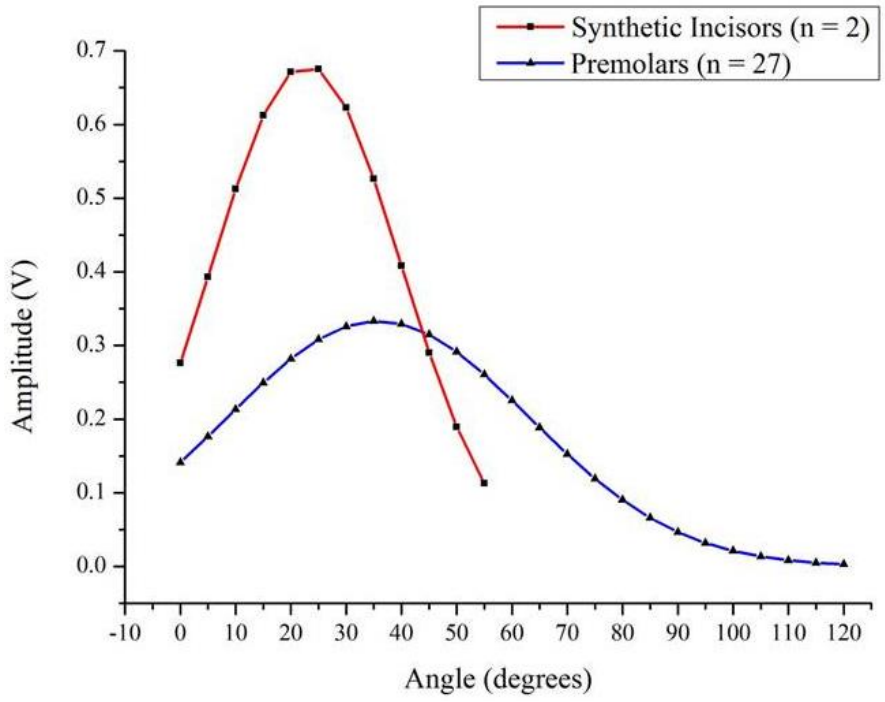

Figure 3.10. Fitted regression lines between angle and amplitude for each group. The size of interaction between group and angle indicated that there was a statistically significant difference between premolars and synthetic incisors (p-value < 0.001). The lines were back-transformed to the original scale for presentation.

3.4 Discussion

The issue of angle dependency is very important for the use of ultrasound to image human teeth. This is because teeth have complex geometry and multi-layered tissues, each with their own physical and chemical properties. Enamel, the hardest tissue in the human body, is composed of 98% hydroxyapatite crystals and 2% water. These crystals form the hierarchy of enamel in the form of hexagonal rods, known as enamel rods, which are 5 μm in diameter (Habelitz *et al.*, 2001). The orientation of these rods within the enamel is another important aspect when looking at ultrasound imagery of teeth (Lees and Rollins Jr, 1972).

Because enamel is anisotropic, the SOS tends to be higher in enamel sections where the rods are oriented along the path of the ultrasound beam and *vice versa* (Lees and Rollins Jr, 1972; Ng *et al.*, 1989; Maev *et al.*, 2002). This aspect does not affect the aim of this Chapter because it is focussed on the water-enamel interface in terms of echo reflection off that interface. However, in later Chapters, the orientation of enamel rods is more relevant.

In this Chapter ultrasound was examined in premolars and incisor teeth, which have very different shapes, and echo ultrasound differently. Ideally, a comparison of natural premolars with natural maxillary central incisors would have been done, but because there were no natural incisors available, synthetic incisors were used. The choice of synthetic maxillary central incisors does not undermine this work because the goal of this work was to investigate the ultrasonic reflection from the outer surface; thus, effects from the subsurface layer were not considered. The effects of anisotropy and orientation of the enamel rods in a real tooth were also irrelevant

here. The only relevant feature was the labial topography of the synthetic maxillary central incisors.

The results showed that the angle dependency in premolars did not reflect ultrasonic signal from the ‘start’ position and that several rotations of 5° ±0.45° were necessary to find an echo. It took some premolars 50° ±2.5° (ten rotations) until the highest echo was seen; comparatively, this angle was 10° ±0.50° (two rotations) for the synthetic maxillary central incisors. This means that the relationship between angle and amplitude significantly varies between the premolars and the synthetic maxillary central incisors (p-value < 0.001).

These differences are observed because premolars have non-planar buccal surfaces (the start position of ultrasound scans) and more often than not, the ultrasound beam does not hit the water-enamel interface at a right-angle, causing most of the reflected wave to scatter and not return back to the transducer. When the ultrasonic beam begins to meet a planar surface, the echoes begin to register. These planar surfaces were towards the mesial and distal aspects of the premolars, which explains why the stronger echoes were generated at those locations (angles 15–85°). The ultrasound signal amplitude in the premolars plummeted when the teeth deviated from their ideal angle range of 15–85° (dashed lines in Figure 3.7).

On the other hand, the synthetic maxillary central incisors had their strongest reflected ultrasonic signal at 10°, which was near the ‘start’ position (Figure 3.8). It was apparent from the results that the synthetic maxillary central incisors had a smaller signal angle range of 0–55°, compared to premolars with an angle range of 0–120°(Figure 3.9). This can be attributed to the fact that synthetic central incisors were inherently planar at the labial surface, and consequently, when the tooth rotates

beyond 55° ±2.75°, no planar surfaces were present to reflect the signal. In premolars, this was not the case. The premolars at any one time may not reflect a signal due to their non-planar surface, and at other times, a planar surface might exist at any location around their circumference, which is why their signal angle range was higher.

The mean amplitude measurements for the premolars demonstrated a wide spread (standard deviation) across the specimens and, indeed, within each specimen. Again, this is due to two factors: First, the varying surface topography of the premolars; second, the ultrasonic incident beam angle. This also explains the wide standard deviation of the mean amplitude measurements for the synthetic maxillary central incisors (although the surface was planar, the ultrasonic beam did not meet it at a right-angle consistently). Unlike the non-contact ultrasound scanning mode used in this experiment, contact ultrasound measurements (used in later Chapters) will help ensure that a right-angle is consistently present because the small transducer tip will be level with the enamel surface.

In summary, the results in this Chapter indicate that synthetic maxillary central incisors can readily produce ultrasonic echoes; thus, ultrasonic measurements were easier to obtain than in premolars. However, the limitations of this approach are threefold: First, knowing how much movement in a clinical hand-held mode will be equivalent to the angle of 25° ±1.25° (the angle in incisors after which 50% of the echo amplitude drops) is a problem and an interesting area for future research; second, the apparatus used here did not simulate a clinical setting, even though it demonstrated important aspects of the angle dependency for both premolars and incisors; third, the relatively small sample size of the synthetic incisors, may not accurately have covered the true variation seen in patients. However, the incisors are

produced from the same mould so they may not have different topographies reflecting the natural situation.

3.5 Conclusions

The conclusions that can be drawn from this Chapter are twofold:

- The measurement is made more difficult by the curvature of the tooth surface and it seems likely that larger, planar, incisors would give more satisfactory results.
- Premolars will be more sensitive to angle issues if B-mode imaging is used.

Nevertheless, the question remains on how adequate B-mode images are when performed on premolars? This will be discussed in the following Chapter.

4 Cross-Sectional Imaging

4.1 Introduction

It is apparent from the study of the A-mode echoes and their angle dependency described in Chapter 3 that confidently identifying anatomical features with ultrasound is not trivial. Nonetheless, other authors such as Hua *et al.* (2009) have used B-mode ultrasound imaging to identify such features and to successfully measure enamel thickness. Hua *et al.* have built upon the work of Culjat *et al.* (2003) and demonstrated that image processing could facilitate measurement of the enamel layer on B-mode images and improve its detection, providing hope that ultrasound could be used to monitor progressive enamel loss (erosive TSL). Hua *et al.* used a 13 MHz linear array transducer and reported good results after comparing their measurements with μ-CT.

Based on these promising results, it was therefore decided to evaluate the feasibility of B-mode ultrasound imaging of the enamel layer on human premolar teeth. Two experiments were set up, the first used an ultrasound apparatus built in-house (Figure 4.1), while the second B-mode experiment was done utilising a commercial high-frequency ultrasound scanner (Figure 4.16, p.99). Since this creates a family of cross-sectional images, it is convenient to validate such studies with μ-CT. The main purpose of this Chapter was to investigate whether the B-mode images obtained from both experiments were clear enough to measure enamel thickness and to assess their agreement with μ-CT. The aims of this chapter are:

- to extend this approach to assess more teeth
- use a higher frequency and a potentially more automated system
- to compare the agreement of two ultrasonic systems with μ-CT

4.2 B-Mode Imaging Using In-House Ultrasound Apparatus

4.2.1 Introduction

Harput *et al.* (2011) used a custom-made ultrasonic imaging system for human teeth with good results *in vitro*. They used this imaging system to circumferentially scan a human molar tooth with ultrasound to produce an ultrasonic echo map of the enamel layer. Their raw ultrasonic A-mode data was subsequently converted to greyscale images (B-mode image) of the enamel layer, from which enamel thickness measurements were calculated. The results were verified with μ-CT which showed that the standard error of the mean was 13.4% after using a filter and 5.5% after using fractional Fourier transform (FrFT). This section explores the use of an ultrasound apparatus built in-house to image human premolar teeth and compare the B-mode images generated with μ-CT.

4.2.2 Materials and Methods

4.2.2.1 Tooth Selection and Storage

Fifteen human premolars were randomly selected from the sample set described in Chapter 3. The teeth were kept hydrated in 0.1% thymol (Sigma Aldrich, MO, USA) solution and stored in the laboratory refrigerator at 5 °C.

4.2.2.2 Ultrasonic Setup

An ultrasonic pulse-echo technique was used to circumferentially scan each tooth with a 20 MHz transducer (V208-RM, Olympus® Inc., MA, USA) using the apparatus described in Chapter 3, which is similar to the apparatus used by Culjat *et*

al. (2003) and Harput *et al.* (2011) but with a change of transducer frequency (20 MHz) and the use of a macro (written by Mr Mohammed Khan, University of Leeds) for automating the scans and converting them into B-mode images (Appendix 2). The premolar tooth was mounted into a brass holder using impression compound (Kemco, Kemdent®, UK). The tooth was then rotated while the A-mode ultrasound scans were captured. To improve the signal-to-noise ratio, 1000 pulses were averaged for each scan by the oscilloscope to create an ASCII data file for export to a PC via an RS-232 cable (Figure 4.1).

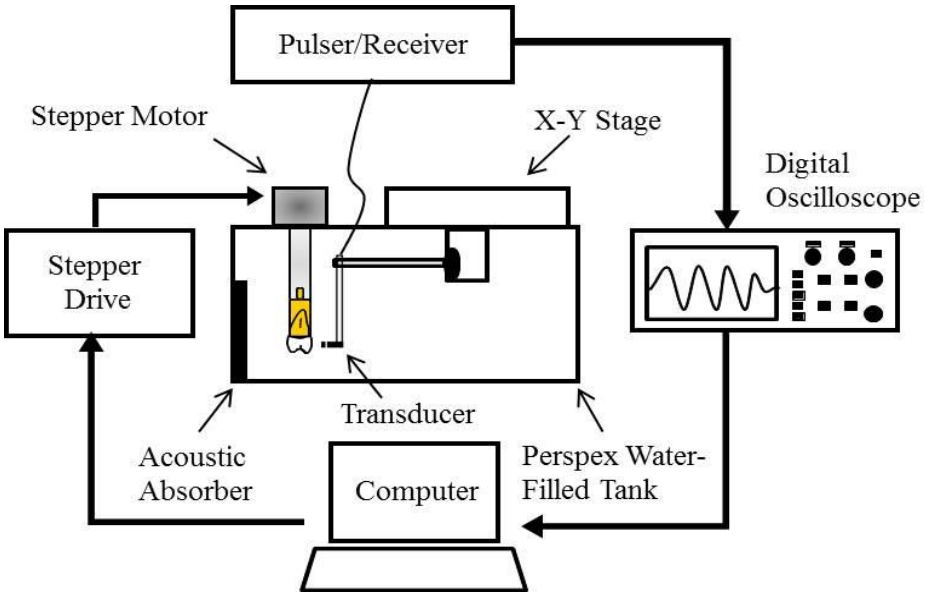

Figure 4.1. Ultrasonic apparatus used for the scans.

4.2.2.3 Phantom Test

In order to determine whether the experimental setup was operational and could perform as required (creation of a B-mode image from A-mode data); a cylindrical 1 mm thick plastic tube with a diameter of 8 mm was mounted in the brass holder with impression compound to approximate this test to the actual tooth experiment. To avoid bias in the ultrasound measurements, the internal diameter of the tube was

measured after the ultrasonic scans were made via a digital calliper with a resolution of 0.01 mm (101-45, Hitek, China).

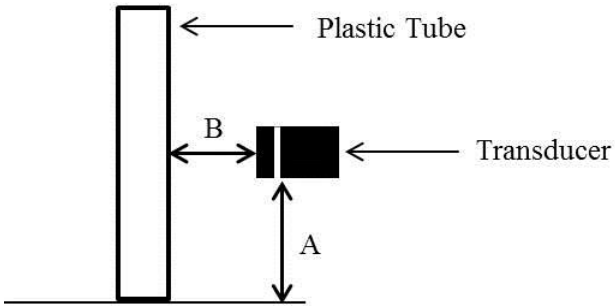

Figure 4.2. Location of transducer relative to the plastic tube.

The transducer was placed opposing the plastic tube to circumferentially scan it. The transducer was kept stationary while continuously firing signals at the tube. In Figure 4.2 the transducer at the start of the circumferential ultrasonic scan was at a vertical distance, 'A', and a horizontal distance, 'B'. Distance 'A' was recorded and used when verifying the ultrasonic A-mode scans with thickness of the tube. The horizontal distance was kept static at all times once the vertical distance was known.

In the screen capture in Figure 4.3, the transducer diameter is 3.175 mm because only one transducer was used; the normalised focal length (SF), which is set to 1 for transducers that have a flat front face (unfocussed). After measuring the external diameter of the tube with the digital calliper at the level of scan, the value was inserted in its field (in this example it was 8 mm). Once all values were inserted as seen in Figure 4.3, the button "Calculate" was clicked to generate, based on the macro code, the beam width, circumference, number of steps (1000 steps = 10°), beam overlap and the rotation angle required for a full scan around the tube.

The stepper drive, which controls the rotation of the stepper motor, was programmed (via the manufacturer's software) to allow the tube to rotate in ~6 ±0.30º until the

tube was fully scanned. At the start of the scan and before the tube rotated, the received signal from that site was saved in ASCII format. When the first 6º rotation was made, a second signal was received and saved. The rotation angle was chosen such that the second ultrasonic scan line overlapped the initial one by half a beam width, and the third scan line slightly overlapped the second one by the same amount and so forth. This overlap was important to ensure all the tube was scanned and will result in a continuous tube wall when the B-mode image is formed later. This cycle continued until the tube was fully scanned and a signals database was generated for a 'slice' through the tube.

The number of ultrasonic scans for the tube is dependent on its circumference and beam width. After calculating the circumference, the number of ultrasonic scan lines required can be derived by dividing the circumference by the beam width. However, because an overlap of half a beam width is required, the number of ultrasonic scans ('number of increments' in Figure 4.3) is multiplied by two. After completing the scans for the tube, the steel rod and the brass holder attached to it were removed from the stepper motor and placed in a bowl of warm water, so the tube could be taken out from the brass holder.

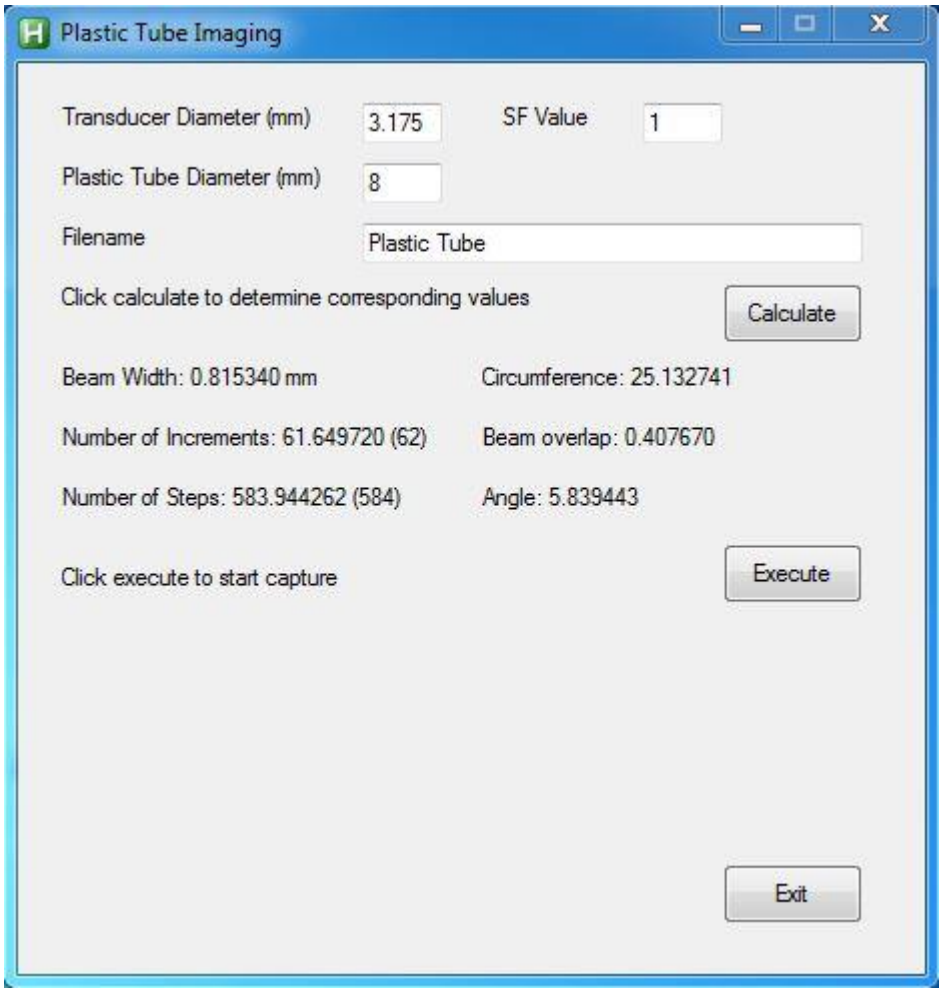

Figure 4.3. A screen capture of the macro's user interface depicting the input parameters for the plastic tube.

4.2.2.4 A-Mode Scans of Premolars

The same process for scanning the tube was used for scanning teeth. The transducer was placed opposing the premolar (Figure 4.4 below) at a planar area determined visually. The level of the circumferential scan was determined by the topology of the premolar surface. When there was a relatively planar area on the buccal surface; it was chosen as the 'start' point for the scan. The scan was a 'slice' in the horizontal plane of the tooth's crown. The number of ultrasonic scans for each tooth was dependent on its circumference and beam width. Assuming that the teeth are circular in cross-section, a circumference was calculated from the measured diameter (Figure 4.5).

The first ultrasonic scan was always started on the buccal surface of the tooth and each scan was repeated three times and the mean taken (Figure 4.6). A trial scan was performed to make sure that the tooth rotated freely, was in line with the transducer and that the ultrasound scans could be successfully stored.

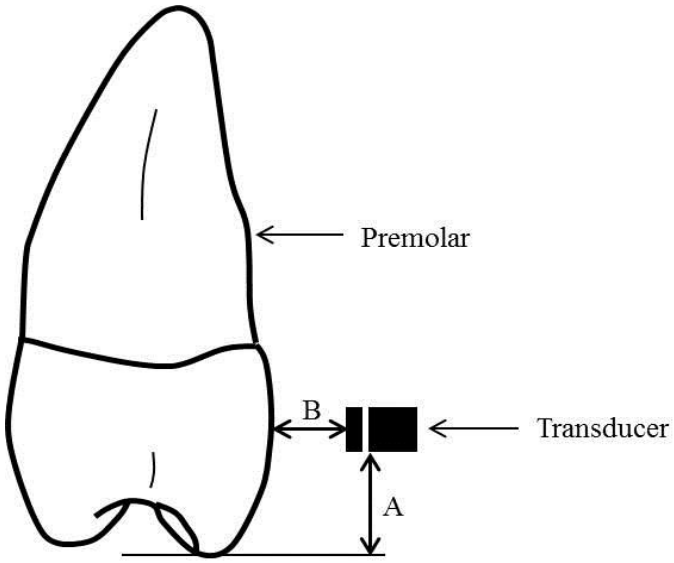

Figure 4.4. The location of the 20 MHz transducer relative to the tooth at the start of the scan.

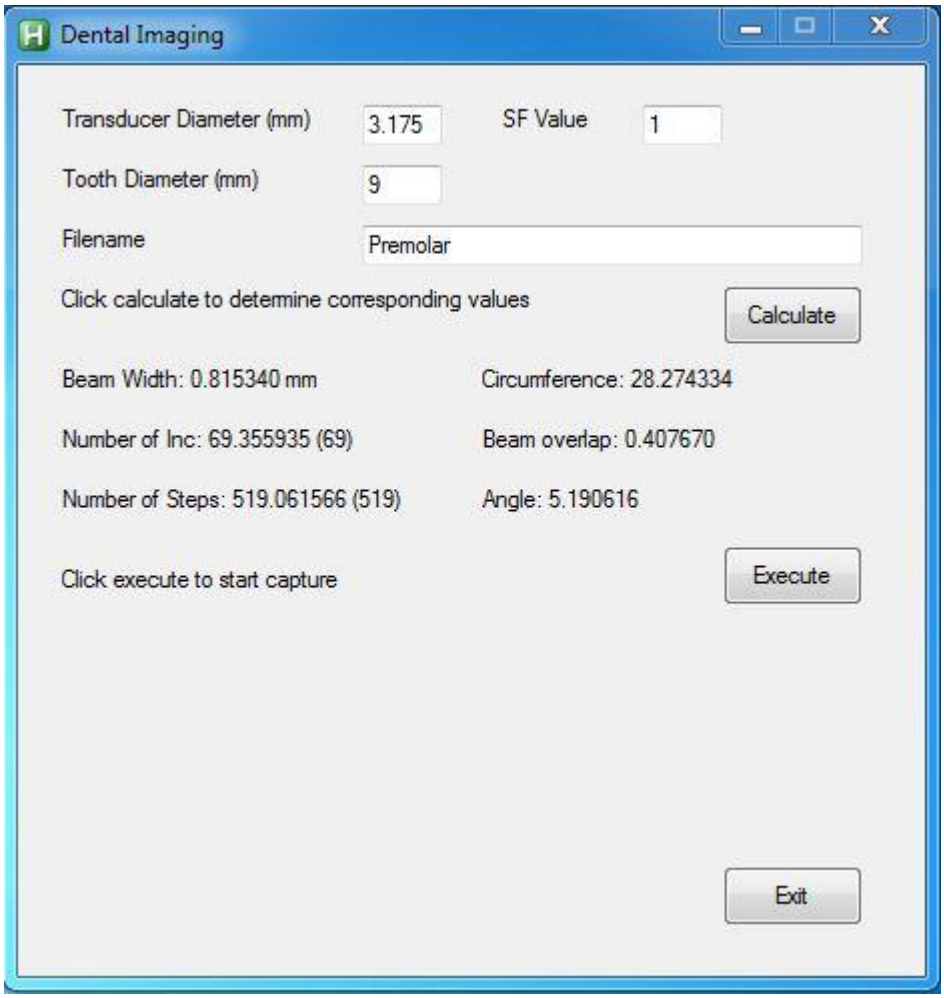

Figure 4.5. A screen capture of the macro's user interface depicting the input parameters for the premolar tooth.

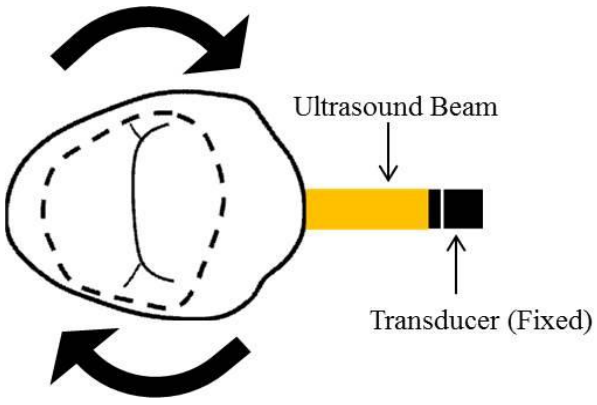

Figure 4.6. A schematic of the premolar and the transducer's position at the start of the ultrasonic scan.

4.2.2.5 Conversion of A-Mode Scans of the Plastic Tube to B-mode Images

The B-mode image created for the plastic tube was a result of the collected signals (A-mode scans), where the external and internal tube wall echo amplitudes were converted into pixel values (via a macro) which could be viewed as a greyscale image (B-mode image). Each signal obtained had the same number of data points (2500 points). A data point represents a value of amplitude at a certain period of time. The time base on the oscilloscope was 0.5 μm per division.

When the ultrasound signal arrived at the surface of the plastic tube, an echo was generated and when the remainder of the signal continued its path until it reached the internal wall of the plastic tube, a second echo developed. The amplitude values of the two echoes were extracted from each signal by the macro. These two amplitude values, separated by TOF, were used to create two pixels in the B-mode image. After the first scan line was created on the B-mode image, the second scan line (obtained when the plastic tube rotated) had a second pair of amplitude values separated by another TOF and these were also fed into the B-mode image to create the second scan line.

Because the pixels had spatial coordinates on the blank image they will fall adjacent to the first scan line and so forth until the circumferential cross-section of the plastic tube is plotted in B-mode. The greyscale intensity of each pixel in the B-mode image is determined by the original amplitude of the data point from which the pixel was formed.

For each line of A-mode data, the angle of the beam, θ, is known (stepper motor rotation angle) and the distance between the transducer and any reflector, r', is calculated from the TOF, t, assuming $r' = vt/2$ where v is the SOS. To map this onto

x and *y* coordinates required for B-mode display, the raw polar coordinates were transformed by means of a macro into *x* and *y* (Cartesian coordinates). To plot the tube echoes in an optimal position relative to the centre of rotation in the B-mode display, the distance between the transducer and the centre of rotation had to be known. To calculate this distance, a thin metal rod was embedded in the brass holder (attached to the motor axle) and ultrasound was fired at the metal rod.

The TOF between the echo generated at the transducer-water interface and the water-metal rod interface was calculated from the oscilloscope. In this experiment, θ had to be a value that allows for an overlap to occur between subsequent ultrasound beams around the tube. If the angle is larger than the beam width there would be missing sections from the final B-mode image of the tube. As mentioned earlier, each ultrasonic scan line creates two echoes in the form of greyscale pixels in the image, corresponding to the tube external and internal wall.

4.2.2.6 Conversion of A-Mode Scans of the Premolars to B-mode Images

The same process for the plastic tube was used for creating B-mode images of premolars.

4.2.2.7 Data Analysis

For the plastic tube, a total of 62 ASCII data files were imported into MATLAB® and plotted to create a waveform onto which an imaging macro (written by Mr Mohammed Khan, University of Leeds) was applied. For premolars, a total of 1030 ASCII data files were imported into MATLAB® for analysis. Each tooth had its own ASCII data files that were plotted to produce the A-mode waveform. A MATLAB® macro was used so that all the waveforms were plotted to form the B-mode image. Because there was some noise in the raw A-mode waveform, a Butterworth filter (Butterworth, 1930) was incorporated in the macro to remove

irrelevant noise from the waveform. The macro incorporated a final step in which the envelope of the waveform was obtained, further clarifying the echo peaks before conversion into B-mode images.

4.2.2.8 μ-CT Scans

All teeth that underwent ultrasound imaging were scanned with μ-CT (μ-CT 80, Scanco Medical AG, Switzerland) so that the ultrasound enamel thickness was verified (Figure 4.8 and Figure 4.9 on p.88). Each tooth was placed in a clear acrylic container and secured from the root end with impression compound (Kemco, Kemdent®, UK). Blu-Tac® (Bostik, Inc., WI, USA) was used as a radio-opaque reference point that was placed near the distal surface of the crown. The scans were at a resolution of 0.072 mm and were in the corono-apical direction. The images were saved in digital imaging and communications in medicine (DICOM) format for further analysis.

4.2.2.9 Cross-Sectional Image Measurements

After converting the A-mode scans into B-mode, fifteen B-mode images were imported to ImageJ software, version 1.46r (Schneider *et al.*, 2012) where the enamel thickness measurements were made using the line selection tool. The scale of the line selection tool in ImageJ was set to conform to the scale of the tooth so that precise measurements were obtained. Three repeat radial measurements for the enamel thickness were made at three sites (on the buccal surface of the tooth in each B-mode image) and the results were compared with their μ-CT counterparts to verify the enamel thickness at the three sites.

The resolution of μ-CT images (0.072 mm) is higher than the ultrasound beam width (0.81 mm); therefore, the mean of ~11 μ-CT images was taken by creating an image stack comprised of 11 μ-CT images in ImageJ and an ‘average intensity’ function

was chosen to combine the images into one averaged image. The number of μ-CT images required for averaging was determined by dividing the ultrasound 'slice' thickness of 0.81 mm by the slice thickness for the μ-CT, which was 0.072 mm (Figure 4.7 below).

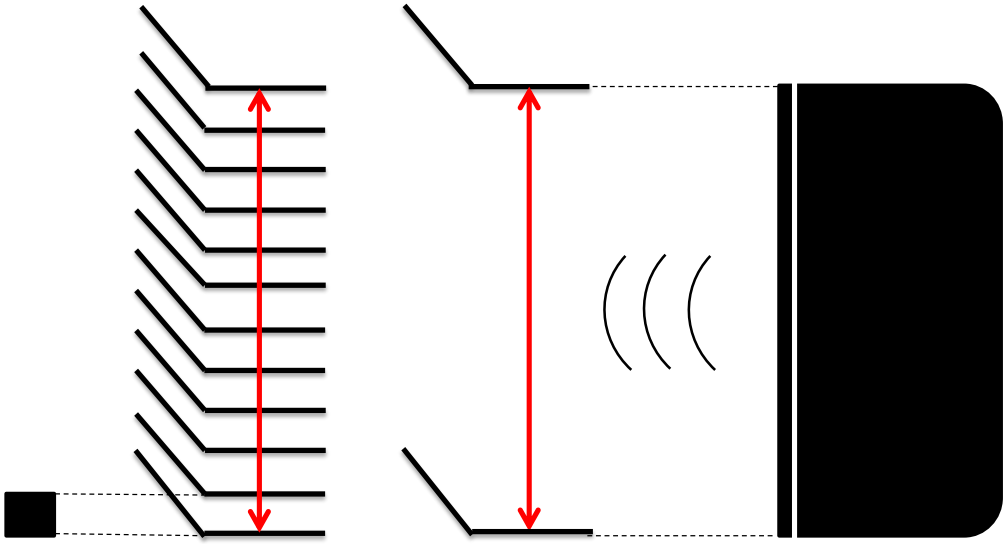

Figure 4.7. Schematic depicting ultrasound beam width versus μ-CT.

4.2.2.10 Statistical Methods for In-house Ultrasound Apparatus

The statistical analysis was performed to determine the agreement between the enamel thickness measurement obtained from B-mode imaging using the in-house ultrasound apparatus and their μ-CT counterparts. The data was examined using the Bland-Altman limits of agreement method (Bland and Altman, 1986). This method measures, in real terms, the size of differences between pairs of values that are likely to occur. This measure is obtained by first calculating the difference between the two values for each tooth. The 95% limits of agreement (within which 95% of all differences between values should occur) are then calculated as follows:

Mean difference +/- 1.96 × (standard deviation of differences)

In addition, a hypothesis test was performed.

- The null hypothesis was: there is no difference between the in-house ultrasound apparatus and μ-CT in measuring enamel thickness of human premolars.
- The alternative hypothesis was: there is a difference between the in-house ultrasound apparatus and μ-CT in measuring enamel thickness of human premolars.

Prior to hypothesis testing, the Shapiro-Wilk test was used to check if the data was normally distributed. The significance level for the normality test was set at $\alpha = 0.05$. If the *p*-value for the test was < 0.05 then the data were not normally distributed and a non-parametric test, such as the Wilcoxon sign rank test was used instead of the paired t-test. However, if the *p*-value was > 0.05 then the data were deemed normally distributed and the paired t-test was used. The significance level for the hypothesis test was set at $\alpha = 0.05$. All statistical analyses were done using IBM® SPSS® version 20 (IBM SPSS®, IBM® Corp., NY, USA).

Figure 4.8. μ-CT 80 Scanco Machine.

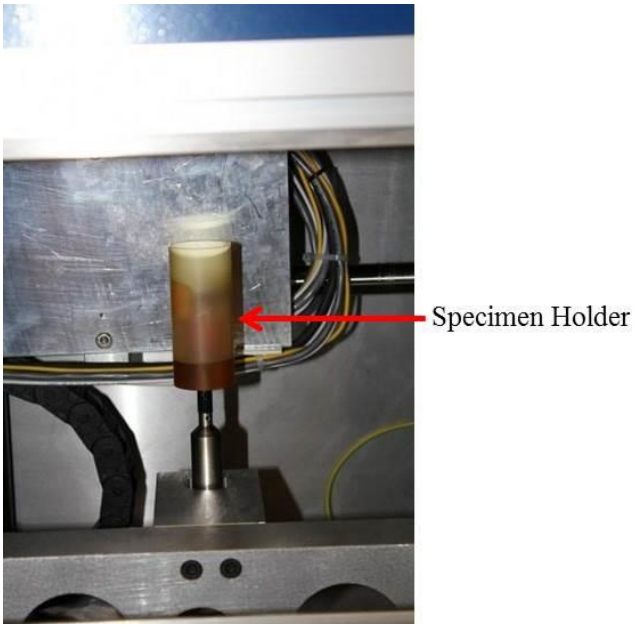

Figure 4.9. μ-CT Scanco Machine's specimen holder *in-situ*.

4.2.3 Results

The A-mode ultrasound scans for the plastic tube and the premolar teeth were captured and generation of the B-mode images was successfully performed using the macro programme. The 'true' thicknesses of both the plastic tube and the enamel layer of the premolar teeth were successfully verified.

4.2.3.1 Phantom Test

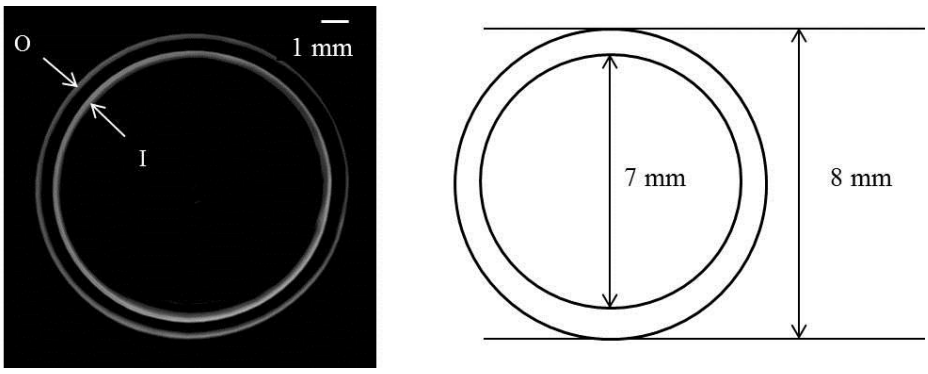

Figure 4.10. A circumferential B-mode image of a plastic tube that was used to test the ultrasonic setup. The image displays the tube's outer, O, and inner, I, borders with a thickness of 1 mm.

4.2.3.2 A-Mode Scans of Premolars

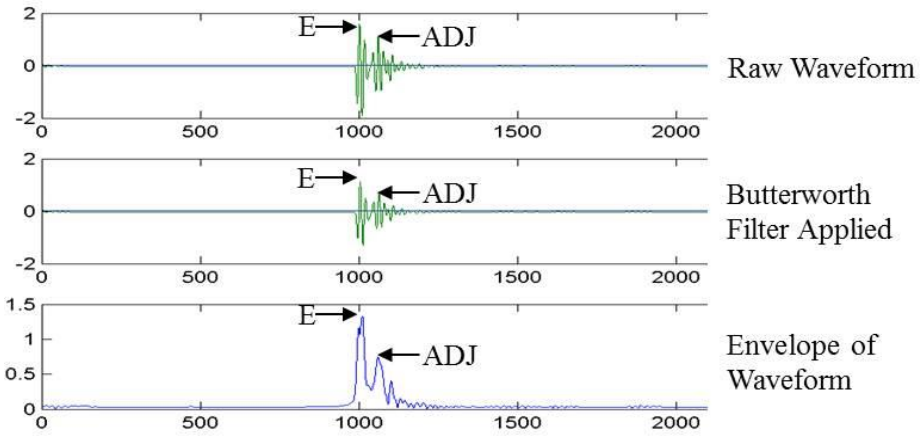

Figure 4.11. A sample waveform of a scanned premolar with a Butterworth filter applied, after which the envelope of the waveform was obtained, all in MATLAB®. 'E' depicts the enamel echo and 'ADJ' depicts the amelo-dentinal junction's echo.

4.2.3.3 Conversion of A-Mode Scans of Premolars to B-mode Images

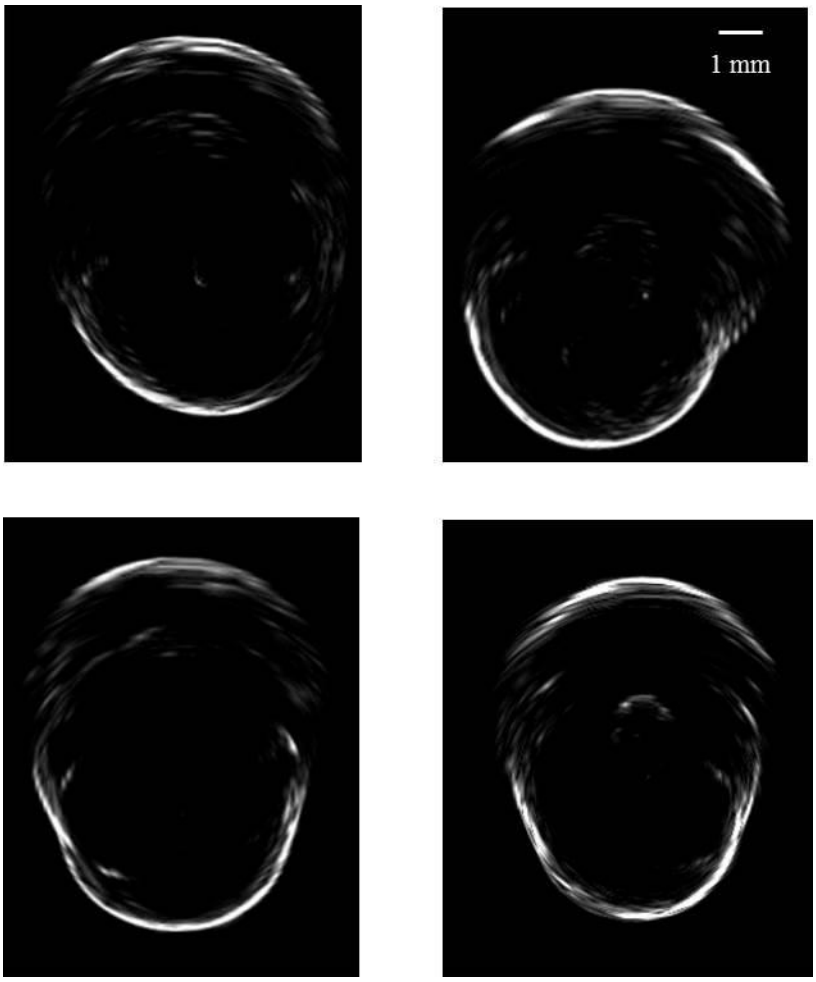

Figure 4.12. Representative sample of B-mode images obtained from A-mode ultrasound scans of four premolar teeth

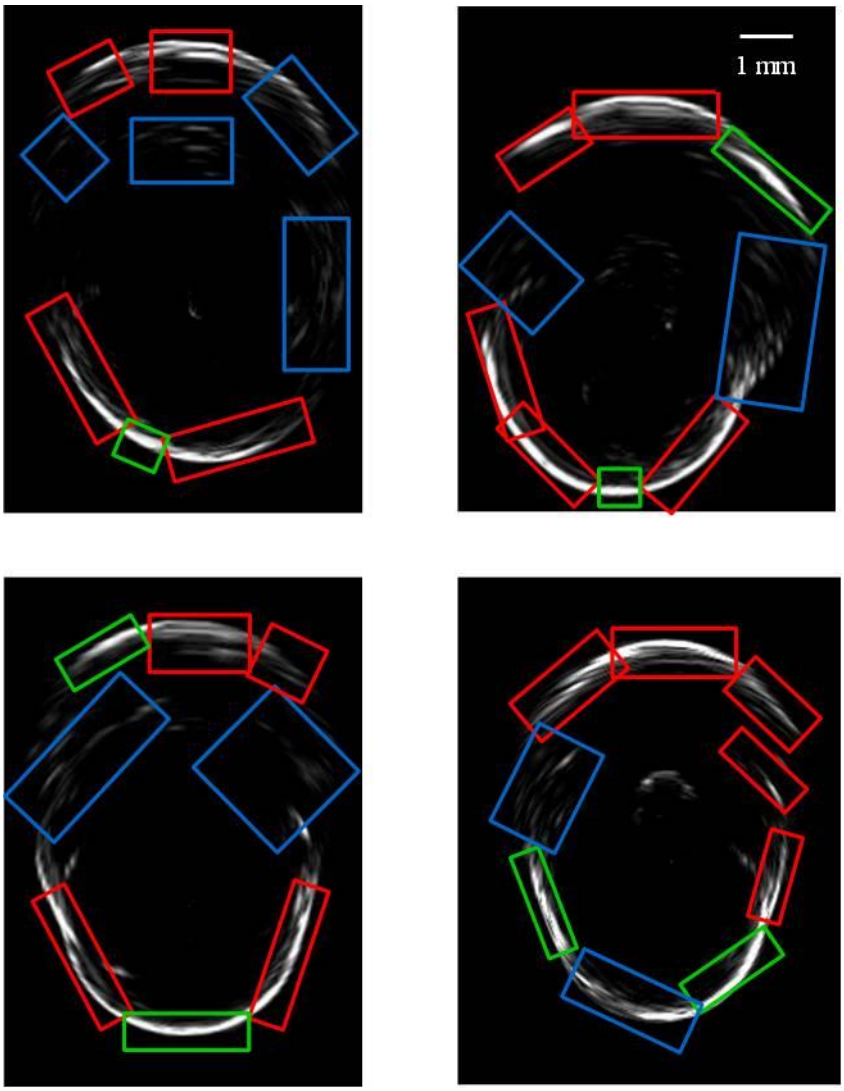

Figure 4.13. The same teeth in Figure 4.12 with identifiable enamel layer in red borders.

4.2.3.4 Cross-Sectional Images' Measurements

Table 4.1. Summary of results obtained from measuring enamel thickness with the in-house ultrasound apparatus and μ-CT (mm).

Tooth	B-mode enamel thickness (±SD)*	μ-CT enamel thickness (±SD)*	Difference
1	0.69 (0.02)	1.93 (0.03)	-1.25
2	0.67 (0.02)	0.87 (0.01)	-0.21
3	0.64 (0.01)	1.03 (0.04)	-0.39
4	1.30 (0.06)	0.86 (0.02)	0.44
5	1.46 (0.01)	1.45 (0.13)	0.01
6	0.81 (0.02)	1.19 (0.09)	-0.38
7	0.91 (0.01)	1.11 (0.08)	-0.20
8	1.42 (0.01)	0.47 (0.03)	0.95
9	0.89 (0.03)	1.12 (0.08)	-0.22
10	0.74 (0.03)	1.37 (0.06)	-0.63
11	0.61 (0.02)	1.52 (0.05)	-0.92
12	0.74 (0.02)	0.56 (0.07)	0.18
13	0.55 (0.01)	0.63 (0.01)	-0.08
14	0.57 (0.05)	0.57 (0.05)	0.00
15	0.68 (0.01)	0.58 (0.04)	0.10
			Range (-1.25 – 0.95)

*Each measurement was a mean of 3 repeat measurements.

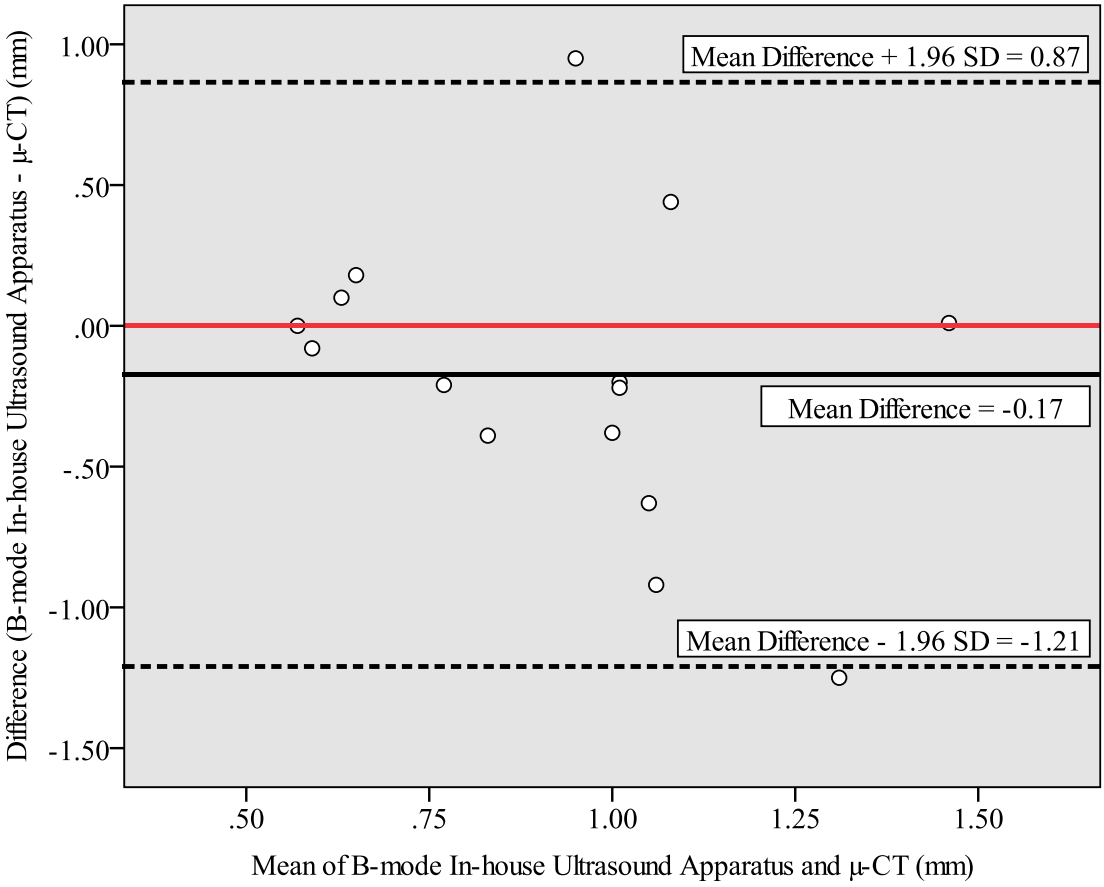

Figure 4.14. Bland-Altman plot showing the agreement in measuring enamel thickness between B-mode of in-house ultrasound apparatus and μ-CT (n = 15).

The lines marked in Figure 4.14 are the upper and lower limits of agreement (dashed black lines), the mean difference between the two pairs of measurements (solid black line) and the zero line as reference (red line).

Table 4.2. Summary of the Bland-Altman results obtained from B-mode of in-house ultrasound apparatus and μ-CT (mm).

Mean Difference (B-mode of in-house ultrasound apparatus – μ-CT)	SD Difference	95% Bland-Altman Limits of Agreement
-0.17	0.53	(-1.21, 0.87)

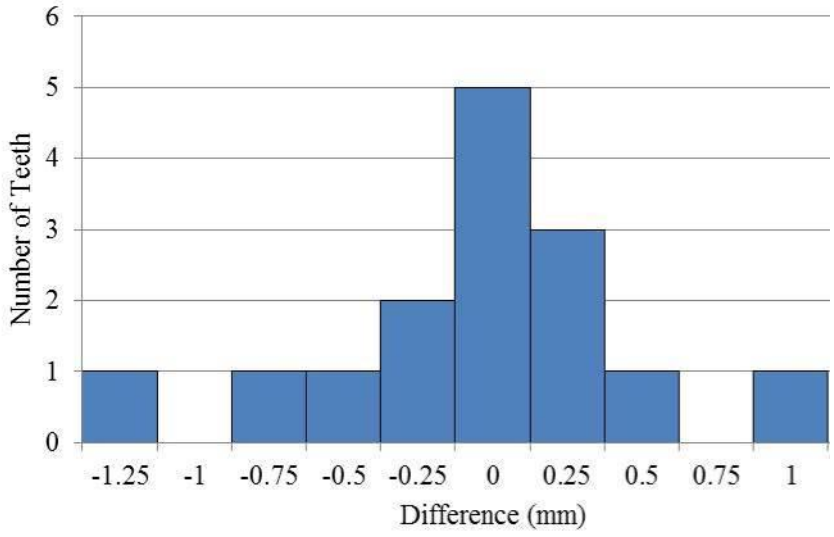

Figure 4.15. Difference between B-mode of in-house ultrasound apparatus and μ-CT in measuring enamel thickness in premolars at the same site (n = 15).

4.2.3.5 Test of Normality

The Shapiro-Wilk test result gave a *p*-value of 0.90 (Table 4.3), therefore the data followed a normal distribution.

Table 4.3. Shapiro-Wilk normality test for the difference in enamel thickness measurements obtained with in-house ultrasound apparatus and μ-CT

Method	Statistic	df	Sig.
Ultrasound - μ-CT	0.97	15	0.90

4.2.3.6 Paired t-test

Table 4.4. Hypothesis test result

Method	Mean Difference (mm)	SE Mean Difference	95% CI of Difference (Lower)	95% CI of Difference (Upper)	T	df	Sig.
Ultrasound and μ-CT	-0.17	0.17	-0.46	0.12	-1.26	14	0.23

The results of the paired t-test indicated that the *p* value was > 0.05 (*p*-value = 0.23) therefore the null hypothesis was not rejected. This means that there was no

statistically significant difference between both methods in measuring enamel thickness.

4.2.3.7 Descriptive Statistics

Table 4.5. Paired samples descriptive statistics (mm).

Method(s)	n	Range	Minimum	Maximum	Mean	SE
Ultrasound	15	0.91	0.55	1.46	0.85	0.08
μ-CT	15	1.46	0.47	1.93	1.02	0.11

4.2.4 Discussion

This section was primarily focussed on using B-mode ultrasound to measure enamel thickness. Like X-rays, but without ionising radiation, ultrasound can generate images of teeth (B-mode) provided the right frequency is used.

The results from the phantom test experiment using the in-house ultrasonic scanner were encouraging because the setup functioned appropriately and the automation process proceeded as anticipated. Furthermore, the phantom test result revealed that the actual thickness of the plastic tube has matched that seen in the B-mode image, where the actual thickness was 1 ± 0.01 mm and the ultrasound thickness was 1 ± 0.09 mm (Figure 4.10). This agreement was not surprising as the SOS did not vary across the plastic tube (i.e. there was no SOS anisotropy). Another reason for this agreement is the clarity of the tube boundaries in the B-mode image, which was due to less ultrasonic signal loss in the fairly homogenous plastic tube.

Figure 4.11 depicts a sample waveform with the enamel and ADJ echoes present. It is these echoes (Enamel and ADJ) from each waveform that were used to generate the pixels of the B-mode image using the macro programme, which was written by

Mr Mohammed Khan, University of Leeds. The envelope of the waveform made it easier to locate the peaks of the enamel and ADJ boundaries.

The results demonstrated that the in-house ultrasound apparatus was able to generate B-mode images of the premolars (Figure 4.12). The enamel thickness measurements from the B-mode images of the premolar teeth showed some discrepancy when compared to their μ-CT counterparts and the Bland-Altman 95% limits of agreement ranged from -1.21 to 0.87 mm with a mean difference of -0.17 mm. Despite having no statistically significant difference between both methods (p-value = 0.23), it is unlikely that this apparatus will be able to measure enamel thickness accurately. This is because the disagreement between both methods can reach 1.04 mm on average. However, there were some occasions in which the apparatus showed very good agreement with μ-CT on 5 teeth (see Figure 4.15). The reason for the large discrepancy between both techniques lies primarily in the boundary detection capability of the in-house apparatus (water-enamel and ADJ). Boundary detection is dependent on the amount of ultrasound energy returning to the transducer. More energy returning means more pixel intensity on the image and therefore boundaries are easier to detect.

In the red marked areas of Figure 4.13 the front surface of the enamel layer is more visible than the less echogenic ADJ because the received echoes from the ADJ were lower than those of the front enamel surface, resulting in lower greyscale intensity for the pixels (the pixel greyscale intensity is directly proportional to the echo generating it).

The weaker ADJ echo could be due to several causes: First, attenuation of the sound wave can sometimes be problematic, especially in hard dental tissues; second, the

ultrasound wave might not have met the enamel surface at an appropriate angle, resulting in minimal echoes from the ADJ. This signal loss complicated enamel thickness measurements in some areas of the image, where no thickness was measured; a third factor underlying the weaker ADJ echo was operator error arising from selecting an inaccurate ADJ interface.

This inaccuracy stems from multiple consecutive echoes known as reverberations (Zagzebski, 1996) that mimic the actual interface, which add an element of uncertainty as to which one of the echoes is the real interface. The reverberations appear as small opaque lines in the B-mode image marked in blue (Figure 4.13). This problem is seen when ultrasound travels in materials with high SOS, causing the sound to rattle back and forth and generating those echoes. Fourth, the SOS in enamel was assumed at ~6000 ms^{-1} based on the mean value from the literature (see Table 1.1 in Chapter 1).

All these reasons render B-mode enamel thickness measurements using the in-house apparatus challenging. It is important to mention that the imaging process in our work was too time consuming to be acceptable clinically. Typically, the time required to obtain all necessary data from the tooth in A-mode is ~17 minutes for each tooth; second, the time required to transform A-mode data to B-mode images (~5 minutes); third, the time spent in image analysis and measuring enamel thickness from the B-mode images and their μ-CT counterpart (~5 minutes).

4.3 B-mode Imaging Using a Commercial Ultrasound Scanner

4.3.1 Introduction

B-mode images can be obtained automatically by using a commercial ultrasound scanner or, manually where the processing part is done through a programme written specifically for this purpose (section 4.2, p.76). In this Chapter, both modes were explored; manual (in-house ultrasonic scanner) B-mode image generation and automatic (commercial ultrasonic scanner). Since the time required for B-mode imaging was a critical issue in the previous experiment, a real-time commercial ultrasound scanner that automatically produces B-mode images was investigated.

Commercial ultrasonic scanners are widely available both at low frequencies 3-10 MHz for clinical scanning and high frequency between 30 – 50 MHz for preclinical scanning, but all of these are designed for work with soft tissues with an assumed SOS of 1540 ms^{-1} (around four times slower than the mean SOS in enamel, which is 6000 ms^{-1} (see Table 1.1, p.20). Nonetheless, it was decided to evaluate the feasibility of using such a scanner for dental work. Previous research was performed using single element transducers that were able to produce B-mode images of human teeth (Culjat *et al.*, 2003; Hughes *et al.*, 2009; Harput *et al.*, 2011). However, multiple problems were identified such as missed areas on the tooth surface where the incident ultrasound beam was scattered due to an angled surface or due to high anisotropy in that area.

Another feature of the commercial scanner used in this Chapter was its high-frequency transducer, which yields better images resolution. The ability of an ultrasonic transducer to mechanically vibrate whilst sending and receiving ultrasonic signals improves the quality of the resultant B-mode image. This is because multiple

sequential ultrasound beams are sent to the object and therefore more data are collected from it. The ultrasonic scanner used in this section benefited from such a transducer.

4.3.2 Materials and Methods

4.3.2.1 Commercial Ultrasound Scanner

The scans were done using a commercial high-frequency ultrasound scanner (Vevo 770®, Visual Sonics® Inc., Canada) shown in Figure 4.16 that benefited from a 40 MHz focussed transducer (VS-11170, RMV 704, Visual Sonics® Inc., Canada) shown in Figure 4.17.

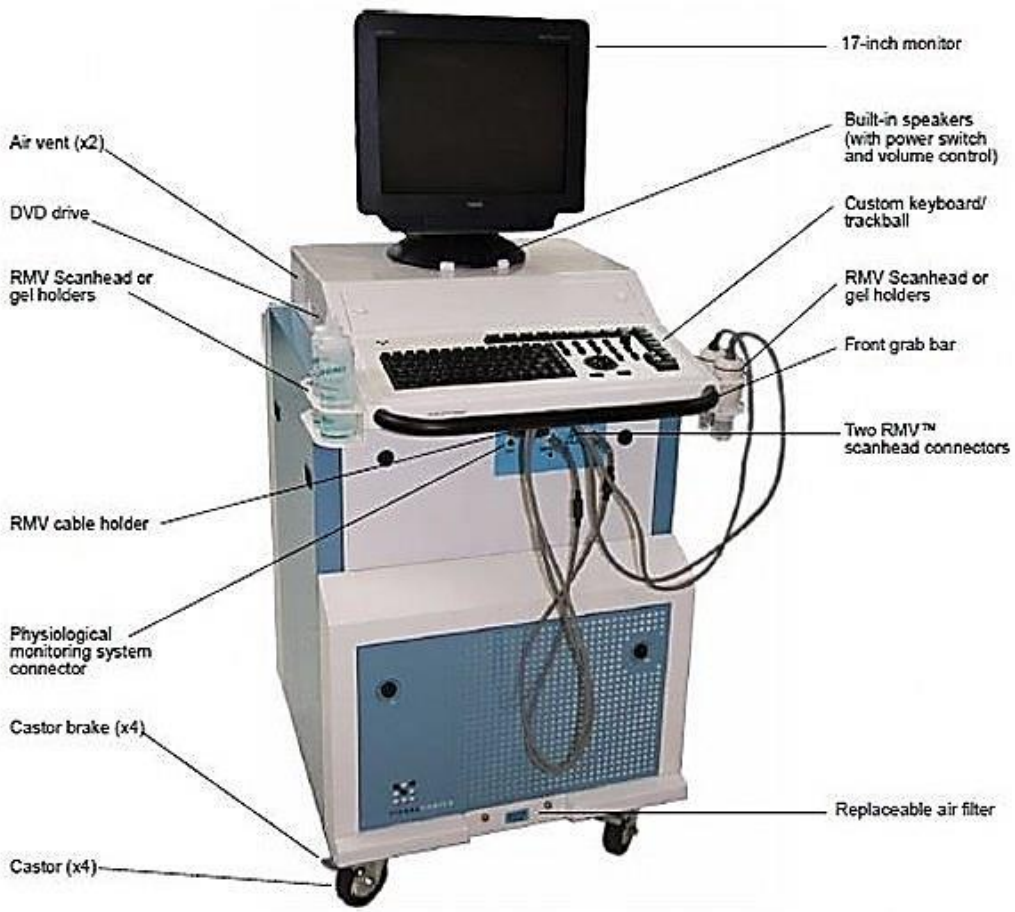

Figure 4.16. Vevo 770® high-frequency ultrasound scanner, front view. [Reproduced with permission from Visual Sonics®, Inc].

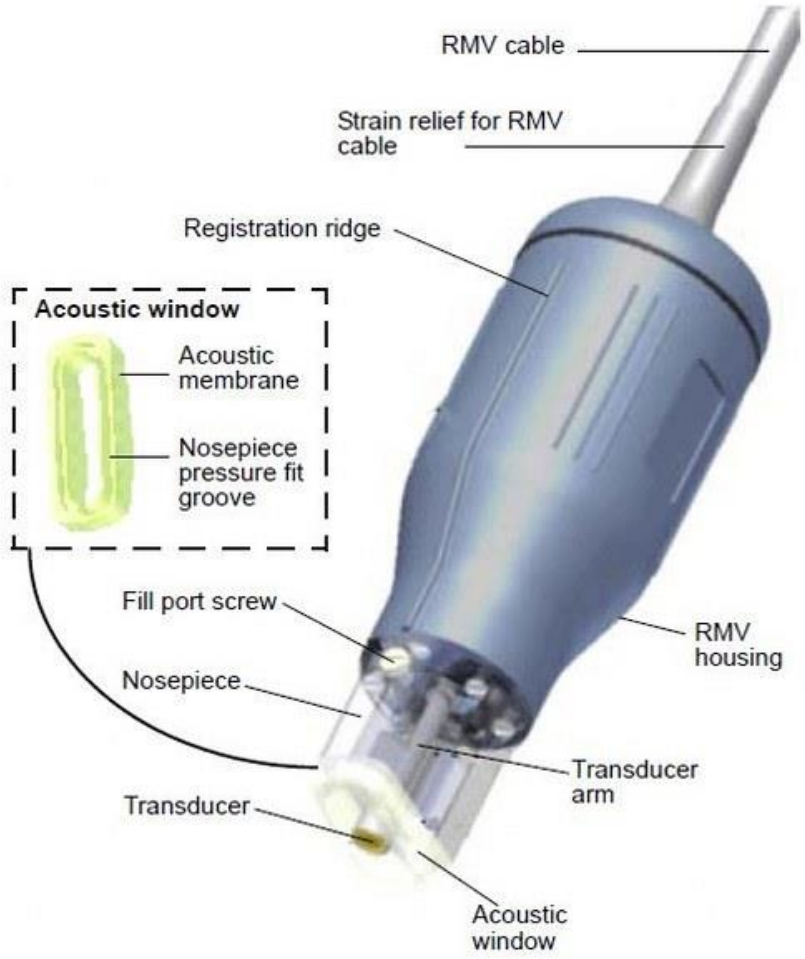

Figure 4.17. RMV 704 scan head with 40 MHz focussed transducer. [Reproduced with permission from Visual Sonics®, Inc].

This transducer mechanically vibrates so it can produce cross-sectional images. It can be clamped to be stationery or used in a hand-held mode. The acoustic window has a replaceable acoustic membrane, which can be replaced if damaged.

4.3.2.2 Tooth Selection, Preparation and Storage

Five premolar teeth were randomly selected from the tooth sample set used in section 4.2.2, and each tooth was secured with impression compound (Kemco, Kemdent®, UK) on the internal wall of a small acrylic pot (40 × 26 × 23 mm). The pots had an open window at the transducer side, which enabled it to be filled with fresh tap water as a couplant. The teeth were kept hydrated with fresh tap water during the

experiment. At the end of the experiment, they were placed back in the 0.1% thymol (Sigma Aldrich, MO, USA) solution and stored in a refrigerator at 5 ºC.

4.3.2.3 B-mode Ultrasound Scans

A total of 200 B-mode images were taken from 5 premolar teeth. Ten ultrasonic scans were made on each surface (buccal, mesial, palatal and distal) for each tooth as follows:

The first pot was placed on the *xyz* translation stage of the machine, and secured so that it lay within the focal distance of the ultrasonic transducer (6 mm). The pot was placed so that the buccal surface of the tooth was facing the transducer; the ultrasound transducer in this machine has its own housing (scan head) as shown in Figure 4.17 above.

The scan head was secured by a clamp (Figure 4.18) so that the transducer was perpendicular to the buccal surface of the tooth. The scan head remained stationary while the translation stage moved. The relation between transducer movement and the translation stage is shown in Figure 4.19.

A trial scan was performed to ensure that the tooth can be scanned and that the pot lay at the focal point of the scanner. Thereafter, the first scan started from the top of the buccal surface (coronal most part) and in 1 mm steps (toward the cervical part), ten cross-sectional B-mode images were captured, named and saved. After imaging the buccal surface, the mesial, palatal and distal surfaces were imaged using the same technique.

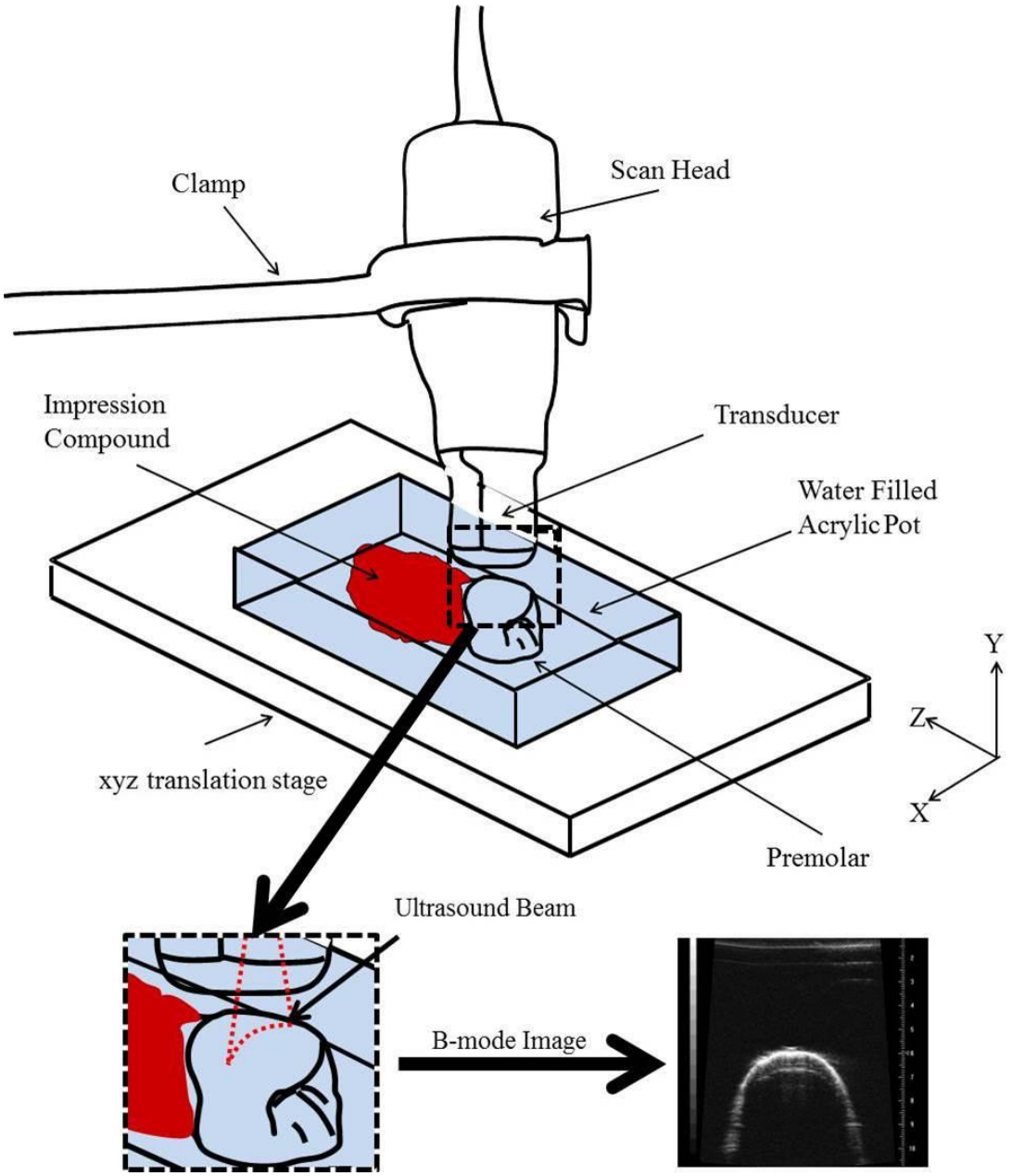

Figure 4.18. Ultrasound scan head and transducer relationship with the premolar tooth while scanning.

The transducer in Figure 4.18 vibrated in the '*x*' axis, emitting multiple ultrasound beams that were processed instantaneously to produce a B-mode image. The example

in this figure shows a cross-sectional image of a premolar tooth, with the enamel layer demarcated by the top bright boundary.

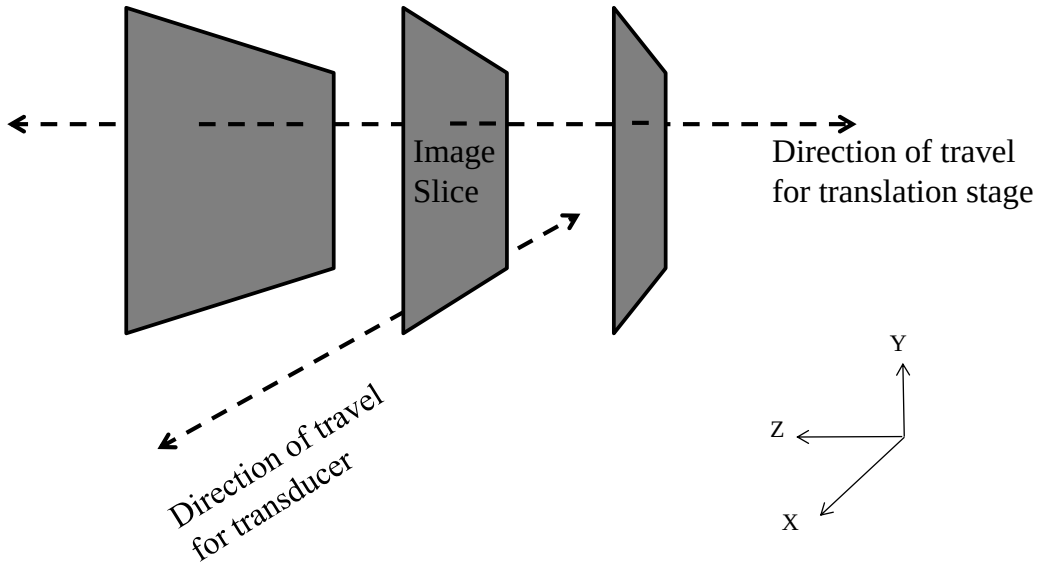

Figure 4.19. The relationship between the movement of the transducer and the translation stage [Adapted with permission from Visual Sonics®, Inc].

As the transducer scans the first section producing a slice, the translation stage is moved by 1 mm in the '*z*' axis and the next slice scanned and saved.

4.3.2.4 Cross-Sectional Image Measurements

The B-mode image had a slice thickness of 0.30 mm, which is equal to the beam width of the transducer at the depth of focus (6 mm). Therefore, when verifying the B-mode image enamel thickness μ-CT, the thickness of the B-mode image was divided by the μ-CT thickness (0.30/0.072) to produce the equivalent number of μ-CT images required for B-mode comparison of 4 μ-CT images. These 4 μ-CT images were combined in ImageJ software, version 1.46r (Schneider *et al.*, 2012) to form an averaged single image from which to take enamel thickness measurements, in the same way as section 4.2.2.

The B-mode images were saved in tagged image file format (TIFF) and were transferred to a memory stick for analysis in ImageJ on a PC. The images were opened one by one, and each image was measured using the line selection feature, where a line is drawn between the boundary of interest (enamel in this case) and the software calculates the distance. For precise measurements, the scale of the image in question requires being set first, this is done by opening the software measure tab, selecting ‘set scale’ and inputting the ‘known distance’. This known distance is obtained from the B-mode image itself, hence it has a scale embedded in it (see section 4.3.3 below). This ensures that measurements made in ImageJ are precise.

4.3.2.5 μ-CT Scans

The μ-CT scans for the 5 premolars used here were from section 4.2.2.

4.3.2.6 Statistical Methods for Commercial Ultrasound Scanner

The methods used here were the same as in section 4.2.2. The null hypothesis here is: there is no difference between the commercial ultrasound scanner and μ-CT in measuring enamel thickness of human premolars. The alternative hypothesis: there is a difference between the commercial ultrasound scanner and μ-CT in measuring enamel thickness of human premolars.

4.3.3 Results

4.3.3.1 B-mode Ultrasound Scans

A total of 200 B-mode scans (B-mode images) were successfully performed on 5 premolar teeth.

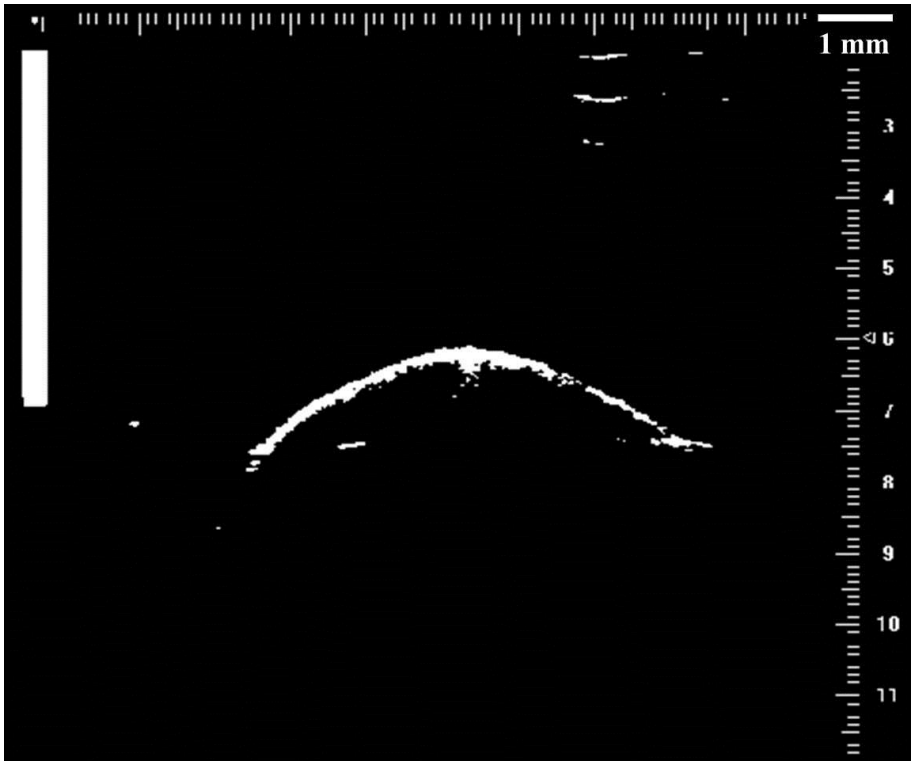

Figure 4.20. Representative B-mode image across the buccal aspect of a premolar obtained from the commercial ultrasound scanner after thresholding.

See Appendix 3 for representative raw B-mode images.

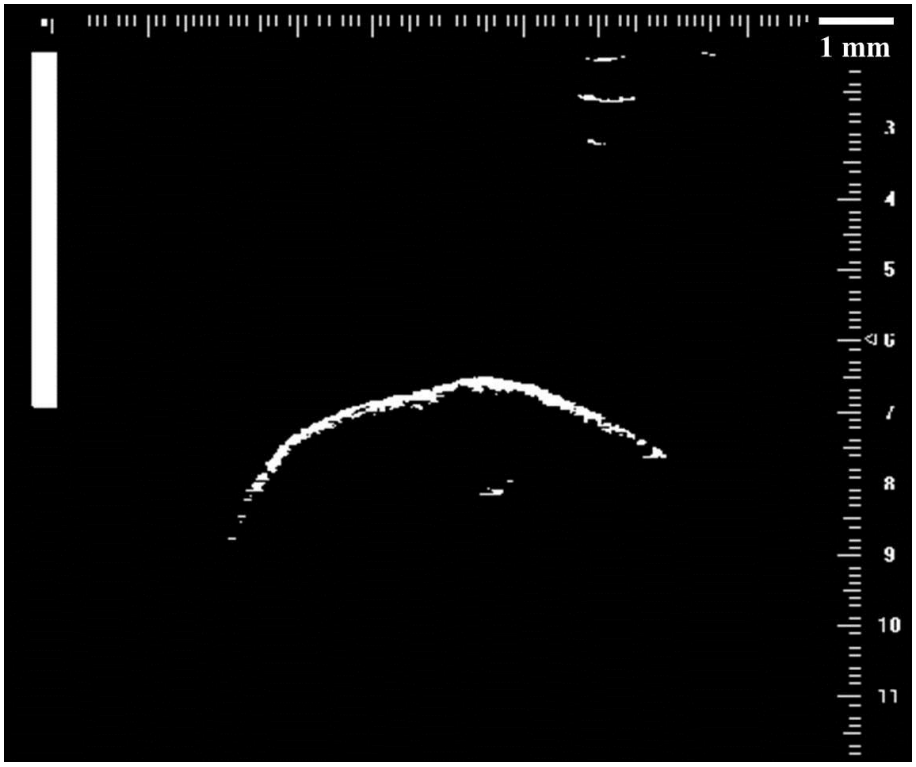

Figure 4.21. Representative B-mode image across the buccal aspect of a premolar obtained from the commercial ultrasound scanner after thresholding.

4.3.3.2 μ-CT Scans

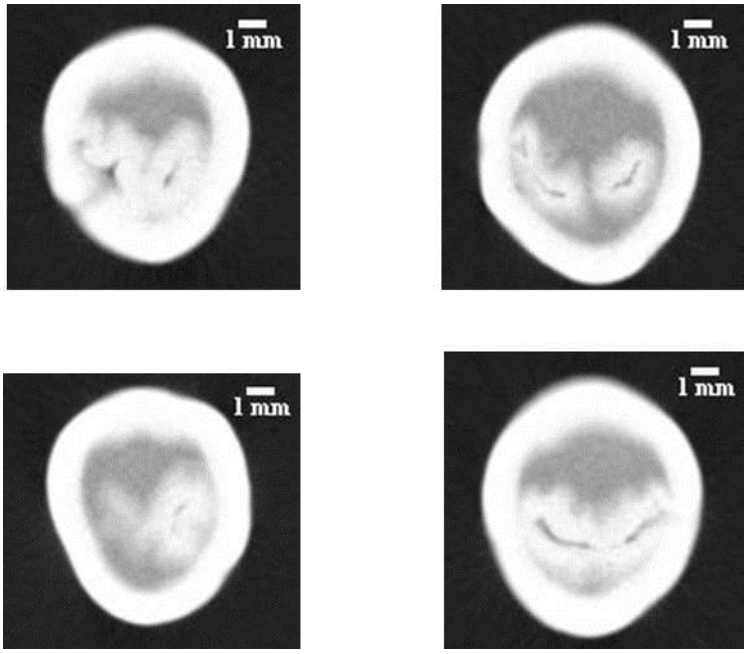

Figure 4.22. A representative sample of averaged μ-CT scans

4.3.3.3 Cross-Sectional Images' Measurements

A total of 113 B-mode images were suitable for enamel thickness measurements obtained from 5 premolars.

Table 4.6. Difference in enamel thickness between commercial ultrasound and μ-CT for the same sites.

Tooth	**Difference from μ-CT (mm)**			
	Buccal	**Mesial**	**Palatal**	**Distal**
1	-0.03	-0.24	-0.14	0.18
	-0.02	-0.45	0.00	0.02
	-0.24	-0.40	-0.03	0.10
	-0.02	-0.04	0.01	0.09
	0.02	0.41	-	0.29
	0.03	0.21	-	0.29
	0.01	-	-	0.29
	0.02	-	-	-
Mean Difference	-0.03	-0.09	-0.04	0.18
SD Difference	0.08	0.31	0.06	0.10
2	-1.14	-0.46	-0.22	-0.08
	-0.12	-0.06	-0.09	-0.2
	-0.07	0.32	-0.09	-0.10
	-	0.05	0.00	0.00
	-	0.58	0.29	-
	-	0.13	0.32	-
	-	0.22	0.27	-
	-	0.11	0.25	-
	-	-0.12	-	-
Mean Difference	-0.44	0.09	0.09	-0.10
SD Difference	0.49	0.28	0.20	0.07

Tooth	Difference from μ-CT (mm)			
	Buccal	**Mesial**	**Palatal**	**Distal**
3	-0.33	-0.16	-0.23	-0.29
	-0.31	-0.26	-0.49	-0.16
	-0.36	-0.04	-0.36	-0.07
	-0.30	0.06	-	0.05
	-0.12	-	-	-
	-0.04	-	-	-
	0.29	-	-	-
	0.36	-	-	-
	0.16	-	-	-
	0.37	-	-	-
	0.14	-	-	-
Mean Difference	-0.01	-0.10	-0.36	-0.12
SD Difference	0.28	0.12	0.11	0.12
4	0.25	-0.26	-0.08	0.38
	0.73	0.08	0.03	-0.26
	0.1	-0.18	0.05	-0.03
	-0.27	-0.27	0.05	0.19
	-0.22	-0.10	0.16	0.03
	-	-	0.01	0.28
Mean Difference	0.12	-0.15	0.04	0.10
SD Difference	0.36	0.13	0.07	0.21
5	-0.05	0.03	0.17	-0.07
	-0.08	-0.06	-0.23	0.00
	0.01	0.11	-0.19	0.00
	-0.34	0.04	0.14	0.01
	-0.08	-	0.22	0.06
	-	-	-	0.07
Mean Difference	-0.11	0.03	0.02	0.01
SD Difference	0.12	0.06	0.19	0.05

4.3.3.4 Test of Normality

The Shapiro-Wilk test results gave a *p*-value of 0.00 (Table 4.7 below), which indicate that the data did not follow a normal distribution therefore a paired Wilcoxon test was used (Table 4.9).

Table 4.7. Shapiro-Wilk normality test for the difference in enamel thickness measurements obtained with the commercial ultrasound scanner and μ-CT

Method	Statistic	df	Sig.
Commercial Ultrasound - μ-CT	0.95	113	0.00

Table 4.8. Descriptive statistics for ultrasound and μ-CT measurements from all sites (mm)

	n	Range	Minimum	Maximum	Mean	SE
Commercial Ultrasound	113	1.87	-1.14	0.73	-0.01	0.02
μ-CT	113	2.15	0.19	2.34	1.03	0.04

4.3.3.5 Paired Wilcoxon Test Between μ-CT and the Commercial Ultrasound Scanner

The results of the paired Wilcoxon test indicated that *p*-value was < 0.05 (*p*-value= 0.00) therefore the null hypothesis was rejected in favour of the alternative hypothesis. This means that there was a statistically significant difference between both methods in measuring enamel thickness.

Table 4.9. Paired Wilcoxon test result for the difference in enamel thickness measurements between μ-CT and the commercial ultrasound scanner

Methods	Exact Sig.
μ-CT – Commercial Ultrasound	0.00

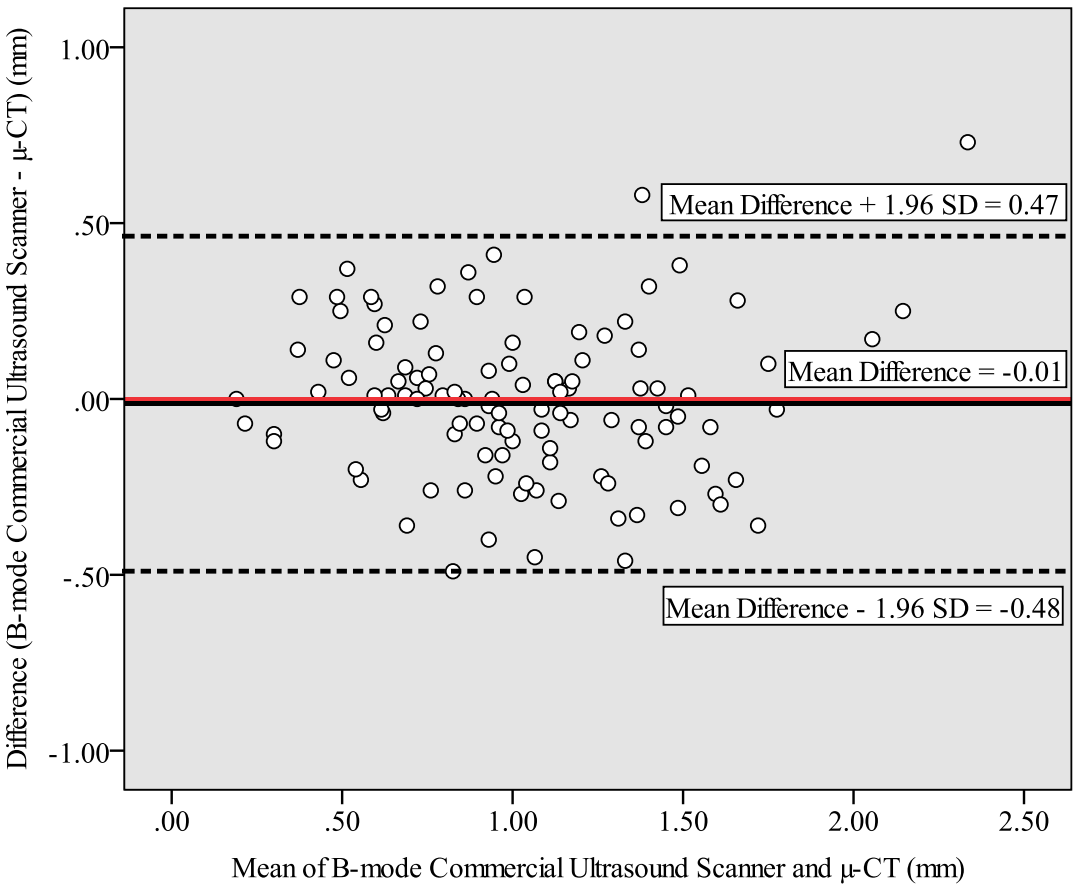

Figure 4.23. Bland-Altman plot showing the agreement in measuring enamel thickness between B-mode of commercial ultrasound scanner and μ-CT (n = 113)

Table 4.10. Summary of the Bland-Altman results obtained from B-mode of commercial ultrasound scanner and μ-CT

Mean Difference (mm) (B-mode of commercial ultrasound scanner – μ-CT)	SD Difference (mm)	95% Bland-Altman Limits of Agreement
-0.01	0.24	(-0.48, 0.47)

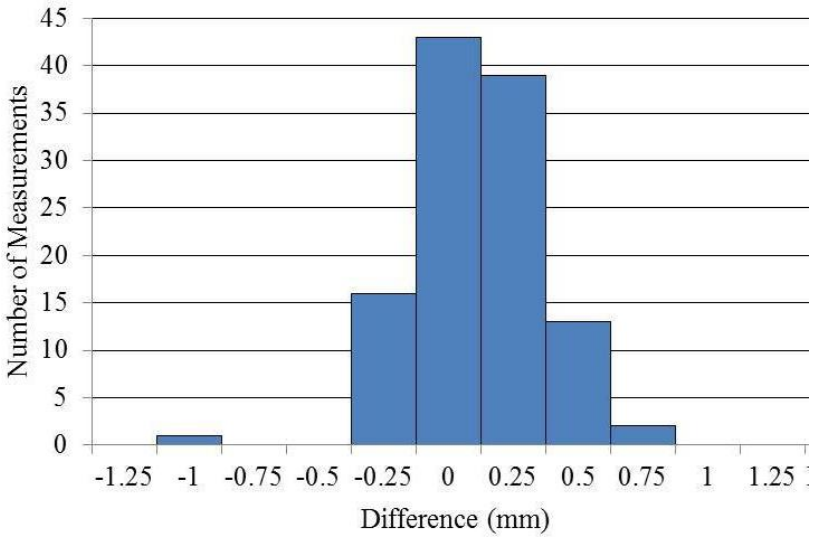

Figure 4.24. Difference between B-mode of commercial ultrasound scanner and μ-CT in measuring enamel thickness (n = 113).

4.3.4 Discussion

Commercial ultrasonic scanners are used in several research areas worldwide. However, their use in the dental arena has been limited to few studies demonstrating their potential in dental imaging. The earliest reported use of a commercial ultrasound scanner to produce a B-mode image of teeth was in the 1960s (Baum *et al.*, 1963). The image barely showed the anatomic structure of the teeth, but was deemed acceptable by researchers at that time as a 'proof of principle'.

The computing power of ultrasound machines in the 1960s was small in comparison to now, which may be a factor for the B-mode image quality produced, both in soft tissue research and dental research. Berson *et al.* (1999) has used a commercial ultrasound scanner to produce a cross-section of the periodontium in a tooth. In this study, the B-mode images were acquired with a linear array transducer. Although the authors did not attempt to measure the enamel thickness, the study demonstrated the potential of the device for examining the periodontium and teeth.

The results from the commercial ultrasound scanner experiment in this section demonstrated that there was a good overall agreement between B-mode ultrasonic image measurements of enamel thickness and their μ-CT counterparts. The mean difference from the surface of all teeth was –0.01 mm with a standard deviation of 0.24 mm. However, given this standard deviation the accuracy of this scanner in measuring in enamel thickness was lower than reported enamel loss of 17.6-108.2 μm/6 months due to erosive TSL (Bartlett *et al.*, 1997). Thus the scanner is not useful as clinical tool to monitor erosive TSL.

Hua *et al.* (2009) compared enamel thickness measurements from ultrasonic B-mode images of a commercial scanner obtained with a 13 MHz linear array transducer with μ-CT and found that there was a mean difference in agreement of about 0.55 mm (from 4 observers) between the two images when measuring occlusal enamel of a human molar. This difference was attributed to the inability to easily locate the ADJ boundary, resulting in reduced accuracy of measurements.

Hua *et al.* enhanced the accuracy of their technique by using image processing algorithms and this led to a decrease in the difference between B-mode and μ-CT to 0.32 mm. Image processing focussed on refining the ADJ to result in a clearer B-mode image. The improvement after image processing was seen on occlusal but not on buccal and palatal enamel, where the mean difference from μ-CT from 4 observers was 0.53 mm.

The results obtained with the commercial ultrasound scanner in our work produced a mean difference on all sites (-0.01 mm) that is lower than that reported by Hua *et al.* (2009) at all sites (0.43 mm). This could be due to the higher frequency used in our work (40 MHz) which produces higher axial resolution and therefore clearer B-mode

images. Furthermore, the image processing in our work was performed in real time within the scanner and this may be an advantage when deciding on selecting an image before capturing it for enamel thickness measurements.

It is pertinent to highlight that this commercial scanner used a built-in SOS value of 1540 ms^{-1} to generate the B-mode images. This value was not user-controllable thus it was not possible to adjust to the assumed SOS in enamel (6000 ms^{-1}). Therefore, the enamel layer in the B-mode image appeared ~1/4 of its actual size. To account for this, the enamel thickness in the B-mode image was multiplied by a factor of 4.

To ascertain the accuracy of the technique for every paired measurement it is best to use the limits of agreement as an indication, because this checks for the accuracy of the measurements for every observation and not just an 'overall' accuracy of all measurements. The highest limit of agreement in this work was 0.48 mm (Table 4.10), which is still better than the accuracy reported in the work of Hua and co-workers (2009) for buccal and palatal surfaces (0.53 mm).

Although the results are encouraging, it is important to highlight that these were obtained from 5 teeth and require confirmation with a larger sample size. Another issue with this commercial scanner is its size as shown in Figure 4.16, which makes its routine use in the dental clinic cumbersome. Nonetheless, a smaller version of this scanner may be of benefit.

4.4 Conclusions

In summary of these studies on cross-sectional imaging of teeth using ultrasound, the conclusions are:

- μ-CT is the most accurate technique in measuring enamel thickness of human premolars followed by the commercial ultrasound scanner and the in-house ultrasound apparatus.
- Even with B-mode imaging, there is the anatomical challenge that renders ultrasonic B-mode imaging unfavourable for measuring enamel thickness because of the curvature of the teeth and the problems with SOS.
- For clinical use, the relatively large B-mode commercial ultrasound scanner is likely to be cumbersome and expensive. Therefore, it is thought that A-mode imaging may be better, which renders it the next logical area to investigate. This will be discussed in the following Chapter.

5 *In Vitro* Enamel Thickness Measurements with A-Mode Ultrasound

5.1 Introduction

For the development of a clinically useful tool it was thought that a relatively simple approach such as A-mode ultrasound would be preferred for measuring the enamel thickness at certain areas on the tooth. This takes the form of a 'spot measurement' on the labial or buccal surface of the tooth, rather than 'bulk measurement' as in the 3D laser scanning and image registration technique. A series of spot measurements will give enough information to monitor erosive TSL because the erosive agent will contact the labial surface of the tooth equally.

In vitro enamel thickness measurements are mainly performed by destructive methods, however with the use of a pulse-echo ultrasound technique it is possible to obtain thickness measurements non-destructively (Tagtekin *et al.*, 2005). Indeed, several studies have compared these types of measurements with histology, the gold standard in the field, with mixed results (see section 1.5).

One factor that may explain the variation between these studies is the assumed SOS in enamel; in most cases the authors have used a mean value obtained from the literature. However, it is well established that there is variation in the SOS within the enamel tissue because of the enamel rods (see section 1.3.2.1, p.18). Sound travels faster in enamel rods that are parallel to the sound beam and the opposite holds true. The aim of this Chapter is to assess the agreement between enamel thickness measurements of A-mode ultrasound and histology measurements using the SOS value for each tooth.

5.2 Materials and Methods

5.2.1 Tooth Selection and Storage

Fifteen human premolar teeth were randomly chosen from the samples described in Chapter 3. The teeth were kept hydrated in 0.1% thymol (Sigma Aldrich, MO, USA) solution and stored in the laboratory refrigerator at 5 ºC.

5.2.2 Sectioning of the Premolar Teeth and Storage Media

The crowns of all premolars were inspected for near planar areas (buccally, palatally, mesially and distally) so that the cut sections could include these acoustically preferential regions. All 15 premolars were sectioned coronally using a cutting machine employing a 250 μm water cooled diamond cut-off wheel (Accutom, Struers, Denmark). Two disc shaped specimens with a thickness of 2.50 ±0.02 mm were obtained from each premolar's crown (an 'occlusal' and 'cervical' specimen) shown Figure 5.1, which resulted in a total of 30 specimens. The specimen thickness was determined with a digital micrometer (293-766-30, Mitutoyo, Japan). The remainder of the tooth was discarded using an approved clinical waste disposal route. The specimens were stored in labelled vials filled with HBSS (Thermoscientific, Hyclone Laboratories Inc., USA) in a refrigerator at 5 ºC for subsequent ultrasound measurements.

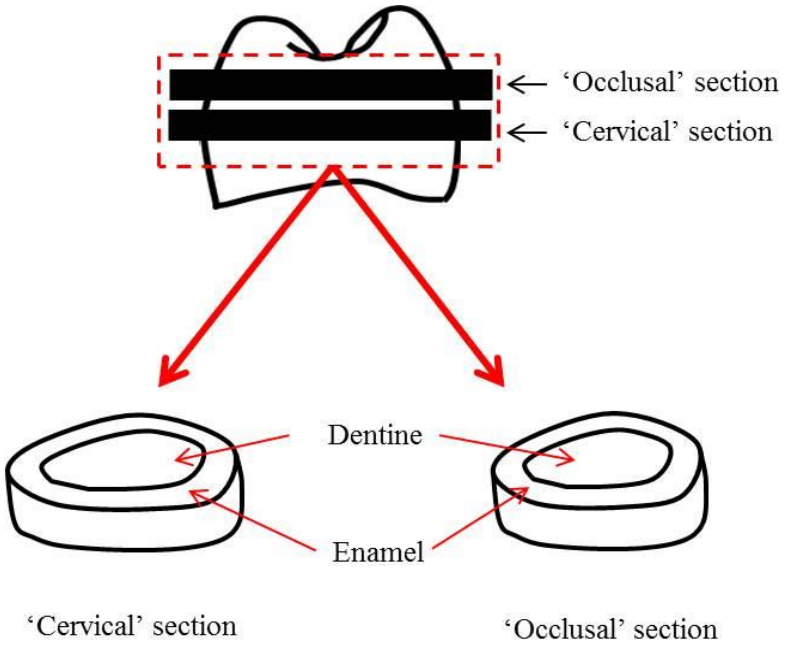

Figure 5.1. Schematic for the location and orientation of the sections.

5.2.3 Marking Specimens

Each specimen was marked with a permanent marker (Twin tip, Sharpie™, Newell Rubbermaid, Inc., USA) at two locations on the enamel surface (V and T in Figure 5.2 below). For each specimen, the V marked area was used to determine the SOS in that specimen. The T marked area was used to measure enamel thickness with ultrasound, which was then validated with histological measurements. Marks were made on the most planar areas of the specimens. The specimens were kept hydrated in HBSS at all times, except when measurements were performed.

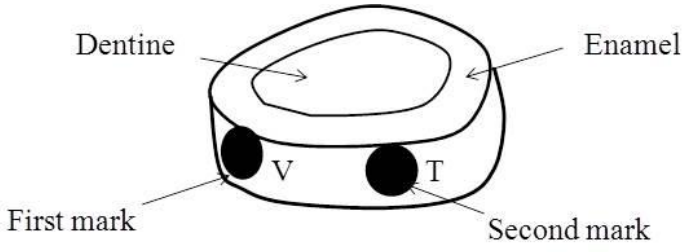

Figure 5.2. Schematic of a section in a premolar tooth, depicting two marked areas, one for SOS (V) and one for enamel thickness measurement (T).

5.2.4 Ultrasound Setup

Due to specimen dimensions, dental boxing wax (00609, Kerr, CA, USA) was used to secure the specimens on a microscopic glass slide in order to prevent moving or rocking while ultrasound readings were made from the pre-marked areas. A direct contact pulse-echo technique using a 15 MHz focussed transducer (VR-260, Olympus® Inc., Waltham, USA) with a replaceable Perspex delay line that had a 2 mm tip was coupled to the enamel surface with a water drop (Huysmans and Thijssen, 2000). The transducer was excited with a pulser-receiver unit (PR-5742, Olympus®, MA, USA), and the waveforms were displayed on a digital oscilloscope (LT-342, Lecroy®, USA) with a sampling rate of 500 megasamples per second. When recognisable enamel layer echoes were displayed on the oscilloscope, 1000 echoes were averaged and saved in ASCII format on a computer coupled to the oscilloscope by an RS-232 cable. A macro, written by a laboratory colleague, was required in order to automate the waveform capture while simultaneously holding the transducer against the enamel surface. The ultrasonic setup was calibrated for enamel with a tooth section before commencing the actual measurements.

5.2.5 SOS Measurements in Enamel at V Marked areas

As described earlier the SOS was calculated using the range equation (see section 1.2, Equation 1.1, p.3) (Slak *et al.*, 2011). To calculate the SOS, equation 1.1 becomes Equation 5.1. In order to satisfy this equation and derive the SOS (v), the TOF (t) and the enamel thickness (d) at the ‘V’ marked area in Figure 5.2 should be known.

$$v = \frac{2\,d}{t}$$

Equation 5.1

5.2.5.1 Time of Flight Calculation at V Marked Areas

The TOF measurements were made while the specimen was held with one hand and the transducer in the other (Tagtekin *et al.*, 2005). The transducer tip was placed perpendicular to the 'V' marked area on the enamel surface, while ensuring intimate contact between the tip and the surface (Figure 5.3 below).

Three repeat measurements were obtained from each V marked area of each section. In the repeat measurements, the transducer was removed from the enamel surface and reapplied. The signal from each repeat measurement was averaged 1000 times by the oscilloscope before saving. A total of 90 TOF measurements were obtained from all sections. The TOF was calculated from the first peak corresponding to the Perspex-enamel interface and the second peak representing the ADJ. When there were multiple consecutive peaks, the first peak was chosen. Once all TOF's were carried out for the 30 sections, thickness measurements of the V marked site was completed as discussed in the following section.

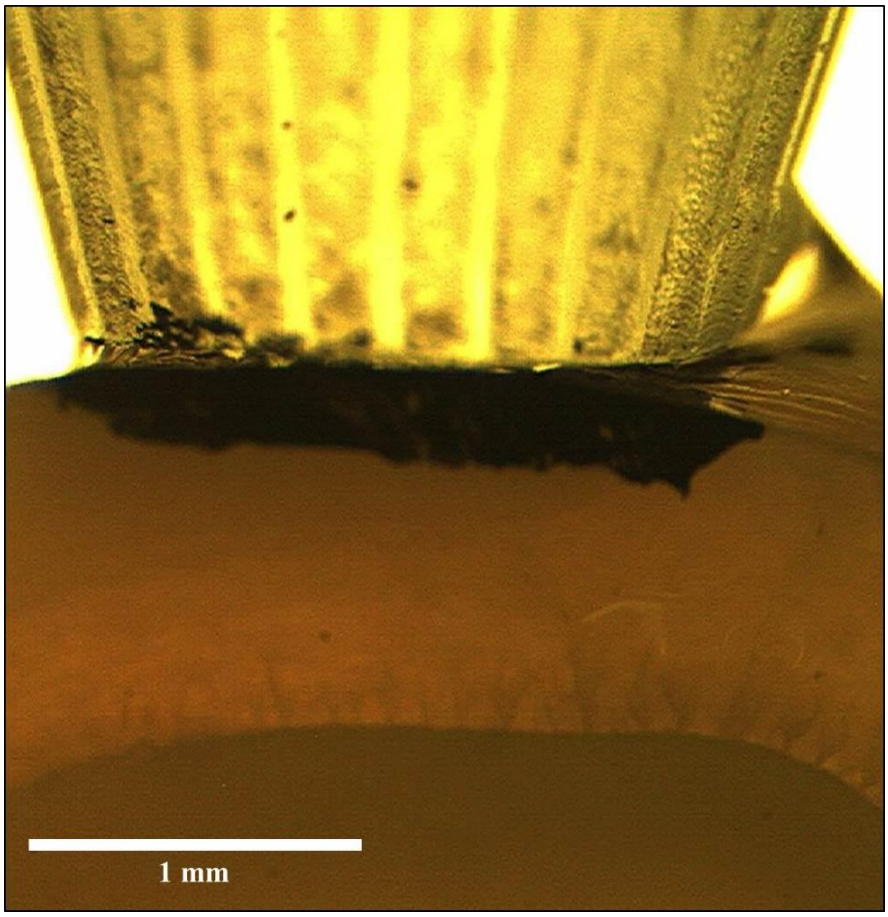

Figure 5.3. The transducer's Perspex tip coupled with water to enamel on the pre-marked area. Note the marker colour on the proximal area.

5.2.5.2 Thickness Calculation at V Marked Areas

Each tooth section was placed under a stereo microscope (Nippon, Kogako, Tokyo), equipped with a 20 W fibre-optic light source (Leica L2, Leica Microsystems GmbH, Wetzlar, Germany) and viewed at 20x magnification. A computer controlled digital microscope camera (Moticam 2300, Motic®, Inc. Ltd., China) with a resolution of 3 Megapixels was mounted on one of the ocular eye pieces via an eye piece adapter, so that images could be taken without moving the setup. Before images were captured, a calibration slide provided by the manufacturer (Figure 5.4) was used in order to calibrate the software (Motek Images Plus, version 2.0 ML).

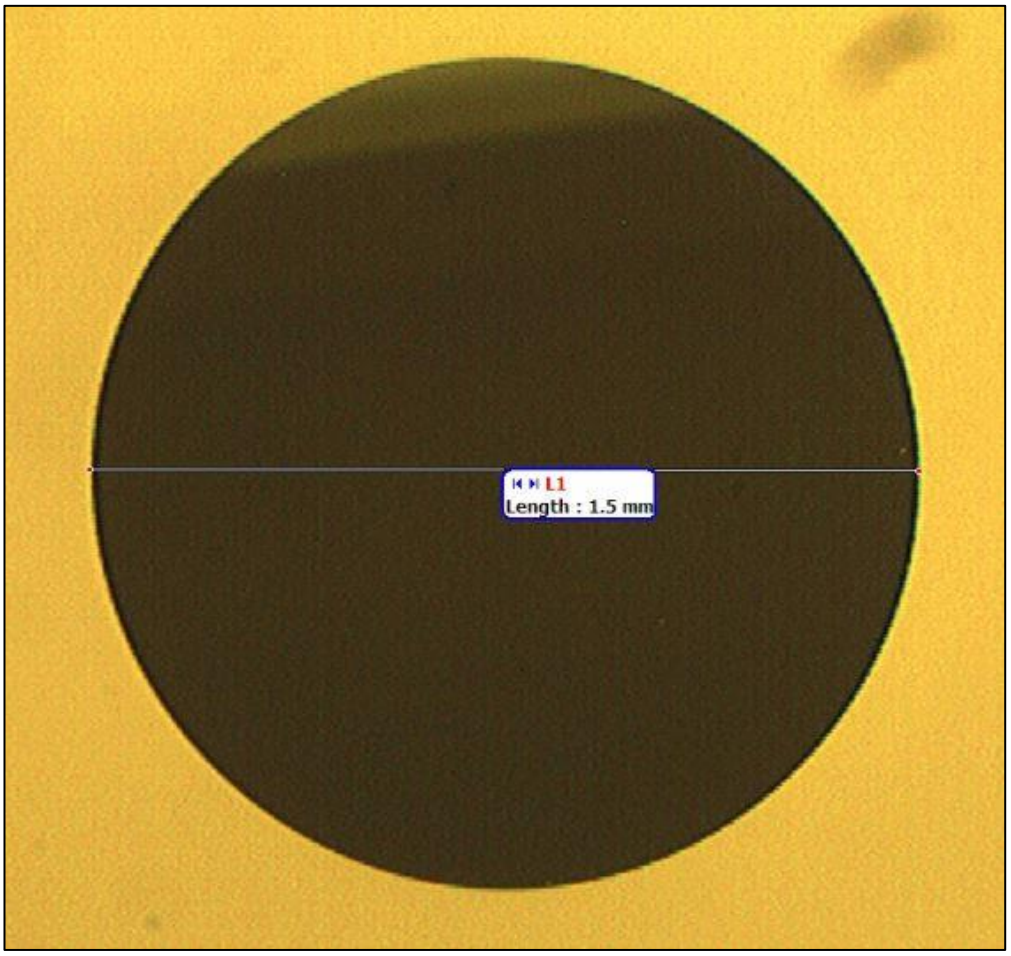

Figure 5.4. A calibration slide depicting a reference circle with a radius of 1.5 mm

Once the V marked area of the specimen was in the field of view and the enamel layer was in sharp focus, a digital image was taken and saved in TIFF file format. The software that captured the images had a built-in line-measurement tool which was used to measure enamel thickness (*d*). Three radial measurements were made at the V marked area and the mean was taken. The line measurement tool cursor was placed on the external enamel surface and was extended to the ADJ. The ADJ was sometimes ambiguous and therefore the contrast was adjusted until the boundary became clearer for a measurement to be taken. Care was exercised not to spend unnecessary 'dry time' for the specimen.

5.2.5.3 SOS in Enamel at V Marked Areas

The SOS in enamel at the V marked area on all 30 specimens was obtained by incorporating the TOF and thickness values from this area in Equation 5.1

5.2.6 Enamel Thickness Measurements with A-Mode Ultrasound at T Marked Areas

To avoid bias in enamel thickness measurements, a different area (T in Figure 5.2) was chosen within the same section to measure enamel thickness, but this was not in the area from which SOS measurements were made (V marked area) because the thickness was already known in that area. In order to obtain the enamel thickness at the 'T' marked area in Figure 5.2 for the 30 specimens, the TOF and the SOS must first be known to satisfy the range formula.

5.2.6.1 Time of Flight Calculation at T Marked Areas

The TOF for the T marked area on the specimens was measured with ultrasound using the same method described in section 5.2.5.

5.2.6.2 Enamel Thickness Calculation at T Marked Areas (A-Mode Ultrasound)

The range equation was used to calculate enamel thickness at the T marked area using the SOS determined for region V of each specimen. The mean SOS from all specimens was also used to calculate the enamel thickness at the T marked areas to see if the thicknesses differed.

5.2.6.3 Verifying A-Mode Ultrasonic Enamel Thickness Measurements with Histology at T Marked Areas

The ultrasonic enamel thickness values at the T marked areas were verified by measuring enamel thickness at these areas using a stereo microscope following the method described section 5.2.5.

5.2.7 Statistical Methods

The aim of the analysis was to examine the agreement in enamel thickness between histology and ultrasound, and also to examine SOS in enamel. This was done using three different statistical approaches. The first method examined agreement using the Bland-Altman limits of agreement method (Bland and Altman, 1986). In order to achieve a holistic evaluation of the agreement, the intra-class correlation coefficient (ICC) test was used as a second method (Gilligan *et al.*, 2011). This method involves dividing the total variability in enamel thicknesses into two components, the variation between different teeth, and the variation within measurements of the same teeth (i.e. measurements of the same teeth by different methods). The ICC is the proportion of the total variability between teeth. If the method is accurate, then the majority of variation should be between teeth, with little variation between repeat measurements of the same teeth (within teeth). This would give an ICC value close to 1.

The difference in SOS values between tooth sections was also examined. As the specimens came in pairs from the same teeth, the paired t-test was used for analysis.

The third statistical method used was a hypothesis test.

- The null hypothesis was: there is no difference between measurements made with A-mode ultrasound and histology.
- The alternative hypothesis was: there is a difference between measurements made with A-mode ultrasound and histology.

Prior to hypothesis testing, the Shapiro-Wilk test was used to check if the data was normally distributed. The significance level for the normality test was set at $\alpha = 0.05$. If the *p*-value for the test was < 0.05 then the data were not normally distributed and a non-parametric test, such as the Wilcoxon sign rank test was used instead of the paired t-test. However, if the *p*-value was > 0.05 then the data were deemed normally distributed and the paired t-test was used. The significance level for the hypothesis test was set at $\alpha = 0.05$.

5.3 Results

5.3.1 Sectioning of the Premolar Teeth and Storage Media

All teeth were sectioned successfully yielding 30 sections and stored in HBSS.

5.3.2 Marking Teeth Sections

Permanent marks (V and T areas) were successfully placed in each of the 30 sections

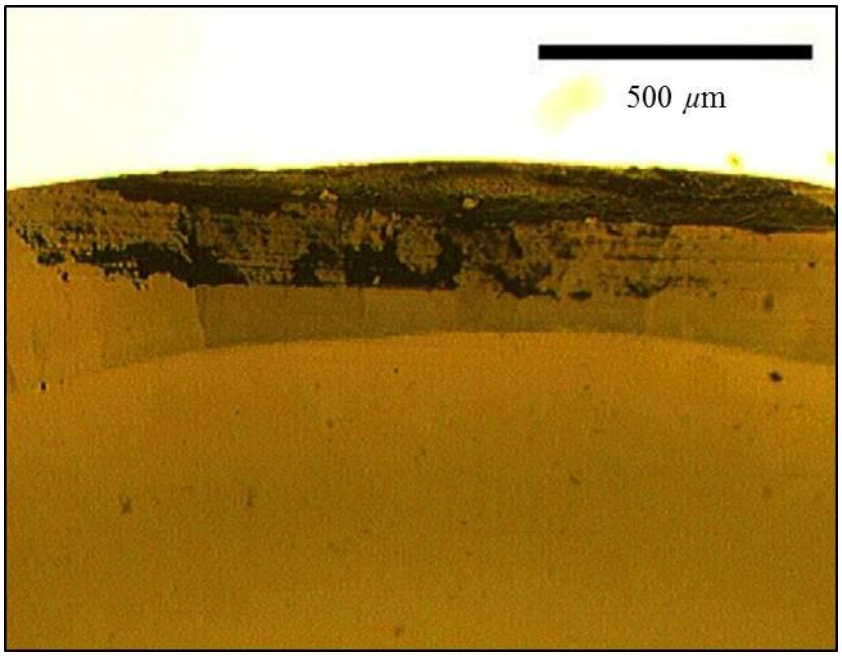

Figure 5.5. Coronal section of a representative specimen at a V marked area on enamel. Note that extending the mark to the cut surface was necessary for the histological measurements**.**

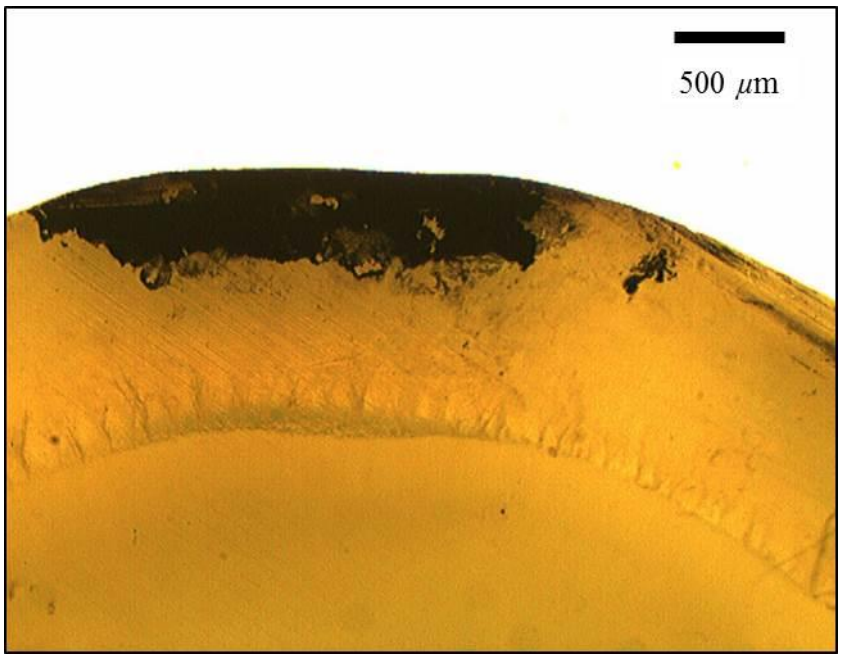

Figure 5.6. Coronal section of a representative specimen at a T marked area on enamel. Note that extending the mark to the cut surface was necessary for the histological measurements.

5.3.3 SOS Measurement in Enamel at V Marked Areas

5.3.3.1 Time of Flight Calculation at V marked Areas

Table 5.1. Mean TOF for all tooth sections. Note that the TOF here is the round trip time and is not divided by 2.

Specimen	Mean TOF (μs)	±SD (μs)
1	0.36	0.01
2	0.31	0.00
3	0.22	0.02
4	0.32	0.03
5	0.31	0.01
6	0.26	0.00
7	0.37	0.02
8	0.30	0.01
9	0.30	0.02
10	0.37	0.00
11	0.38	0.03
12	0.34	0.02
13	0.31	0.02
14	0.30	0.01
15	0.37	0.03
16	0.32	0.02
17	0.36	0.00
18	0.28	0.01
19	0.57	0.01
20	0.40	0.01
21	0.46	0.00
22	0.44	0.00
23	0.36	0.01
24	0.20	0.03
25	0.32	0.02
26	0.27	0.03
27	0.28	0.02
28	0.33	0.01
29	0.22	0.01
30	0.29	0.00

5.3.3.2 Enamel Thickness Calculation at V Marked Areas (Histology)

Table 5.2. Enamel thickness measurments from 30 specimens obtained from histology (mm).

Specimen	Mean Thickness (Histology)	±SD
1	1.30	0.05
2	1.00	0.00
3	0.70	0.00
4	0.86	0.05
5	1.00	0.00
6	0.80	0.00
7	1.00	0.00
8	0.90	0.00
9	1.06	0.05
10	1.20	0.00
11	1.13	0.05
12	1.10	0.00
13	1.03	0.05
14	0.97	0.05
15	1.20	0.08
16	0.83	0.05
17	1.20	0.04
18	0.87	0.00
19	1.60	0.00
20	1.40	0.00
21	1.37	0.05
22	1.37	0.05
23	1.03	0.05
24	0.63	0.05
25	0.97	0.05
26	0.80	0.00
27	0.96	0.05
28	0.93	0.05
29	0.70	0.00
30	0.87	0.00

5.3.3.3 SOS in Enamel at V Marked Areas

Table 5.3. SOS obtained with A-mode ultrasound at V marked areas from 30 specimens (ms^{-1}).

Specimen	Mean SOS	±SD
1	7222	179
2	6451	196
3	6363	250
4	5375	169
5	6451	196
6	6153	207
7	5404	138
8	6000	177
9	7066	208
10	6486	165
11	5947	156
12	6470	191
13	6645	202
14	6466	218
15	6486	165
16	5187	163
17	6667	184
18	6214	225
19	5614	247
20	6000	287
21	5956	128
22	6227	140
23	5722	158
24	6300	330
25	6062	190
26	5926	207
27	6857	248
28	5636	161
29	6363	300
30	6000	195
Mean	6191	199

The mean SOS in enamel was determined in this work at 6191 ± 199 ms^{-1}.

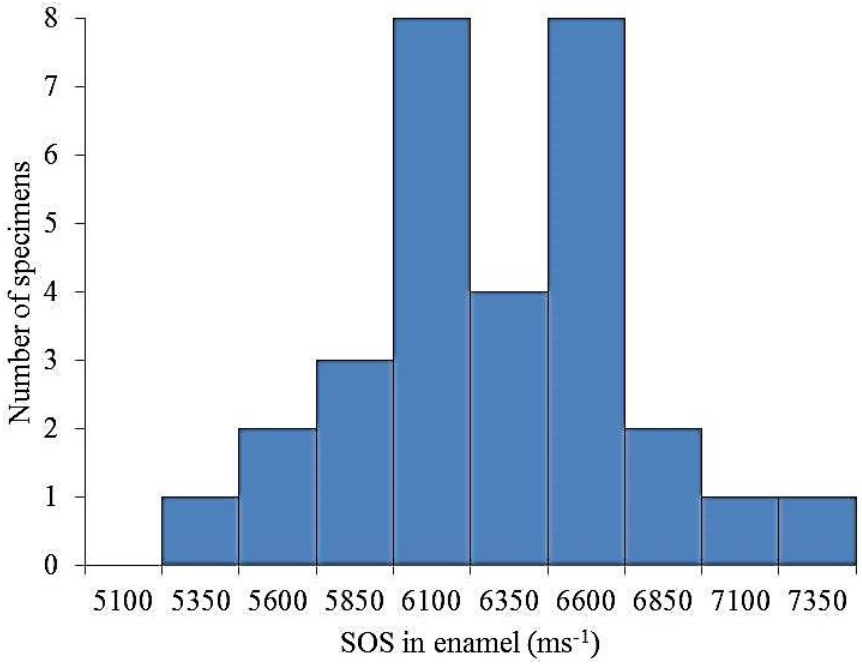

Figure 5.7. Distribution of SOS across a sample of 30 sections from 15 premolar teeth.

The paired t-test was used to compare the differences in SOS between sections, and the results are summarised in the next table. The figures reported are the mean and standard deviation in each section, along with the *p*-value indicating the significance of the results. The Shapiro-Wilk test gave a *p*-value of > 0.05 indicating that the SOS values were normally distributed.

Table 5.4. Comparison of SOS between occlusal and cervical sections (ms^{-1}).

Section	Mean (±SD)	*p*-value
'Occlusal'	6267 (549)	0.34
'Cervical'	6063 (479)	

5.3.4 Enamel Thickness Measurements with A-Mode Ultrasound at T Marked Areas

5.3.4.1 Time of Flight Calculation at T Marked Areas

Table 5.5. TOF obtained with A-mode ultrasound at T marked areas from 30 specimens (μs).

Specimen	Mean TOF	±SD
1	0.29	0.01
2	0.19	0.02
3	0.25	0.01
4	0.23	0.01
5	0.30	0.03
6	0.24	0.02
7	0.35	0.01
8	0.33	0.01
9	0.34	0.01
10	0.37	0.02
11	0.42	0.02
12	0.38	0.01
13	0.25	0.01
14	0.33	0.02
15	0.34	0.01
16	0.43	0.02
17	0.36	0.02
18	0.26	0.01
19	0.56	0.01
20	0.56	0.01
21	0.47	0.02
22	0.42	0.02
23	0.34	0.01
24	0.28	0.01
25	0.33	0.01
26	0.30	0.01
27	0.35	0.02
28	0.34	0.01
29	0.30	0.01
30	0.28	0.01

5.3.4.2 SOS in Enamel at T Marked Areas

Refer to Table 5.3.

5.3.4.3 Enamel Thickness Calculation at T Marked Areas (A-Mode Ultrasound)

Table 5.6. Enamel thickness measurements obtained with A-mode ultrasound at T marked areas from 30 specimens (mm), using the SOS of each specimen.

Specimen	Mean Thickness (A-Mode Ultrasound)	±SD
1	1.06	0.02
2	0.60	0.05
3	0.78	0.02
4	0.61	0.02
5	0.94	0.09
6	0.75	0.05
7	0.92	0.03
8	0.99	0.03
9	1.20	0.04
10	1.16	0.05
11	1.26	0.05
12	1.24	0.02
13	0.80	0.03
14	1.09	0.04
15	1.07	0.03
16	1.12	0.05
17	1.21	0.05
18	0.81	0.03
19	1.54	0.03
20	1.96	0.03
21	1.38	0.03
22	1.29	0.04
23	0.98	0.02
24	0.88	0.03
25	1.00	0.03
26	0.86	0.03
27	1.19	0.02
28	0.92	0.02
29	0.94	0.02
30	0.80	0.02

Table 5.7. Enamel thickness measurements obtained with A-mode ultrasound at T marked areas from 30 specimens (mm), using mean SOS from all specimens.

Specimen	Mean Thickness (A-Mode Ultrasound)	±SD
1	0.91	0.02
2	0.59	0.05
3	0.77	0.03
4	0.71	0.03
5	0.93	0.09
6	0.74	0.05
7	1.08	0.03
8	1.02	0.03
9	1.05	0.03
10	1.16	0.06
11	1.30	0.05
12	1.18	0.03
13	0.77	0.03
14	1.02	0.06
15	1.05	0.03
16	1.33	0.06
17	1.11	0.05
18	0.80	0.03
19	1.73	0.03
20	1.73	0.03
21	1.44	0.05
22	1.30	0.06
23	1.05	0.03
24	0.86	0.04
25	1.02	0.03
26	0.93	0.03
27	1.09	0.05
28	1.04	0.02
29	0.93	0.03
30	0.87	0.03

5.3.4.4 Verifying A-Mode Ultrasonic Enamel Thickness Measurements (using SOS of each specimen) with Histology at T Marked Areas

Table 5.8. Enamel thickness measurements obtained with A-mode ultrasound (using SOS of each specimen) and histology[†] at T marked areas from 30 specimens (mm).

Specimen	Mean A-Mode Thickness	±SD	Mean Histology Thickness	±SD	Difference
1	1.06	0.02	1.07	0.05	-0.01
2	0.60	0.05	0.60	0.00	0.00
3	0.78	0.02	0.80	0.00	-0.02
4	0.61	0.02	0.60	0.05	0.01
5	0.94	0.09	0.97	0.00	-0.03
6	0.75	0.05	0.70	0.00	0.05
7	0.92	0.03	0.90	0.00	0.02
8	0.99	0.03	1.00	0.00	-0.01
9	1.20	0.04	1.30	0.05	-0.10
10	1.16	0.05	1.16	0.00	0.00
11	1.26	0.05	1.27	0.05	-0.01
12	1.24	0.02	1.17	0.00	0.07
13	0.80	0.03	0.73	0.05	0.07
14	1.09	0.04	0.97	0.05	0.12
15	1.07	0.03	1.13	0.08	-0.06
16	1.12	0.05	1.07	0.05	0.05
17	1.21	0.05	1.20	0.04	0.01
18	0.81	0.03	0.83	0.00	-0.02
19	1.54	0.03	1.70	0.00	-0.16
20	1.96	0.03	1.57	0.00	0.39
21	1.38	0.03	1.40	0.05	-0.02
22	1.29	0.04	1.27	0.05	0.02
23	0.98	0.02	1.00	0.05	-0.02
24	0.88	0.03	0.90	0.05	-0.02
25	1.00	0.03	1.03	0.05	-0.03
26	0.86	0.03	0.87	0.00	-0.01
27	1.19	0.02	1.17	0.05	0.02
28	0.92	0.02	0.97	0.05	-0.05
29	0.94	0.02	0.90	0.00	0.04
30	0.80	0.02	0.80	0.00	0.00

[†] See Appendix 4 for histology images at T marked areas

5.3.4.5 Agreement between A-Mode Ultrasound and Histology

Analyses were performed to examine the agreement in enamel thickness between ultrasound and histology. The initial analysis considered the agreement in terms of the actual difference (in mm). The Bland-Altman method was used for the analysis, and the results are summarised in Table 5.9 and Figure 5.8 below.

Table 5.9. Summary of Bland-Altman results using SOS of each specimen (mm).

Mean Difference (A-mode Ultrasound - Histology)	SD Difference	95% Bland-Altman Limits of Agreement
0.01	0.09	(-0.16, 0.18)

The agreement analysis using ICC was 0.97 which means there is almost excellent agreement between the methods.

Table 5.10. Summary of Bland-Altman results using mean SOS for all specimens (mm).

Mean Difference (A-mode Ultrasound - Histology)	SD Difference	95% Bland-Altman Limits of Agreement
0.02	0.10	(-0.17, 0.21)

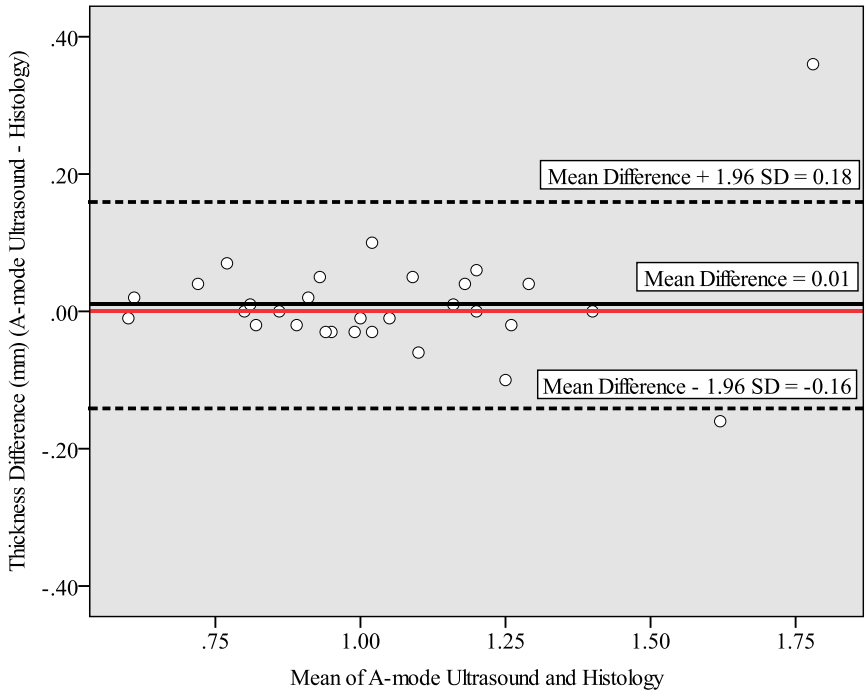

Figure 5.8. Bland-Altman plot for enamel thickness measurements with histology and A-mode ultrasound using the SOS from each specimen (n = 30). The dashed black lines represent the limits of agreement which range from 0.18 to -0.16 mm. The solid black line represents the mean difference between ultrasound and histology which was 0.01 mm. The red line is the reference at 0.00 mm.

5.3.4.6 Test of Normality

The Shapiro-Wilk test result was < 0.05 (*p*-value = 0.00) which indicated that the data was not normally distributed.

Table 5.11. Shapiro-Wilk test of normality for the data obtained from A-mode ultrasound and histology.

	Statistic	df	Sig.
Difference between A-mode Ultrasound and Histology	0.76	30	0.00

Table 5.12. Wilcoxon sign rank test of A-mode ultrasound and histology

	Histology - Ultrasound
Asymp. Sig. (2-tailed)	0.55

Table 5.13. Descriptive statistics for measurements with A-mode ultrasound and histology (mm)

	n	Mean	SD	Minimum	Maximum
A-mode Ultrasound	30	1.04	0.28	0.59	1.96
Histology	30	1.03	0.26	0.60	1.70

5.3.4.7 Verifying A-Mode Ultrasonic Enamel Thickness Measurements (using mean SOS from all specimens) with Histology at T Marked Areas

Table 5.14. Enamel thickness measurements obtained with A-mode ultrasound (using mean SOS from all specimens) and histology at T marked areas from 30 specimens (mm)

Specimen	Mean A-Mode Thickness	±SD	Mean Histology Thickness	±SD	Difference
1	0.91	0.02	1.07	0.05	-0.16
2	0.59	0.05	0.60	0.00	-0.01
3	0.77	0.03	0.80	0.00	-0.03
4	0.71	0.03	0.60	0.05	0.11
5	0.93	0.09	0.97	0.00	-0.04
6	0.74	0.05	0.70	0.00	0.04
7	1.08	0.03	0.90	0.00	0.18
8	1.02	0.03	1.00	0.00	0.02
9	1.05	0.03	1.30	0.05	-0.25
10	1.16	0.06	1.16	0.00	0.00
11	1.30	0.05	1.27	0.05	0.03
12	1.18	0.03	1.17	0.00	0.01
13	0.77	0.03	0.73	0.05	0.04
14	1.02	0.06	0.97	0.05	0.05
15	1.05	0.03	1.13	0.08	-0.08
16	1.33	0.06	1.07	0.05	0.26
17	1.11	0.05	1.20	0.04	-0.09
18	0.80	0.03	0.83	0.00	-0.03
19	1.73	0.03	1.70	0.00	0.03
20	1.73	0.03	1.57	0.00	0.16
21	1.44	0.05	1.40	0.05	0.04
22	1.30	0.06	1.27	0.05	0.03
23	1.05	0.03	1.00	0.05	0.05
24	0.86	0.04	0.90	0.05	-0.04
25	1.02	0.03	1.03	0.05	-0.01
26	0.93	0.03	0.87	0.00	0.06
27	1.09	0.05	1.17	0.05	-0.08
28	1.04	0.02	0.97	0.05	0.07
29	0.93	0.03	0.90	0.00	0.03
30	0.87	0.03	0.80	0.00	0.07

Table 5.15. Difference in enamel thickness from histology using SOS of each specimen and mean SOS from all specimens (mm).

Specimen	Difference using SOS of each specimen	Difference using mean SOS from all specimens
1	-0.01	-0.16
2	0.00	-0.01
3	-0.02	-0.03
4	0.01	0.11
5	-0.03	-0.04
6	0.05	0.04
7	0.02	0.18
8	-0.01	0.02
9	-0.10	-0.25
10	0.00	0.00
11	-0.01	0.03
12	0.07	0.01
13	0.07	0.04
14	0.12	0.05
15	-0.06	-0.08
16	0.05	0.26
17	0.01	-0.09
18	-0.02	-0.03
19	-0.16	0.03
20	0.39	0.16
21	-0.02	0.04
22	0.02	0.03
23	-0.02	0.05
24	-0.02	-0.04
25	-0.03	-0.01
26	-0.01	0.06
27	0.02	-0.08
28	-0.05	0.07
29	0.04	0.03
30	0.00	0.07
Mean	0.01 ±0.09	0.02 ±0.10

5.4 Discussion

The conventional and most convenient method for monitoring TSL at present is sequential study casts (Bartlett, 2003), which are compared longitudinally. The other method, which is more accurate and reproducible but time consuming, is laser profilometry (Bartlett, 2003). This requires an impression of the teeth from which the replicas are made but it has been shown that impressions can lead to inaccurate measurements (Rodriguez and Bartlett, 2011). Also, the measurement of progressive enamel loss by laser profilometry is done in the laboratory using expensive equipment. A-mode ultrasound has been proposed as a potential tool for direct, non-destructive enamel thickness measurements. The majority of ultrasonic enamel thickness measurements reported in the literature assumed a constant SOS within the tooth and across other teeth. This attracts an element of uncertainty in the enamel thickness measurements because the SOS varies within and across teeth. A solution for this problem is to use information in the relative TOFs in the serial measurements. When the ultrasound transducer is placed on the enamel surface to take a measurement, what is being measured is the TOF, not the thickness (which requires an SOS to be calculated using the range equation). The TOF will be the point of interest here, because if it decreases, it means that some enamel has been lost, provided the transducer was perpendicular to the enamel surface.

5.4.1 SOS Measurement in Enamel at V Marked Areas

In this work, the mean SOS value for the 30 sections, 6191 ±199 ms^{-1}, was in very good agreement with the reported literature values (see Table 1.1, p.20 and Figure 5.9 below). The results showed no statistically significant difference (p-value = 0.34) in SOS values between the two sections (occlusal and cervical). This might be due to

the relatively close proximity of both sections. There appears to be a wide range in SOS across the specimens (5187-7222 ms^{-1}), which was not surprising as the SOS was known to be different across different teeth and within the same teeth. John (2005) has demonstrated that SOS in a tooth can vary depending on how parallel the ultrasound wave is to the enamel rods. Enamel rods vary in orientation along the enamel layer where some rods lie perpendicular to the ADJ others lie parallel to it (Lees and Rollins Jr, 1972) which explains the higher SOS values shown in the histogram (Figure 5.9). Furthermore, anisotropy in teeth has been reported by several studies as a primary obstacle for the utilisation of diagnostic ultrasound in dentistry (Huysmans and Thijssen, 2000; Habelitz *et al.*, 2001; Louwerse *et al.*, 2004; John, 2005; Harput *et al.*, 2009; Harput *et al.*, 2011; Slak *et al.*, 2011). Therefore, careful awareness of the ultrasound transducer orientation during measurements is crucial for consistent results.

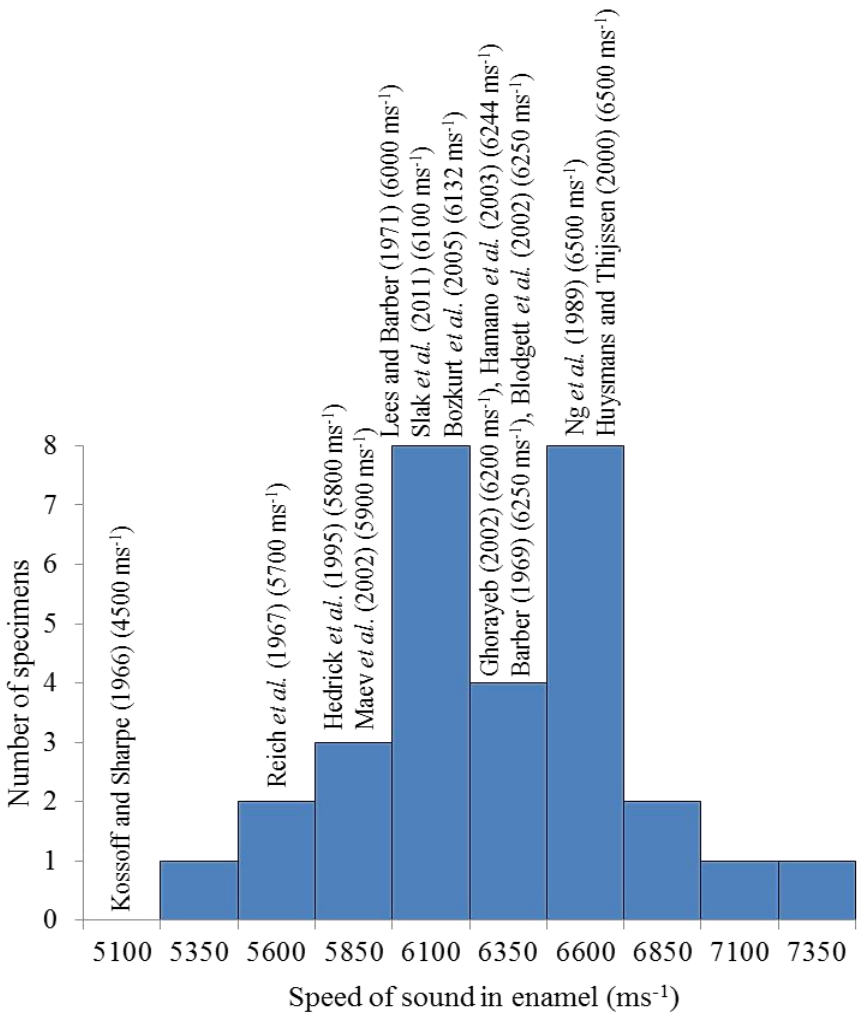

Figure 5.9. SOS result across a sample of 30 sections from 15 premolar teeth. SOS values from the literature are also shown

5.4.2 Enamel Thickness Measurements with A-Mode Ultrasound at T Marked Areas

The results from this Chapter showed very good agreement between A-mode ultrasound and histology in measuring enamel thickness in premolars, which means that the ultrasonic system was accurate and effective in measuring enamel thickness. The results indicated that in all analyses there was a relatively small mean difference between the two methods. This means there is no consistent trend of A-mode ultrasound over- or under-predicting enamel thickness. The mean percentage difference between A-mode ultrasound and histology was 1.05 ±6.34%. This is better

than the *in vitro* findings of Slak *et al.* (2011) which reported a ~12.00% difference in enamel thickness between A-mode ultrasound and histology from a sample of 4 human central incisors.

It is well established that the accuracy of ultrasound in measuring the true enamel thickness depends on the SOS in enamel, which varies across different individuals and different teeth (Huysmans and Thijssen, 2000). Since Slak and co-workers (2011) have determined the SOS in enamel in one of the teeth and used its mean SOS value in subsequent measurements for other teeth, it is not surprising to see a difference between the measured value and the true value. This explains the higher accuracy achieved in this Chapter because the SOS was determined for each specimen and a mean SOS value was not used for all specimens. Also, the paired t-test results demonstrated that there was no statistically significant difference between A-mode ultrasound and histology (p-value = 0.46).

Using the mean difference as a measure of accuracy between two methods is acceptable for assessing the 'overall' accuracy of the measurements which shows how ultrasound under/overestimates the histology measurements. However, if the aim was to assess for each tooth how ultrasound agrees with the histology measurements, then it is best to calculate the 95% limits of agreement (Bland and Altman, 1986) and report this value as the accuracy of the ultrasonic technique. Using this approach, the results showed that the majority of the ultrasound measurements are within approximately 10% of the histology measurements. The 10% difference in the measurements may have arisen due to the non-planar nature of premolars which means that the transducer tip was not perpendicular to the enamel surface while taking measurement. This results in smaller echoes that are difficult to recognise in the waveform (Slak *et al.*, 2011). The ICC obtained in this work (0.96)

means that the majority of the differences were between teeth and not within measurements of the same teeth (measurements of the same teeth by ultrasound and histology). Therefore there is a high level of agreement between ultrasound and histology measurements.

An *in vitro* study has measured enamel thickness on worn cusps of molar teeth with A-mode ultrasound before and after abrading the cusps with abrasive paper (Tagtekin *et al.*, 2005). They verified the results with histological sections and found a moderate correlation between both methods (ultrasound and histology) but not perfect agreement. This could be due to the use of one SOS value (6132 ± 2.5 ms^{-1}) for all teeth which may have caused inaccuracies in their results.

To investigate this further, the mean SOS for all the specimens in this Chapter was used to calculate the enamel thickness using the same TOF data used earlier. The 95% limits of agreement increased to -0.17 to 0.21 mm compared to -0.16 to 0.18 mm. This demonstrates that using the specific SOS rather than mean values results in a more accurate measurement. This is an important distinction between previous work by other researchers and the work in this Chapter, where the enamel thickness obtained for each section was based on its own SOS measurement.

For the purpose of measuring progressive loss of enamel thickness the important thing is the ability to reproducibly measure the ***change*** in thickness from baseline rather than the ***remaining*** enamel thickness value (discussed in Chapter 6). If the current system was to be used on maxillary central incisors it would be expected to produce more accurate results, because planar and larger central incisors would reflect stronger echoes that are easier to identify.

It is important to note that there is scope for improving the agreement between A-mode ultrasound and histological measurements. This could be achieved by signal processing, to increase the signal-to-noise ratio which renders reflected echoes easier to locate. Harput *et al* (2011) have investigated signal loss in human teeth and used a custom-made wave excitation technique known as linear frequency modulated (LFM) chirp excitation that is tailored for individual teeth. This allows most of the ultrasound wave to be targeted into the tooth and separated from overlapping echoes which makes their detection easier. However, implementing this technique requires a solid background in signal analysis and programming, which is beyond the scope of this thesis. Nevertheless, it would be an interesting method to learn and adopt in future experiments involving ultrasound and dental applications.

5.5 Conclusions

- A-mode ultrasound shows promise as a non-destructive technique for measuring enamel and monitoring TSL.
- The A-mode ultrasound technique used here was accurate and within 10% of histological measurements.
- The reproducibility of this A-mode ultrasound technique must be assessed in order to see if it can measure progressive loss in enamel thickness with sufficient precision. This will be discussed in the following Chapter.

6 *In Vivo* Reproducibility of Enamel Thickness Measurements with A-Mode Ultrasound

6.1 Introduction

In the previous Chapter it was demonstrated that ultrasound can measure enamel thickness *in vitro*. However it was apparent that measurements on teeth which had marked curvature, such as premolars, were not ideal since there was strong angle dependency. It was therefore concluded that any further work should focus on incisors since these normally have more planar surfaces. It proved impossible to investigate this further *in vitro* because extracted human incisors were not available from the University of Leeds Skeletal Tissue Bank. This prompted the designing of an *in vivo* study.

Taking into account the results from the studies described in the earlier Chapters, it was concluded that a simple A-mode approach would be the most useful. There were two reasons for this choice: Firstly, the potential for the creation of a simple hand-held tool for routine clinical use is much greater if there is no need to display and interpret a B-mode image; secondly, the operator of such a device would be able to make angle adjustments easily, guided by the instantaneous height of the received echoes. In the first instance this would be a manually optimised system but there is clear potential for a more automated approach in which the machine would monitor the received signal and feedback to the operator, either visually or by sound, when the optimal angle has been attained.

There are a number of possible clinical applications for such a device but the detection and monitoring of TSL is definitely one of them (Huysmans and Thijssen, 2000; Tagtekin *et al.*, 2005; Hua *et al.*, 2009; Huysmans *et al.*, 2011).

For any technique to be useful in monitoring TSL, its reproducibility has to be better than the change which is to be detected (Schlueter *et al.*, 2005). There is little quantitative data on the amount of TSL in affected patients. Generally, the range of the reported values for pathologic TSL varied from 17.6-108.2 μm/6 months (Bartlett *et al.*, 1997) and 250 μm/year (Wilder-Smith *et al.*, 2009). However, these TSL rates were from GORD patients and caution is required before generalising to different populations (Huysmans *et al.*, 2011). A recent study on patients referred for management of erosive TSL reported a wear rate of < 15 μm/6 months (Rodriguez *et al.*, 2012) but the patients enrolled had dietary counselling before commencement of the study which might have contributed to lower wear rates, as it has been shown that consuming acidic food and drinks increases erosive TSL. That said, erosive TSL is cyclical in nature (Rodriguez *et al.*, 2012) and the ability to monitor it at an early stage with a precise method is important to permit instigation of dietary counselling and preventive measures, avoiding further loss of enamel. The technique must also be simple to perform, acceptable for patients and cost effective in the dental surgery (Schlueter *et al.*, 2005).

One important issue is to distinguish between absolute accuracy and reproducibility. If monitoring erosive TSL requires accurate and precise measurement of enamel thickness on each occasion, the variation in the SOS in enamel between patients will be a limiting factor. Clearly the accuracy of the thickness measurement depends on the reliability of the SOS value. However, the aim of this study was to measure the reproducibility of the technique *in vivo* rather than the true thickness of the enamel.

The challenge in the case of TSL measurements is not to make the individual measurement very accurate but rather to enable detection of change between visits so that the rate of enamel loss can be determined. The key performance parameter in such cases is not accuracy (i.e. agreement with a gold standard) but rather reproducibility. For the purposes of time dependent erosion assessment, it is the difference in serial measurements which is critical and this hinges on reproducibility. The smallest amount of detectable change in enamel thickness will be greater than the reproducibility of individual measurements. It was therefore decided to proceed to an *in vivo* reproducibility study using incisors of normal healthy volunteers.

The literature has addressed the reproducibility of the A-mode ultrasonic technique to measure enamel thickness with good results, but this was in an *in vitro* setting (Huysmans and Thijssen, 2000). Therefore establishing the reproducibility of this technique *in vivo* would determine its viability as a non-destructive, non-invasive approach for monitoring erosive TSL. The aim of this Chapter is to determine whether ultrasound can be used to reproducibly measure enamel thickness in human teeth *in vivo* and to assess whether it is a reproducible and reliable technique for use within a clinical environment.

6.2 Materials and Methods

6.2.1 Ethical Approval

The study was conducted after obtaining local ethical approval (020712/KS/46, Appendix 5) from the Dental Research Ethics Committee (DREC) and Leeds Research and Development Directorate (DT12/10538, Appendix 6). Good Clinical Practice (GCP) standards were followed in line with the recommendations guiding physicians in biomedical research involving human volunteers adopted by the 18th World Medical Assembly, Helsinki, Finland, 1964, amended at the 52nd World Medical Association General Assembly, Edinburgh, Scotland, October 2000.

6.2.2 Recruitment

The assessment of eligibility and the informed consent process was undertaken by the Principal Investigator at the Leeds Dental Translational and Clinical Research Unit (DenTCRU) who is qualified by training and/or experience in taking informed consent to GCP standards. Informed, written consent for entry into the study was obtained prior to recruitment**.**

An ethically approved advertisement (Appendix 7) was posted on the University of Leeds campus and volunteers interested in taking part in the study were provided with verbal and written details about the study (Participant Information Sheet and Participant Consent Form, Appendix 8 and 9 respectively). This included detailed information about the rationale, design and personal implications of the study. Following information provision, volunteers had as long as they needed to consider participation (minimum of 24 hours) and were given the opportunity to discuss the study with their family and other healthcare professionals before they were asked whether they would be willing to participate.

Assenting volunteers were then formally assessed for eligibility and invited to provide informed, written consent. The Principal Investigator or any other clinically qualified member of the trial team, who had received GCP training and had been approved by the Principal Investigator as detailed on the Authorised Personnel Log, was permitted to take informed consent. The right of the volunteer to refuse consent without giving reasons was respected. Further, the volunteer remained free to withdraw from the study at any time without giving reasons and without prejudicing any further treatment.

A total of 30 (27 females and 3 males) healthy consenting volunteers with a mean age of 35 years (range 20-63 years) were recruited to the study from members of staff, undergraduate and postgraduate students (excluding dental students) at the University of Leeds (30 volunteers came forward and none were rejected). This was a pilot study and further studies would require data on reproducibility in order to facilitate a power calculation which would determine the sample size. Since this was the first specific study of this problem, the choice of sample size was inevitably arbitrary. Each volunteer underwent an initial dental examination visit to determine his/her suitability for the study. The tooth chosen for this study was one of the maxillary central incisors, as these large and more planar teeth would be more echogenic and less angle dependent, as confirmed by preliminary *in vitro* work prior to commencing the study (see Chapter 3). There was a preference for the upper right maxillary central incisor for practical operational reasons.

Both maxillary central incisors underwent assessment and the one which was not restored nor had cracks was included in the study. Before the start of the study a trial scan was performed on the chosen intact maxillary central incisor to assess whether it was echogenic or not. If it was not echogenic the contralateral incisor was selected

instead. If the contralateral incisor was also not echogenic, the volunteer was not included in the study and a replacement volunteer was recruited.

6.2.3 Exclusion Criteria

Volunteers with the following were excluded: abnormal, replaced, hypoplastic enamel on maxillary central incisors; teeth that had orthodontic appliances, removable appliances, fixed crown or bridgework, hypersensitivity and periodontal disease.

6.2.4 Inclusion Criteria

Consenting healthy adults over 18 years (females and males) with at least one maxillary central incisor that was intact with no obvious cracks in its crown could be included. At least one maxillary central incisor had to be caries-free and with no obvious periodontal disease and had to also be echogenic.

6.2.5 Cross Infection Control

The ultrasound transducer and attached cable, pulser and digital oscilloscope were cleaned at the beginning of the session and after each volunteer with a soap and water wipe. The laptop, membrane keyboard and USB hub underwent external surface clean with a soap and water wipe at the beginning of each session and after each volunteer use. During a clinical session, gloves were worn whilst the transducer was applied to the surface of the tooth and changed between participants.

To eliminate cross infection risks, a new Perspex tip was used on the transducer for each volunteer at every visit. In addition, to ensure that volunteers were not inconvenienced and to enable continuity of the trial, an additional transducer was available for use.

6.2.6 Data Protection

The ultrasound measurements generated ultrasound waveforms which were anonymised and stored on a secure password protected laptop backed up on an encrypted memory stick for analyses.

6.2.7 A-Mode Ultrasound Enamel Thickness Measurements

The transducer was excited by a pulser/receiver (PR-5742, Olympus® Inc., MA, USA) and the ultrasound waveform was captured on a digital oscilloscope (LT-3542, Teledyne LeCroy®, NY, USA) and digitized to 2500 data points. 1000 such pulses were averaged by the oscilloscope to create an ASCII data file for export. A drop of water was used to couple a 15 MHz focussed delay line transducer (VR-260, Olympus® Inc., MA, USA) to the tooth (Figure 6.1 below). In order to automate the waveform capturing and saving process, a macro programme written by a colleague was used. A dental research coordinator assisted in entering data whilst taking measurements.

Figure 6.1. Ultrasound transducer applied to maxillary right central incisor.

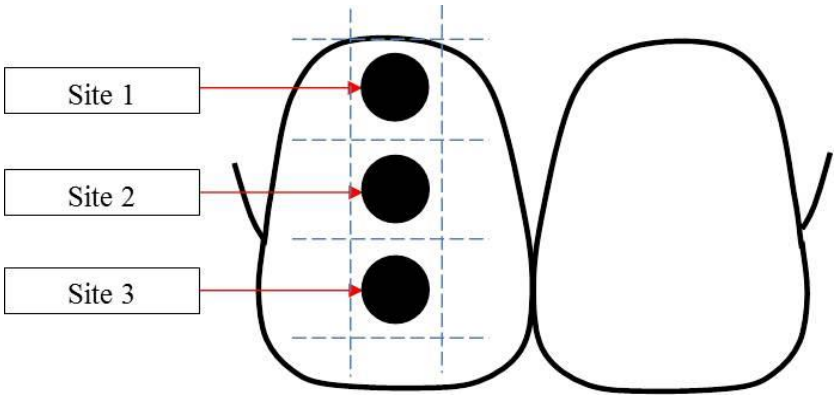

Figure 6.2. Schematic of maxillary central incisor and the measurement sites. The dashed lines represent the 'visual' marking of the scan sites.

6.2.7.1 Week 1 Visit

A trial ultrasonic scan was completed on the chosen tooth to check if it was echogenic. A cotton wool roll was used to clean the tooth surface from plaque residues. Three readings were taken for each site. Readings were repeated on the second and third visits, which were a week apart, to assess reproducibility.

6.2.7.2 Week 2 and 3 Visits

The same procedure from the week 1 visit was repeated in the week 2 and then 3 visits, except for the trial scan. The second visit took place one week after the initial visit while the third visit took place two weeks after the initial visit. The Principal Investigator did not have access to the data obtained from prior weeks to avoid bias when seeing the waveform on the oscilloscope.

6.2.8 Data Analysis

A total of 810 ASCII data files were analysed using OriginPro 8.6 (OrigLabs, MA, USA). Each file was plotted and a waveform was produced. A "find peaks" function in the programme was used to locate the peaks. The first peak corresponded to the transducer-enamel interface and the second peak corresponded to the ADJ. When there were multiple peaks for an echo, the first echo was used. When a waveform

was uninterpretable its measurement was omitted. The time difference from the first and second peak was used in the range formula to calculate the enamel thickness, based on a mean SOS of 6000 ms^{-1}.

6.2.9 Statistical Methods

The primary aim of the analysis was to examine the reproducibility of the method. This was done using the same statistical tests as in Chapter 5 (Bland-Altman limits of agreement and the ICC tests).

6.3 Results

The data showed that for sites one and two there was one tooth where the agreement was substantially different to that for the rest of the teeth. As the data from this tooth was very influential in the results obtained the analyses for these two sites was performed twice, firstly considering all data (n = 30), and then secondly omitting this tooth as an outlier (n = 29).

6.3.1 A-Mode Ultrasound Enamel Thickness Measurements

Table 6.1. Site 1 mean enamel thickness measurements for all teeth on weeks 1, 2 and 3 (mm).

Site	Tooth	Age	Week 1	SD	Week 2	SD	Week 3	SD
1	1	27	1.22	0.02	1.17	0.25	1.09	0.06
1	2	28	1.37	0.10	0.61	0.03	0.58	0.02
1	3	34	0.57	0.00	0.56	0.02	0.55	0.03
1	4	26	0.59	0.05	0.57	0.00	0.57	0.00
1	5	63	0.57	0.00	0.54	0.00	0.56	0.02
1	6	38	0.55	0.03	0.53	0.03	0.55	0.03
1	7	55	0.56	0.02	0.56	0.03	0.59	0.03
1	8	30	0.55	0.09	0.53	0.05	0.59	0.06
1	9	21	0.59	0.07	0.59	0.06	0.63	0.11
1	10	36	0.55	0.07	0.51	0.03	0.56	0.02
1	11	51	0.54	0.02	0.55	0.02	0.6	0.06
1	12	27	0.57	0.02	0.57	0.00	0.57	0.00
1	13	20	0.59	0.00	0.63	0.00	0.62	0.05
1	14	40	0.54	0.00	0.54	0.00	0.56	0.02
1	15	35	0.56	0.02	0.56	0.05	0.56	0.02
1	16	35	0.58	0.00	0.58	0.06	0.56	0.02
1	17	42	0.58	0.00	0.58	0.02	0.55	0.12
1	18	27	0.56	0.02	0.55	0.03	0.55	0.02
1	19	32	0.56	0.03	0.58	0.05	0.56	0.03
1	20	22	0.57	0.02	0.57	0.00	0.57	0.00
1	21	27	0.56	0.02	0.56	0.05	0.56	0.02
1	22	41	0.57	0.03	0.57	0.00	0.57	0.03
1	23	41	0.55	0.08	0.58	0.03	0.56	0.02
1	24	42	0.58	0.00	0.58	0.02	0.57	0.03
1	25	38	0.57	0.05	0.59	0.03	0.57	0.06
1	26	41	0.56	0.00	0.58	0.05	0.54	0.00
1	27	29	0.56	0.03	0.58	0.05	0.57	0.03
1	28	36	0.63	0.03	0.55	0.02	0.55	0.05
1	29	25	0.56	0.02	0.53	0.05	0.56	0.02
1	30	49	0.56	0.03	0.56	0.02	0.57	0.00

Table 6.2. Site 2 mean enamel thickness measurements for all teeth on week 1, 2 and 3 (mm).

Site	Tooth	Age	Week 1	SD	Week 2	SD	Week 3	SD
2	1	27	0.66	0.00	1.25	0.09	1.42	0.03
2	2	28	0.79	0.08	0.75	0.05	0.84	0.20
2	3	34	0.56	0.02	0.70	0.23	0.56	0.02
2	4	26	0.60	0.00	0.59	0.02	0.59	0.02
2	5	63	0.57	0.00	0.55	0.03	0.57	0.00
2	6	38	0.55	0.02	0.56	0.02	0.56	0.02
2	7	55	0.54	0.00	0.56	0.02	0.55	0.02
2	8	30	0.57	0.00	0.53	0.03	0.59	0.03
2	9	21	0.55	0.02	0.57	0.03	0.59	0.03
2	10	36	0.56	0.02	0.52	0.02	0.55	0.02
2	11	51	0.54	0.00	0.56	0.02	0.53	0.03
2	12	27	0.58	0.05	0.61	0.05	0.58	0.02
2	13	20	0.54	0.00	0.60	0.03	0.56	0.02
2	14	40	0.54	0.00	0.57	0.00	0.57	0.00
2	15	35	0.57	0.00	0.57	0.00	0.58	0.02
2	16	35	0.54	0.03	0.65	0.06	0.61	0.07
2	17	42	0.54	0.00	0.61	0.05	0.55	0.05
2	18	27	0.57	0.00	0.57	0.00	0.56	0.03
2	19	32	0.54	0.03	0.56	0.02	0.62	0.07
2	20	22	0.56	0.02	0.56	0.02	0.57	0.04
2	21	27	0.55	0.02	0.56	0.03	0.56	0.02
2	22	41	0.56	0.02	0.55	0.02	0.57	0.03
2	23	41	0.56	0.03	0.57	0.05	0.58	0.02
2	24	42	0.57	0.00	0.57	0.08	0.57	0.00
2	25	38	0.54	0.00	0.57	0.00	0.57	0.00
2	26	41	0.60	0.00	0.54	0.00	0.54	0.00
2	27	29	0.56	0.02	0.54	0.00	0.56	0.02
2	28	36	0.57	0.00	0.60	0.03	0.57	0.00
2	29	25	0.57	0.00	0.57	0.00	0.56	0.02
2	30	49	0.57	0.00	0.57	0.00	0.56	0.02

Table 6.3. Site 3 mean enamel thickness measurements for all teeth on week 1, 2 and 3 (mm).

Site	Tooth	Age	Week 1	SD	Week 2	SD	Week 3	SD
3	1	27	0.96	0.00	1.36	0.12	1.27	0.05
3	2	28	1.31	0.06	1.15	0.05	0.99	0.13
3	3	34	0.57	0.00	1.00	0.12	0.57	0.00
3	4	26	0.57	0.00	0.60	0.00	0.58	0.02
3	5	63	0.85	0.02	0.86	0.03	0.9	0.00
3	6	38	1.56	0.00	1.22	0.06	1.30	0.03
3	7	55	1.36	0.11	1.45	0.07	1.19	0.09
3	8	30	0.84	0.08	0.96	0.03	0.93	0.05
3	9	21	0.87	0.03	0.83	0.03	0.88	0.02
3	10	36	0.87	0.06	0.73	0.06	0.98	0.07
3	11	51	1.19	0.08	0.86	0.06	0.87	0.05
3	12	27	1.39	0.02	1.16	0.09	1.22	0.03
3	13	20	1.05	0.03	1.22	0.11	1.25	0.02
3	14	40	1.07	0.03	1.02	0.06	1.05	0.00
3	15	35	1.08	0.08	0.83	0.03	0.84	0.00
3	16	35	0.91	0.12	0.88	0.03	0.91	0.03
3	17	42	1.04	0.08	0.86	0.03	0.92	0.05
3	18	27	1.17	0.14	1.10	0.02	1.00	0.11
3	19	32	1.27	0.05	1.19	0.03	1.10	0.03
3	20	22	1.18	0.14	0.84	0.05	1.05	0.04
3	21	27	1.27	0.18	0.91	0.07	0.84	0.00
3	22	41	1.03	0.17	1.00	0.06	1.11	0.00
3	23	41	1.14	0.03	1.03	0.17	1.11	0.03
3	24	42	0.86	0.02	0.92	0.03	1.03	0.09
3	25	38	1.11	0.03	1.04	0.05	1.08	0.00
3	26	41	0.84	0.13	1.04	0.11	1.07	0.12
3	27	29	1.05	0.18	0.87	0.00	0.88	0.02
3	28	36	0.85	0.02	0.88	0.07	0.91	0.06
3	29	25	0.95	0.12	0.92	0.09	0.87	0.05
3	30	49	0.87	0.06	1.02	0.05	1.02	0.08

6.3.2 Week 1 to Week 2 - Intra-Examiner Reproducibility

The first set of analyses examined the agreement between the measurements from week 1 and week 2 using the Bland-Altman method. The results of the analysis are summarised in Table 6.4.

Table 6.4. A summary of the Bland-Altman results obtained from week 1 and 2 (mm).

Site	Mean Difference (Bias) (Week 2 - Week 1)	SD Difference	95% Bland-Altman Limits of Agreement
Site 1	- 0.03	0.14	(- 0.30, 0.24)
Site 1 (*)	- 0.01	0.02	(- 0.05, 0.04)
Site 2	0.03	0.11	(- 0.19, 0.25)
Site 2 (*)	0.01	0.04	(- 0.07, 0.09)
Site 3	- 0.04	0.20	(- 0.43, 0.34)

(*) Analysis repeated omitting one outlying value

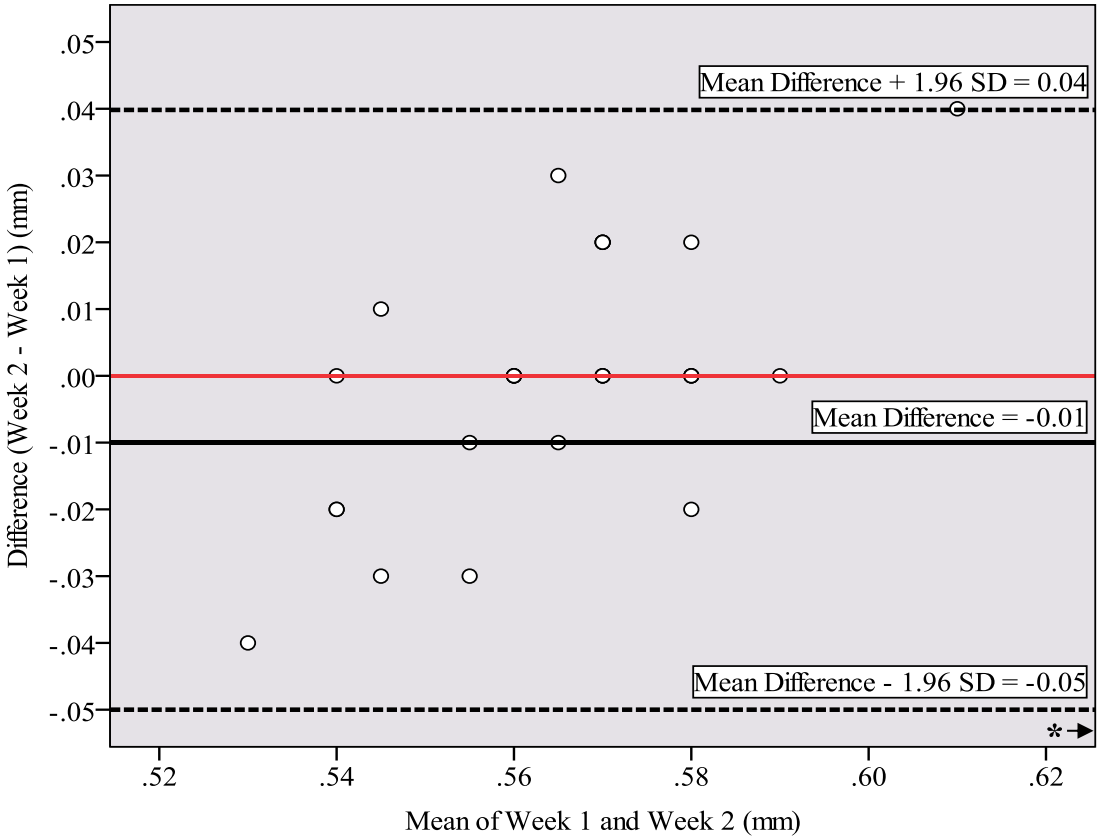

Figure 6.3. A Bland-Altman plot comparing week 1 and 2 on site 1 (n = 29). The asterisk represents a data point removed for graph clarification (data point location was $x = 1.02$, $y = -0.05$)

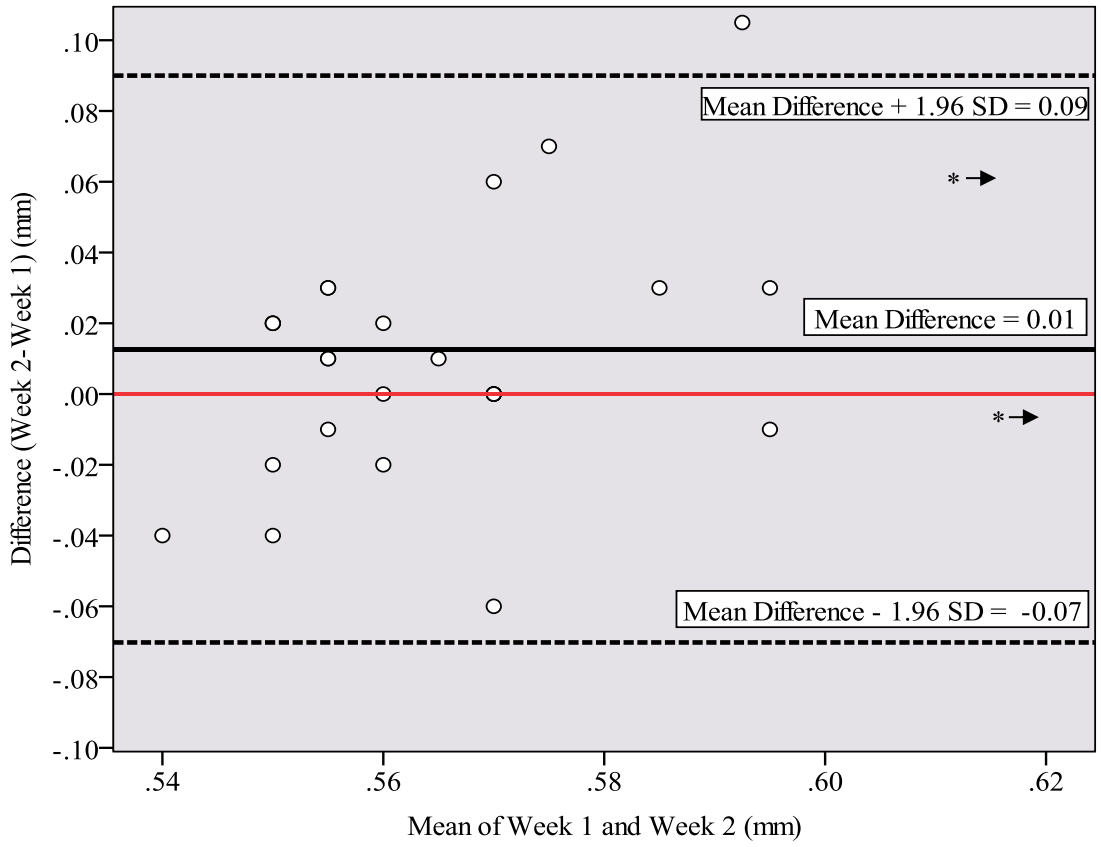

Figure 6.4. A Bland-Altman plot comparing week 1 and 2 on site 2 (n = 29). The asterisks represent data points removed for graph clarification (top to bottom their locations are $x = 0.63$, $y = 0.14$ and $x = 0.77$, $y = -0.04$)

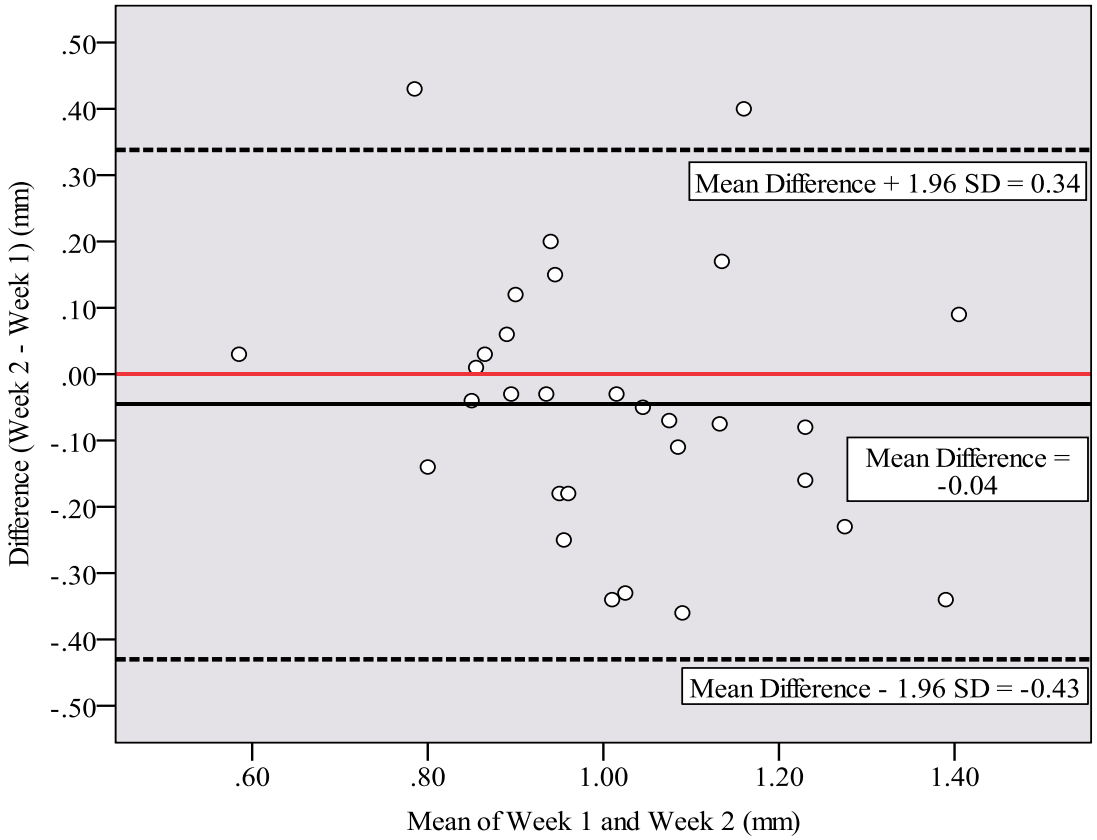

Figure 6.5. A Bland-Altman plot comparing week 1 and 2 on site 3 (n = 30)

6.3.3 Week 1 to Week 3 - Intra-Examiner Reproducibility

The Bland-Altman analyses were repeated using the change in values from week 1 to week 3. The results are summarised in Table 6.5.

Table 6.5. A summary of the Bland-Altman results obtained from week 1 and 3 (mm).

Site	Mean Difference (Bias) (Week 3 - Week 1)	SD Difference	95% Bland-Altman Limits of Agreement
Site 1	- 0.03	0.15	(- 0.32, 0.26)
Site 1 (*)	0.00	0.04	(- 0.07, 0.06)
Site 2	0.04	0.14	(- 0.24, 0.31)
Site 2 (*)	0.01	0.03	(- 0.04, 0.06)
Site 3	- 0.05	0.18	(- 0.39, 0.30)

(*) Analysis repeated omitting one outlying value

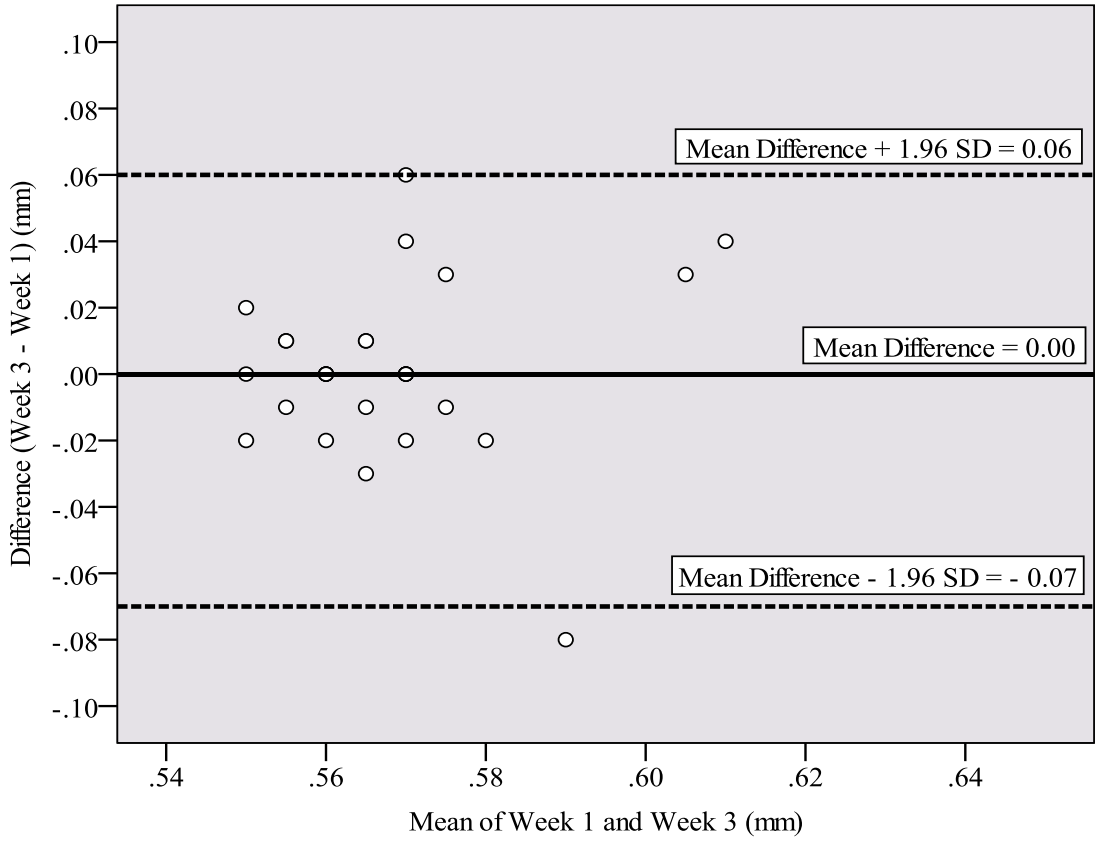

Figure 6.6. A Bland-Altman plot comparing week 1 and 3 on site 1 (n = 29).

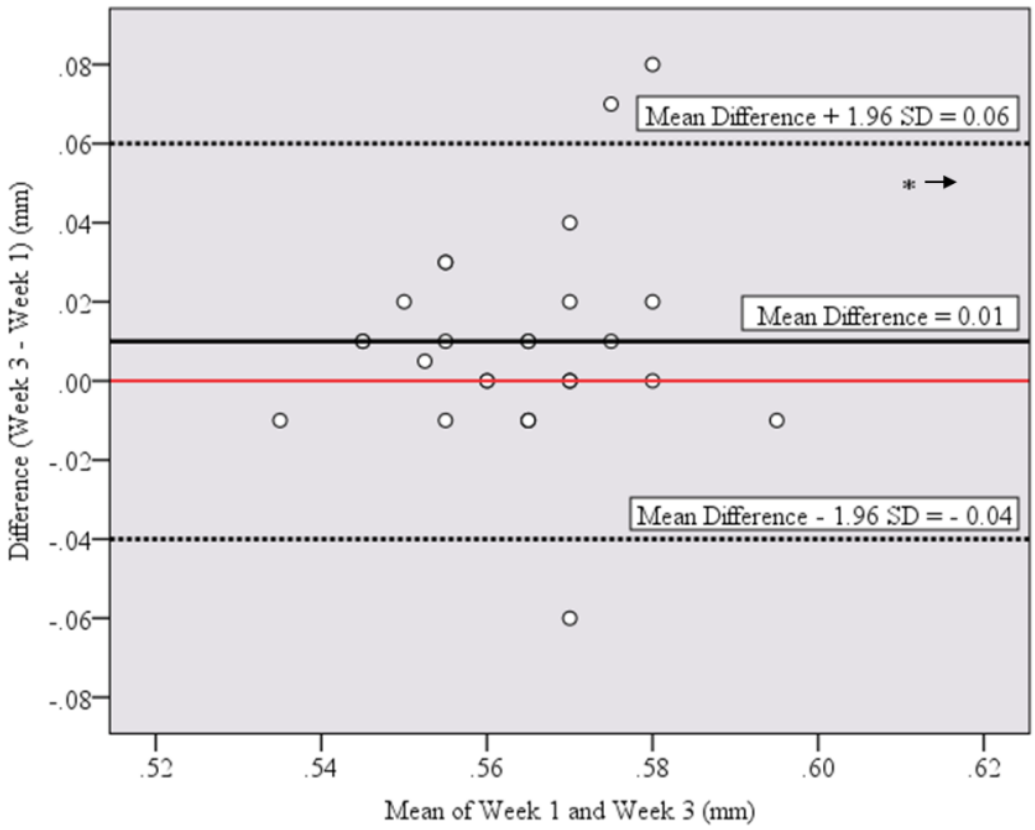

Figure 6.7. A Bland-Altman plot comparing week 1 and 3 on site 2 (n = 29). The asterisk represents a data point removed for graph clarification (data point location was $x = 0.82$, $y = 0.05$).

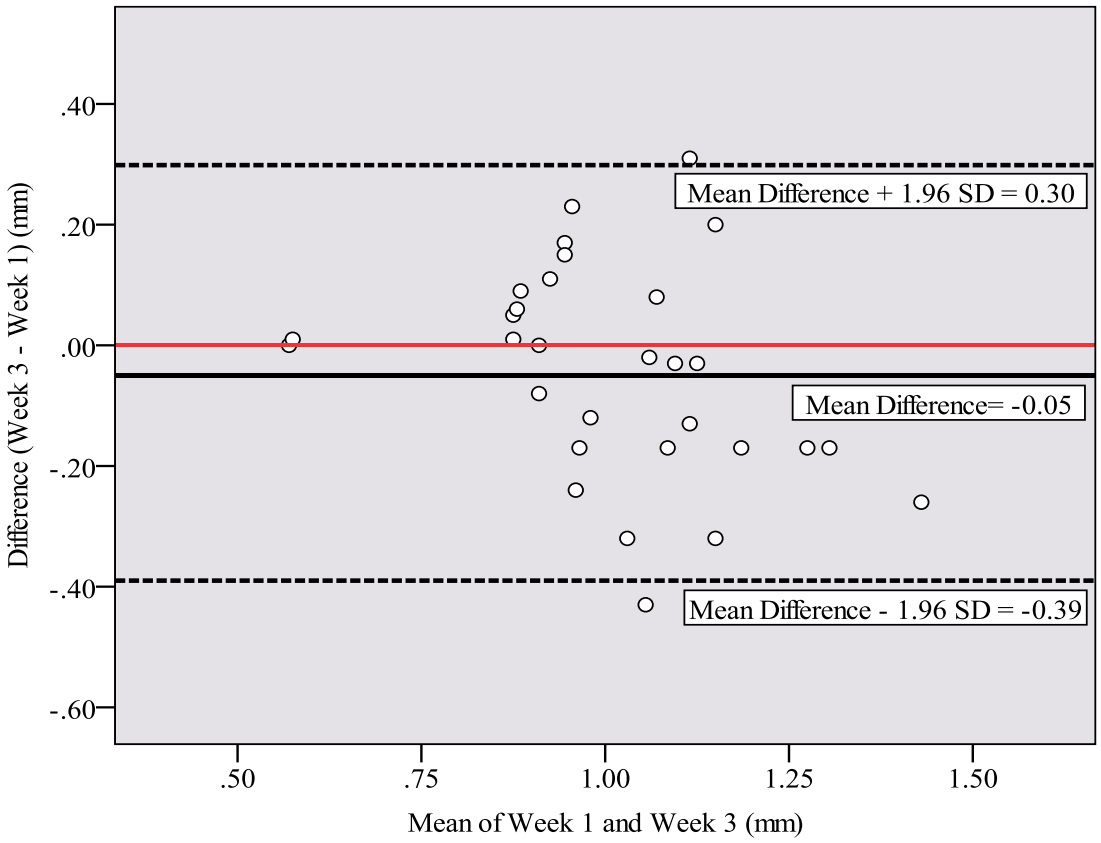

Figure 6.8. A Bland-Altman plot comparing week 1 and 3 on site 3 (n = 30).

6.3.4 Week 2 to Week 3 - Intra-Examiner Reproducibility

A similar set of analyses were performed to examine the differences between measurements made on week 2 and week 3, with the analysis results summarised in Table 6.6.

Table 6.6. A summary of the Bland-Altman results obtained from week 2 and 3 (mm).

Site	Mean Difference (Bias) (Week 3 - Week 2)	SD Difference	95% Bland-Altman Limits of Agreement
Site 1	0.00	0.03	(- 0.06, 0.06)
Site 2	0.00	0.05	(- 0.10, 0.10)
Site 3	0.00	0.13	(- 0.25, 0.25)

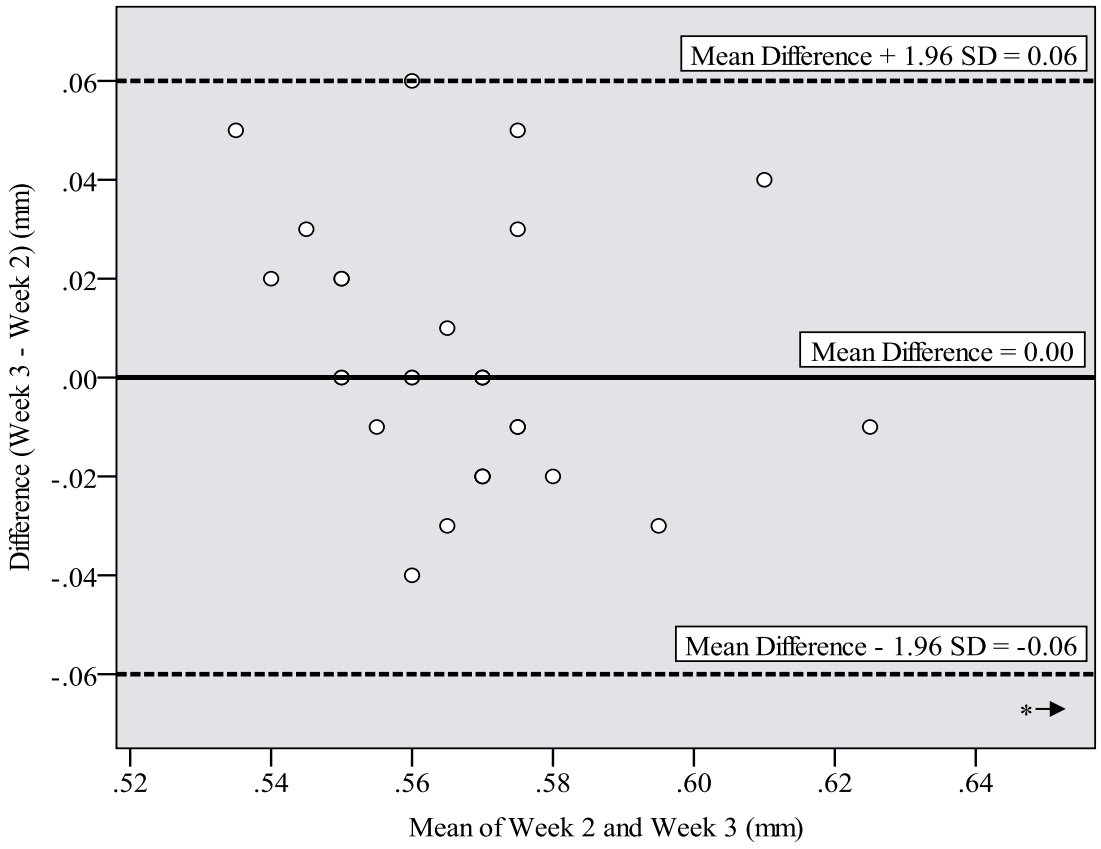

Figure 6.9. A Bland-Altman plot comparing week 2 and 3 on site 1 (n = 30). The asterisk represents a data point removed for graph clarification (data point location was $x = 1.13$, $y = -0.08$).

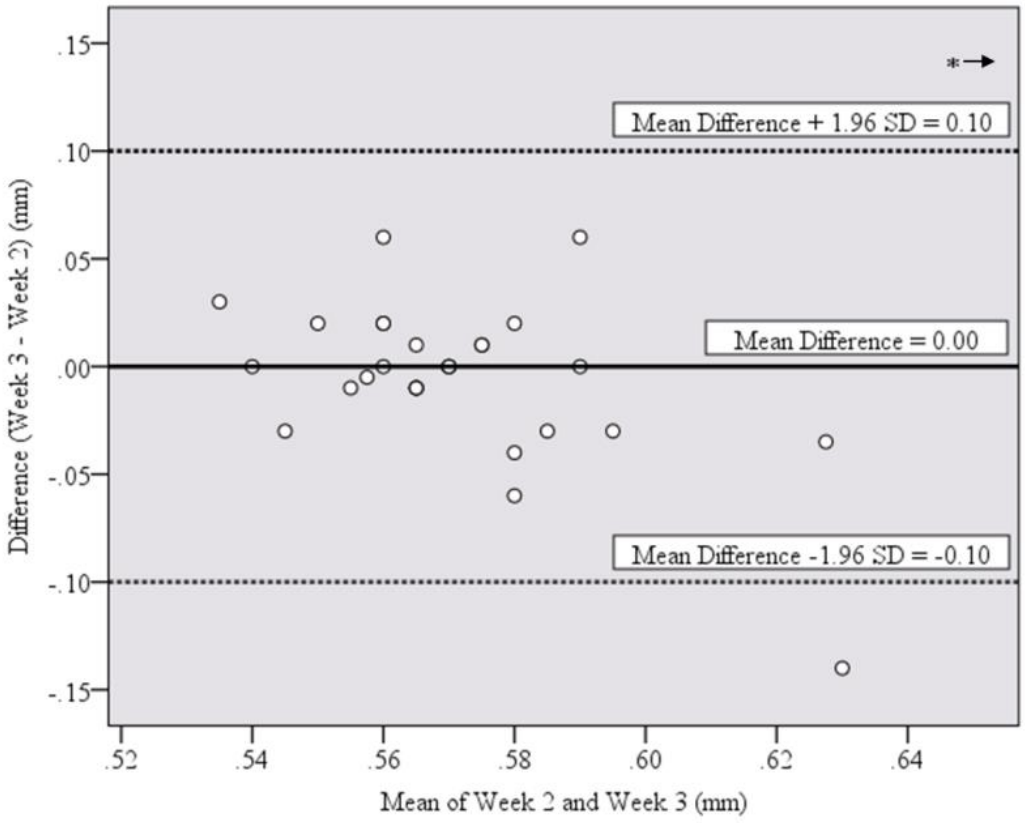

Figure 6.10. A Bland-Altman plot comparing week 2 and 3 on site 2 (n = 30). The asterisk represents a data point removed for graph clarification (data point location was $x = 1.34$, $y = 0.17$).

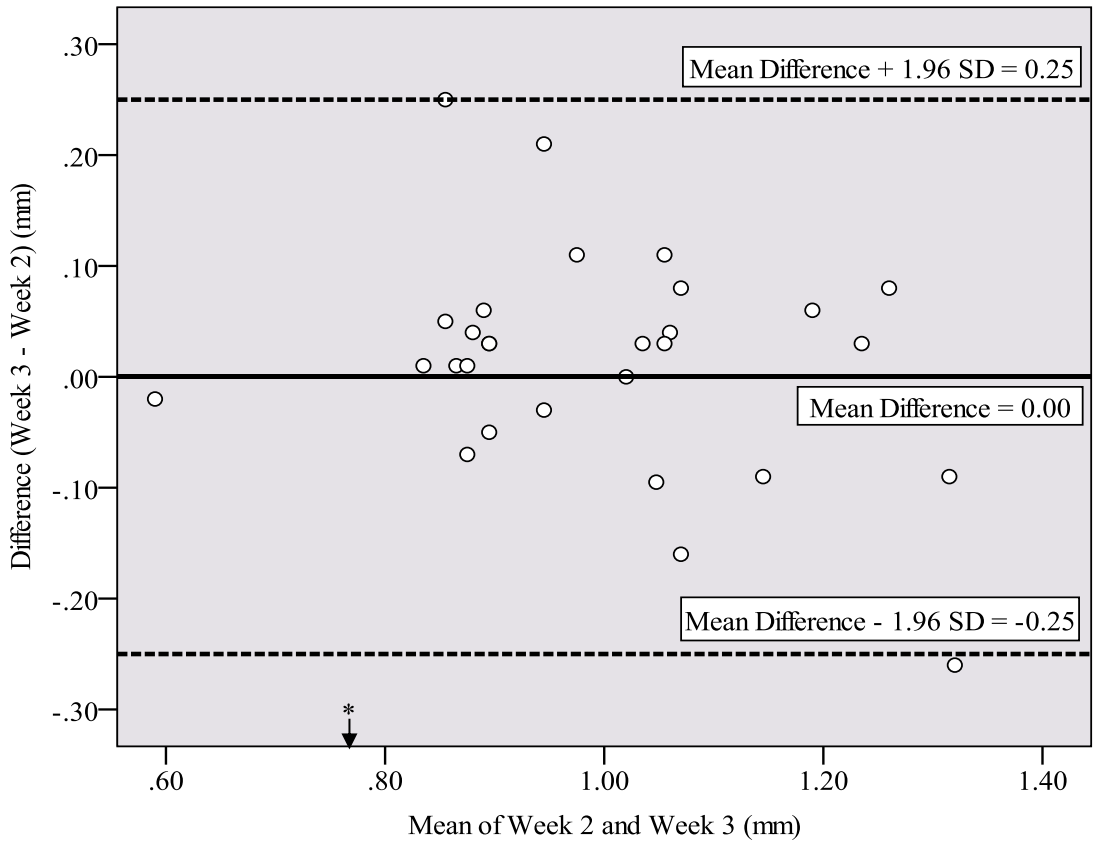

Figure 6.11. A Bland-Altman plot comparing week 2 and 3 on site 3 (n = 30). The asterisk represents a data point removed for graph clarification (data point location was $x = 0.79$, $y = -0.43$).

6.3.5 Intra-Class Correlation

The agreement between the repeat measurements was also assessed using the ICC test. A summary of the values obtained from each of the sites is given in Table 6.7. For sites 1 and 2, the analyses were repeated omitting one outlying tooth from the analyses.

Table 6.7. A summary of the ICC values across the three sites.

Site	ICC (*)	ICC (**)
Site 1	0.63	0.96
Site 2	0.61	0.71
Site 3	0.62	-

(*) Analysis using data from all teeth

(**) Omitting 1 outlier

6.3.6 Agreement between Repeat Measures at the Same Visit

This analysis examined the agreement between repeat measurements of the same teeth at the same visit. The ICC was calculated for each site/visit combination, and the results are summarised in the next table. The agreement was lowest for site 1 at week 3, where the ICC value was only 0.75.

Table 6.8. A summary of the ICC values across the three sites on all visits.

Site	Visit	ICC
Site 1	Week 1	0.96
	Week 2	0.84
	Week 3	0.75
Site 2	Week 1	0.82
	Week 2	0.85
	Week 3	0.92
Site 3	Week 1	0.86
	Week 2	0.86
	Week 3	0.90

6.4 Discussion

Erosive tooth surface loss is a problem of great concern to both patients and dentists. The patient's appearance and dental function become compromised as the enamel gradually wears away. Dentists strive to monitor this disease in a reproducible way, but at present the only resort for them is to use study casts or the very subjective erosion indices. One important aspect in the monitoring of erosion *in vivo* is having a fixed reference point from which measurements can be taken. Fortunately, the ADJ is a good reference point as it does not move or change with erosion. This is of key importance and potentially makes ultrasound a simpler procedure when compared, for example, to techniques like profilometry where metal discs are cemented on the teeth to serve as reference points (Bartlett *et al.*, 1997).

6.4.1 Week 1 to Week 2 - Intra-Examiner Reproducibility

The results showed that in all analyses there was a relatively small mean difference between the repeat measurements (i.e. one set of scores is not consistently higher than the other). This indicates no consistent trend of higher or lower values at week 2 compared to week 1.

The site 1 results gave Bland-Altman limits of agreement of -0.30 to 0.24 when all measurements were included in the analysis. This means that 95% of all differences between the two sets of measurements should lie within this range. However this result was masked by one tooth where the differences were very large. If this tooth was excluded from the analysis, the limits of agreement were drastically reduced to -0.05 to 0.04 (Figure 6.3).

In an *in vitro* study researchers found that the cervical site (site 1 in this Chapter) had the lowest reproducibility because enamel was thin in that area and because of difficulty in aligning the ultrasound transducer at the site; they added that if this measurement were performed *in vivo*, the reproducibility would be higher as teeth are stationary in the jawbone (Huysmans and Thijssen, 2000). However, this was not the case in the work described here, as demonstrated by the reproducibility results for the cervical site in in this Chapter (Table 6.4, Table 6.5 and Table 6.6). It would be interesting to know why the cervical site examined in this Chapter resulted in reproducible measurements, contrary to the previously reported results of Huysmans and Thijssen (2000). A reason for this could be that the measurements were made further away from the cervical region where enamel thickness changes rapidly with position. A second reason could be that the tooth was stationery and thus the position of the measurements was defined more reproducibly (Huysmans and Thijssen, 2000).

It is important to consider why there was an outlying value in the data set. This outlying value was from the second volunteer (Table 6.1). The reasons as to why this might have occurred are twofold: First, the transducer might not have been at a right angle to the enamel surface and as such the reflected echo took a longer TOF resulting in larger apparent enamel thickness (Culjat *et al.*, 2005a); second, a small echo from the ADJ of that tooth may lead to inaccurate location of the echo peak on the waveform during data analysis might have contributed to this larger thickness value.

The results for site 2 showed a similar pattern to those from site 1, in that the Bland-Altman limits are relatively wide when all teeth are included (with the outlier tooth). The interval is narrower with the exclusion of data from the one outlying tooth, although the interval is wider than that observed for site 1 (Figure 6.4).

The site 3 data showed the widest limits of agreement, ranging from -0.43 to +0.34 (Figure 6.5). This could be due to the ultrasound beam not meeting the ADJ at a right angle (due to the undulation of the ADJ), which causes the ultrasound beam to scatter away from the transducer, resulting in no echoes from that site.

6.4.2 Week 1 to Week 3 - Intra-Examiner Reproducibility

The results showed a similar pattern to those observed when considering the change from week 1 to week 2. There were relatively wide limits for sites 1 and 2 when all data values were used, but these limits were much reduced after omitting one outlying value. Site 3 again demonstrated the poorest agreement, with the widest Bland-Altman limits.

6.4.3 Week 2 to Week 3 - Intra-Examiner Reproducibility

The outlying values were primarily due to data from week 1, with no outlying values found when assessing differences between weeks 2 and 3. Thus all analyses were performed based on the data from all teeth. The intra-examiner reproducibility results showed relatively narrow intervals for sites 1 and 2, with the interval for site 1 the narrowest, indicating the best agreement. The Bland-Altman intervals for site 3 are much wider that those for sites 1 and 2, which indicates the poorest agreement for this site from week 2 to week 3.

6.4.4 Overall Reproducibility for All Weeks at Different Sites

Overall, the cervical and mid-buccal sites scored highest in terms of reproducibility of enamel thickness measurements with 95% limits of agreement of -0.05 to 0.04 and -0.04 to 0.06 mm respectively. This is similar to the intra-examiner reproducibility results of Huysmans and Thijssen (2000) where the 95% limits of

agreement for cervical, mid-buccal, incisal and palatal sites of human incisors were -0.064 to 0.061 mm for the first observer and -0.084 to 0.061 for the second observer. However, the observers did not indicate whether the incisors were maxillary, mandibular, lateral or central. It is likely that the reproducibility on lateral incisors (maxillary and mandibular) will not deviate significantly from this as they have planar surfaces. The authors have also investigated the influence of temperature on ultrasonic measurements using a thermostatically controlled chamber at either 34 ºC or 21 ºC. They reported no statistically significant difference between measurements at either temperature and concluded that ultrasound measurements appeared to be independent of temperature. This finding links their *in vitro* work with the *in vivo* work in this Chapter and makes the comparison between these two approaches more valid. The data presented in this Chapter, shows that the incisal site had the lowest reproducibility with 95% limits of agreement ranging from -0.43 to 0.34 mm. This wide range of agreement could be due to the fact that the ADJ is least parallel to the enamel surface and consequently a weak echo is produced from the incisal site, which is difficult to detect.

The enamel thickness obtained in this Chapter assumed that the SOS in enamel is consistently equal to 6000 ms^{-1}. It is well known that the actual value varies considerably between individuals and between teeth for any one individual (Slak *et al.*, 2011). However it is not necessary to know the correct SOS to detect a change in thickness by serial measurement as long as the SOS in the tooth in question remains constant. The requirement in this case is that the percentage change in thickness is greater than the percentage reproducibility.

Another *in vitro* investigation of the reproducibility of enamel thickness measurements with A-mode ultrasound led to the conclusion that ultrasonic

measurements of enamel thickness are not clinically useful because of the low level of reproducibility (Louwerse *et al.*, 2004). This might be due to the high anisotropy in the enamel of their 12 incisor sample set, or the orientation of the ultrasonic transducer on the enamel surface. It is known that the transducer must be oriented at a right-angle to the enamel surface for optimum ultrasonic energy transfer, which may not be the case in their study. In addition, some of the examiners in the Louwerse study only had 2 hours of training on how to perform ultrasonic measurements, which could contribute to the poor reproducibility in this study. However, the results in this Chapter do not support these findings and are in agreement with the work of Huysmans and Thijssen (2000), who showed that reproducible data could be obtained using ultrasound.

6.4.5 Intra-Class Correlation

For all three sites, when all teeth were included in the analysis, the ICC values were around 0.6. This means that only around 60% of the total variability in enamel thickness was due to differences between individual teeth with the remaining 40% of variability due to differences between repeat measurements of the same teeth. This is a high percentage, and indicates that agreement is not particularly good for all of the three sites. However, as discussed previously, the results for sites 1 and 2 were influenced by one potentially outlying value. Therefore the ICC analyses were repeated omitting this tooth. The revised results yielded an ICC of 0.96 for site 1 indicating that there is potentially excellent reproducibility in this method.

The ICC value was 0.96 for site 1 which means that 96% of the total variability was between teeth, with only 4% within teeth (i.e. between repeat measurements of the same teeth). This data, based on triplicate measures for each data point is a high

value demonstrating good reproducibility. The ICC for site 2 also increased after omitting the one outlying tooth. However, it only increased to 0.71, indicating a relatively large proportion of variability was due to repeat measurements of the same teeth. Thus the level of agreement at site 2 is not particularly high. An ICC test for each site on all three visits was made and the values demonstrated that there was very good agreement with the majority of the ICC values around 0.85 or higher.

These are fairly high values, which mean that 85% of the total variability was between teeth, with only 15% within teeth (i.e. between repeat measurements of the same teeth). The ICC was then calculated for the three sites on all visits combined to give an overall value. The overall ICC was 0.85 and it means that 85% of the total variability in enamel thicknesses was between different teeth with the remaining 15% between repeat measurements of the same teeth (at the different visits). This is a relatively good value which shows that the overall agreement was reasonable. This data emphasizes the importance of the scan site when making serial ultrasonic measurements on a tooth. Previous *in vitro* work (Louwerse *et al.*, 2004) demonstrated that using ink markers to guide ultrasound measurements did not have significant effect on the reproducibility of the measurements. On the other hand, a different study of pulpal blood flow with ultrasound used a positioning stent to aid in placement of the tip of the transducer in order to obtain reproducible measurements (Yoon *et al.*, 2010).

The data presented in this Chapter show that reproducible measurements can be obtained both during the same visit and on different visits without the use of positioning stents or ink marks in agreement with the findings of Louwerse and co-workers (2004). This was achieved by visually dividing the maxillary central incisor into 3 sites and orienting the transducer in the middle of the site under

investigation and at a perpendicular angle (Figure 6.2). This approach contributes to the simplicity of the proposed clinical ultrasound technique described in the current study.

6.4.6 Agreement between Repeat Measures at the Same Visit

ICC analysis of repeat measures during the same visit showed that the agreement was lowest for site 1 at week 3, where the ICC value was only 0.75. Also, an equivalent overall agreement value was calculated, this time combining the results for all three sites together. The ICC was calculated to be 0.85, which indicates good agreement for all sites combined.

6.5 Conclusions

- Ultrasound is a highly reproducible and reliable technique for monitoring enamel thickness *in vivo*. The preferable site for making ultrasonic measurement is the cervical site (site 1) followed by the mid-buccal site (site 2).
- This study is of great clinical significance in that it demonstrates for the first time *in vivo* that ultrasound has sufficient precision (0.05 mm) to allow it to be used serially for assessing erosive TSL.

7 General Discussion

The development of an approach to monitor erosive TSL *in vivo* with a reproducible, quantitative and direct method is important because current methods are either subjective or require expensive laboratory equipment. Relatively new methods are emerging, such as QLF (Pretty *et al.*, 2004) and OCT (Wilder-Smith *et al.*, 2009) but both have limitations (see section 1.4.2). Ultrasound is a direct, quantitative and non-invasive method that has potential for monitoring enamel thickness in patients with erosive TSL. However, much of the work so far has been performed *in vitro* (Huysmans and Thijssen, 2000; Tagtekin *et al.*, 2005). This thesis investigated the feasibility and optimisation of ultrasound as a dental tool aiding in monitoring erosive TSL *in vitro* and *in vivo*. This was achieved through several experiments each investigating a different but related problem that hinders the use of ultrasound in the area of monitoring erosive TSL.

Ultrasound can detect boundaries and interfaces (e.g. enamel and ADJ) but this requires the use of a suitable couplant. Several potential couplants were explored in Chapter 2, however the only suitable one was Perspex because it was able to deliver the ultrasonic energy to the target and back again and was appropriate for use clinically (biocompatible). Indeed, Perspex, although not ideal, has been the couplant of choice in several investigations of enamel thickness measurement by direct placement of the transducer (with a Perspex tip) on the enamel surface (Huysmans and Thijssen, 2000; Louwerse *et al.*, 2004; Tagtekin *et al.*, 2005; Harput *et al.*, 2011).

Perspex was also used in these studies as a delay line to provide a time offset between the transducer's excitation echo and the echo from the interface of interest.

Without such an offset overlap between the two echoes occurs and complicates the localisation of the echo peaks. This was the main reason for choosing Perspex in the *in vitro* and *in vivo* work (in addition to being the default delay line and couplant in the ultrasound transducer supplied by the manufacturer which was used later in this work). However, to achieve intimate contact between the Perspex and the tooth surface (i.e. enamel), and therefore transfer more ultrasound energy into the tooth, it is helpful to use a liquid medium, such as a drop of water or water-based gel. This water drop itself also acts as couplant in addition to the Perspex. Thus, both Perspex and water work as couplants to transfer the ultrasound energy into the enamel and back to the transducer.

Lees and co-workers (1969) examined the use of aluminium as a sole couplant and a delay line at the same time. They used aluminium because it has a similar impedance to enamel thus maximising the ultrasound energy transfer into the enamel. However, there was a trade-off as they had to grind the native enamel surface flat before they could receive echoes from the enamel. This is obviously an invasive method and therefore would not be amenable for use *in vivo*.

The approach that was used in Chapter 6 of this work (use of a Perspex and water drop) for coupling ultrasound to enamel was non-invasive and resulted in sufficient ultrasound energy transfer into the enamel and back to the transducer (Slak *et al.*, 2011), although the Perspex and water impedances of 3.6 MRayls and 1.5 MRayls, respectively (Singh *et al.*, 2008) was not similar to enamel impedance of 18 MRayls (Ng *et al.*, 1988). Following some initial ultrasonic measurements it was apparent that the topography of the surface greatly affected the reflected echoes, which was not unexpected. The hypothesis tested was that premolar teeth, due to their non-planar topography, reflected echoes less readily than the relatively planar synthetic

maxillary central incisors. The results corroborated the hypothesis and it was evident that planar teeth reflect ultrasound more favourably. The results from Chapter 3 demonstrated that the more planar the surface was the better the echo received and thus it would be logical to choose maxillary central incisors as 'landmark teeth' for ultrasonic measurements of the enamel layer (Chapter 6).

Dwyer-Joyce *et al.* (2010) reported that no echo was observed from the ADJ at an ultrasound beam angle more than 10º from perpendicular in molar teeth *in vitro*. The *in vivo* study (Chapter 6) examined the reproducibility of ultrasound in monitoring enamel thickness. The results demonstrated that the ADJ echo was detectable using a hand-held transducer. This means that the incident ultrasound beam was always within the signal-angle dependency limit of 10º reported by Dwyer-Joyce *et al.* (2010). Furthermore, this signal-angle dependency limit is expected to be more than 10º in the planar maxillary central incisors, which gives more leeway for orienting and positioning the transducer on the palatal surfaces of maxillary central incisors in addition to the labial surfaces. This would be helpful in monitoring enamel thickness in patients with eating disorders or patients with GORD.

It is pertinent to remember that the surface topography, albeit important in ultrasonic measurements, is not the only determinant for the accuracy and reproducibility of the enamel thickness value, hence other factors are involved (enamel anisotropy, ultrasound transducer position and orientation, SOS, ultrasonic coupling and the undulation of the ADJ). As previously stated in Chapter 3, having a relatively planar enamel surface does not necessarily indicate a planar ADJ. Some manual adjustment of transducer orientation on the enamel surface may be required in order for the ultrasonic beam to meet both enamel and ADJ as close as possible to a right angle.

Because medical ultrasound scanners display images of tissues, attempts were made to use these scanners to image hard and soft dental tissues. The first reported use of ultrasound imaging in dentistry was by Baum *et al.* (1963), after which several studies of ultrasound to image dental hard and soft tissue were performed. It is convenient to have an ultrasound scanner that generates a 2D ultrasonic image, which can be of diagnostic value when monitoring progressive loss of enamel thickness over time. However, the size of the equipment involved makes this challenging for every day use in a typical dental practice. In addition, the transducers used for modern medical ultrasound scanners are too large for dental use although it seems probable that a miniaturised version would prove popular in the dental arena. The results from Chapter 4 demonstrated that ultrasound imaging in B-mode could potentially be of value if the resolution could be improved. This could be done by increasing the frequency of the transducer and/or applying signal and image processing to increase contrast and decrease noise (Mahmoud *et al.*, 2010).

Neither of the ultrasonic systems (in-house and commercial ultrasound scanner) described in Chapter 4 allowed scanning of the same enamel site over a wide range of angles, which stems from the dependency of the ultrasonic signal on the incident angle. This further supports the findings in Chapter 3 demonstrating that premolars are particularly dependent on the signal-angle. Although the enamel thickness could not be reliably measured with the ultrasonic systems explored in B-mode, they were not the only option and it was decided to investigate A-mode ultrasound as a potential way forward.

It can be seen from Chapter 5 that A-mode ultrasound can be used to accurately measure enamel thickness. This was supported by comparison with histological findings and highlights the value of ultrasound in complementing the dentist's

arsenal of diagnostic instruments. It could be envisaged that a hand-held ultrasonic transducer could be used like a dental hand piece to measure enamel thickness and indeed monitor the future loss of enamel thickness in patients with moderate to severe erosive TSL. The instrument in this work achieved accuracy levels that are within 10% of the histological measurements, which is higher than the reported accuracy in a similar study (Slak *et al.*, 2011). The work in Chapter 5 has shown that the use of the SOS value in enamel belonging to an individual tooth section can improve the accuracy of the enamel thickness measurement, which has not been investigated previously. This technique is of special interest in *in vitro* studies evaluating the use of ultrasound for enamel thickness measurements. The majority of previous studies used a mean SOS value obtained either from the literature or from the teeth examined, which could undermine the accuracy of the ultrasonic measurement (Huysmans and Thijssen, 2000; Tagtekin *et al.*, 2005; Harput *et al.*, 2011; Slak *et al.*, 2011).

Monitoring erosive TSL *in vivo* has been recognised as a challenge due to the uncertainty of the progression pattern of erosion and the lack of control over the multifactorial nature of TSL, which makes it impossible to isolate and assess the effects of erosion alone (Huysmans *et al.*, 2011). Nevertheless, it is clinically desirable to attempt to monitor the progressive loss of enamel thickness due to the interplay of erosion, abrasion and attrition. Whatever the cause of TSL, the enamel thickness might be very conveniently monitored with a direct, non-destructive method such as A-mode ultrasound.

There are a plethora of studies describing TSL measurements using profilometry assessments of study casts and impressions but these have drawbacks, such as the dimensional changes that occur within impression materials. These materials are

known to shrink or expand which introduces errors in the measured TSL value (Rodriguez and Bartlett, 2011). The American National Standard Institute/American Dental Association (ANSI/ADA) specification number 19 states that elastomeric impression materials should not have linear dimensional changes exceeding 1.5% within a 24 hour period (ANSI/ADA specification 19, 2004). Rodriguez and Bartlett (2011) argue that this 1.5% change of up to 0.1 mm might sometimes be permissible in certain clinical situations, for example in removable prosthodontics, but is not acceptable for the purposes of laboratory studies investigating TSL as it will affect data interpretation. Furthermore, they point out that most studies do not mention how the impressions were handled, or if they were scanned within similar timescales, and often report small TSL values that may be within the dimensional change values of impression materials in their study.

Enamel thickness was accurately measured in Chapter 5 which prompted the investigation of the reproducibility of the measurements *in vivo* in Chapter 6. This demonstrated that A-mode ultrasound had an *in vivo* resolution of 0.05 mm (50 μm) on both cervical and mid-buccal sites, and an ICC of 0.96 in the best conditions indicating that the method could be very reproducible. This is an important finding given the fact that no previous studies addressed the applicability and reproducibility of ultrasound for use *in vivo* to monitor erosive TSL.

West and co-workers (1998) performed a study on 10 participants to investigate the effect of consuming proprietary orange juice on enamel thickness. The participants had to wear an intra-oral appliance with human enamel specimens attached palatally for seven hours each day. They found that the consumption of proprietary orange juice 4 times a day for 15 days led to enamel loss of 2.69 ±0.49 μm *in situ* and 24.06 ±1.62 μm *in vitro*. Although the study was conducted over a short period of

time, it demonstrated the erosive potential of acidic drinks. However, the volunteers were not allowed to brush their teeth while the appliance was worn. It is reasonable to assume that the enamel loss would be higher if tooth brushing had also taken place. The TSL value quoted above equates to a loss of 65 ±11.76 μm/12 months. This is from orange juice only and it is expected that this value would be higher in real oral conditions, especially labially because of the direct contact with the erosive agent when consumed. This level of TSL renders the ultrasonic system described in Chapter 6 capable of monitoring erosive TSL every 12-18 months and more frequently than this in GORD patients.

Directly measuring the progressive loss of enamel due to erosive TSL with this level of precision and reliability is something that would be of great value to the dental and research community. This could be commenced as soon as the permanent maxillary central incisor erupts in children and adolescents, so that preventive measures could be used if the condition progresses into adulthood. It could aid in flagging up cases requiring conservative restorative intervention, such as dental composites, to protect the remaining enamel layer. This could be part of a dental examination where preventative measures are applied and oral hygiene instructions are reinforced, although the frequency of dental visits is dependent on the level of oral health of each patient.

It is known that incisors are prone to acid attack from frequent acidic intake and erosive TSL in patients with frequent consumption of acidic fruit juice and carbonated beverages is an increasing concern in young patients. Unusual drinking habits, such as swishing, sucking or retaining drinks in the mouth also aggravate the erosive process (O'Sullivan and Curzon, 2000) as it has been shown that the drinking method significantly affects the pH of the tooth surface (Lussi and Hellwig, 2006).

Patients with suspected anorexia or patients with GORD could also be monitored using this technology. The level of erosive TSL occurring in patients as a result of the habits mentioned above cannot be monitored reliably in the dental surgery with available methods (indices, study casts, photographs), whereas ultrasound has shown excellent precision (0.05 mm), making it a promising alternative for reliably monitoring erosive TSL in the dental surgery on native teeth.

It has been shown that the SOS increases proportionally with the volumetric concentration of inorganic content *in vitro* (Lees, 1971). This could render the ultrasonic system useful for non-destructive *in vitro* monitoring of uptake or release of minerals from enamel to study the effect of dairy products on remineralisation (Yamaguchi *et al.*, 2006). Other research areas in which ultrasound could be applied include evaluating newly approved formulations of fluoride supplements, such as mouthwashes, toothpastes and gels. This, of course, does not substitute for established techniques, such as transverse microradiography (Gonzalez-Cabezas *et al.*, 1998) used for such studies, but highlights some of the potential and important applications of ultrasound in dental research.

7.1 Conclusions

1. Perspex is a suitable ultrasonic couplant to enamel for the purpose of enamel thickness measurements. The tightness of the coupling at an interface (e.g. the Perspex-enamel interface) is of importance if ultrasound energy is to be transmitted efficiently into a tooth.
2. Planar maxillary central incisors are less angle-dependent compared to non-planar premolars and therefore incisors are more echogenic.
3. B-mode ultrasound imaging of the enamel layer is not a suitable method for measuring enamel thickness because of the associated limitations.
4. The difference between the enamel thicknesses obtained with histology (true value) and the values obtained by the hand-held A-mode ultrasound transducer was 10%. This demonstrates that the measurements made with the hand-held transducer had good accuracy.
5. A-mode ultrasound is a highly reproducible and reliable technique for monitoring enamel thickness *in vivo*. The preferable site for making ultrasonic measurement is the cervical site (site 1) followed by the mid-buccal site (site 2).
6. This study is of great clinical significance in that it demonstrates for the first time *in vivo* that A-mode ultrasound is a reproducible, reliable and ***direct method*** with sufficient precision (0.05 mm) that can be used to quantify and serially monitor erosive TSL.

7.2 Limitations of This Work

1. The use of synthetic teeth in Chapter 3 was not ideal but natural central incisors were lacking from the Skeletal Tissue Bank, and these were the best alternative available.
2. The impedance mismatch between enamel and the couplant (Perspex and water) will decrease the amount of ultrasound enamel is exposed to. Nonetheless, useful echoes can be generated as demonstrated in Chapters 5 and 6.
3. Anisotropy in enamel can yield different SOS values and therefore an element of uncertainty can be introduced to the thickness measurement. However, carefully orientating the transducer on the baseline mark can reduce this uncertainty.
4. Landmark teeth, such as central or lateral incisors can currently be used to assess the level of TSL, excluding other teeth, such as molars, which could suffer erosive TSL to a greater extent.
5. Teeth presenting with severe TSL might have lost the enamel layer completely with only dentine remaining. Ultrasound has not been investigated in this study in measurement of the dentine layer.
6. The instrument was not tested on primary dentition but it could potentially be validated on this group using the same method described here.
7. Measuring the true enamel thickness *in vivo* depends on enamel's SOS in the tooth, which varies between patients. Using a mean SOS would therefore introduce uncertainties in the measured thickness. Thus the

thickness value would not necessarily be absolute but would be a useful indicative value.

8. Analysing small echoes in captured waveforms is sometimes difficult.

7.3 Future Research

1. Revisit the *in vitro* signal angle dependency experiment and use natural teeth subjected to erosive challenge to determine if there is a relationship between surface roughness and amplitude of reflected echoes from the enamel.
2. Compare this ultrasonic system with an established technique such as profilometry assessments of sequential study casts.
3. Investigate the use of ultrasound on dentine specimens. The technology could then be used to monitor patients with advanced erosive TSL with exposed dentine.
4. Verify the resolution limit of the ultrasound system *in vitro*.
5. Optimise the technique by using signal processing, such as the FrFT, which could increase the resolution to detect finer changes (< 0.05 mm).
6. Creating an SOS database for teeth from different age groups to calculate a more representative mean SOS, which is then used to help calculate the enamel thickness *in vivo.*

8 References

Al-Dlaigan Y, Shaw L and Smith A. 2001. Dental erosion in a group of British 14-year-old, school children. Part i: Prevalence and influence of differing socioeconomic backgrounds. *British Dental Journal.* **190** (3), pp.145-149.

Al-Omiri M, Harb R, Abu Hammad O, Lamey P-J, Lynch E and Clifford T. 2010. Quantification of tooth wear: Conventional vs new method using toolmakers microscope and a three-dimensional measuring technique. *Journal of Dentistry.* **38** (7), pp.560-568.

American National Standard Institute/ American Dental Association. 2004. *Specification no. 19: Elastomeric dental impression materials.* Chicago: American Dental Association.

Assaf A, Kahl-Nieke B, Feddersen J and Habermann C. 2013. Is high-resolution ultrasonography suitable for the detection of temporomandibular joint involvement in children with juvenile idiopathic arthritis?. *Dentomaxillofacial Radiology.* **42** (3), pp.1-9.

Attin T. 2006. Methods for assessment of dental erosion. *Monographs in Oral Science.* **20**, pp.152-172.

Azzopardi A, Bartlett DW, Watson TF and Smith BG. 2000. A literature review of the techniques to measure tooth wear and erosion. *European Journal of Prosthodontics and Restorative Dentistry.* **8** (3), pp.93-97.

Bab IA, Feuerstein O and Gazit D. 1997. Ultrasonic detector of proximal caries. *Caries Research.* **31**, p322.

Barber FE, Lees S and Lobene RR. 1969. Ultrasonic pulse-echo measurements in teeth. *Archives of Oral Biology.* **14** (7), pp.745-760.

Bardsley P, Taylor S and Milosevic A. 2004. Epidemiological studies of tooth wear and dental erosion in 14-year-old children in North West England. Part 1: The relationship with water fluoridation and social deprivation. *British Dental Journal.* **197** (7), pp.413-416.

Bartlett DW, Blunt L and Smith BGN. 1997. Measurement of tooth wear in patients with palatal erosion. *British Dental Journal.* **182** (5), pp.179-184.

Bartlett D, Coward P, Nikkah C and Wilson R. 1998. The prevalence of tooth wear in a cluster sample of adolescent schoolchildren and its relationship with potential explanatory factors. *British Dental Journal.* **184** (3), pp.125-129.

Bartlett D. 2003. Retrospective long term monitoring of tooth wear using study models. *British Dental Journal.* **194** (4), pp.211-213.

Bartlett D and Dugmore C. 2008. Pathological or physiological erosion–is there a relationship to age?. *Clinical Oral Investigations.* **12 Suppl 1**, pp.27-31.

Bartlett D, Ganss C and Lussi A. 2008. Basic Erosive Wear Examination (BEWE): A new scoring system for scientific and clinical needs. *Clinical Oral Investigations.* **12 Suppl 1**, pp.65-68.

Bartlett DW, Lussi A, West NX, Bouchard P, Sanz M and Bourgeois D. 2013. Prevalence of tooth wear on buccal and lingual surfaces and possible risk factors in young European adults. *Journal of Dentistry*. **41** (11), pp.1007-1013.

Baum G, Greenwood I, Slawski S and Smirnow R. 1963. Observation of internal structures of teeth by ultrasonography. *Science.* **139** (3554), pp.495–496.

Berson M, Gregoire JM, Gens F, Rateau J, Jamet F, Vaillant L *et al.* 1999. High frequency (20 MHz) ultrasonic devices: Advantages and applications. *European Journal of Ultrasound.* **10** (1), pp.53-63.

Bland JM and Altman DG. 1986. Statistical methods for assessing agreement between two methods of clinical measurement. *Lancet.* **1** (8476), pp.307-310.

Blodgett DW. 2002. Ultrasonic assessment of tooth structure. *In: Proceedings of the Society of Photo-optical Instrumentation Engineers conference , Laser Tissue Interaction XIII: Photochemical, Photothermal, and Photomechanical, 27 June 2002, San Jose, California, USA*, pp.284-288.

Bozkurt F, Tagtekin D, Hayran O, Stookey G and Yanikoglu F. 2005. Accuracy of ultrasound measurement of progressive change in occlusal enamel thickness. *Oral Surgery, Oral Medicine, Oral Pathology, Oral Radiology and Endodontics.* **99** (1), pp.101-105.

Butterworth S. 1930. On the theory of filter amplifiers. *Experimental Wireless and the Wireless Engineer.* **7**, pp.536-541.

Carlsson G, Johansson A and Lundqvist S. 1985 Occlusal wear. A follow-up study of 18 subjects with extensively worn dentitions. *Acta Odontologica Scandinavica.* **43** (2), pp.83-90.

Catuna M. 1953. Sonic energy: A possible dental application (preliminary report of an ultrasonic cutting method). *Annals of Dentistry.* **12**, pp.256-260.

Centerwall BS, Armstrong CW, Funkhouser LS and Elzay RP. 1986. Erosion of dental enamel among competitive swimmers at a gas-chlorinated swimming pool. *American Journal of Epidemiology.* **123** (4), pp.641-647.

Chadwick R. 1998. 'Toothwear—towards the third dimension'. *Bulletin of the Royal College of Physicians and Surgeons of Glasgow*. **27**, pp.31-32.

Chadwick B and Pendry L. 2004. *Non-carious dental conditions* London: Office for National Statistics.

Chapple ILC. 1997. Periodontal disease diagnosis: Current status and future developments. *Journal of Dentistry.* **25** (1), pp.3-15.

Chifor R, Badea ME, Hedesiu M, Serbanescu A and Badea AF. 2010. Experimental model for measuring and characterisation of the dento-alveolar system using high frequencies ultrasound techniques. *Medical Ultrasonography*. **12** (2), pp.127-132.

Contaldo M, Serpico R and Lucchese A. 2013. In vivo imaging of enamel by reflectance confocal microscopy (RCM): Non-invasive analysis of dental surface. *Odontology.* pp.1-5.

Costa MR, Silva VC, Miqui MN, Sakima T, Spolidorio DMP and Cirelli JA. 2007. Efficacy of ultrasonic, electric and manual toothbrushes in patients with fixed orthodontic appliances. *The Angle Orthodontist.* **77** (2), pp.361-366.

Cotti E, Campisi G, Garau V and Puddu G. 2002. A new technique for the study of periapical bone lesions: Ultrasound real time imaging. *International Endodontic Journal.* **35** (2), pp.148-152.

Crabb H. 1976. The porous outer enamel of unerupted human premolars. *Caries Research.* **10** (1), pp.1-7.

Culjat M, Singh R, Yoon D and Brown E. 2003. Imaging of human tooth enamel using ultrasound. *IEEE Transactions on Medical Imaging.* **22** (4), pp.526-529.

Culjat MO, Singh RS, Brown ER, Neurgaonkar RR, Yoon DC and White SN. 2005a. Ultrasound crack detection in a simulated human tooth. *Dento-Maxillo-Facial Radiology.* **34** (2), pp.80-85.

Culjat MO, Singh RS, White SN, Neurgaonkar RR and Brown ER. 2005b. Evaluation of gallium-indium alloy as an acoustic couplant for high-impedance, high-frequency applications. *Acoustics Research Letters Online.* **6** (3), pp.125-130.

d'Incau E, Couture C and Maureille B. 2012. Human tooth wear in the past and the present: Tribological mechanisms, scoring systems, dental and skeletal compensations. *Archives of Oral Biology.* **57** (3), pp.214-229.

de Josselin de Jong E, Sundstrom F, Westerling H, Tranaeus S, ten Bosch JJ and Angmar-Mansson B. 1995. A new method for in vivo quantification of changes in initial enamel caries with laser fluorescence. *Caries Research.* **29** (1), pp.2-7.

DeLong R. 2006. Intra-oral restorative materials wear: Rethinking the current approaches: How to measure wear. *Dental Materials.* **22** (8), pp.702-711.

Denisova LA, Maev RG, Leontjev VK, Denisov AF, Grayson GG, Rusanov FS *et al.* 2009. A study of the adhesion between dental cement and dentin using a nondestructive acoustic microscopy approach. *Dental Materials.* **25** (5), pp.557-565.

Dugmore CR and Rock WP. 2003. Awareness of tooth erosion in 12-year-old children and primary care dental practitioners. *Community Dental Health.* **20** (4), pp.223-227.

Dugmore C and Rock W. 2004. The prevalence of tooth erosion in 12-year-old children. *British Dental Journal.* **196** (5), pp.279-282.

Dwyer-Joyce RS, Goodman MA and Lewis R. 2010. A comparative study of ultrasonic direct contact, immersion, and layer resonance methods for assessment of enamel thickness in teeth. *Proceedings of the Institution of Mechanical Engineers Part J: Journal of Engineering Tribology, 1 June 2010.* London: SAGE, pp.519-528.

Eccles JD. 1979. Dental erosion of nonindustrial origin. A clinical survey and classification. *Journal of Prosthetic Dentistry.* **42** (6), pp.649-653.

Eisenburger M, Hughes J, West NX, Jandt KD and Addy M. 2000. Ultrasonication as a method to study enamel demineralisation during acid erosion. *Caries Research.* **34** (4), pp.289-294.

Eisenburger M, Shellis RP and Addy M. 2004. Scanning electron microscopy of softened enamel. *Caries Research.* **38** (1), pp.67-74.

Elton V, Cooper L, Higham SM and Pender N. 2009. Validation of enamel erosion in vitro. *Journal of Dentistry.* **37** (5), pp.336-341.

Field J, Waterhouse P and German M. 2010. Quantifying and qualifying surface changes on dental hard tissues in vitro. *Journal of Dentistry.* **38** (3), pp.182-190.

Freed HK, Gapper RL and Kalkwarf KL. 1983. Evaluation of periodontal probing forces. *Journal of Periodontology.* **54** (8), pp.488-492.

Fukukita H, Yano T, Fukumoto A, Sawada K, Fujimasa T and Sunada I. 1985. Development and application of an ultrasonic-imaging system for dental diagnosis. *Journal of Clinical Ultrasound.* **13** (8), pp.597-600.

Gateno J, Miloro M, H. Hendler B and Horrow M. 1993. The use of ultrasound to determine the position of the mandibular condyle. *Journal of Oral and Maxillofacial Surgery.* **51** (10), pp.1081-1086.

Ghorayeb SR and Valle T. 2002. Experimental evaluation of human teeth using noninvasive ultrasound: Echodentography. *Ultrasonics, Ferroelectrics and Frequency Control, IEEE Transactions on.* **49** (10), pp.1437-1443.

Ghorayeb S, Bertoncini C and Hinders M. 2008. Ultrasonography in dentistry. *IEEE transactions on ultrasonics, ferroelectrics, and frequency control.* **55** (6), pp.1256-1266.

Gilligan T, Nelson L, McLeod L and Dalal AA. 2011. Prm42 visually evaluating the measurement comparability between paper-based and alternate versions of administration of the lung function questionnaire. *Value in Health.* **14** (3), pA153.

Giunta J. 1983. Dental erosion resulting from chewable vitamin C tablets. *Journal of the American Dental Association.* **107** (2), pp.253-256.

Gonzalez-Cabezas C, Fontana M, Dunipace AJ, Li Y, Fischer GM, Proskin HM *et al.* 1998. Measurement of enamel remineralization using microradiography and confocal microscopy. A correlational study. *Caries Research.* **32** (5), pp.385-392.

Grenby TH. 1996. Methods of assessing erosion and erosive potential. *European Journal of Oral Sciences.* **104** (2), pp.207-214.

Gundappa M, Ng S and Whaites E. 2006. Comparison of ultrasound, digital and conventional radiography in differentiating periapical lesions. *Dento-Maxillo-Facial Radiology.* **35** (5), pp.326-333.

Habelitz S, Marshall SJ, Marshall Jr GW and Balooch M. 2001. Mechanical properties of human dental enamel on the nanometre scale. *Archives of Oral Biology.* **46** (2), pp.173-183.

Hall AF, Sadler JP, Strang R, De Josselin De Jong E, Foye RH and Creanor SL. 1997. Application of transverse microradiography for measurement of mineral loss by acid erosion. *Advances in Dental Research.* **11** (4), pp.420-425.

Hall A and Girkin JM. 2004. A review of potential new diagnostic modalities for caries lesions. *Journal of Dental Research.* **83** (suppl 1), pp.C89-C94.

Hamano N, Hanaoka K, Ebihara K, Toyoda M and Teranaka T. 2003. Evaluation of adhesive defects using an ultrasonic pulse-reflection technique. *Dental Materials Journal.* **22** (1), pp.66-79.

Harput S, Cowell DMJ, Evans JA, Bubb N and Freear S. 2009. Tooth characterization using ultrasound with fractional Fourier transform. In: *Ultrasonics Symposium (IUS), 2009 IEEE International, 20-23 September 2009, Rome,* pp.1906-1909.

Harput S, Evans T, Bubb N and Freear S. 2011. Diagnostic ultrasound tooth imaging using fractional fourier transform. *IEEE transactions on ultrasonics, ferroelectrics, and frequency control.* **58** (10), pp.2096-2106.

Hedrick WR, Hykes DL, Starchman DE and Wilson TA. 1995. Ultrasound physics and instrumentation. St. Louis, MI, USA: Mosby.

Hellwig E and Lussi A. 2006. Oral hygiene products and acidic medicines. *Monographs in Oral Science.* [Online]. **20**, pp.112-118. [Accessed 11 November 2013]. Available from: http://www.karger.com/Article/Pdf/93358.

Hill M. 2012. The role of oral health assessments. *British Dental Journal: Oral Health Report.* pp.8-11.

Hinds K and Gregory J. 1995. National diet and nutrition survey: Children aged 1 1/2 to 4 1/2 years. Volume 2: Report of the dental survey. London: Her Majesty's Stationary Office.

Hua J, Chen SK and Kim Y. 2009. Refining enamel thickness measurements from B-mode ultrasound images. In: *Annual International Conference of the IEEE Engineering in Medicine and Biology Society, 3-6 September 2009, Minneapolis, MN*. pp.440-443.

Hughes DA, Girkin JM, Poland S, Longbottom C, Button TW, Elgoyhen J *et al.* 2009. Investigation of dental samples using a 35 MHz focussed ultrasound piezocomposite transducer. *Ultrasonics.* **49** (2), pp.212-218.

Huysmans MC and Thijssen JM. 2000. Ultrasonic measurement of enamel thickness: A tool for monitoring dental erosion? *Journal of Dentistry*. **28** (3), pp.187-191.

Huysmans MC, Chew HP and Ellwood RP. 2011. Clinical studies of dental erosion and erosive wear. *Caries Research.* **45(suppl 1)**, pp.60-68.

International Standards Organisation. *Dental materials - guidance on testing of wear resistance- part 1: Wear by tooth brushing. Technical specification 1999; no. 14569-1*.

Jarvinen VK, Rytomaa, II and Heinonen OP. 1991. Risk-factors in dental erosion. *Journal of Dental Research.* **70** (6), pp.942-947.

Johansson A, Haraldson T, Omar R, Kiliaridis S and Carlsson GE. 1993. A system for assessing the severity and progression of occlusal tooth wear. *Journal of Oral Rehabilitation.* **20** (2), pp.125-131.

Johansson A-K, Lingström P and Birkhed D. 2002. Comparison of factors potentially related to the occurrence of dental erosion in high- and low-erosion groups. *European Journal of Oral Sciences.* **110** (3), pp.204-211.

John C. 2005. Directing ultrasound at the cemento-enamel junction (CEJ) of human teeth: I. Asymmetry of ultrasonic path lengths. *Ultrasonics.* **43** (6), pp.467-479.

Johnson W and Wilson J. 1957. Application of the ultrasonic dental unit to scaling procedures. *Journal of Periodontology.* **28**, pp.264-271.

Jones SG and Nunn JH. 1995. The dental health of 3-year-old children in Cast Cumbria 1993. *Community Dental Health.* **12** (3), pp.161-166.

Kossoff G and Sharpe CJ. 1966. Examination of the contents of the pulp cavity in teeth. *Ultrasonics.* **4** (2), pp.77-83.

Kreulen CM, Van 't Spijker A, Rodriguez JM, Bronkhorst EM, Creugers NH and Bartlett DW. 2010. Systematic review of the prevalence of tooth wear in children and adolescents. *Caries Research.* **44** (2), pp.151-159.

Krikken JB, Zijp JR and Huysmans MC. 2008. Monitoring dental erosion by colour measurement: An in vitro study. *Journal of Dentistry.* **36** (9), pp.731-735.

Lambrechts P, Braem M, Vuylsteke-Wauters M and Vanherle G. 1989. Quantitative in vivo wear of human enamel. *Journal of Dental Research.* **68** (12), pp.1752-1754.

Larsen IB, Westergaard J, Stoltze K, Larsen AI, Gyntelberg F and Holmstrup P. 2000. A clinical index for evaluating and monitoring dental erosion. *Community Dentistry and Oral Epidemiology.* **28** (3), pp.211-217.

Lea SC and Walmsley AD. 2009. Mechano-physical and biophysical properties of power-driven scalers: Driving the future of powered instrument design and evaluation. *Periodontology 2000.* **51**, pp.63-78.

Lee A, He L, Lyons K and Swain M. 2012. Tooth wear and wear investigations in dentistry. *Journal of Oral Rehabilitation.* **39** (3), pp.217-225.

Lees S and Barber FE. 1968. Looking into teeth with ultrasound. *Science.* **161** (3840), pp.478-479.

Lees S. 1968. Specific acoustic impedance of enamel and dentine. *Archives of Oral Biology.* **13** (12), pp.1491-1500.

Lees S, Barber FE and Lobene RR. 1970. Dental enamel: Detection of surface changes by ultrasound. *Science.* **169** (3952), pp.1314-1316.

Lees S and Barber FE. 1971. Looking into the tooth and its surfaces with ultrasonics. *Ultrasonics.* **9** (2), pp.85-87.

Lees S. 1971. Ultrasonics in hard tissues. *International Dental Journal.* **21** (4), pp.403-417.

Lees S and Rollins Jr FR. 1972. Anisotropy in hard dental tissues. *Journal of Biomechanics.* **5** (6), pp.557-566.

Lees S, Gerhard Jr FB and Oppenheim FG. 1973. Ultrasonic measurement of dental enamel demineralization. *Ultrasonics.* **11** (6), pp.269-273.

Lempriere BM. 2002. *Ultrasound and elastic waves frequently asked questions.* Amsterdam: Academic Press.

Linkosalo E and Markkanen H. 1985. Dental erosions in relation to lactovegetarian diet. *Scandinavian Journal of Dental Research.* **93** (5), pp.436-441.

Louwerse C, Kjaeldgaard M and Huysmans MC. 2004. The reproducibility of ultrasonic enamel thickness measurements: An in vitro study. *Journal of Dentistry.* **32** (1), pp.83-89.

Lussi A, Schaffner M, Hotz P and Suter P. 1991. Dental erosion in a population of Swiss adults. *Community Dentistry and Oral Epidemiology.* **19** (5), pp.286-290.

Lussi A, Jaeggi T and Zero D. 2004. The role of diet in the aetiology of dental erosion. *Caries Research.* **38** (Suppl. 1), pp.34-44.

Lussi A and Hellwig E. 2006. Risk assessment and preventive measures. *Monographs in Oral Science.* **20**, pp.190-199.

Lussi A. 2006. Erosive tooth wear—a multifactorial condition of growing concern and increasing knowledge. In: Lussi, A ed. *Monographs in oral science.* Switzerland, Basel: Karger, pp.1-8.

Lussi A and Jaeggi T. 2008. Erosion—diagnosis and risk factors. *Clinical Oral Investigations.* **12 Suppl 1**, pp.S5-13.

Lynch JE and Hinders MK. 2002. Ultrasonic device for measuring periodontal attachment levels. *Review of Scientific Instruments.* **73** (7), pp.2686-2693.

Maev RG, Denisova LA, Maeva EY and Denissov AA. 2002. New data on histology and physico-mechanical properties of human tooth tissue obtained with acoustic microscopy. *Ultrasound in Medicine and Biology.* **28** (1), pp.131-136.

Mahmoud AM, Ngan P, Crout R and Mukdadi OM. 2010. High-resolution 3D ultrasound jawbone surface imaging for diagnosis of periodontal bony defects: An in vitro study. *Annals of Biomedical Engineering.* **38** (11), pp.3409-3422.

Mair LH. 1992. Wear in dentistry—current terminology. *Journal of Dentistry.* **20** (3), pp.140-144.

McCabe JF and Walls A. 2009. *Applied dental materials.* 9th ed. Oxford: Wiley-Blackwell.

Mehta S, Banerji S, Millar B and Suarez-Feito J. 2012. Current concepts on the management of tooth wear: Part 1. Assessment, treatment planning and strategies for the prevention and the passive management of tooth wear. *British Dental Journal.* **212** (1), pp.17-27.

Millward A, Shaw L and Smith A. 1994. Dental erosion in four-year-old children from differing socioeconomic backgrounds. *ASDC Journal of Dentistry for Children.* **61** (4), pp.263-266.

Milosevic A, Young PJ and Lennon MA. 1994. The prevalence of tooth wear in 14-year-old school children in Liverpool. *Community Dental Health.* **11** (2), pp.83-86.

Milosevic A. 1997. Sports drinks hazard to teeth. *British Journal of Sports Medicine.* **31** (1), pp.28-30.

Mitchell HL, Chadwick RG, Ward S and Manton SL. 2003. Assessment of a procedure for detecting minute levels of tooth erosion. *Medical and Biological Engineering and Computing.* **41** (4), pp.464-469.

Moazzez R, Smith BGN and Bartlett DW. 2000. Oral pH and drinking habit during ingestion of a carbonated drink in a group of adolescents with dental erosion. *Journal of Dentistry.* **28** (6), pp.395-397.

Ng SY, Ferguson MWJ, Payne PA and Slater P. 1988. Ultrasonic studies of unblemished and artificially demineralized enamel in extracted human teeth: A new method for detecting early caries. *Journal of Dentistry.* **16** (5), pp.201-209.

Ng SY, Payne PA, Cartledge NA and Ferguson MWJ. 1989. Determination of ultrasonic velocity in human enamel and dentine. *Archives of Oral Biology.* **34** (5), pp.341-345.

Nuttall NM, Steele JG, Pine CM, White D and Pitts NB. 2001. Adult Dental Health Survey: The impact of oral health on people in the UK in 1998. *British Dental Journal.* **190** (3), pp.121-126.

O' Brien M. 1994. Children's dental health in the United Kingdom 1993. London:Office of Population Censuses and Surveys, Her Majesty's Stationary Office.

O'Sullivan EA and Curzon ME. 2000. A comparison of acidic dietary factors in children with and without dental erosion. *ASDC Journal of Dentistry for Children.* **67** (3), pp.186-192, 160.

O'Sullivan E. 2000. A new index for the measurement of erosion in children. *European Journal of Paediatric Dentistry.* **1** (1), pp.69-74.

O'Sullivan E and Milosevic A. 2008. UK national clinical guidelines in paediatric dentistry: Diagnosis, prevention and management of dental erosion. *International Journal of Paediatric Dentistry.* **18 Suppl 1**, pp.29-38.

Peck SD and Briggs GA. 1987. The caries lesion under the scanning acoustic microscope. *Advances in Dental Research.* **1** (1), pp.50-63.

Pindborg J. 1970. *Pathology of dental hard tissues.* Copenhagen: Munksgaard.

Postle HH. 1958. Ultrasonic cavity preparation. *The Journal of Prosthetic Dentistry.* **8** (1), pp.153-160.

Pretty IA, Edgar WM and Higham SM. 2004. The validation of quantitative light-induced fluorescence to quantify acid erosion of human enamel. *Archives of Oral Biology.* **49** (4), pp.285-294.

Pretty IA. 2006. Caries detection and diagnosis: Novel technologies. *Journal of Dentistry.* **34** (10), pp.727-739.

Raghav N, Reddy SS, Giridhar AG, Murthy S, Devi Y, Santana N *et al.* 2010. Comparison of the efficacy of conventional radiography, digital radiography, and ultrasound in diagnosing periapical lesions. *Oral Surgery Oral Medicine Oral Pathology Oral Radiology and Endodontology.* **110** (3), pp.379-385.

Raum K, Kempf K, Hein HJ, Schubert J and Maurer P. 2007. Preservation of microelastic properties of dentin and tooth enamel in vitro-a scanning acoustic microscopy study. *Dental Materials.* **23** (10), pp.1221-1228.

Reich F, Brenden B and Porter N. 1967. Ultrasonic imaging of teeth. Report of battelle memorial institute. *Pacific Northwest Laboratory, Richland, Washington.*

Rodriguez JM and Bartlett DW. 2011. The dimensional stability of impression materials and its effect on in vitro tooth wear studies. *Dental Materials.* **27** (3), pp.253-258.

Rodriguez JM, Austin RS and Bartlett DW. 2012. In vivo measurements of tooth wear over 12 months. *Caries Research.* **46** (1), pp.9-15.

Scheven BAA, Shelton RM, Cooper PR, Walmsley AD and Smith AJ. 2009. Therapeutic ultrasound for dental tissue repair. *Medical Hypotheses.* **73** (4), pp.591-593.

Schlueter N, Ganss C, De Sanctis S and Klimek J. 2005. Evaluation of a profilometrical method for monitoring erosive tooth wear. *European Journal of Oral Sciences.* **113** (6), pp.505-511.

Schneider C, Rasband W and Eliceiri K. 2012. NIH Image to ImageJ: 25 years of image analysis. *Nature Methods.* **9** (7), pp.671-675.

Shaw L, Walmsley D, Barclay C, Perryer G and Smith A. 1999. *Tooth wear.* [Manuscript]. At*:* The University of Birmingham, Computer assisted learning for general dental practitioners.

Singh RS, Culjat MO, Cho JC, Neurgaonkar RR, Yoon DC, Grundfest WS *et al.* 2007. Penetration of radiopaque dental restorative materials using a novel ultrasound imaging system. *American Journal of Dentistry.* **20** (4), pp.221-226.

Singh RS, Culjat MO, Grundfest WS, Brown ER and White SN. 2008. Tissue mimicking materials for dental ultrasound. *Journal of the Acoustical Society of America.* **123** (4), pp.EL39-EL44.

Slak B, Ambroziak A, Strumban E and Maev RG. 2011. Enamel thickness measurement with a high frequency ultrasonic transducer-based hand-held probe for potential application in the dental veneer placing procedure. *Acta of Bioengineering and Biomechanics.* **13** (1), pp.65-70.

Smith BG and Knight JK. 1984a. A comparison of patterns of tooth wear with aetiological factors. *British Dental Journal.* **157** (1), pp.16-19.

Smith BG and Knight JK. 1984b. An index for measuring the wear of teeth. *British Dental Journal.* **156** (12), pp.435-438.

Smith B and Robb N. 1996. The prevalence of toothwear in 1007 dental patients. *Journal of Oral Rehabilitation.* **23** (4), pp.232-239.

Spranger H. 1971. Ultrasonic diagnosis of marginal periodontal diseases. *International Dental Journal.* **21** (4), pp.442-455.

Stefanoff V, Hausamen J-E and van den Berghe P. 1992. Ultrasound imaging of the TMJ disc in asymptomatic volunteers: Preliminary report. *Journal of Cranio-Maxillofacial Surgery.* **20** (8), pp.337-340.

Tagtekin D, Oztürk F, Lagerweij M, Hayran O, Stookey G and Caliskan Yanikoglu F. 2005. Thickness measurement of worn molar cusps by ultrasound. *Caries Research.* **39** (2), pp.139-143.

Toda S, Fujita T, Arakawa H and Toda K. 2005. An ultrasonic nondestructive technique for evaluating layer thickness in human teeth. *Sensors and Actuators, A: Physical.* **125** (1), pp.1-9.

Toumba KJ, Tahmassebi JF and Balmer R. 2003. Paediatric dentistry in the new millennium: 5. Clinical prevention: The role of the general dental practitioner. *Dental Update.* **30** (9), pp.503-508, 510.

Tsiolis FI, Needleman IG and Griffiths GS. 2003. Periodontal ultrasonography. *Journal of Clinical Periodontology.* **30** (10), pp.849-854.

Van't Spijker A, Rodriguez JM, Kreulen CM, Bronkhorst EM, Bartlett DW and Creugers NH. 2009. Prevalence of tooth wear in adults. *International Journal of Prosthodontics.* **22** (1), pp.35-42.

Walker A, Britain G, Gregory J and Bradnock G. 2000. National diet and nutrition survey: Young people aged 4 to 18 years; volume 2: Report of the oral health survey. London: Stationery Office.

Walmsley AD. 1988. Applications of ultrasound in dentistry. *Ultrasound in Medicine and Biology.* **14** (1), pp.7-14.

West NX, Maxwell A, Hughes JA, Parker DM, Newcombe RG and Addy M. 1998. A method to measure clinical erosion: The effect of orange juice consumption on erosion of enamel. *Journal of Dentistry.* **26** (4), pp.329-335.

Wetselaar P, Lobbezoo F, Koutris M, Visscher CM and Naeije M. 2009. Reliability of an occlusal and nonocclusal tooth wear grading system: Clinical use versus dental cast assessment. *International Journal of Prosthodontics.* **22** (4), pp.388-390.

White D, Pitts N, Steele J, Sadler K and Chadwick B. 2011. Disease and related disorders – a report from the Adult Dental Health Survey 2009. London: The Health and Social Care Information Centre. [Online]. pp.1-55.[Accessed 10 December 2013]. Available from: http://www.dhsspsni.gov.uk/theme2_disease_and_related_disorders.pdf

Wichard R, Schlegel J, Haak R, Roulet JF and Schmitt RM. 1996. Dental diagnosis by high frequency ultrasound. *Acoustical Imaging.* **22**, pp.329-334.

Wickens J. 1999. Tooth surface loss. 6. Prevention and maintenance. *British Dental Journal.* **186** (8), pp.371-376.

Wilder-Smith C, Wilder-Smith P, Kawakami-Wong H, Voronets J, Osann K and Lussi A. 2009. Quantification of dental erosions in patients with GERD using optical coherence tomography before and after double-blind, randomized treatment with esomeprazole or placebo. *American Journal of Gastroenterology.* **104** (11), pp.2788-2795.

Williams D, Croucher R, Marcenes W and O'Farrell M. 1999. The prevalence of dental erosion in the maxillary incisors of 14-year-old schoolchildren living in tower Hamlets and Hackney, London, UK. *International Dental Journal.* **49** (4), pp.211-216.

Yamaguchi K, Miyazaki M, Takamizawa T, Inage H and Moore BK. 2006. Effect of CPP-ACP paste on mechanical properties of bovine enamel as determined by an ultrasonic device. *Journal of Dentistry.* **34** (3), pp.230-236.

Yanikoğlu FC, Öztürk F, Hayran O, Analoui M and Stookey GK. 2000. Detection of natural white spot caries lesions by an ultrasonic system. *Caries Research.* **34** (3), pp.225-232.

Yoon MJ, Kim E, Lee SJ, Bae YM, Kim S and Park SH. 2010. Pulpal blood flow measurement with ultrasound Doppler imaging. *Journal of Endodontics.* **36** (3), pp.419-422.

Yoon MJ, Lee SJ, Kim E and Park SH. 2012. Doppler ultrasound to detect pulpal blood flow changes during local anaesthesia. *International Endodontic Journal.* **45** (1), pp.83-87.

Young A, Amaechi BT, Dugmore C, Holbrook P, Nunn J, Schiffner U *et al.* 2008. Current erosion indices—flawed or valid? Summary. *Clinical Oral Investigations.* **12 Suppl 1**, pp.S59-63.

Zagzebski J. 1996. *Essentials of ultrasound physics.* Missouri: Mosby.

Zheng YP, Maeva EY, Denisov AA and Maev RG. 2002. Ultrasound imaging of human teeth using a desktop scanning acoustic microscope. In: Lee, H ed. *Acoustical imaging.* USA: Springer, pp.165-171.

Zimmer S, Nezhat V, Bizhang M, Seemann R and Barthel C. 2002. Clinical efficacy of a new sonic/ultrasonic toothbrush. *Journal of Clinical Periodontology.* **29** (6), pp.496-500.

Zinner DD. 1955. Recent ultrasonic dental studies, including periodontia, without the use of an abrasive. *Journal of Dental Research.* **34**, pp.748-749.

9 Appendix 1: Signal Angle Dependency Raw Data

Premolars Signal Angle Dependency Table

		Angle (degrees)																								
Tooth	**Scan No.**	**0**	**5**	**10**	**15**	**20**	**25**	**30**	**35**	**40**	**45**	**50**	**55**	**60**	**65**	**70**	**75**	**80**	**85**	**90**	**95**	**100**	**105**	**110**	**115**	**120**
1	**1**	0.00	0.18	0.21	0.30	0.23	0.41	0.88	0.89	0.45	0.33	0.30	0.24	0.07	0.06											
	2	0.00	0.18	0.26	0.34	0.23	0.30	0.86	0.92	0.57	0.24	0.36	0.24	0.08	0.05											
2	**1**	0.00	0.07	0.21	0.20	0.05	0.16	0.12	0.14	0.26	0.41	0.49	0.43	0.22	0.10	0.10	0.08	0.04								
	2	0.00	0.07	0.21	0.20	0.05	0.16	0.12	0.16	0.26	0.43	0.51	0.44	0.22	0.09	0.10	0.08	0.02								
3	**1**	0.04	0.09	0.05	0.05	0.05	0.04	0.02	0.00																	
	2	n/a	0.05	0.04	0.06	0.04	0.05	0.02	n/a																	
4	**1**	0.02	0.05	0.12	0.05	0.08	0.10	0.17	0.20	0.25	0.32	0.07	1.04	0.79	0.40	0.29	0.04									
	2	0.05	0.06	0.11	0.04	0.03	0.02	0.13	0.20	0.26	0.30	0.64	0.96	0.85	0.42	0.30	0.06									
5	**1**	0.02	0.08	0.13	0.17	0.16	0.23	0.17	0.30	0.20	0.20	0.02														
	2	0.04	0.08	0.13	0.19	0.17	0.24	0.19	0.31	n/a	0.04	n/a														
6	**1**	0.01	0.01	0.01	0.05	0.05	0.08	0.05	0.10	0.04	0.02															
	2	0.01	0.02	0.02	0.05	0.08	0.02	0.08	0.01	0.02	0.02															

Amplitude (V)

		Angle (degrees)																								
Tooth	**Scan No.**	**0**	**5**	**10**	**15**	**20**	**25**	**30**	**35**	**40**	**45**	**50**	**55**	**60**	**65**	**70**	**75**	**80**	**85**	**90**	**95**	**100**	**105**	**110**	**115**	**120**
7	**1**	0.01	0.03	0.06	0.10	0.16	0.17	0.19	0.17	0.02																
	2	0.04	0.10	0.08	0.14	0.19	0.14	0.28	0.05	0.02																
8	**1**	0.00	0.00	0.10	0.16	0.25	0.35	0.33	0.33	0.39	0.43	0.51	0.59	0.68	1.02	0.84	0.70	0.59	0.43	0.22	0.16	0.15	0.16	0.13	0.06	0.04
	2	0.00	0.00	0.10	0.16	0.25	0.34	0.34	0.34	0.41	0.43	0.49	0.59	0.72	1.03	0.85	0.72	0.63	0.45	0.25	0.18	0.15	0.12	0.13	0.05	0.04
9	**1**	0.00	0.10	0.18	0.07	0.25	0.29	0.50	0.69	0.78	0.66	0.16	0.10	0.02												
	2	0.00	0.10	0.16	0.06	0.26	0.31	0.49	0.69	0.80	0.68	0.16	0.11	0.01												
10	**1**	0.07	0.06	0.66	0.23	0.10	0.23	0.45	0.46	0.44	0.42	0.13	0.06	0.09	0.08	0.08	0.01									
	2	0.03	0.03	0.35	0.15	0.10	0.13	0.42	0.49	0.41	0.26	0.17	0.09	0.06	0.12	0.18	0.04									
11	**1**	0.01	n/a	0.01	0.11	0.90	0.31	0.07	0.10	0.24	0.10	0.03														
	2	n/a	0.05	0.10	0.09	0.13	0.58	0.53	0.10	0.03	0.24	0.15														
12	**1**	0.06	0.12	0.35	0.31	0.65	0.53	1.21	1.83	1.41	1.13	1.03	0.78	0.62	0.32	0.12	0.11									
	2	0.05	0.11	0.28	0.23	0.58	0.51	1.18	1.73	1.39	1.17	1.03	0.78	0.53	0.3	0.18	0.11									

Amplitude (V)

		Angle (degrees)																									
Tooth	**Scan No.**	**0**	**5**	**10**	**15**	**20**	**25**	**30**	**35**	**40**	**45**	**50**	**55**	**60**	**65**	**70**	**75**	**80**	**85**	**90**	**95**	**100**	**105**	**110**	**115**	**120**	**Amplitude (V)**
13	**1**	0.04	0.12	0.18	0.19	0.10	0.11	0.16	0.30	0.33	0.61	0.93	0.76	0.75	0.63	1.30	0.49	0.23	0.11	0.04							
	2	0.05	0.13	0.10	0.10	0.11	0.21	0.29	0.37	0.67	1.06	0.73	0.68	1.36	0.34	0.22	0.10	0.03	0.05	0.02							
14	**1**	0.01	0.02	0.12	0.23	0.26	0.45	0.43	0.46	0.24	0.13	0.12	0.07	0.04													
	2	0.01	0.03	0.12	0.23	0.28	0.46	0.43	0.50	0.25	0.13	0.13	0.07	0.03													
15	**1**	0.05	0.06	0.10	0.15	0.29	0.68	0.42	0.31	0.32	0.30	0.19	0.08	0.07													
	2	0.05	0.06	0.11	0.15	0.28	0.63	0.39	0.26	0.29	0.29	0.20	0.07	0.05													
16	**1**	0.02	0.06	0.08	0.17	0.28	0.31	0.35	0.23	0.10	0.10	0.08	0.05	0.03													
	2	0.02	0.07	0.08	0.18	0.27	0.32	0.35	0.24	0.10	0.11	0.08	0.04	0.03													
17	**1**	0.03	0.05	0.16	0.35	0.42	0.54	0.64	0.14	0.06	0.00																
	2	0.01	0.04	0.16	0.32	0.41	0.54	0.64	0.13	0.05	0.00																
18	**1**	0.09	0.26	0.32	0.27	0.24	0.23	0.37	0.28	0.16	0.09	0.11	0.07	0.01	0.00												
	2	0.03	0.06	0.23	0.31	0.24	0.26	0.22	0.34	0.38	0.17	0.12	0.11	0.10	0.03												

		Angle (degrees)																								
Tooth	**Scan No.**	**0**	**5**	**10**	**15**	**20**	**25**	**30**	**35**	**40**	**45**	**50**	**55**	**60**	**65**	**70**	**75**	**80**	**85**	**90**	**95**	**100**	**105**	**110**	**115**	**120**
19	**1**	0.05	0.18	0.12	0.13	0.09	0.10	0.20	0.20	0.45	0.33	0.23	0.21	0.25	0.06											
	2	0.05	0.05	0.17	0.11	0.20	0.22	0.20	0.23	0.22	0.44	0.34	0.24	0.24	0.32											
20	**1**	0.04	0.06	0.34	0.14	0.11	0.39	0.55	0.30	0.13	0.02															
	2	0.04	0.06	0.29	0.14	0.11	0.39	0.52	0.29	0.14	0.02															
21	**1**	0.02	0.09	0.14	0.11	0.20	0.07	0.11	0.22	0.49	0.48	0.31	0.13	0.16	0.13	0.04										
	2	0.01	0.01	0.01	0.09	0.08	0.08	0.09	0.20	0.47	0.48	0.27	0.11	0.10	0.06	0.02										
22	**1**	0.00	0.02	0.06	0.03	0.08	0.15	0.26	0.33	0.53	0.16	0.16	0.08	0.06	0.07	0.13	0.05	0.05	0.00							
	2	0.02	0.02	0.06	0.03	0.07	0.15	0.27	0.32	0.54	0.16	0.18	0.07	0.07	0.07	0.14	0.05	0.03	0.00							
23	**1**	0.03	0.12	0.07	0.08	0.11	0.15	0.31	0.40	0.60	0.77	0.58	0.70	0.24	0.14	0.02										
	2	0.02	0.05	0.08	0.11	0.19	0.30	0.34	0.36	0.50	0.75	0.62	0.70	0.23	0.15	0.02										
24	**1**	0.04	0.06	0.10	0.13	0.18	0.18	0.10	0.11	0.16	0.26	0.15	0.11	0.13	0.17	0.21	0.15	0.07								
	2	0.04	0.05	0.11	0.13	0.21	0.05	0.15	0.11	0.17	0.23	0.22	0.15	0.13	0.26	0.13	0.16	0.07								

Amplitude (V)

		Angle (degrees)																								
Tooth	**Scan No.**	**0**	**5**	**10**	**15**	**20**	**25**	**30**	**35**	**40**	**45**	**50**	**55**	**60**	**65**	**70**	**75**	**80**	**85**	**90**	**95**	**100**	**105**	**110**	**115**	**120**
25	**1**	0.03	0.04	0.16	0.29	0.38	0.41	0.12	0.02	0.02																
	2	0.02	0.02	0.21	0.33	0.57	0.18	0.09	0.07	0.03																
26	**1**	0.01	0.09	0.22	0.31	0.52	0.60	0.22	0.08	0.07	0.02															
	2	0.01	0.07	0.08	0.23	0.32	0.56	0.58	0.02	0.07	0.01															
27	**1**	0.01	0.08	0.37	0.30	0.16	0.26	0.11	0.03	0.08	0.17	0.32	0.16	0.06	0.05	0.03										
	2	0.02	0.09	0.38	0.30	0.16	0.34	0.11	0.03	0.08	0.19	0.30	0.15	0.07	0.05	0.03										

Amplitude (V)

Synthetic Central Incisors Signal Angle Dependency Table

		Angle (degrees)																								
Tooth	**Scan No.**	**0**	**5**	**10**	**15**	**20**	**25**	**30**	**35**	**40**	**45**	**50**	**55**	**60**	**65**	**70**	**75**	**80**	**85**	**90**	**95**	**100**	**105**	**110**	**115**	**120**
1	**1**	0.01	0.84	0.84	0.69	0.70	0.13	0.09	0.07	0.08	0.05	0.10	0.00													
	2	0.00	0.09	1.44	1.52	1.55	1.58	1.52	0.25	0.19	0.14	0.24	0.28													
2	**1**	0.02	0.72	0.73	0.58	1.60	1.16	0.59	0.37	0.08	0.15	0.10	0.00													
	2	0.01	0.06	1.35	1.55	1.46	1.47	1.52	0.26	0.17	0.15	0.23	0.28													

Amplitude (V)

10 Appendix 2: MATLAB® Imaging Programme Code

This is the code used in MATLAB® to process and display the ultrasound image.

Green comments are included to aid in any future advancement on the software.

```
inputname = get(handles.uifilename,'String');

cp = str2num(get(handles.centerpoint,'String'));

cutoff = str2num(get(handles.cutoffpoint,'String'));

cplength = str2num(get(handles.tdistance,'String'));

inc = str2num(get(handles.increments,'String'));

threshold = str2num(get(handles.threshold,'String')); % The percentage lower than the maximum value in the envelope array (A) is returned as 0.

scale = str2num(get(handles.ratio,'String')); % The scale factor used for correct imaging. This is the ratio between speed of sound in enamel and speed of sound in water.

smoothness = str2num(get(handles.smoothamount,'String'));


threshold = 1 - threshold; % Adjusts value of threshold for use in equation

N = cp - cutoff; % Point of centre of rotation

data = zeros(N,inc); % Creates empty array called data for use later on

inc1 = 360/inc;

inc2 = (inc1 * 3.14)/180;

 h = waitbar(0,'Forming Image...');

 if (get(handles.checkbox1,'Value') == get(hObject,'Max'))

   % Checkbox is checked-take appropriate action

   for i = 1:inc

    waitbar(i/(inc*5),h)

    filename = [inputname ' ' num2str(i) '.txt']; % Change filename as accordingly

    F=dlmread(filename, ',',cutoff,0); % Reads the file

    [Bb,Aa] = butter(1,smoothness); % First filter set up

    FData = filter(Bb,Aa,F); % Applying first filter
```

```
    mag = abs(hilbert(FData(:,2))); % Turning data into 'envelope'
form

    A = mag;

    A(A < (max(A)*threshold)) = 0; % Sets all values lower than
stated number to 0

     C = diff(A); %edge detection via use of differentiation

    C(C < 0) = 0; %only keeping positive values of C

    empty_test = any(C); %Test to see if array C is empty, returns 0
if it is empty, 1 if it is not empty

    if empty_test == 1

        indices = find(C); %Finding indices of non zero values

        M = indices(1,1); %Store index of first non zero value in M

        x = N - M;  %Remainder elements

        y = round(x / scale); %Remainder elements after applying
scaling factor

        secondlayer = C(M:(M+y));

        firstlayer = C(1:(M-1));

        fixedsecondlayer = interp(secondlayer,4); %Resamples the
sequence in vector 'secondlayer' at 4 times the original sample
rate.

        final_array = [firstlayer; fixedsecondlayer]; %Concatenate 2
layers vertically

        final_array = final_array(1:N);

        data(:,i) = final_array;

else

continue

end

end

data = flipud(data);

data = resample(data,1,4);

[nrows, ncols] = size(data);

increment = inc2; % for an increment angle in radians (x pi/180)

startAngle = 0;

%prepare matrices containing the polar coordinate data

rho = repmat([1:nrows]',1,ncols);
```

```
theta = repmat([startAngle:increment:startAngle + increment*(ncols-
1)],nrows,1);

waitbar(2/5,h)


%convert the polar coordinates to cartesian

[x,y] = pol2cart(theta,rho);

waitbar(3/5,h)

%use ffgrid to prepare the data

[zz, xx, yy] = ffgrid(x, y, data, 1, 1);

waitbar(4/5,h)

%use griddata to produce the final image

Z = griddata(x,y,data,xx,yy');

waitbar(5/5,h)

iptsetpref('ImshowAxesVisible', 'on');

r = max(max(data));

imax = cplength*2;

figure;

imshow(Z, [0 r], 'XData', [0 imax], 'YData', [0 imax])

else

   % Checkbox is not checked-take appropriate action

   for i = 1:inc

    waitbar(i/(inc*5),h)

    filename = [inputname ' ' num2str(i) '.txt']; % Change filename
as accordingly

    F=dlmread(filename, ',',cutoff,0); % Reads the file

    [Bb,Aa] = butter(1,smoothness); % First filter set up

    FData = filter(Bb,Aa,F); % Applying first filter

    mag = abs(hilbert(FData(:,2))); % Turning data into 'envelope'
form

    A = mag;

    A(A < (max(A)*threshold)) = 0; % Sets all values lower than
stated number to 0

    empty_test = any(A); %Test to see if array C is empty, returns 0
if it is empty, 1 if it is not empty

    if empty_test == 1
```

```
        indices = find(A); %Finding indices of non zero values

        M = indices(1,1); %Store index of first non zero value in M

        x = N - M;  %Remainder elements

        y = round(x / scale); %Remainder elements after applying
scalling factor

        secondlayer = A(M:(M+y));

        firstlayer = A(1:(M-1));

        fixedsecondlayer = interp(secondlayer,4); %Resamples the
sequence in vector 'secondlayer' at 4 times the original sample
rate.

        final_array = [firstlayer; fixedsecondlayer]; %Concatenate 2
layers vertically

        final_array = final_array(1:N);

        data(:,i) = final_array;

else

continue

end

end

data = flipud(data);

data = resample(data,1,4);

[nrows, ncols] = size(data);

increment = inc2; % for an increment angle in radians (x pi/180)

startAngle = 0;

%prepare matrices containing the polar coordinate data

rho = repmat([1:nrows]',1,ncols);

theta = repmat([startAngle:increment:startAngle + increment*(ncols-
1)],nrows,1);

waitbar(2/5,h)

%convert the polar coordinates to cartesian

[x,y] = pol2cart(theta,rho);

waitbar(3/5,h)

%use ffgrid to prepare the data

[zz, xx, yy] = ffgrid(x, y, data, 1, 1);

waitbar(4/5,h)

%use griddata to produce the final image
```

```
Z = griddata(x,y,data,xx,yy');

waitbar(5/5,h)

iptsetpref('ImshowAxesVisible', 'on');

r = max(max(data));

imax = cplength*2;

figure;

imshow(Z, [0 r], 'XData', [0 imax], 'YData', [0 imax]) %Displays the
image with the correct axis.

end
```

11 Appendix 3: Representative B-Mode Images Using a Commercial Ultrasound Scanner

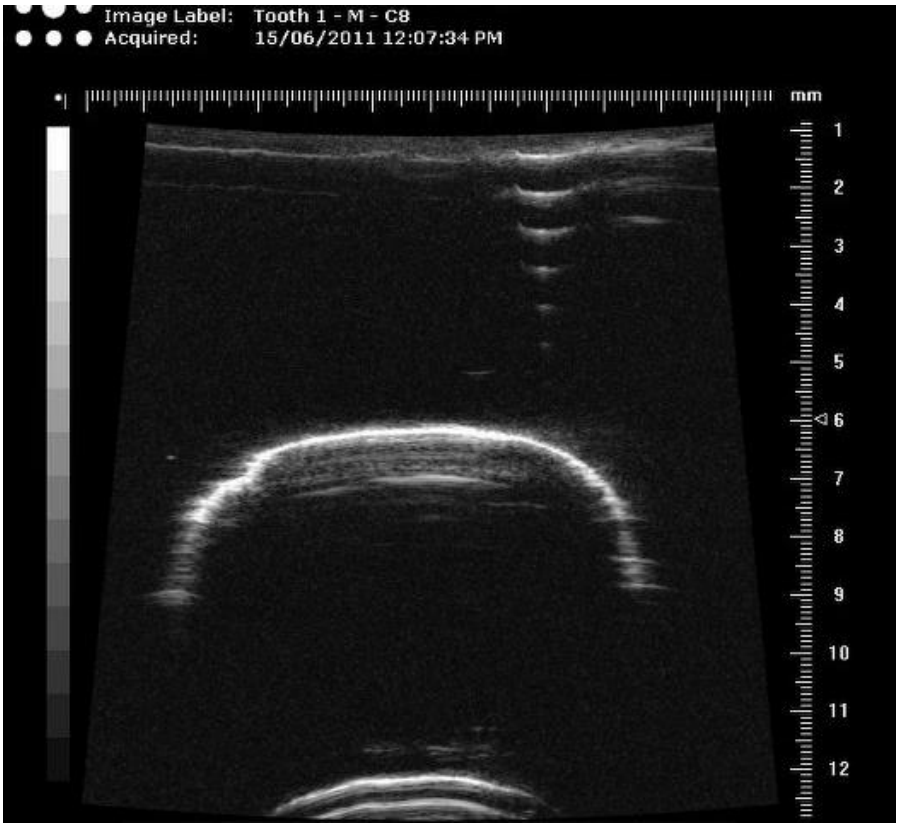

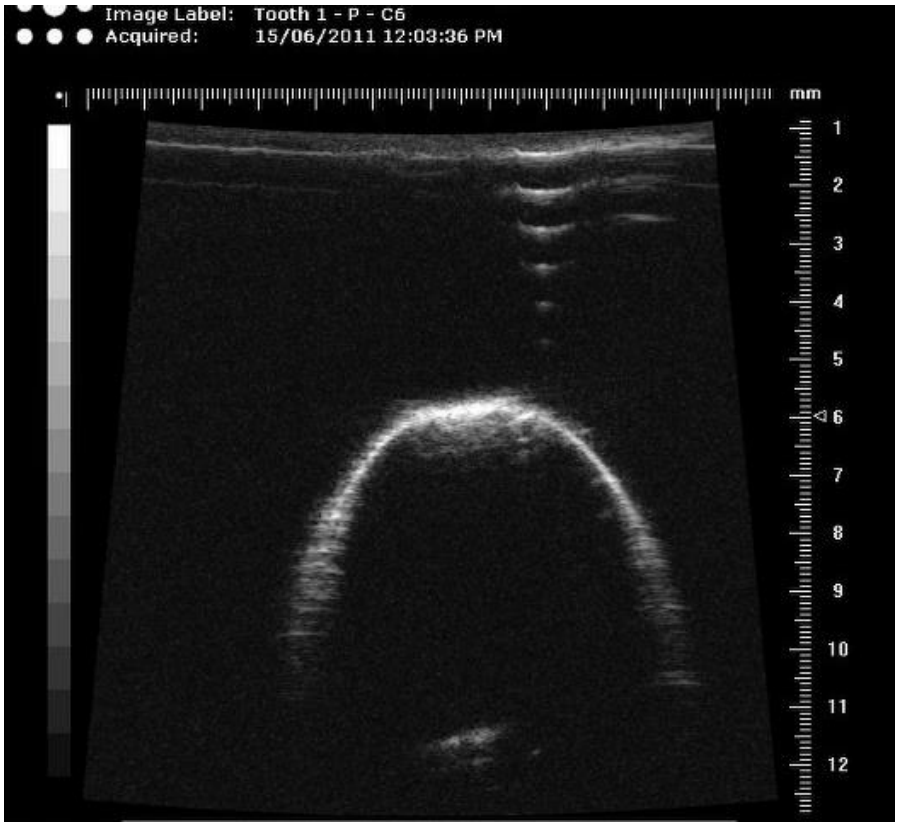
Image Label: Tooth 1 - P - C6
Acquired: 15/06/2011 12:03:36 PM
mm
1
2
3
4
5
6
7
8
9
10
11
12

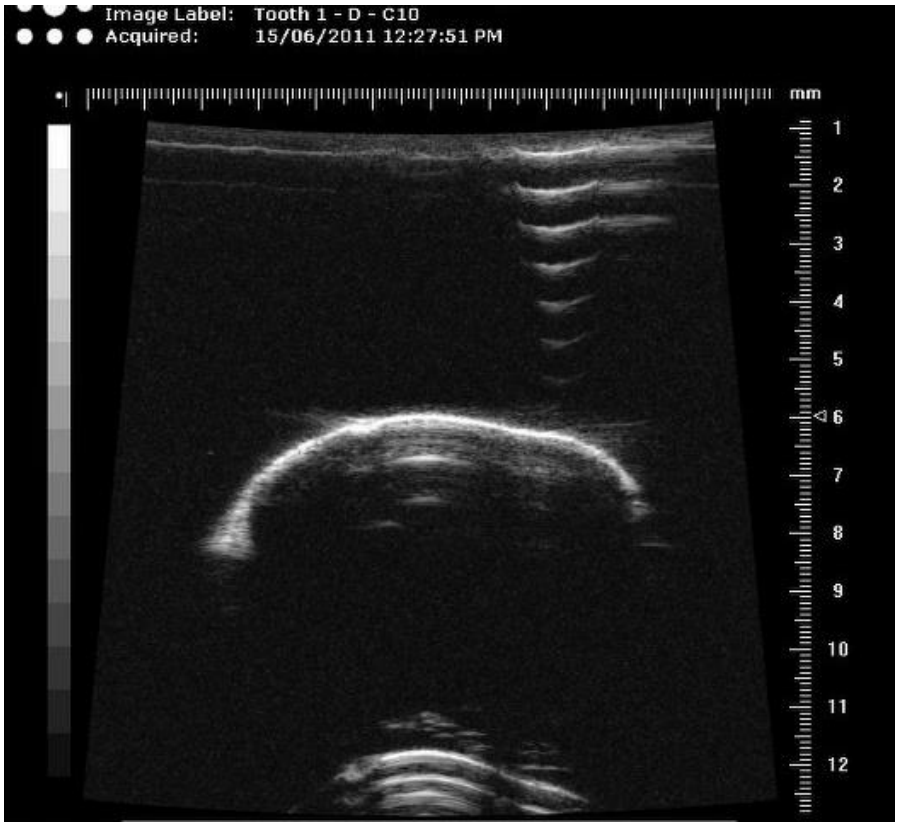
Image Label: Tooth 1 - D - C10
Acquired: 15/06/2011 12:27:51 PM
mm
1
2
3
4
5
6
7
8
9
10
11
12

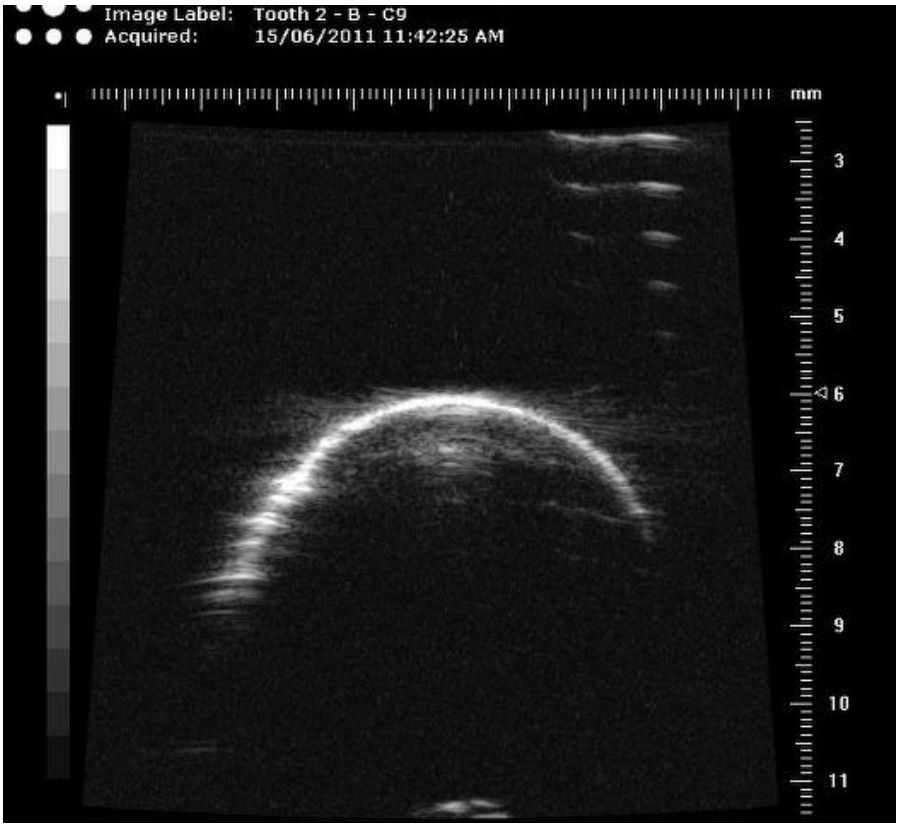
Image Label: Tooth 2 - B - C9
Acquired: 15/06/2011 11:42:25 AM
mm
3
4
5
6
7
8
9
10
11


Image Label: Tooth 2 - M - C6
Acquired: 15/06/2011 11:57:51 AM
mm
1
2
3
4
5
6
7
8
9
10
11
12

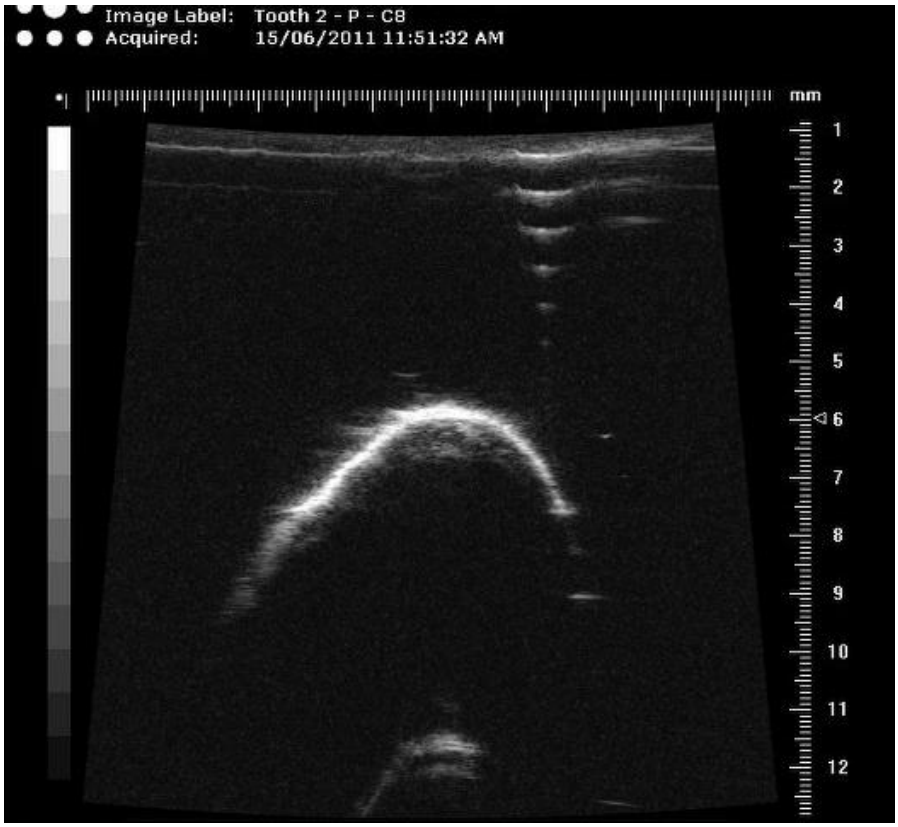
Image Label: Tooth 2 - P - C8
Acquired: 15/06/2011 11:51:32 AM
mm
1
2
3
4
5
6
7
8
9
10
11
12

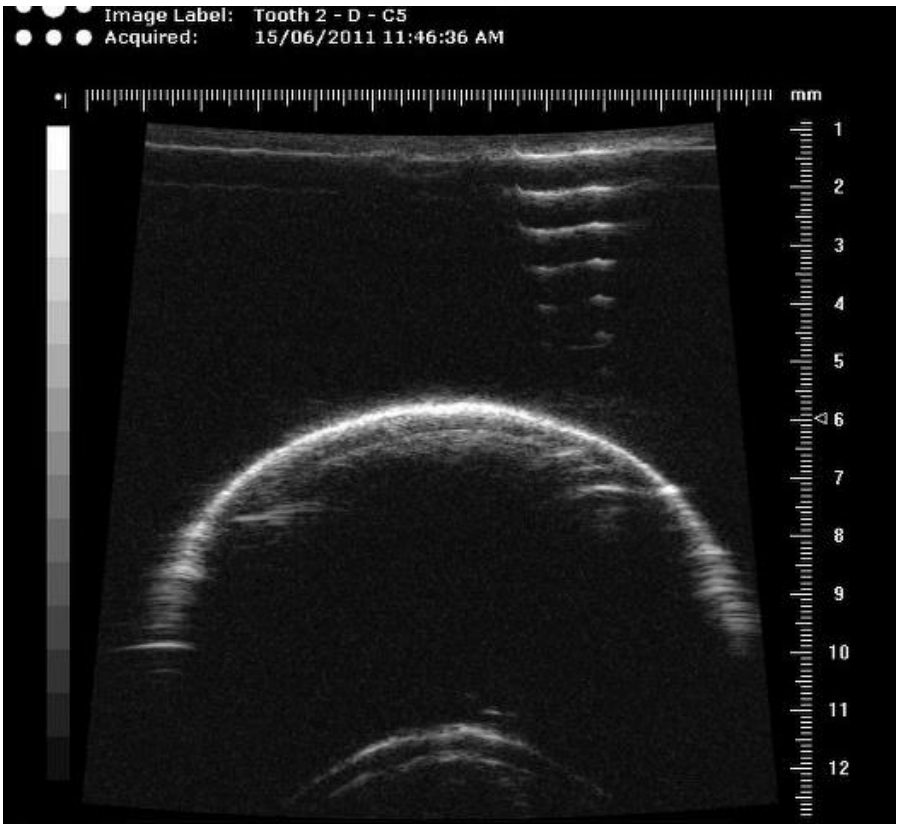
Image Label: Tooth 2 - D - C5
Acquired: 15/06/2011 11:46:36 AM
mm
1
2
3
4
5
6
7
8
9
10
11
12


Image Label: Tooth 3 - B - C7
Acquired: 15/06/2011 11:19:19 AM
mm
2
3
4
5
6
7
8
9
10
11

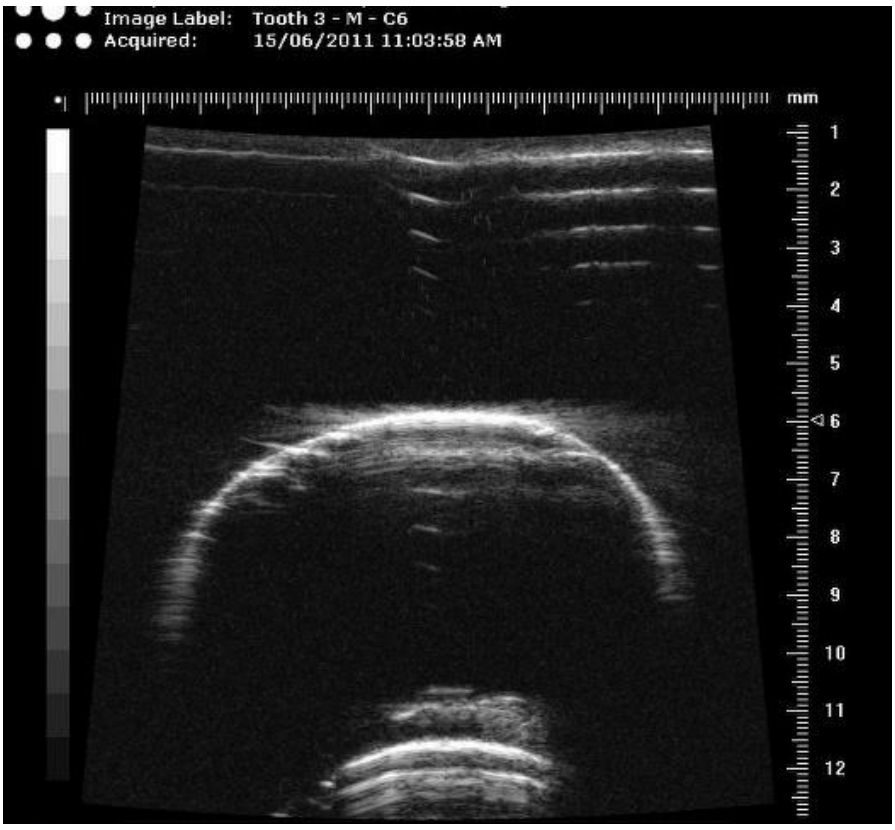
Image Label: Tooth 3 - M - C6
Acquired: 15/06/2011 11:03:58 AM
mm
1
2
3
4
5
6
7
8
9
10
11
12

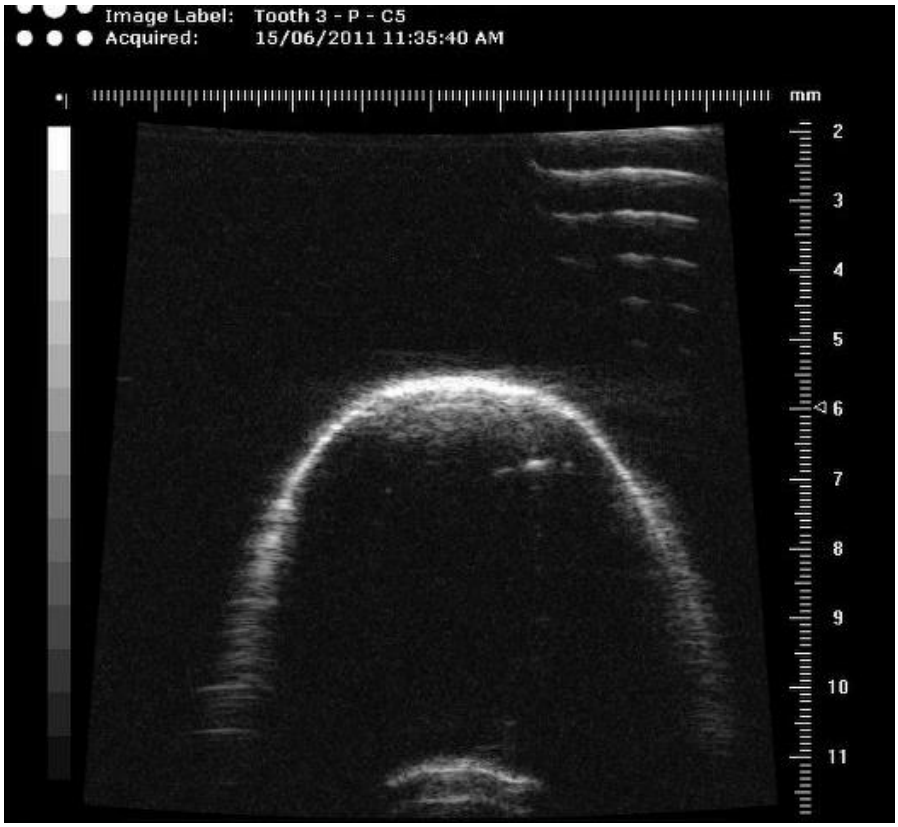
Image Label: Tooth 3 - P - C5
Acquired: 15/06/2011 11:35:40 AM
mm
2
3
4
5
6
7
8
9
10
11

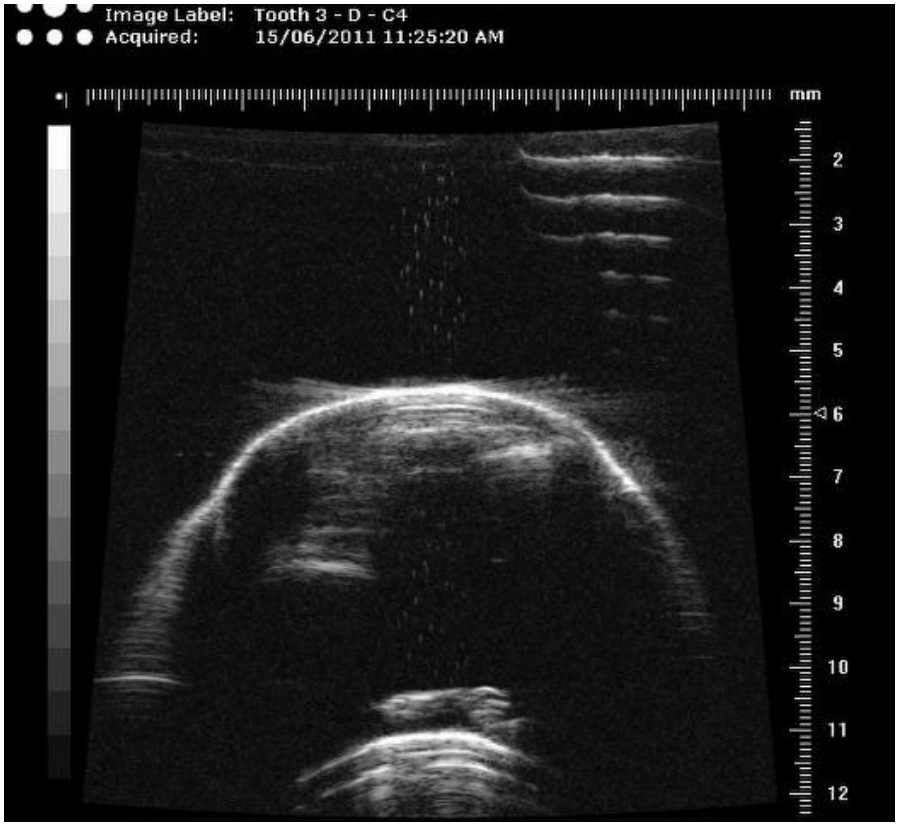
Image Label: Tooth 3 - D - C4
Acquired: 15/06/2011 11:25:20 AM
mm
2
3
4
5
6
7
8
9
10
11
12


Image Label: Tooth 4 - B - C7
Acquired: 15/06/2011 10:33:32 AM
mm
1
2
3
4
5
6
7
8
9
10

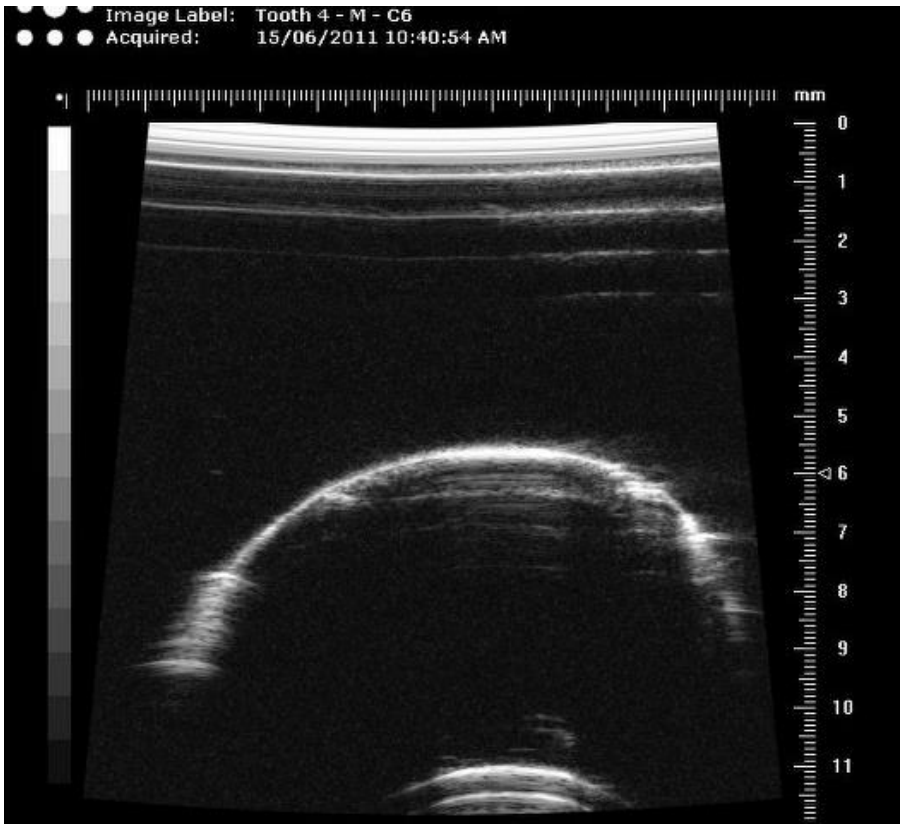
Image Label: Tooth 4 - M - C6
Acquired: 15/06/2011 10:40:54 AM
mm
0
1
2
3
4
5
6
7
8
9
10
11


Image Label: Tooth 4 - P - C5
Acquired: 15/06/2011 10:46:53 AM
mm
2
3
4
5
6
7
8
9
10
11

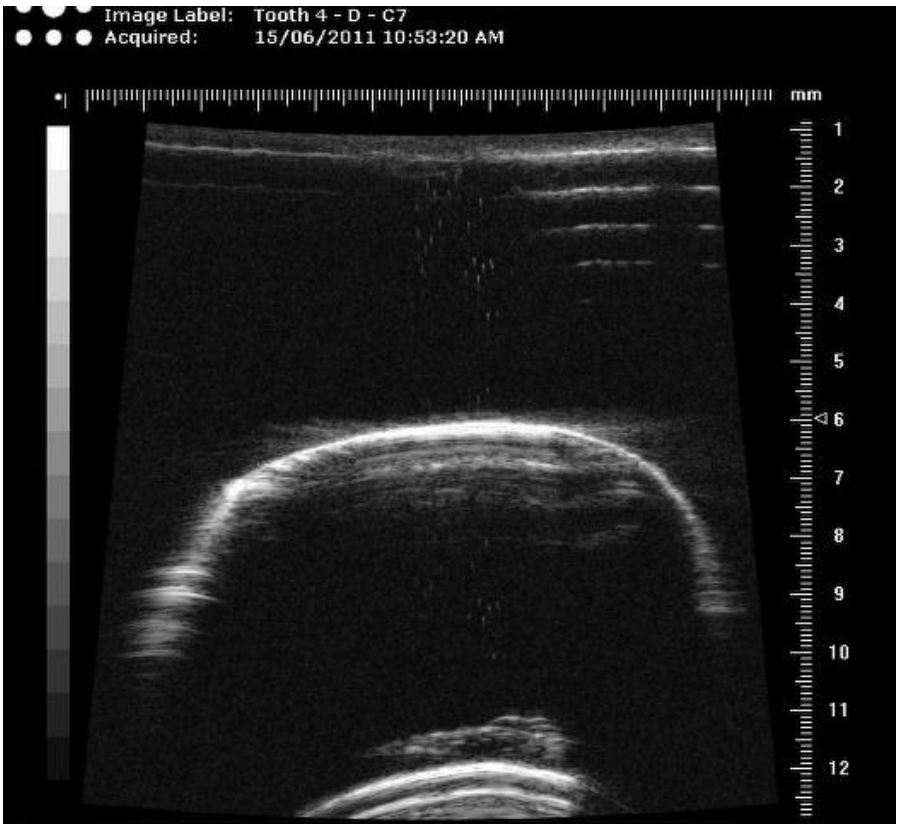
Image Label: Tooth 4 - D - C7
Acquired: 15/06/2011 10:53:20 AM
mm
1
2
3
4
5
6
7
8
9
10
11
12

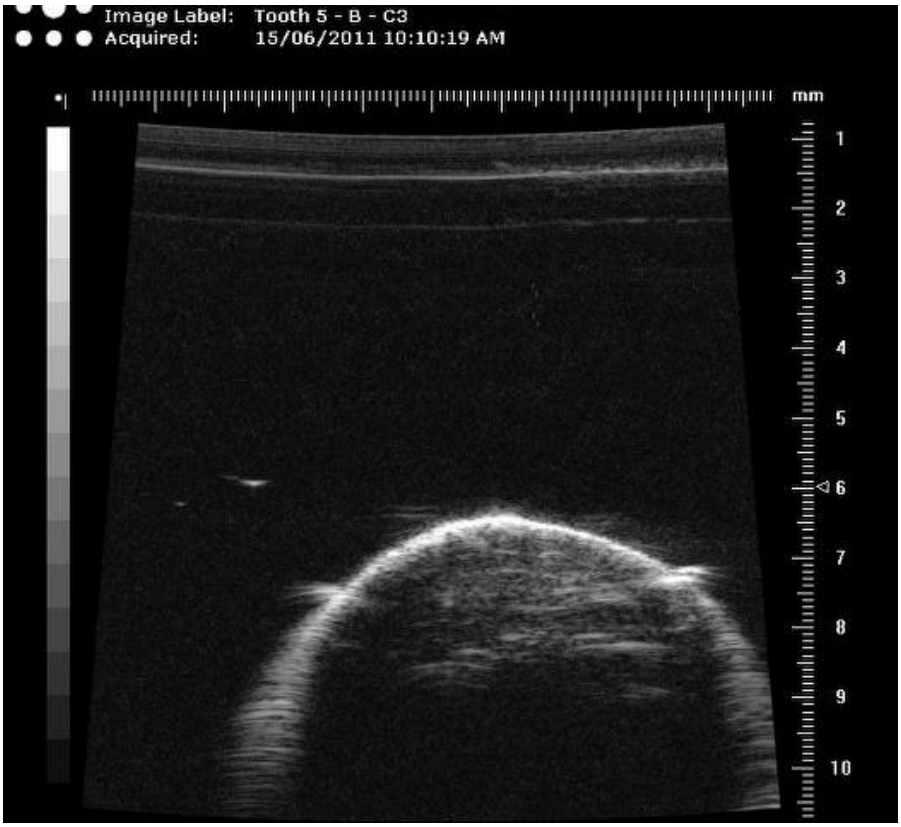
Image Label: Tooth 5 - B - C3
Acquired: 15/06/2011 10:10:19 AM
mm
1
2
3
4
5
6
7
8
9
10


Image Label: Tooth 5 - M - C4
Acquired: 15/06/2011 10:20:36 AM
mm
1
2
3
4
5
6
7
8
9
10


Image Label: Tooth 5 - P - C3
Acquired: 15/06/2011 10:15:39 AM
mm
1
2
3
4
5
6
7
8
9
10

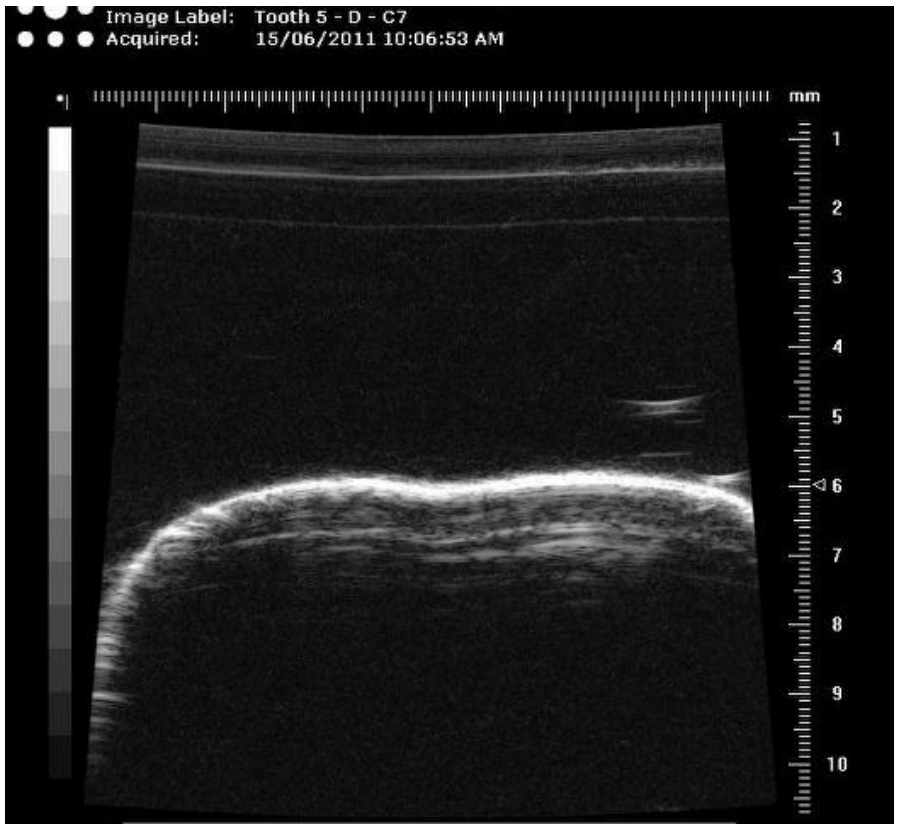
Image Label: Tooth 5 - D - C7
Acquired: 15/06/2011 10:06:53 AM
mm
1
2
3
4
5
6
7
8
9
10

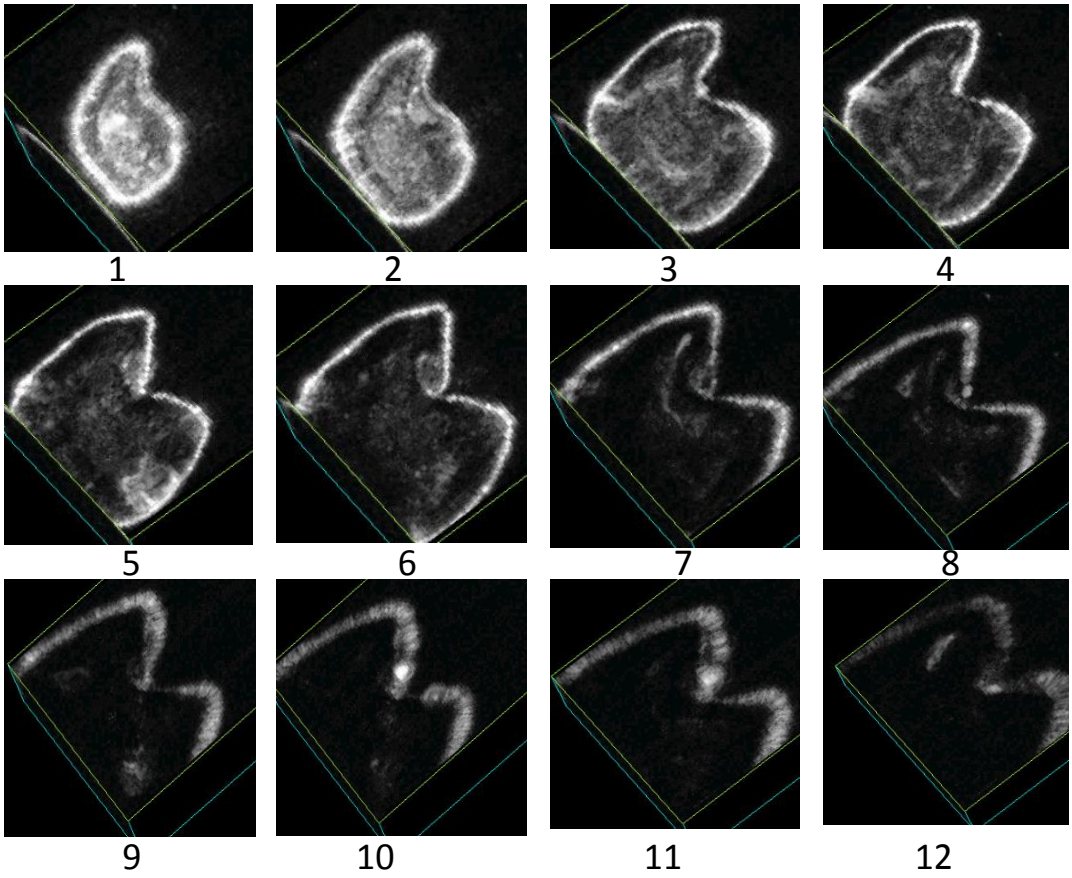

Images of a premolar tooth generated using 3D-mode of the commercial ultrasound scanner. Each 3D image (1 to 12) is itself a series of B-mode ‘slices’ that are assembled by the scanner and rendered to a 3D image.

12 Appendix 4: Histological Images of Premolars at T Marked Areas

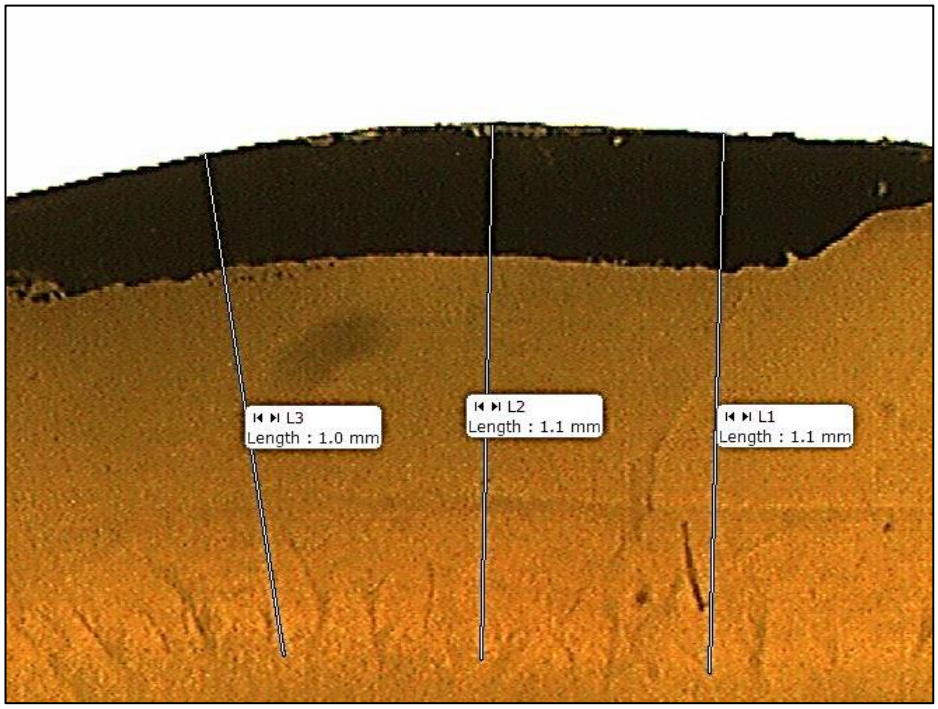

A coronal section of specimen number 1 with three repeat measurements of the enamel layer thickness at the T marked area (black mark).

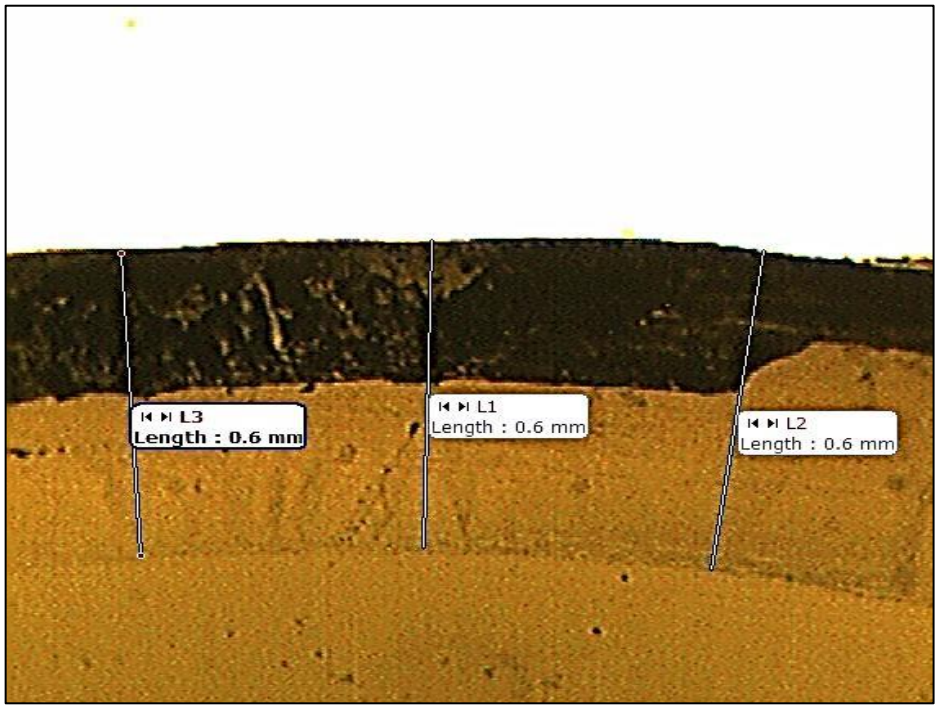

A coronal section of specimen number 2 with three repeat measurements of the enamel layer thickness at the T marked area (black mark).

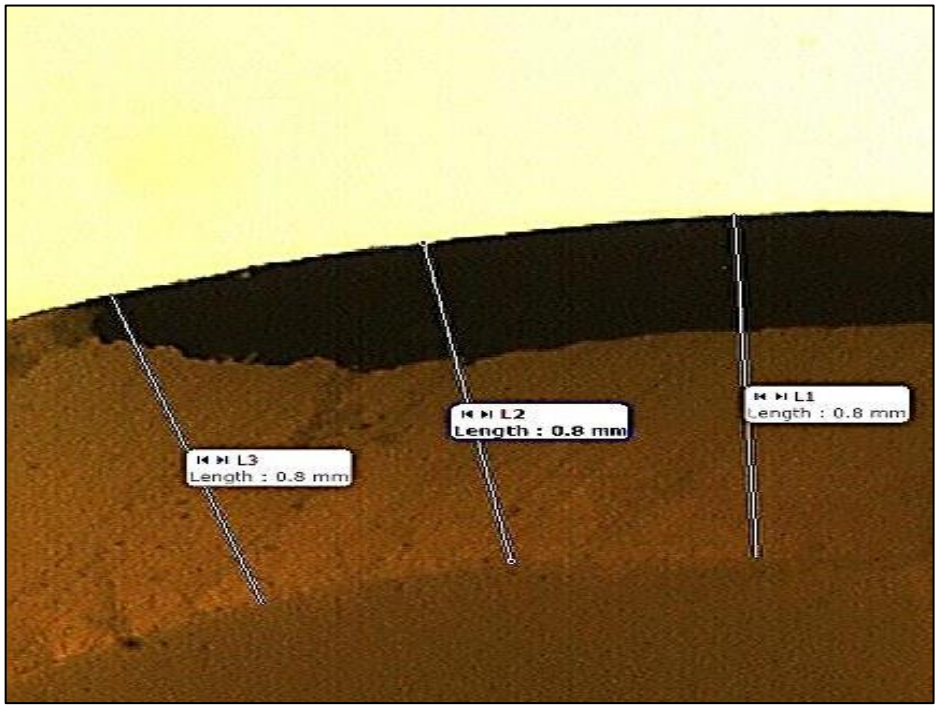

A coronal section of specimen number 3 with three repeat measurements of the enamel layer thickness at the T marked area (black mark).

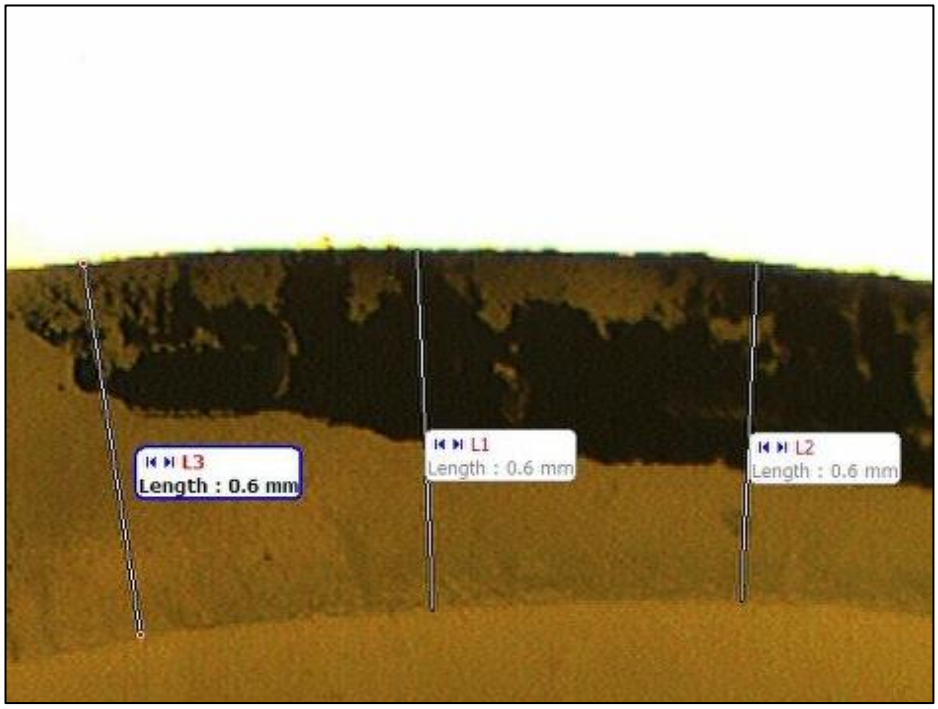

A coronal section of specimen number 4 with three repeat measurements of the enamel layer thickness at the T marked area (black mark).

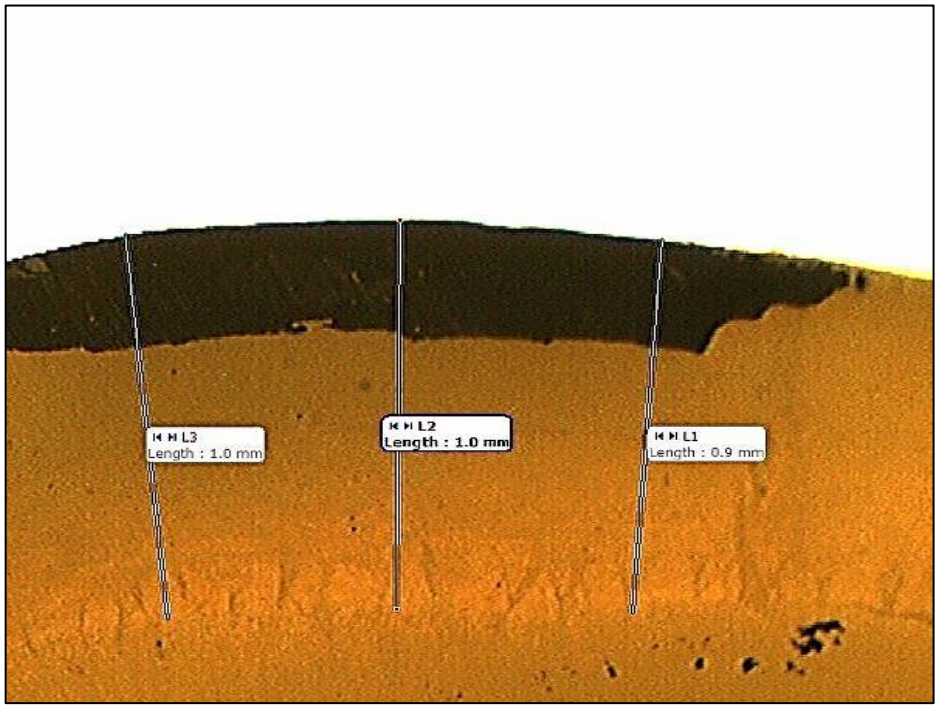

A coronal section of specimen number 5 with three repeat measurements of the enamel layer thickness at the T marked area (black mark).

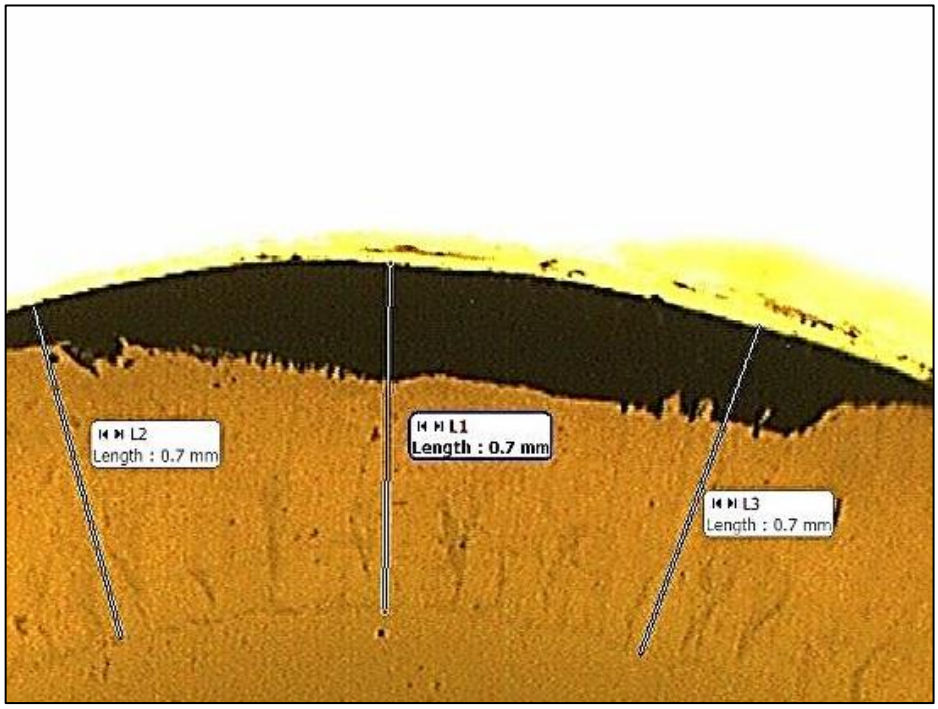

A coronal section of specimen number 6 with three repeat measurements of the enamel layer thickness at the T marked area (black mark).

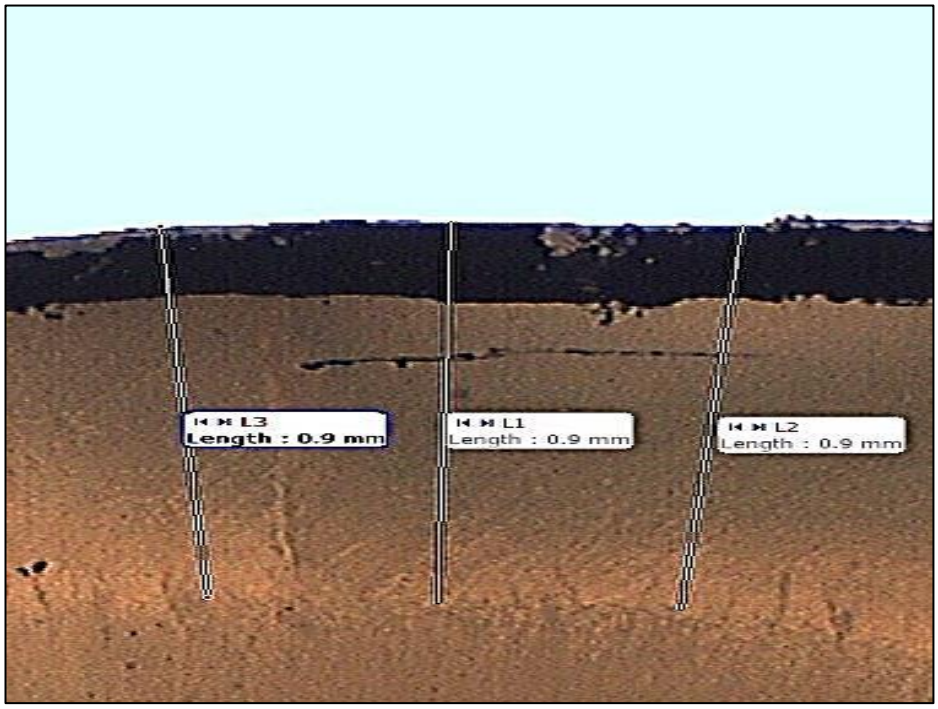

A coronal section of specimen number 7 with three repeat measurements of the enamel layer thickness at the T marked area (black mark).

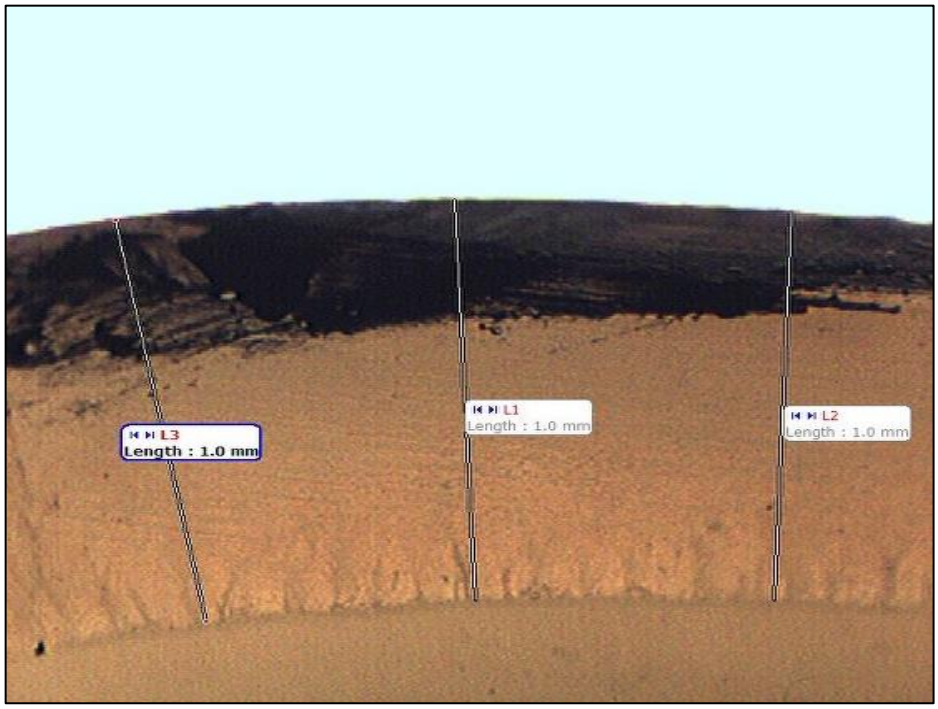

A coronal section of specimen number 8 with three repeat measurements of the enamel layer thickness at the T marked area (black mark).

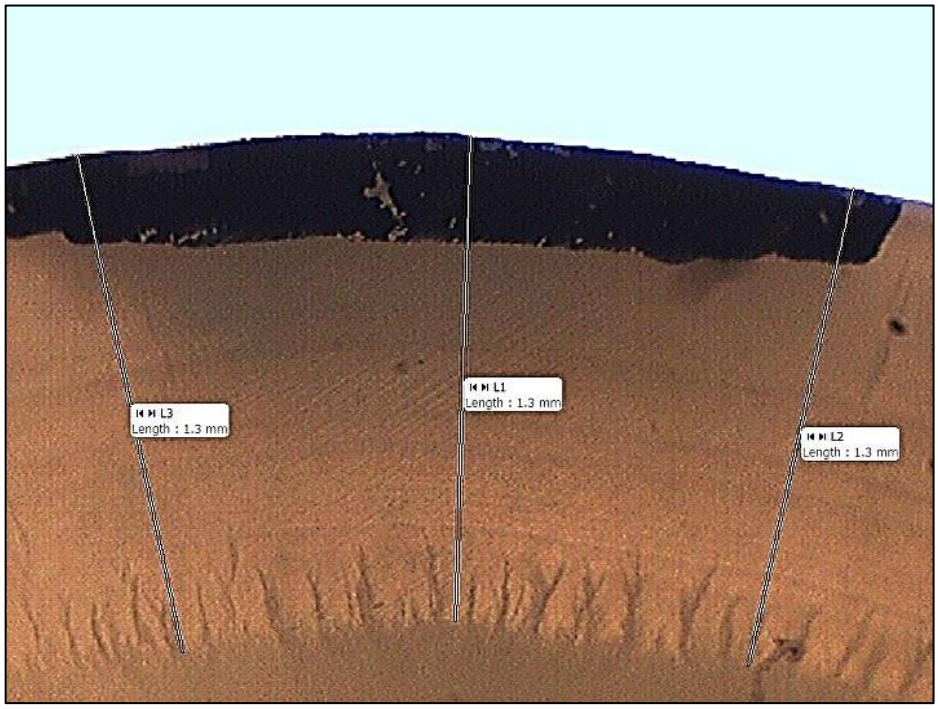

A coronal section of specimen number 9 with three repeat measurements of the enamel layer thickness at the T marked area (black mark).

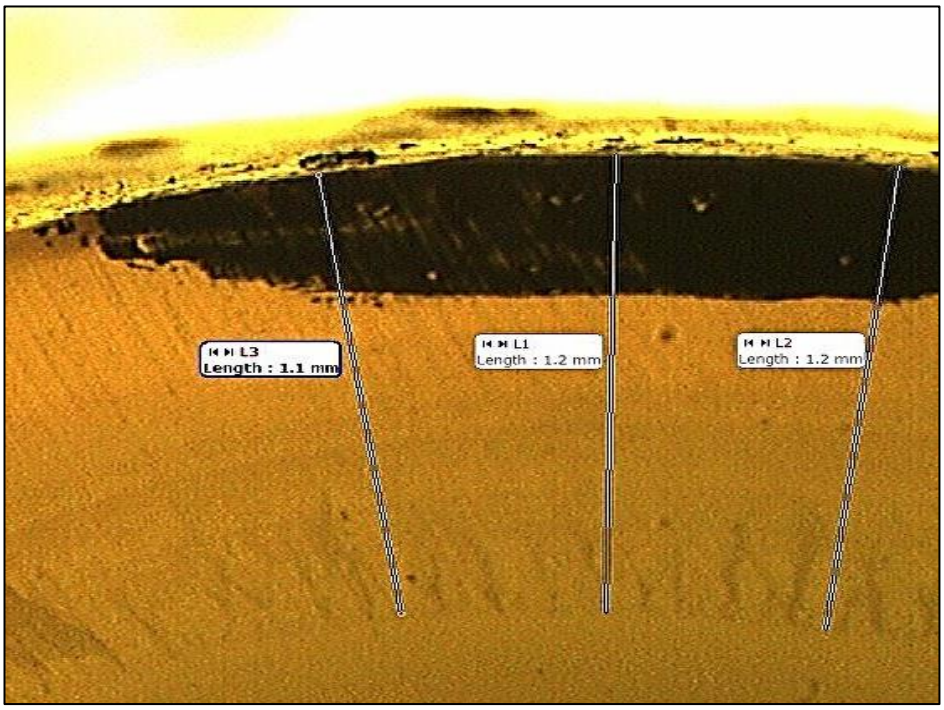

A coronal section of specimen number 10 with three repeat measurements of the enamel layer thickness at the T marked area (black mark).

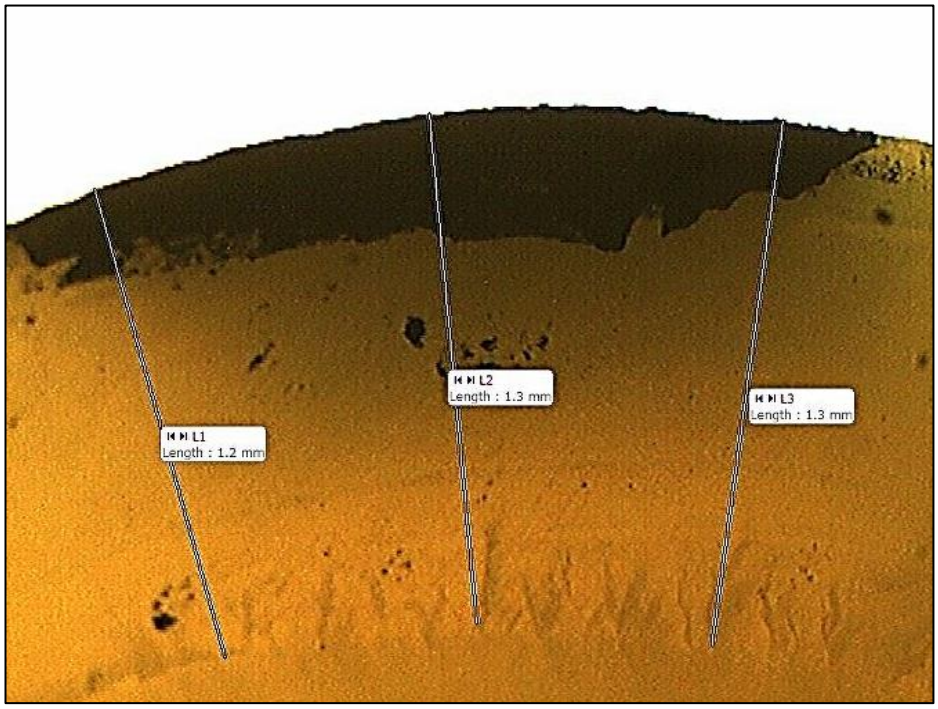

A coronal section of specimen number 11 with three repeat measurements of the enamel layer thickness at the T marked area (black mark).

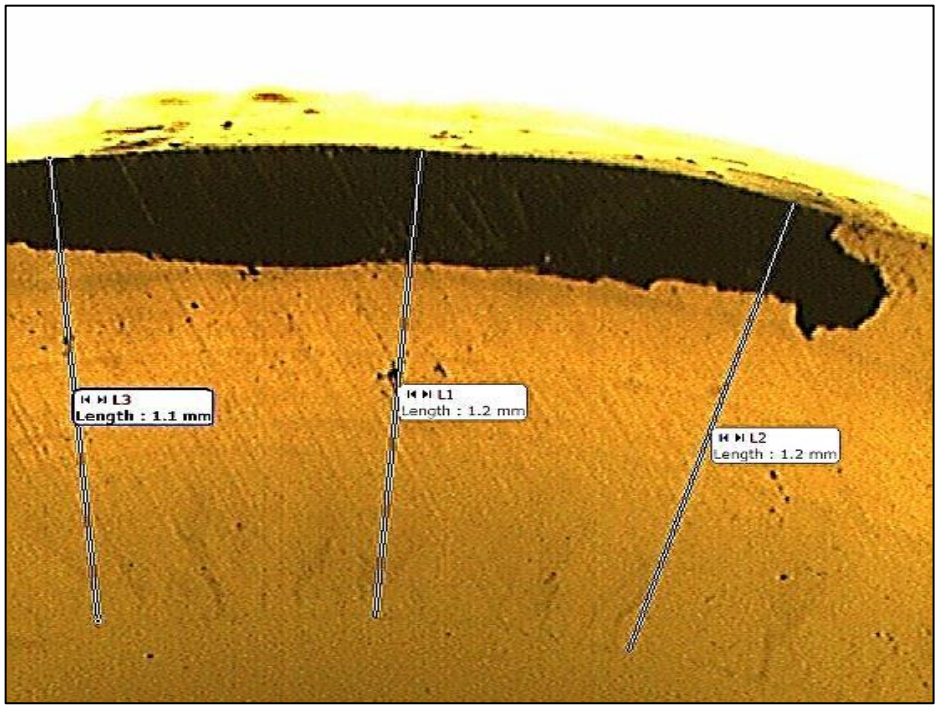

A coronal section of specimen number 12 with three repeat measurements of the enamel layer thickness at the T marked area (black mark).

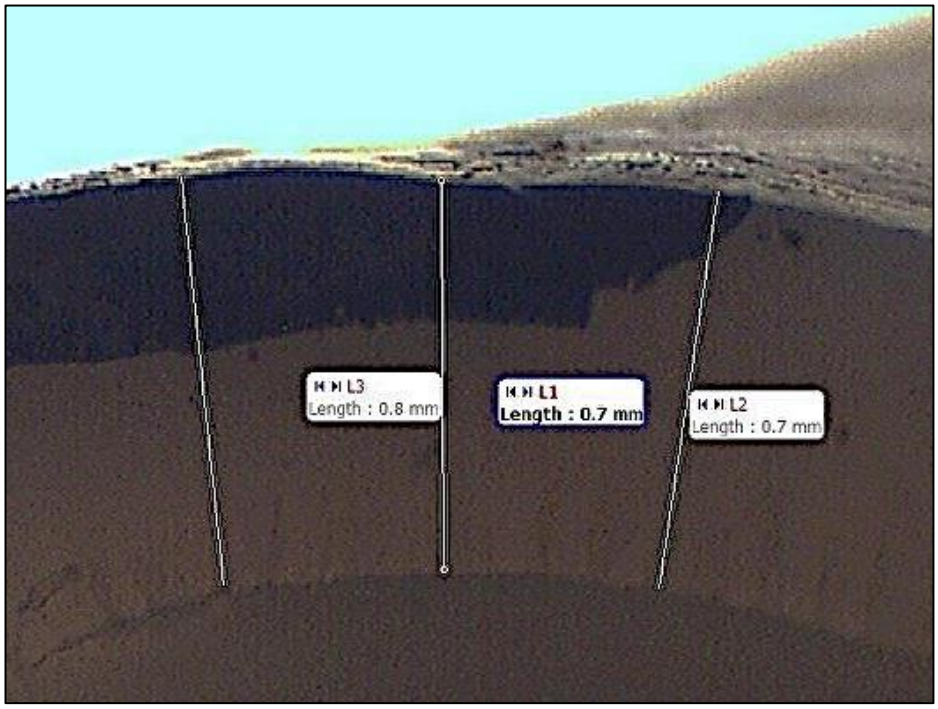

A coronal section of specimen number 13 with three repeat measurements of the enamel layer thickness at the T marked area (black mark).

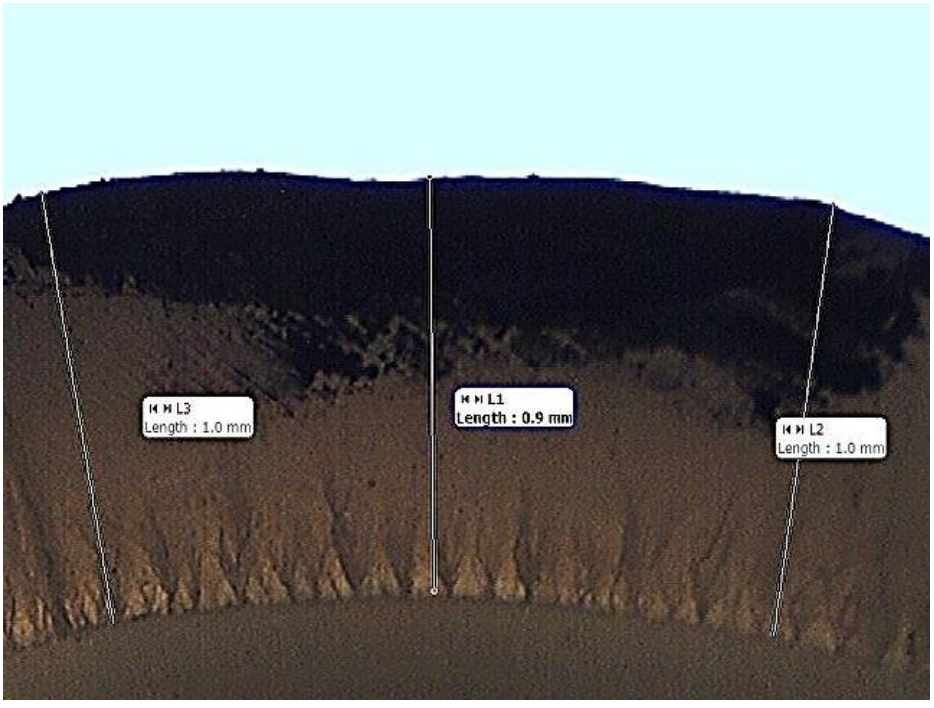

A coronal section of specimen number 14 with three repeat measurements of the enamel layer thickness at the T marked area (black mark).

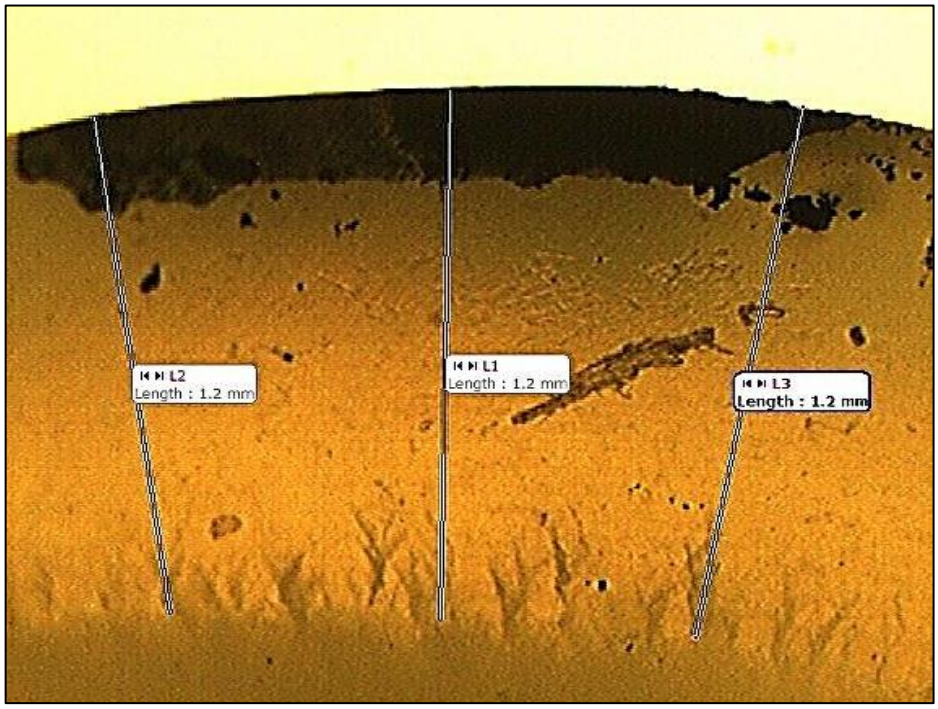

A coronal section of specimen number 17 with three repeat measurements of the enamel layer thickness at the T marked area (black mark).

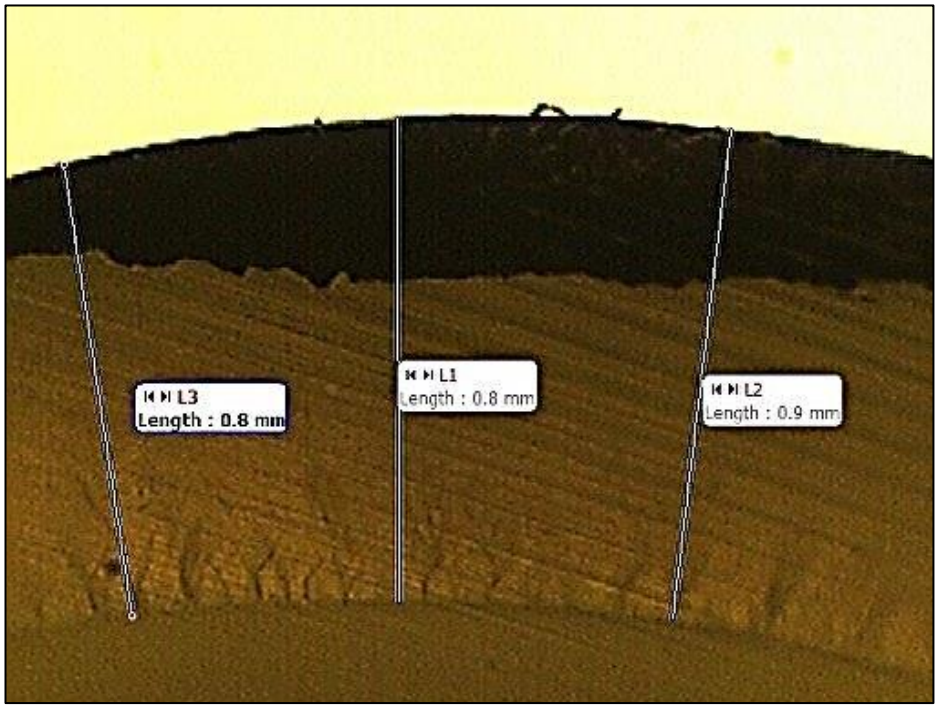

A coronal section of specimen number 18 with three repeat measurements of the enamel layer thickness at the T marked area (black mark).

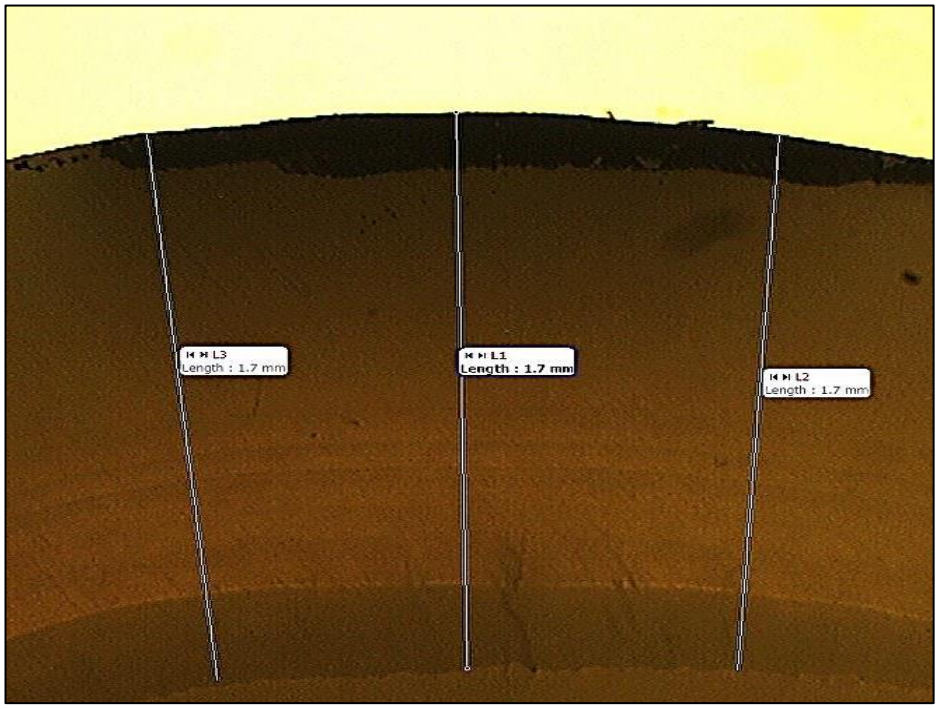

A coronal section of specimen number 19 with three repeat measurements of the enamel layer thickness at the T marked area (black mark).

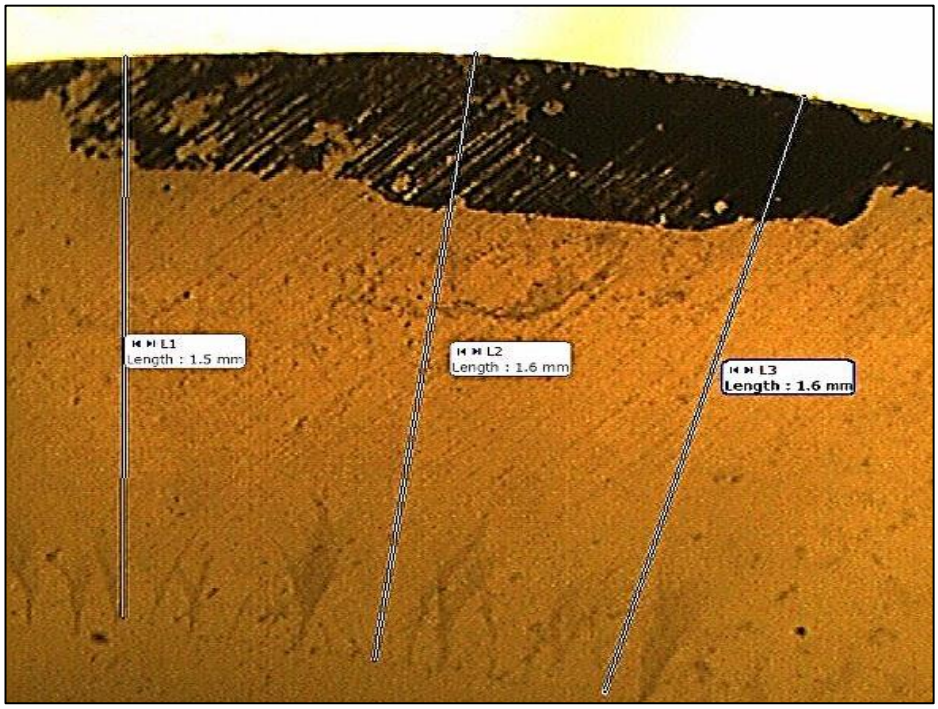

A coronal section of specimen number 20 with three repeat measurements of the enamel layer thickness at the T marked area (black mark).

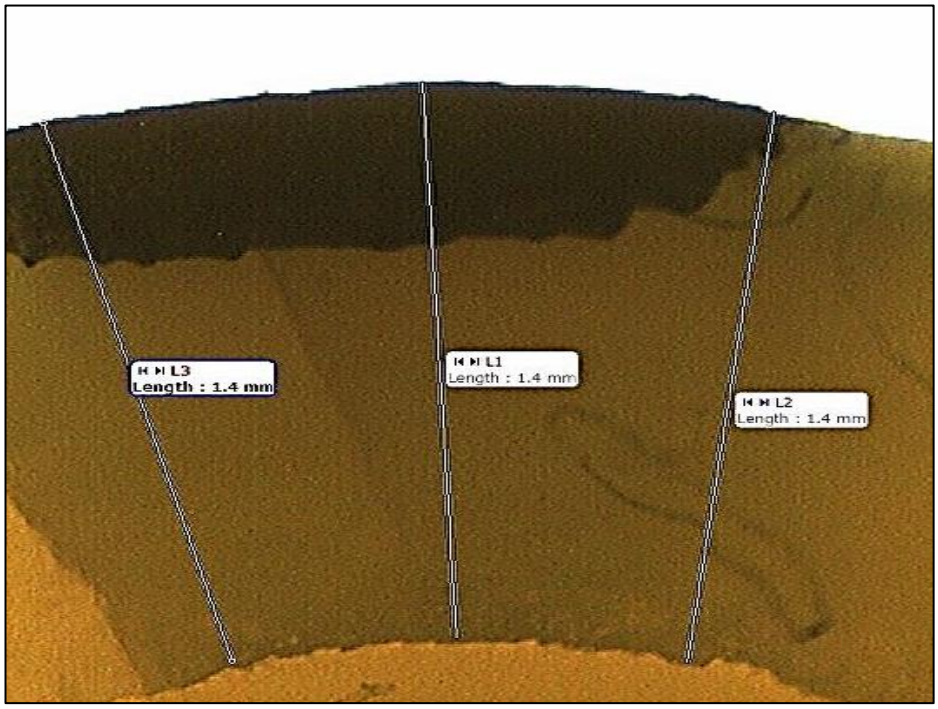

A coronal section of specimen number 21 with three repeat measurements of the enamel layer thickness at the T marked area (black mark).

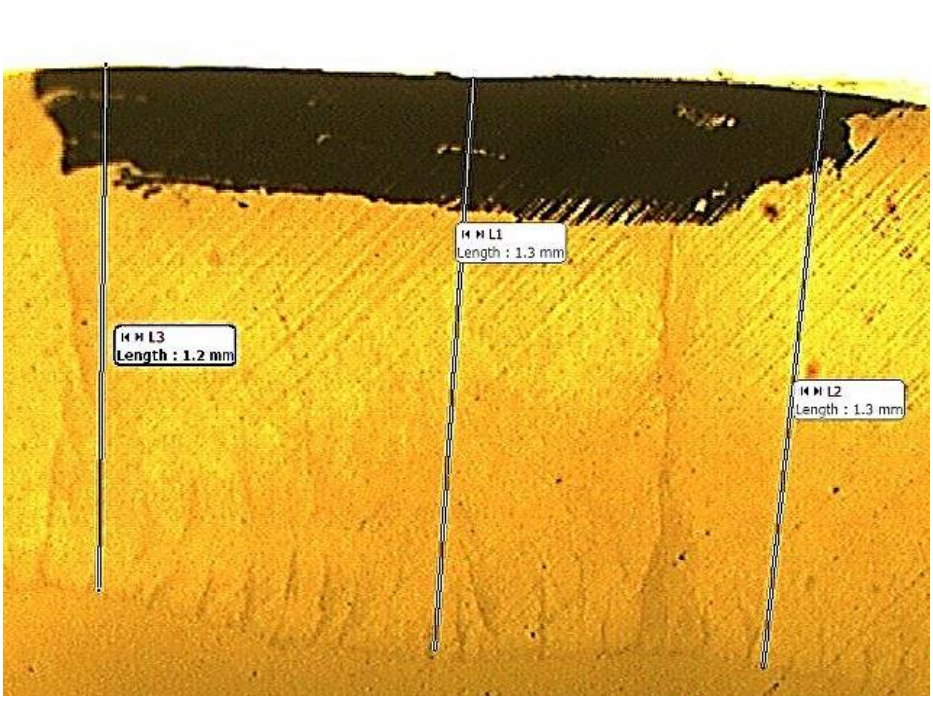

A coronal section of specimen number 22 with three repeat measurements of the enamel layer thickness at the T marked area (black mark).

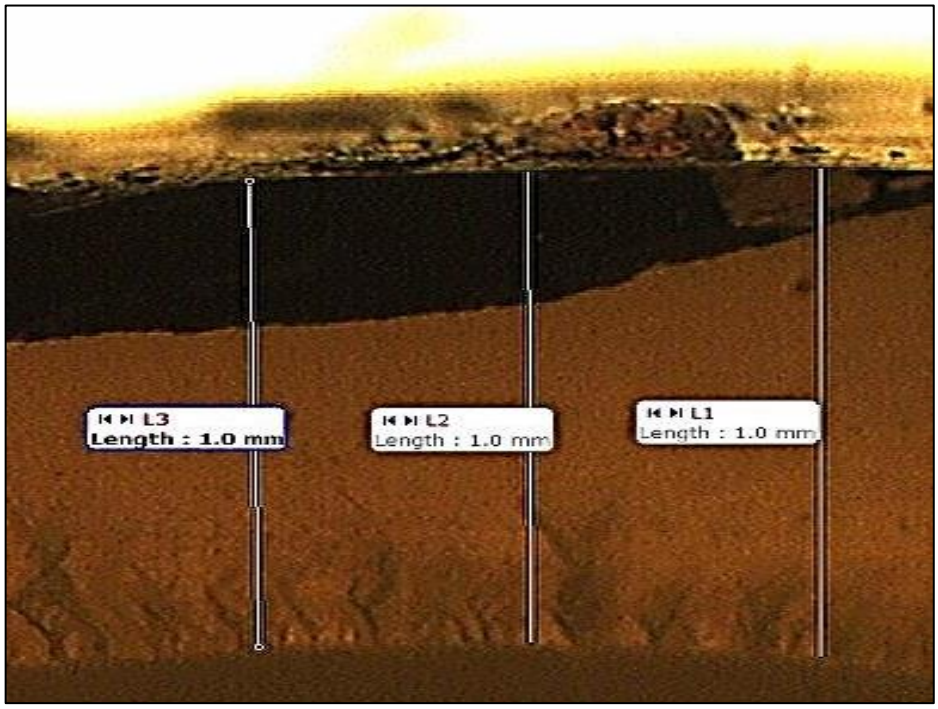

A coronal section of specimen number 23 with three repeat measurements of the enamel layer thickness at the T marked area (black mark).

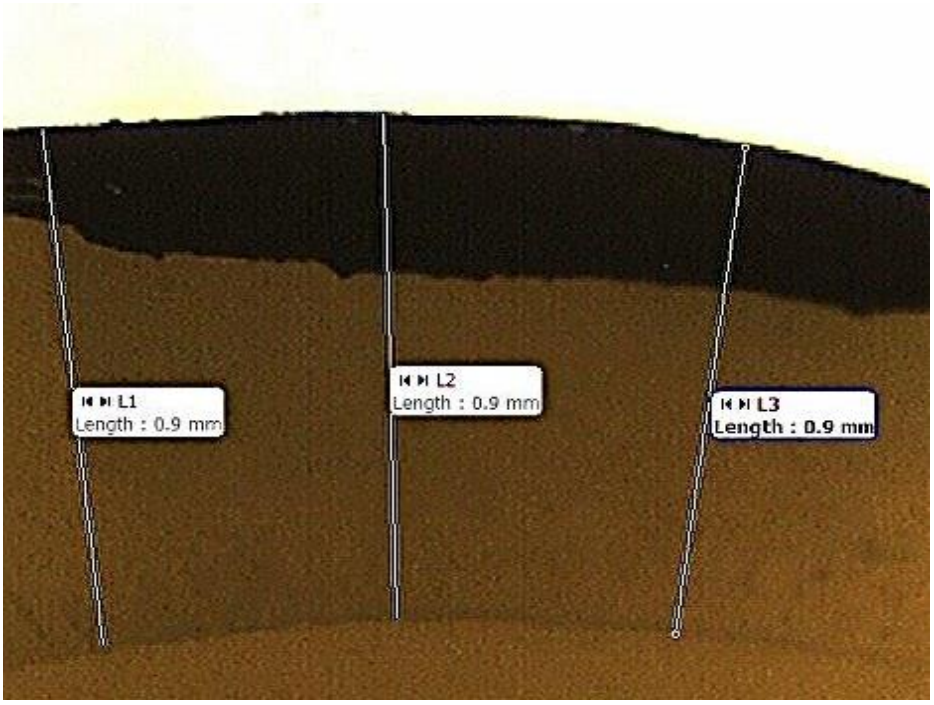

A coronal section of specimen number 24 with three repeat measurements of the enamel layer thickness at the T marked area (black mark).

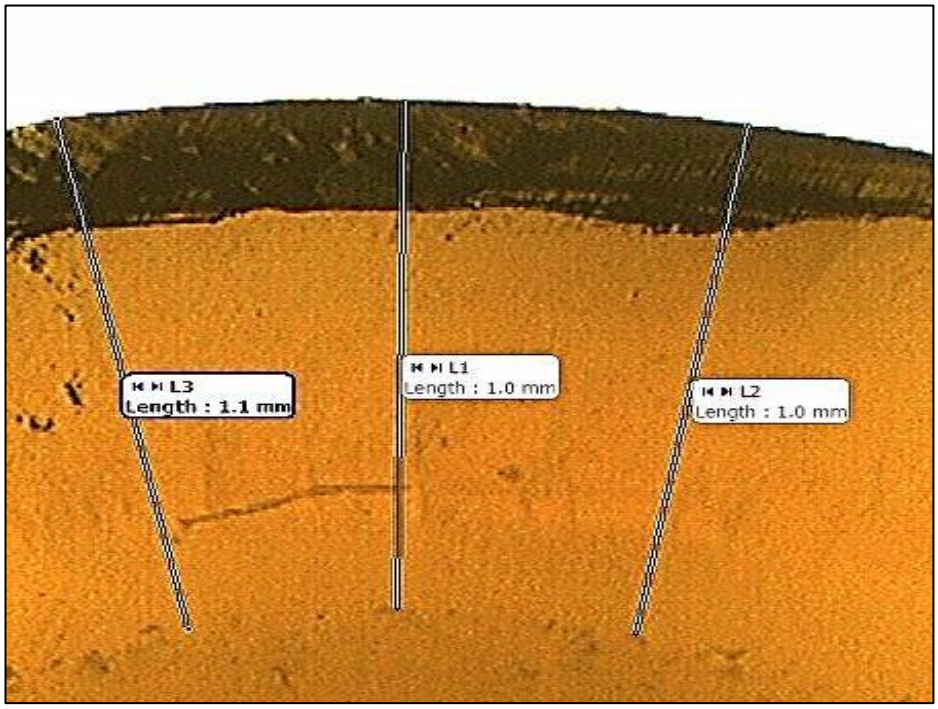

A coronal section of specimen number 25 with three repeat measurements of the enamel layer thickness at the T marked area (black mark).

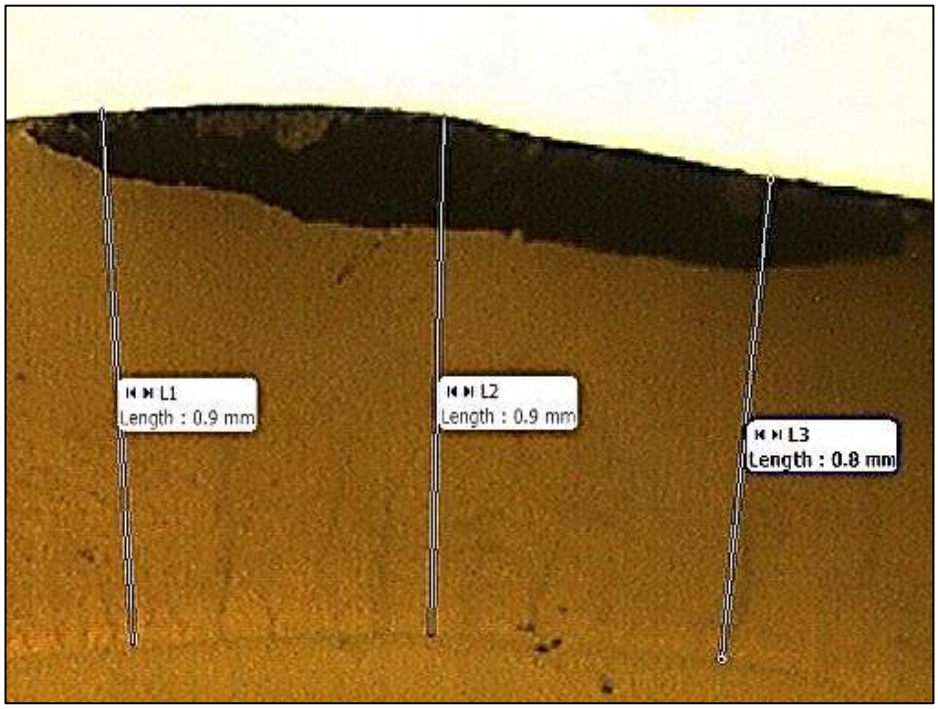

A coronal section of specimen number 26 with three repeat measurements of the enamel layer thickness at the T marked area (black mark).

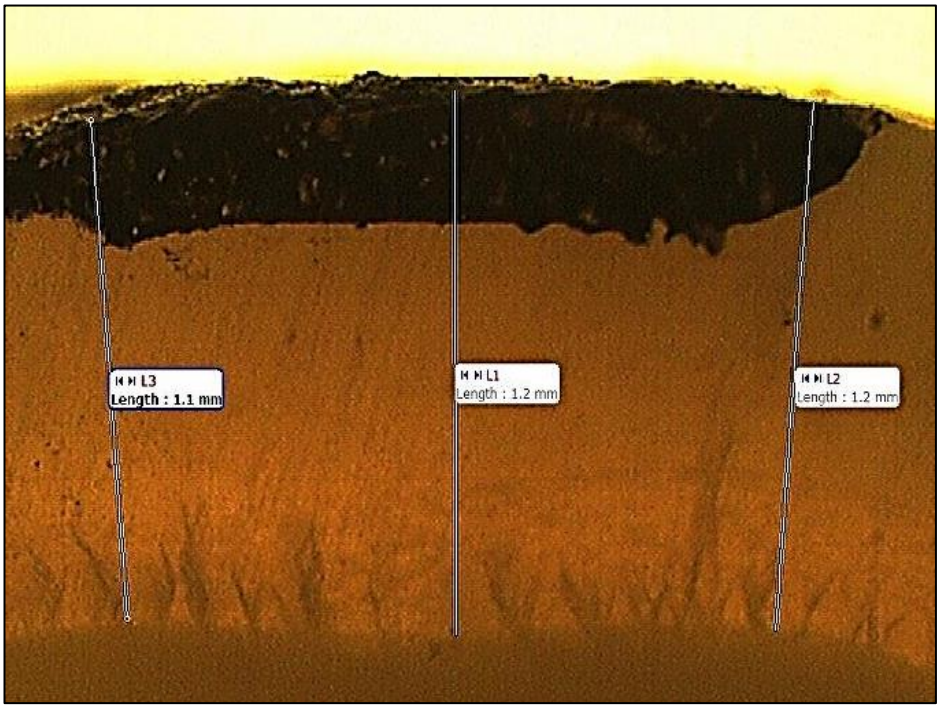

A coronal section of specimen number 27 with three repeat measurements of the enamel layer thickness at the T marked area (black mark).

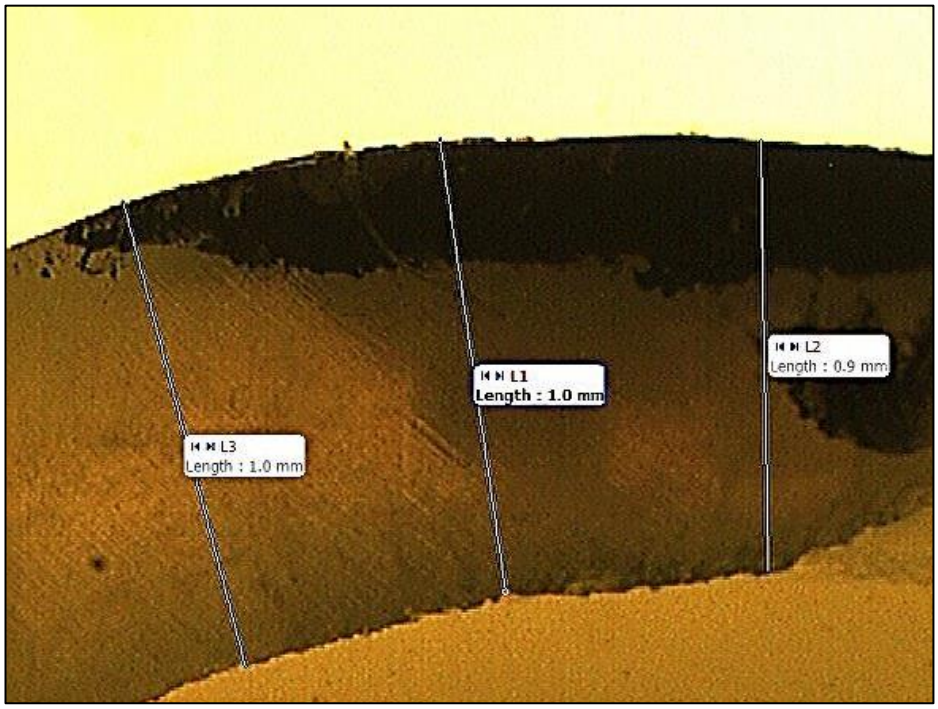

A coronal section of specimen number 28 with three repeat measurements of the enamel layer thickness at the T marked area (black mark).

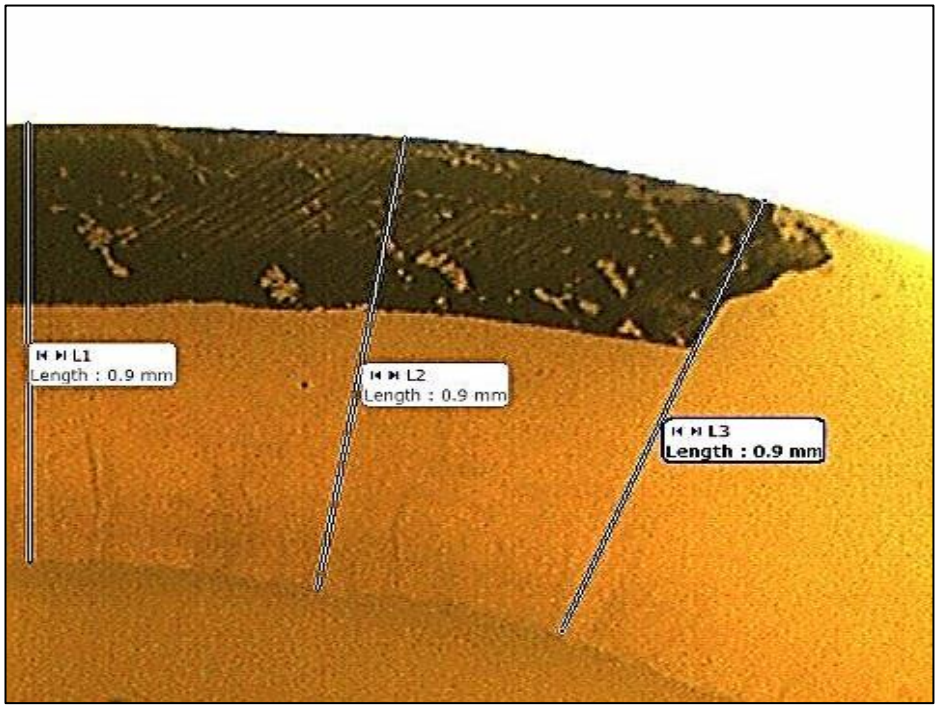

A coronal section of specimen number 29 with three repeat measurements of the enamel layer thickness at the T marked area (black mark).

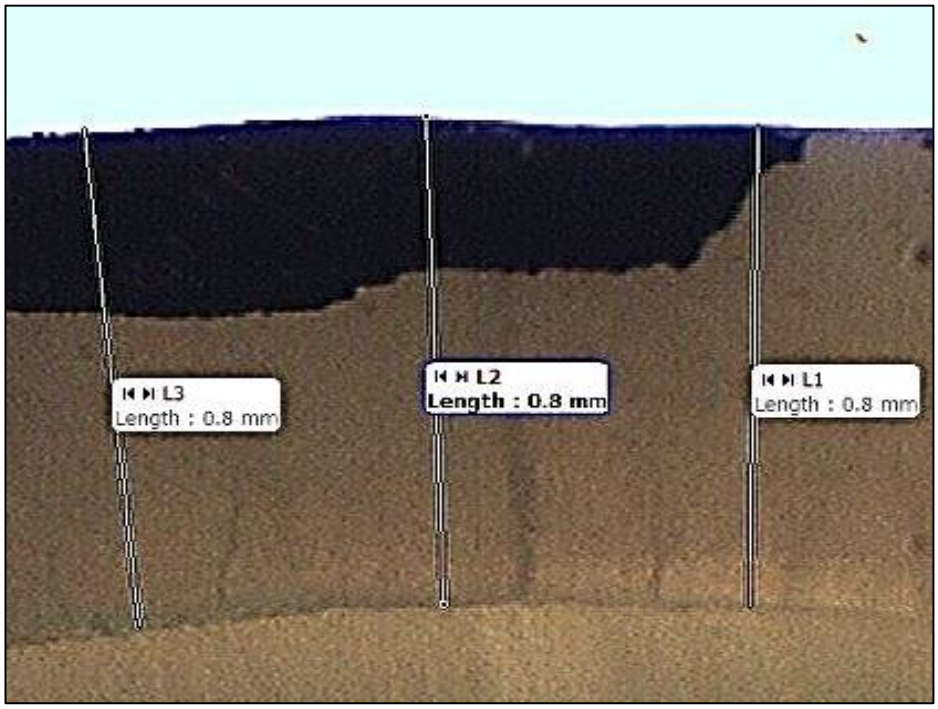

A coronal section of specimen number 30 with three repeat measurements of the enamel layer thickness at the T marked area (black mark).

13 Appendix 5: DREC Ethical Approval

Ethics application 'Preliminary clinical study of ultrasound to measure enamel thickness'

Julie McDermott [J.K.McDermott@leeds.ac.uk]

Sent: 05 October 2012 11:40

To: Sindi, Khalid [dn08khfs@leeds.ac.uk]

Cc: Gail Douglas; Catherine Fernandez; Nigel Bubb; Tony Evans

Dear Khalid,

Thank you for re-submitting the above Ethics application to the Dental Research Ethics Committee. Your application has been re-reviewed and I am pleased to inform you that your application has been accepted.

Documents reviewed by the Committee

Document Name	Date & Version Number
Protocol	Version 2 13.09.2012
Participant Information sheet	Version 1 05.09.2012
Trial Advertisement	Version 1 05.09.2012
Participant Consent form	Version 1 05.09.2012

With best wishes for the success of your project.

Please note: You are expected to keep a record of all your approved documentation, as well as documents such as sample consent forms, signed consent forms, participant information sheets and all other documents relating to the study. This should be kept in your study file, and may be subject to an audit inspection. If your project is to be audited, you will be given at least 2 weeks' notice. It is our policy to remind everyone that it is your responsibility to comply with Health and Safety, Data Protection and any other legal and/or professional guidelines there may be.

Kind regards,

For and on behalf of
Professor Gail Douglas
DREC Chairman

14 Appendix 6: National Health Service Research and Development (R&D) Ethical Approval

The Leeds Teaching Hospitals NHS

NHS Trust

Ref. Anne Gong

08/11/2012

Research & Development Directorate

Mr Khalid Sindi University of Leeds
Oral Biology
Leeds Dental Institute Leeds
LS2 9LU

34 Hyde Terrace

Leeds LS2 9LN

Tel: 0113 392 2878

Fax: 0113 392 6397

www.leedsth.nhs.uk/sites/research and development

Dear Mr Khalid Sindi

Re: Your research project: Preliminary Clinical Study of Ultrasound to Measure Enamel Thickness

LTHT R&D Number: DT12/10538

This project has been reviewed by The Leeds Teaching Hospitals NHS Trust (LTHT) and we are happy confirm support to undertake this project at the Leeds Dental Institute. I can confirm that R&D Approval from the Leeds Teaching Hospitals is not required for your project as you will not be using NHS patients, data, resources or equipment during the course of your work. Please note that the LTHT will not provide indemnity for this research as it is does not involve the NHS.

We wish you well with your interesting project.

Yours sincerely

pp **Dr D R Norfolk**
Associate Director of R&D

15 Appendix 7: Trial Advertisement

VOLUNTEERS REQUIRED

Can you help with research to give people healthier teeth and better smiles?

We are looking for volunteers aged 18 and over, who are willing to participate in a clinical research study looking at the potential use of ultrasound in measuring tooth enamel thickness. If successful, this could form a valuable technique for use in detecting and monitoring acid erosion and may help dentists in future to offer advice on how to prevent further loss of tooth enamel.

- If you have intact upper front teeth that do not have fillings or crowns (middle front upper teeth) you may be suitable to take part.
- At each visit, an ultrasound hand-held probe will be placed on one of your upper front teeth to take several measurements. This is a painless procedure.
- You will be required to attend three visits (approximately 20 minutes/visit) on three different days over a two-week period for further ultrasound measurements.
- The visits will take place at The Dental Translational and Clinical Research Unit (DenTCRU), located within Leeds Dental Institute (Worsley building, Level 5) on Clarendon Way, Leeds.
- A reasonable reimbursement will be paid in recognition of any inconvenience and out of pocket expenses the volunteer may incur.

INTERESTED?

- If you would like to have more information about the study, please call Gillian Dukanovic on 0113 34 36127 or email Gillian on G.Dukanovic@leeds.ac.uk
- If you ring, there may be an answer phone; if so please say that you are calling regarding the UMET Trial and leave your name and number and Gillian will get back to you.

16 Appendix 8: Participant Information Sheet

UNIVERSITY OF LEEDS

PARTICIPANT INFORMATION SHEET

PRELIMINARY CLINICAL STUDY OF ULTRASOUND TO MEASURE ENAMEL THICKNESS

You are being invited to take part in the above research study. Before you decide, it is important for you to understand why the research is being done and what it will involve. Please take time to read the following information carefully and discuss it with others if you wish. Ask us if there is anything that is not clear or if you would like more information. Take time to decide whether or not you wish to take part.

What is the purpose of the study?

The aim of this study is to examine whether an ultrasound technique can be used to measure enamel thickness in teeth. This is important so that dentists can see if enamel is being lost from the surface of the teeth caused by the acids in fruits and fizzy drinks. At present, the amount of enamel lost from teeth can not accurately be measured. Ultrasound is currently only used in scaling of teeth in dentistry, although it is widely used in medicine. If this technique proves useful, this would allow dentists to provide advice to patients to reduce the intake of acidic food/drinks and protect the remaining enamel tissue.

Why have I been chosen?

We are looking to recruit volunteers over 18 years old who have healthy front teeth and who are willing to take part in the study. Before you are enrolled on the study, you will need to have a short dental examination, to allow us to establish whether you are suitable for our study.

Do I have to take part?

Your participation in this study is entirely voluntary. If you decide to take part you will be given this information sheet to keep and be asked to sign a separate consent form. If you decide to take part you are still free to withdraw at any time, and without giving a reason. A decision to withdraw at any time, or a decision not to take part, will not affect the standard of care you receive.

What will happen to me if I take part?

If you are interested in taking part in the study, you will be invited to attend Leeds Dental Institute's Dental Translational and Clinical Research Unit (DenTCRU) for a screening assessment to review your medical history and dental details, and given the opportunity to ask as many questions as you would like. If suitable for the trial we would ask you to sign the consent form (a copy will be returned to you for your records) and begin the study.

You will be asked to attend the clinic on three separate occasions where you will have ultrasound measurements taken from the surface of one of your front teeth. The first visit will involve an ultrasound test to check that a reading can be obtained. The test will involve applying ultrasound on one of your upper front teeth (after massaging the tooth with a cotton wool to dry it) using an ultrasound probe with a replaceable plastic tip which will be placed on the surface of the tooth. A drop of

water will be placed between the plastic tip and the tooth. If it is not possible to obtain a reading, then you will be informed that you are not suitable and you will be withdrawn from the study.

If a reading can be obtained, ultrasound measurements will be taken from three different sites on one of your upper front teeth using the ultrasound probe. Each measurement will be repeated three times at each site to check for reproducibility. You will then be required to visit the clinic at Day 7 and Day 14 so that the same measurement can be taken again, with each visit lasting approximately 20 minutes. You will not be required to do anything extra between the clinic visits.

At the end of the study, you will attend the clinic where a dentist will check your front teeth as a final check-up. If the dentist finds a dental problem, we will inform you and advise you to see your general dental practitioner.

What are the possible disadvantages and risks of taking part?

There are no known risks using ultrasound which is a non-invasive, non-destructive and completely safe procedure with no reported side effects, pain or discomfort.

If you are harmed by taking part in this research project there are no special compensation arrangements. If you are harmed due to someone's negligence, then you may have grounds for a legal action but you may have to pay for it. Regardless of this, if you wish to complain, or have any concerns about any aspect of the way you have been approached or treated during the course of this study you should ask to speak to the researchers who will do their best to answer your questions (Telephone: 0113 3436127). If you remain unhappy and wish to complain formally, you can do this through the NHS Complaints Procedure. Details can be obtained from the Leeds Dental Hospital. If you have private medical insurance, you should

tell your insurer that you are taking part in research and they will let you know if it affects your policy.

What are the possible benefits of taking part?

There are no direct benefits to you in taking part. However, the information gained from the study may provide further knowledge on how enamel thickness may be measured using ultrasound. This may be used in future to produce an ultrasound tool that aids in the diagnosis, monitoring and measuring of enamel erosion.

What if something goes wrong?

Every care will be taken in the course of this study. If you have a concern about any aspect of this study you can speak to your dentist or one of the other researchers who will do their best to answer your questions (Telephone: 0113 3436127).

What if relevant new information becomes available?

If any new information becomes available we will of course let you know.

Will my taking part be kept confidential?

If you decide to participate in this study the information collected about you will be handled strictly in accordance with the consent that you have given and also the 1998 Data Protection Act. Your identity in this trial will be treated as strictly confidential and you will be identified by your study number, date of birth and initials only. Information needed for study purposes will be collected on paper forms and electronically and will be stored securely in DenTCRU and the Department of Oral Biology in the LDI and will be accessible only by authorised members of the team.

Your healthcare records may be inspected by authorised individuals from the research team or the University of Leeds (the study Sponsor) or the regulatory

authorities to ensure that the study is being carried out correctly, although your confidentiality will be maintained. The information collected about you may be shared with other research teams to answer new research questions in the future, but your name will not be provided so you will not be able to be identified.

What will happen if I don't want to carry on with the study?

Your participation in this study is entirely voluntary. You do not have to take part in this trial if you do not wish to do so. If you decide to take part you are free to withdraw at any time. Any present or future treatment which you receive will not be affected in any way if you decide not to take part or if you decide to withdraw at a later date. If you withdraw consent from the study, your data will remain on file and will be included in the final study analysis. In line with Good Clinical Practice guidelines, at the end of the study, your data will be securely archived for a minimum of 5 years. Arrangements for confidential destruction will then be made.

What will happen to the results of the research study?

The results of this study may be published in a scientific journal, as part of the investigator's PhD thesis and at scientific meetings. You will not be identified in any report or publication about this study. If you would like to discuss the results of the study with someone, your dentist will be provided with a copy of the study report.

Who has organised, reviewed and funded the research and who will be supervising it?

The research is being sponsored by the University of Leeds, who are working with the Leeds Teaching Hospitals NHS Trust through the Leeds Dental Institute (LDI). The study has been reviewed by the Dental Research Ethics Committee at the University of Leeds and the local Research and Development Department situated at

the Leeds Teaching Hospital Trust. The study is funded by the Royal Embassy of Saudi Arabia- Ministry of Health.

Contact Details

If you have any further questions about the trial, please do not hesitate to contact:

Name	Telephone	e-mail
Mr Khalid Sindi (Principle Investigator)	0793-9494-877	dn08khfs@leeds.ac.uk
Mrs Gillian Dukanovic (Research coordinator)	0113-343-6127	g.dukanovic@leeds.ac.uk
Miss Lynn Gutteridge (Honorary Consultant in Restorative Dentistry)	0113-343-6132	d.l.gutteridge@leeds.ac.uk

Thank you for reading this information sheet.

17 Appendix 9: Participant Consent Form

UNIVERSITY OF LEEDS

Patient ID :	Initials:
Date of Birth:	Principal Investigator: Mr Khalid Sindi

Preliminary Clinical Study of Ultrasound to Measure Enamel Thickness

PARTICIPANT CONSENT FORM

1. I confirm that I have read and understand the information sheet for dated ..... (version .....) for the above study. I have had the opportunity to consider the information, ask questions and have had these answered satisfactorily. ☐

2. I understand that my participation in this study is voluntary and that I am free to withdraw at any time without my medical care or legal rights being affected. I understand that even if I withdraw from the above study, the data and samples collected from me will be used in analysing the results of the study. ☐

3. I understand that relevant sections of my medical notes and data collected during this study may be looked at by authorised individuals from the research team, regulatory bodies or sponsor in order to check that the study is being carried out correctly. I give permission for these bodies to have access to my records for the above study and any further research that may be conducted in relation to it. ☐

4. I agree to allow any information or results arising from this study to be used for healthcare and/or further medical research upon the understanding that my identity will remain anonymous. ☐

5. I agree to take part in the study.

Participant Consent Form Continued

Patient:

Signature……

Full name of patient (block capitals)……...…….……..

Date…….……

Investigator/Researcher:

I have explained the study to the above named patient and he/she has indicated his/her willingness to participate.

Signature……..……...

Name of Person taking consent(block capitals)……..

Date…….…….……...

(1 copy for patient; 1 for the DenTCRU; Original stored in Investigator Site File)

18 Appendix 10: Ultrasonic Transducers' Standard Test Forms

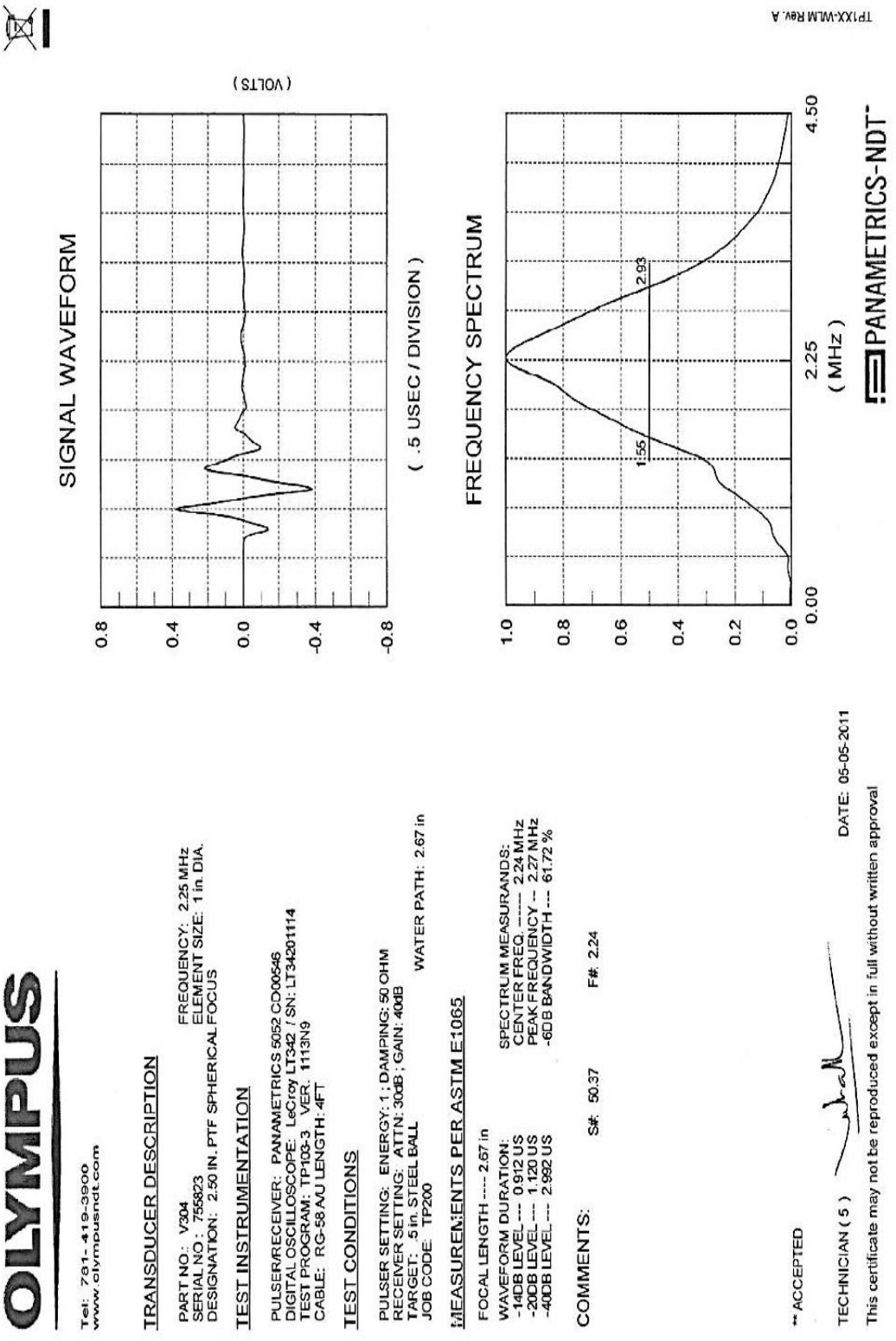

OLYMPUS

Tel: 781- 419-3900
www.olympusndt.com

TRANSDUCER DESCRIPTION

PART NO.: V380 FREQUENCY: 3.50 MHz
SERIAL NO.: 755585 ELEMENT SIZE: 1 in. DIA.
DESIGNATION: 2.5 in. PTF SPHERICAL FOCUS

TEST INSTRUMENTATION

PULSER/RECEIVER: PANAMETRICS 5052 CD00546
DIGITAL OSCILLOSCOPE: LeCroy LT342 / SN: LT34201114
TEST PROGRAM: TP103-3 VER. 1113N9
CABLE: RG-58 A/U LENGTH: 4FT

TEST CONDITIONS

PULSER SETTING: ENERGY: 1 ; DAMPING: 50 OHMS
RECEIVER SETTING: ATTN: 30dB ; GAIN: 40dB
TARGET: .25 STEEL BALL WATER PATH: 2.535 in
JOB CODE: TP200

MEASUREMENTS PER ASTM E1065

FOCAL LENGTH ---- 2.535 in

WAVEFORM DURATION:
-14DB LEVEL --- 0.360 US
-20DB LEVEL --- 0.584 US
-40DB LEVEL --- -1.793 US

SPECTRUM MEASURANDS:
CENTER FREQ. ------ 3.53 MHz
PEAK FREQUENCY -- 3.85 MHz
-6DB BANDWIDTH --- 83.53 %

COMMENTS: S#: 36.14 F#: 3.6

** ACCEPTED

TECHNICIAN (5) DATE: 05-05-2011

SIGNAL WAVEFORM

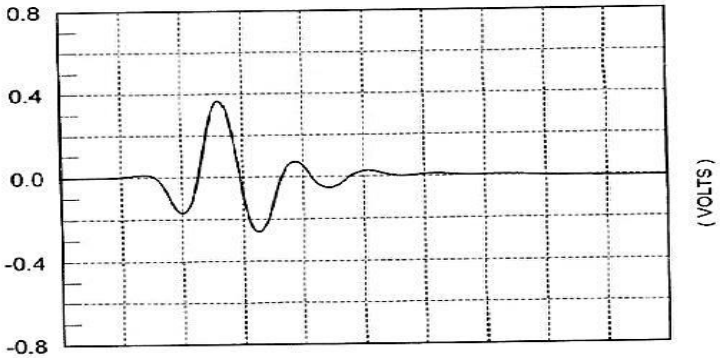

FREQUENCY SPECTRUM

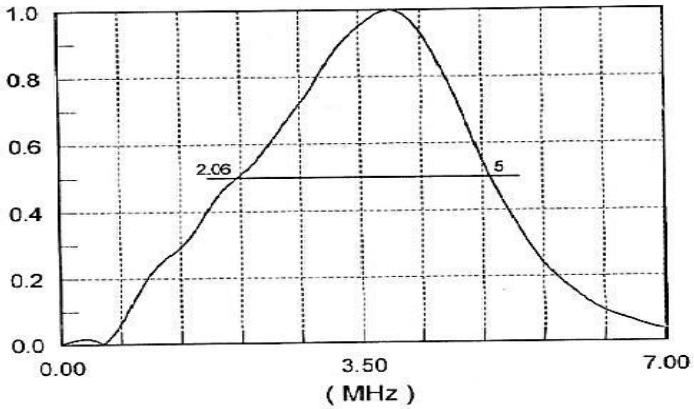

PANAMETRICS-NDT

OLYMPUS

Tel: 781- 419-3900
www.olympusndt.com

TRANSDUCER DESCRIPTION

PART NO.: V307 FREQUENCY: 5.00 MHz
SERIAL NO.: 755301 ELEMENT SIZE: 1 in. DIA.
DESIGNATION: 2.5 in. PTF SPHERICAL FOCUS

TEST INSTRUMENTATION

PULSER/RECEIVER: PANAMETRICS 5052 CD00546
DIGITAL OSCILLOSCOPE: LeCroy LT342 / SN: LT34201114
TEST PROGRAM: TP103-3 VER. 1113N9
CABLE: RG-58 A/U LENGTH: 4FT

TEST CONDITIONS

PULSER SETTING: ENERGY: 1 ; DAMPING: 50 OHM
RECEIVER SETTING: ATTN: 40dB ; GAIN: 40dB
TARGET: .25 IN STEEL BALL
JOB CODE: TP200
WATER PATH: 2.485 in

MEASUREMENTS PER ASTM E1065

FOCAL LENGTH ---- 2.485 in

WAVEFORM DURATION:	SPECTRUM MEASURANDS:
-14DB LEVEL --- 0.440 US	CENTER FREQ. ------ 4.88 MHz
-20DB LEVEL --- 0.552 US	PEAK FREQUENCY -- 5.16 MHz
-40DB LEVEL --- 0.856 US	-6DB BANDWIDTH --- 60.59 %

COMMENTS:

S#: 42.7 F#: 4.95

** ACCEPTED

TECHNICIAN (E) DATE: 05-05-2011

SIGNAL WAVEFORM

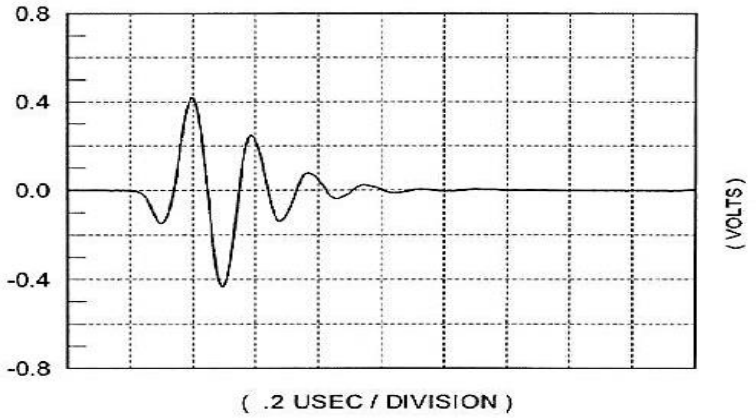

FREQUENCY SPECTRUM

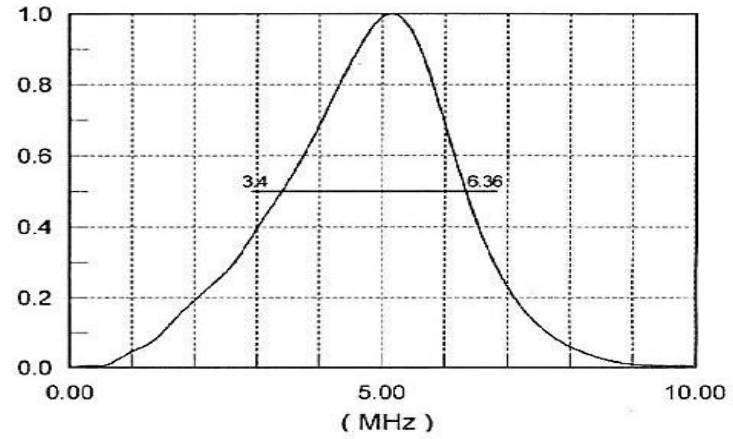

OLYMPUS

CERTIFICATE in ACCORDANCE WITH EN12668-2

TRANSDUCER: V260 **Serial No.: 788704**
PANAMETRICS-NDT

Description: Delay Line Transducer, 15.0 MHz, 3.17mm Element Diameter

Principle Parameters

Reference	Frequency	Active Element	Bandwidth
V260	15 MHz	3.17 mm	N/A

Reference documents
EN12668-2 : 2001
ASTM E-1065
ISO 9001 : 2000
Internal procedure: TP210

Quality system
Fabricant: OLYMPUS NDT, Inc. certified on 2/9/2009 per Intertek

Instrumentation used
Pulser / Receiver: PANAMETRICS 5601
Digitizer: LeCroy LC564A / SN: LC56410253
Cable: RG 174/U Length: 1.22 M

OLYMPUS

Impulse formation
Test conditions:
Pulser Energy 1 ; Damping 30 Ω
Receiver Attenuation: 12 dB ; Gain: 46 dB
Target: Backwall of 1.0 mm steel
Test Date: 11-22-2011

SIGNAL WAVEFORM

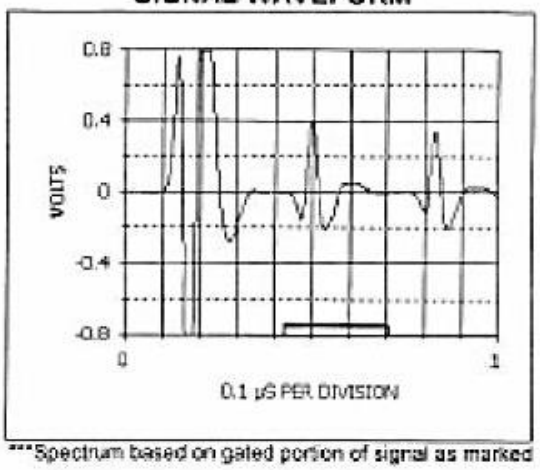

***Spectrum based on gated portion of signal as marked

FREQUENCY SPECTRUM

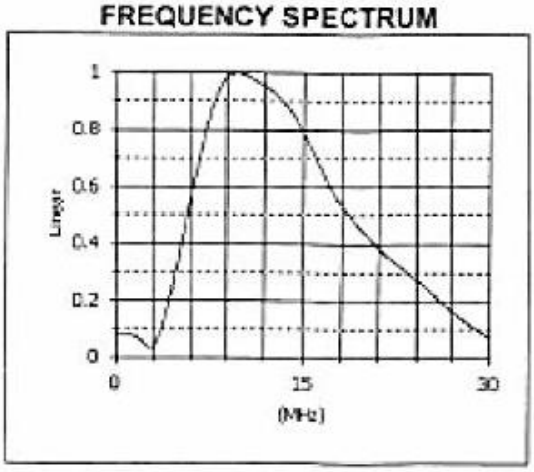

Effective measurands

Parameter	Designation	Min value	Measure	Max value	Units
-14 dB waveform duration	t_{14}	N/A	0.00	N/A	µs
-20 dB waveform duration	t_{20}	N/A	0.00	N/A	µs
Centre Frequency	f_c	10.5	10.33	15.0	MHz
Relative Bandwidth @ -6dB	Δf_{rel}	N/A	126.0	N/A	%

19 Appendix 11: Pulser/Receiver Certificate of Calibration

OLYMPUS 5072PR

OLYMPUS NDT
48 WOERD AVENUE
Waltham, MA 02453 USA
TEL: (781) 419-3900
E-mail: info@panametrics-ndt.com
ISO 9001 CERTIFIED

Certificate of Calibration

Form NDT340C

Certificate Number_____

This certifies that calibration of the Pulser/Receiver model 5072PR described below, has been tested and verified in accordance with the listed Panametrics factory test procedure. This test procedure conforms to the requirements of ISO-9001 section 4.10. The test status below has been generated using National Institute of Standards and Technology (N.I.S.T) Traceable calibrated test equipment.

(Model 5072PR) N.I.S.T FINAL CALIBRATION DATA				
Customer Name:		Serial Number:		060090108
NDT Sales Order / RA:		Date Calibrated:		08-11-06
Temperature:	70.7	Instrument status:		
		New	As received	After repair/cal
Certified by	Michael Hangis	X		
[CALIBRATED TEST EQUIPMENT]				
Network Analyzer Model: 8712ET				
Serial Number:	US39230729	Last NIST Cal Date:		7-14-06
PDL Number:	0054100	Next NIST Cal Date:		7-14-07
Oscilloscope Model: 2445				
Serial Number:	105427	Last NIST Cal Date:		6-21-06
PDL Number:	0021300	Next NIST Cal Date:		6-21-07
Pulse / Function Generator Model: DS 345				
Serial Number:	18512	Last NIST Cal Date:		6-21-06
PDL Number:	0023600	Next NIST Cal Date:		6-21-07
RF Meter Model: 9200A				
Serial Number:	83410BA	Last NIST Cal Date:		6-21-06
PDL Number:	0091600	Next NIST Cal Date:		6-21-07

OLYMPUS

5072PR

OLYMPUS NDT
48 WOERD AVENUE
Waltham, MA 02453 USA
TEL: (781) 419-3900
E-mail: info@panametrics-ndt.com
ISO 9001 CERTIFIED

RECEIVER TEST:

Results for Attenuation/Gain Test					
UUT Gain Setting	**Network Analyzer Setup File**	**Measured Gain**	**Test Limits for Ref Only (Setting ±0.5dB)**	**Pass**	**Fail**
-50 dB	MEAS-50.STA	-49.5	-49.5 to -50.5 dB	X	
±0 dB	MEAS0DB.STA	.006	-0.5 to +0.5 dB	X	
+10 dB	MEAS10DB.STA	10.04	+9.5 to +10.5 dB	X	
+20 dB	MEAS20DB.STA	19.73	+19.5 to +20.5 dB	X	
+30 dB	MEAS30DB.STA	29.86	+29.5 to +30.5 dB	X	
+40 dB	MEAS40DB.STA	40.18	+39.5 to +40.5 dB	X	
+51 dB	MEAS51DB.STA	51.02	+50.5 to +51.5 dB	X	
+52 dB	MEAS52DB.STA	52.05	+51.5 to +52.5 dB	X	
+54 dB	MEAS54DB.STA	54.01	+53.5 to +54.5 dB	X	
+58 dB	MEAS58DB.STA	58.05	+57.5 to +58.5 dB	X	
+59 dB	MEAS59DB.STA	59.0	+58.5 to +59.5 dB	X	

Results for Bandwidth Test							
UUT Setting		**Network Analyzer Setup File**	**Measured -3dB Freq.**		**Test Limit**	**Pass**	**Fail**
HPF Switch	**LPF Switch**		**HPF**	**LPF**			
OUT	FULL BW	BW_FULL.STA	N/A	32.49	> 31 MHz	X	
1 MHz	FULL BW	BW_1-33.STA	1.51	N/A	< 1.7 MHz	X	
OUT	10 MHz	BW_1K-10.STA	N/A	9.61	> 8.5 MHz	X	

Results for Noise Test			
Measured Noise Voltage (RMS)	**Test Limit**	**PASS**	**FAIL**
17.6	35 mV RMS maximum	X	

OLYMPUS

5072PR

OLYMPUS NDT
48 WOERD AVENUE
Waltham, MA 02453 USA
TEL: (781) 419-3900
E-mail: info@panametrics-ndt.com
ISO 9001 CERTIFIED

PULSER TEST:

Results for Pulser Trigger Test					
Setup	**Measured SYNC Pulse**		**Test Limits**	**Pass**	**Fail**
	Ampitude	**Frequency**			
UUT: PRF = EXT Pulse Generator: Pulse Amplitude: +2.4 V Frequency: 5 KHz Width: 210 nS	3.2V	X	Amplitude: ≥ 2.4V @ 50 ohm Frequency: Same as PRF setting	X	
UUT: PRF = all settings from 100 to 5K	3.2V	X		X	

Result for Main Bang Pulse Amplitude Test					
UUT Energy Setting	**UUT Damping Setting**	**Amplitude (Vp)**		**Pass**	**Fail**
		Measured	**Test Limits**		
4	1	380 v	380V min	X	

The above pulser/receiver model 5072PR passes all test requirements (with the exception of cosmetic tests on repaired unit) of PANAMETRICS procedure 714-783.

Technician: Michael Hangis Date: 8-11-06

Printed Name: Michael Hangis

20 Appendix 12: Posters and Presentations

- Speed of Sound Measurements in Ivory, Institute of Physics and Engineering in Medicine (IPEM), York, 2010 (presentation).
- Speed of Sound Measurements in Ivory, School of Dentistry, University of Leeds, Leeds, 2011 (poster).
- Anisotropy in the Speed of Sound in Ivory, British Society of Oral and Dental Research (BSODR), University of Sheffield, Sheffield, 2011 (poster).
- Human Enamel Thickness Measurements with Ultrasound: Will it Work?, Postgraduate Research Day, School of Dentistry, University of Leeds, Leeds, 2012 (presentation).
- Human Enamel Thickness Measurements with Ultrasound: Will it Work?, British Medical Ultrasound Society (BMUS) Conference, Telford, 2012 (presentation).
- *In vivo* Reproducibility of Enamel Thickness Measurements with Ultrasound, School of Dentistry, University of Leeds, Leeds, 2013 (presentation).